



**University
of Antwerp**

Faculty of Science

Department of Bioscience Engineering

Research Group of Sustainable Energy, Air and Water Technology

**Bioreactor strategies for sustainable nitrogen cycling
based on mineralization/nitrification, partial nitrification/anammox
or sulfur-based denitrification**

Thesis submitted for the degree of Doctor in Bioscience Engineering at the
University of Antwerp to be defended by

Ir. Yankai Xie

Promotor

Prof. dr. ir. Siegfried E. Vlaeminck

Antwerpen, 2021

Promotor:

Prof. dr. ir. Siegfried E. Vlaeminck

Department of Bioscience Engineering, Faculty of Science, University of Antwerp,
Belgium

Board of examiners:

Prof. dr. ir. Pieter Billen (Chairman)

Department of Chemistry/Biochemistry, Faculty of Applied Engineering, University of
Antwerp, Belgium

Prof. dr. ir. Ramon Ganigué

Department of Biotechnology, Faculty of Bioscience Engineering, Ghent University,
Belgium

Prof. dr. ir. Jan Dries

Department of Chemistry/Biochemistry, Faculty of Applied Engineering, University of
Antwerp, Belgium

Prof. dr. ir. Eveline Volcke

Department of Green Chemistry and Technology, Faculty of Bioscience Engineering,
Ghent University, Belgium

Prof. dr. ir. Anuska Mosquera Corral

Department of Chemical Engineering, School of Engineering, University of Santiago de
Compostela, Spain

© Yankai Xie, 2021

ISBN: 978-90-5728-707-7

Depot number: D/2021/12.293/28

This research is supported by the China Scholarship Council (CSC).

The author and the promotor give the authorization to consult and to copy parts of this work for personal use only. Every other use is subject to copyright laws. Permission to reproduce any material contained in this work should be obtained from the author.

Notation index

| | |
|---------|--|
| AerAOB | Aerobic ammonium-oxidizing bacteria |
| ADS | Anaerobic digestion sludge |
| AMO | Ammonia monooxygenase |
| Anammox | Anoxic ammonium oxidation |
| AnAOB | Anoxic ammonium-oxidizing bacteria |
| AOA | Ammonium-oxidizing archaea |
| AOB | Ammonium-oxidizing bacteria |
| AS | Activated sludge |
| BAF | Biological aerated filter |
| BAPN | BioAgenasol® profigreen |
| bCOD | Biodegradable chemical oxygen demand |
| BES | Bio-electrochemical system |
| BNS | Baseline nutrient solution |
| BSNLR | Biomass-specific NO_3^- -N loading rate |
| CAB | Consortium of aerobic bacteria |
| CDI | Capacitor deionization technology |
| CHP | Combined heat and power |
| COD | Chemical oxygen demand |
| CSTR | Continuous stirred-tank reactor |
| DHS | Down-flow hanging sponge |

| | |
|------|---|
| DM | Dry matter |
| DN/A | Denigration/anammox |
| DO | Dissolved oxygen |
| EC | Electrical conductivity |
| EPS | Extracellular polymeric substances |
| ES | Earth system |
| EU | European Union |
| FA | Free ammonia |
| FBBR | Fluidized-bed biofilm reactor |
| FNA | Free nitrous acid |
| FO | Forward osmosis |
| GHG | Greenhouse gas |
| HAO | Hydroxylamine oxidoreductase |
| HDH | Hydrazine dehydrogenase |
| HDN | Heterotrophic denitrification |
| HLR | Hydraulic loading rate |
| HNS | Hoagland nutrient solution |
| HRES | H ₂ recycling electrochemical system |
| HRT | Hydraulic retention time |
| HZS | Hydrazine synthase enzyme |
| IFAS | Integrated fixed-film activated sludge |

| | |
|------|--|
| LCA | Life cycle assessment |
| MaB | Microalgae- Consortium of aerobic bacteria |
| MABR | Membrane-aerated biofilm reactor |
| MBBR | Moving bed biofilm reactor |
| MBR | Membrane biofilm reactor |
| MCO | Multicopper oxidase |
| MEC | Microbial electrolysis cell |
| MF | Microbial fertilizer |
| MFC | Microbial fuel cell |
| NAE | Nitrite accumulation efficiency |
| N/DN | Nitrification/denitrification |
| NIR | Nitrite reductase |
| NOB | Nitrite-oxidizing bacteria |
| NPS | Non-point source |
| Nr | Reactive nitrogen |
| NXR | Nitrite oxidoreductase |
| OPEX | Operational expenditure |
| OTE | Oxygen transfer efficiency |
| PN/A | Partial nitrification/anammox |
| PNSB | Purple Non-Sulfur Bacteria |
| RBC | Rotating biological contactor |

| | |
|------|--------------------------------|
| SBR | Sequencing batch reactor |
| SCOD | Soluble chemical oxygen demand |
| SDN | Sulfur-driven denitrataion |
| SOB | Sulfur-oxidizing bacteria |
| SRT | Sludge retention time |
| TAN | Total ammonia nitrogen |
| TCOD | Total chemical oxygen demand |
| TF | Trickling filter |
| TIN | Total inorganic nitrogen |
| TKN | Total Kjeldahl nitrogen |
| TN | Total nitrogen |
| TP | Total phosphorus |
| VSS | Volatile suspended solids |
| WWTP | Wastewater treatment plant |

Table of Contents

| | |
|---|----------|
| Notation index | i |
| Abstract | 1 |
| Chapter 1: Introduction | 5 |
| 1. A planetary problem: too much reactive nitrogen (Nr) | 7 |
| 1.1 Planetary boundaries | 7 |
| 1.2 Nitrogen fertilization in agriculture | 9 |
| 1.3 Nitrogen cascade | 10 |
| 2. Nitrogen management in waste streams | 11 |
| 3. Nitrogen recovery | 12 |
| 3.1 Collected and collectible waste streams containing Nr | 12 |
| 3.1.1 Inorganic Nr waste streams | 13 |
| 3.1.2 Organic Nr waste streams | 16 |
| 3.2 Recovery technologies | 19 |
| 3.2.1 Inorganic Nr recovery | 19 |
| 3.2.2 Organic Nr recovery | 20 |
| 3.2.2.1 General recovery strategies | 20 |
| 3.2.2.2 Application of organic fertilizers | 22 |
| 4. Nitrogen removal | 23 |
| 4.1 Nitrogen and carbon removal processes | 24 |
| 4.1.1 Nitrification | 24 |
| 4.1.1.1 Nitritation | 25 |
| 4.1.1.2 Nitratation | 25 |
| 4.1.1.3 Nitrification = nitritation + nitratation | 26 |
| 4.1.2 Denitrification | 27 |
| 4.1.2.1 Denitratation | 29 |
| 4.1.2.2 Denitritation | 30 |
| 4.1.3 Anammox | 30 |
| 4.1.4 Organic carbon removal | 31 |
| 4.2 Processes for nitrogen (and organic carbon) removal | 32 |

| | | |
|-------|---|----|
| 4.2.1 | Nitrification/denitrification | 32 |
| 4.2.2 | Nitritation/denitritation | 33 |
| 4.2.3 | Partial nitritation/anammox (PN/A)..... | 34 |
| 4.2.4 | Denitratation/anammox | 35 |
| 5. | Bioreactor configurations..... | 36 |
| 5.1 | Growth mode | 36 |
| 5.1.1 | Suspended growth..... | 36 |
| 5.1.2 | Attached growth..... | 37 |
| 5.2 | Aeration approach..... | 39 |
| 6. | Research outline..... | 42 |

Chapter 2: A bioreactor and nutrient balancing approach for the conversion of solid organic fertilizers to liquid nitrate-rich fertilizers: Mineralization and nitrification performance complemented with economic aspects45

| | |
|--|----|
| Abstract | 47 |
| 1. Introduction..... | 48 |
| 2. Material and methods..... | 52 |
| 2.1 Organic fertilizers | 52 |
| 2.2 Batch tests | 52 |
| 2.3 Nitrate conversion in a controlled mineralization and nitrification bioreactor | 53 |
| 2.4 Physicochemical water, biomass, and microbiome analyses..... | 54 |
| 2.5 Nutrient balancing strategy and economic assessment | 55 |
| 3. Results and discussion..... | 57 |
| 3.1 Batch test screen for optimal mineralization conditions | 57 |
| 3.2 Nitrate production in the mineralization and nitrification bioreactor..... | 59 |
| 3.2.1 Performance of nitrate production under various controlling parameters | 59 |
| 3.2.2 The microbial community in the bioreactor..... | 62 |
| 3.3 Nutrient quality balancing and economic analysis..... | 64 |
| 4. Conclusion | 69 |
| 5. Supplementary information | 70 |
| 6. Acknowledgments | 78 |

Chapter 3: A nitrification trickling filter as key to produce hydroponic nutrient solutions from real urine79

| | |
|--|-----|
| Abstract | 81 |
| 1. Introduction..... | 82 |
| 2. Materials and methods | 87 |
| 2.1 Urine collection and alkalization | 87 |
| 2.2 Bioreactor setup..... | 87 |
| 2.2.1 Reactor operation..... | 87 |
| 2.2.2 Reactor inoculation and start-up | 88 |
| 2.2.3 Reactor operation with real urine | 89 |
| 2.3 Sampling and analytical methods..... | 89 |
| 2.4 Calculation of the element supplementation for nutrient balancing | 89 |
| 3. Results and discussion..... | 90 |
| 3.1 Reactor start-up and nitrification performance on synthetic urine..... | 90 |
| 3.2 Nitrification performance on real urine | 92 |
| 3.2.1 Nitrification performance after switching to real urine..... | 92 |
| 3.2.2 Nitrification performance stability under different collection batches | 94 |
| 3.2.3 Impact of hydraulic loading rate on urine nitrification and electrical energy consumption..... | 95 |
| 3.3 Nutrient quality balancing for direct application in hydroponic systems | 96 |
| 4. Conclusion | 99 |
| 5. Supplementary information | 100 |
| 6. Acknowledgments..... | 104 |

Chapter 4: Feasibility of a trickling filter for partial nitrification/anammox: Effects of carrier material, passive ventilation and hydraulic loading rate at lab scale 105

| | |
|--|-----|
| Abstract | 107 |
| 1. Introduction..... | 108 |
| 2. Materials and methods | 113 |
| 2.1 Trickling filter configuration | 113 |
| 2.2 Influent composition | 113 |
| 2.3 Trickling filter operation..... | 114 |
| 2.4 Determination of microbial activity in each compartment..... | 115 |

| | | |
|---|---|------------|
| 2.5 | Physicochemical water analyses and microbial activity calculations..... | 116 |
| 3. | Results and discussion..... | 116 |
| 3.1 | Startup periods: nitrate accumulation | 116 |
| 3.2 | Effect of the top passive ventilation and TN loading rate | 119 |
| 3.3 | Effect of hydraulic loading rate | 121 |
| 3.4 | Effect of top and bottom ventilation..... | 121 |
| 3.5 | Vertical activity stratification in trickling filters | 122 |
| 3.6 | Carrier materials and electrical energy consumption | 124 |
| 4. | Conclusions..... | 125 |
| 5. | Supplementary information | 126 |
| 6. | Acknowledgments..... | 128 |
| Chapter 5: Autotrophic nitrogen polishing of secondary effluents: Challenges in obtaining sulfur-driven denitratation for downstream anammox treatment | | 129 |
| | Abstract | 131 |
| 1. | Introduction..... | 132 |
| 2. | Material and methods..... | 134 |
| 2.1 | Reactor setup | 134 |
| 2.2 | Chemicals and influent | 134 |
| 2.3 | Reactor operation..... | 135 |
| 2.4 | Analytical methods..... | 135 |
| 2.5 | Microbiome Analysis | 136 |
| 3. | Results and discussion..... | 136 |
| 3.1 | Effects of the pH control strategy | 138 |
| 3.2 | Effects of residual nitrate level control | 141 |
| 3.3 | Effects of the BSNLR control..... | 144 |
| 3.4 | Evolution of the microbial community in the long term | 146 |
| 4. | Conclusions..... | 149 |
| 5. | Supplementary information | 150 |
| 6. | Acknowledgments..... | 152 |
| Chapter 6: General discussion and outlook..... | | 153 |
| 1. | Main research outcomes..... | 155 |

| | | |
|-------|--|------------|
| 2. | Nitrogen management to make the N cycle more sustainable | 156 |
| 2.1 | Sustainability | 157 |
| 2.1.1 | Environmental sustainability | 157 |
| 2.1.2 | Human health and sustainability..... | 160 |
| 2.1.3 | Economic sustainability | 162 |
| 2.2 | Nitrogen strength of waste streams..... | 166 |
| 2.3 | Technology performance and feasibility | 168 |
| 3. | Overall conclusions and outlook | 173 |
| | Bibliography..... | 175 |
| | Acknowledgments..... | 199 |
| | Curriculum vitae..... | 203 |

Abstract

In the biogeochemical flows on Earth, the reactive nitrogen (Nr) level has three times surpassed the safe boundary. The severe transgression of this boundary goes against sustainable planetary development. The modern food production process excessively relies on synthetic Nr fertilizers from the Haber– Bosch process. However, the massive loss of valuable nitrogen resources (i.e., 78-89%) from agriculture has been causing severe nitrogen cascade. Besides, the domestic wastewater in some local areas is discharged without proper treatment, making it a nonnegligible source of Nr pollution for local water bodies. Anthropogenic activities keep pumping out Nr pollution via point-source and non-point-source (NPS) emissions. Compared to the NPS emissions, point sources give visible and identified waste streams. It is vital to intervene the nitrogen cascade from point sources and facilitate humanity back to the safe Nr boundary.

The collected and collectible Nr streams from food production, waste management, and recycling secondary raw materials can be used as waste-based fertilizers for agricultural cultivation. Besides the well-investigated recovery of inorganic Nr, organic Nr accounts for a massive Nr proportion on the Earth. Proper handling and treatment make these useful organic fertilizers for soil-based cultivation. However, these organic Nr fertilizers cannot directly apply to fertigation or hydroponic cultivation systems, and further biological conversion via nitrogen mineralization and nitrification to nitrate is essential.

Besides the direct Nr cycling, the indirect Nr cycling ‘over the atmosphere’ should also be considered. In this way, the nitrogen cycle can be completed via converting the waste Nr back to nitrogen gas (i.e., Nr removal) and then synthesizing into Nr again. The municipal wastewater treatment plants receive a vast amount of low-strength Nr wastewater (mainly as ammonium) daily. Compared to the conventional nitrification/denitrification process, partial nitrification/anammox (PN/A) is considered a resource- and cost-effective technology for wastewater with a low COD/N ratio.

Moreover, the novel autotrophic denitrification/anammox process could be a good Nr removal process for wastewater containing both ammonium and nitrate.

This Ph.D. thesis aimed to develop Nr recovery, conversion, and removal bioreactor strategies for different types of waste streams and biomass. Nr recovery was investigated on high-strength Nr waste streams for fertigation or hydroponic applications in **Chapters 2 and 3**. On the other hand, Nr removal was studied on the medium- to low-strength Nr waste streams in **Chapters 4 and 5**.

In **Chapter 2**, a novel mineralization and nitrification system was proposed, producing nutrient solutions from solid organic fertilizers for hydroponic systems. Batch tests showed that aerobic incubation at 35°C could realize the NO_3^- -N production efficiency above 90% from a novel microbial fertilizer. Subsequently, in the stirred tank bioreactor test, NO_3^- -N production efficiency stabilized in a range of 44-51% under the influent loading rate of 400 mg TN $\text{L}^{-1} \text{d}^{-1}$ at a 5-day HRT. Using $\text{Ca}(\text{OH})_2$ and $\text{Mg}(\text{OH})_2$ as pH control reagents generated the nutrient solutions with different P, Ca, and Mg nutrient levels. After modeling the nutrient balancing process, the proportion of organic-sourced NO_3^- -N in the Hoagland nutrient solution (HNS) of $\text{Ca}(\text{OH})_2$ scenario was 92.7%, while only 37.4% in the $\text{Mg}(\text{OH})_2$ scenario. Compared to commercial scenarios, the total costs of the organic-sourced HNS can be cost-competitive for hydroponic cultivation.

In **Chapter 3**, the Nr recovery as nitrate (NO_3^- -N) from diluted human urine (around 670 mg N L^{-1}) was explored in a trickling filter (TF) for the first time. A novel concept of in-situ integrating the TF system into hydroponic systems was proposed as meaningful progress towards sustainable agriculture. The difference between synthetic and real urine in nitrification efficiency was found to be negligible. The full nitrification of alkalized real urine was realized in the pH-controlled TF by calcium hydroxide ($\text{Ca}(\text{OH})_2$) at around pH 6. The TF could handle different urine collection batches and maintain relatively stable nitrification performance, with NO_3^- -N production efficiency and rate of $88\pm 3\%$ and $136\pm 4 \text{ mg N L}^{-1} \text{d}^{-1}$, respectively. The optimal HLR to realize this nitrification performance was $2 \text{ m}^3 \text{ m}^{-2} \text{ h}^{-1}$, with energy consumption of 1.8 kWh electricity $\text{kg}^{-1} \text{NO}_3^-$ -N production. $\text{Ca}(\text{OH})_2$, as a cheap base, its triple advantages on urine alkalization, full nitrification,

and macronutrient supplementation were successfully demonstrated in our proposed concept.

In **Chapter 4**, towards more sustainable wastewater treatment, the feasibility of one-stage partial nitrification/anammox (PN/A) was investigated in three parallel packed-bed trickling filters (TFs), with three types of carrier materials of different specific surface areas. Synthetic wastewater containing 100-250 mg $\text{NH}_4^+\text{-N L}^{-1}$ was tested to mimic medium-strength household waste streams after carbon removal. Interestingly, the cheap carrier based on expanded clay achieved similar rates as commercially used plastic carrier materials. The top passive ventilation combined with an optimum hydraulic loading rate of $1.8 \text{ m}^3 \text{ m}^{-2} \text{ h}^{-1}$ could reach approximately 60% total nitrogen (TN) removal at a rate of $300 \text{ mg N L}^{-1} \text{ d}^{-1}$. A relatively low $\text{NO}_3^-\text{-N}$ production (13%) via PN/A was achieved in TFs. Most of the TN removal took place in the top compartment, where anammox activity was the highest. Energy consumption estimation ($0.78 \text{ kWh electricity g}^{-1} \text{ N removed}$) suggested that the proposed process could be a suitable low-cost alternative for nitrogen removal.

In **Chapter 5**, coupling sulfur-driven denitrification (SDN) with anammox was proposed to treat the wastewater containing both $\text{NO}_3^-\text{-N}$ and $\text{NH}_4^+\text{-N}$, like the secondary effluents of mainstream PN/A processes. To explore the feasibility of sufficient and stable $\text{NO}_2^-\text{-N}$ accumulation via SDN in the long term, the effects of pH setpoints, residual $\text{NO}_3^-\text{-N}$ level, and biomass-specific $\text{NO}_3^-\text{-N}$ loading rate (BSNLR) were investigated. Alternating the pH setpoints between 7.0 and 8.5 could temporarily stimulate the $\text{NO}_2^-\text{-N}$ accumulation. Both the residual $\text{NO}_3^-\text{-N}$ and BSNLR showed highly positive correlations with the $\text{NO}_2^-\text{-N}$ accumulation efficiency. Under the control of pH 8.5, $1.0 \pm 0.8 \text{ mg NO}_3^-\text{-N L}^{-1}$ and $150 \pm 42 \text{ mg NO}_3^-\text{-N g}^{-1} \text{ VSS d}^{-1}$, SDN could produce $6.4 \pm 1.0 \text{ mg NO}_2^-\text{-N L}^{-1}$ in the short term. *Thiobacillus* members may play a crucial role in managing the $\text{NO}_2^-\text{-N}$ accumulation, but the reduction of abundance and possible adaptation significantly impaired the efficacy of control strategies in the long run.

Overall, novel technologies have been proposed to sustainably convert Nr in waste streams and biomass. The decision for Nr recovery versus removal and synthesis should

be based on specific cases with the best environmental, economic, and human-health sustainability. In the future, the Nr management concepts should be further improved to make the nitrogen cycle more sustainable with higher resource use efficiency and less Nr emissions to the environment. Although the thesis is mainly focused on limited types of Nr waste streams, it pointed out the direction of sustainable Nr management and could facilitate the Nr back to the safe boundary in the long run.

Chapter 1

Introduction

1. A planetary problem: too much reactive nitrogen (Nr)

1.1 Planetary boundaries

The planetary environment on Earth has been relatively stable for the past 11,700 years¹. This period of stability known as the Holocene epoch supports human civilizations to arise, develop, and thrive. During the Holocene, the environmental change occurred naturally, and the Earth's regulatory capacity maintained the conditions for human development. Now, the functioning of the Earth system (ES) may be under threat. Since the Industrial Revolution, human actions have become the primary driver of global environmental change², and the Anthropocene era has arisen³. Human activities (e.g., over-reliance on fossil fuel and industrialized agriculture) threaten the ES resilience that keeps the Earth in a Holocene-like state. The consequences could be irreversible and detrimental for large parts of the world⁴.

Facing the challenge of maintaining a Holocene-like state, Rockström et al. (2009) proposed a planetary boundary framework based on the planetary biophysical process regulating the ES stability, to identify levels of human perturbation to the ES⁵. These boundaries define the safe operating space for global societal development. Nine ES processes were used to define the planetary boundaries, including climate change, biosphere integrity, land-system change, freshwater use, biogeochemical flows, ocean acidification, atmospheric aerosol loading, stratospheric ozone depletion, and novel entities (Figure 1.1). As long as the boundaries are not crossed, humanity has the freedom to pursue sustainable development. However, anthropogenic perturbation levels of four ES processes (i.e., climate change, biosphere integrity, biogeochemical flows, and land-system change) have transgressed the proposed safe boundaries.

In the biogeochemical flows, the nitrogen has three times surpassed the safety level to avert the eutrophication of aquatic ecosystems¹. The control variable for interference with the nitrogen circle is the rate at which inert nitrogen (N_2 molecule) is removed from the atmosphere and converted to reactive nitrogen (Nr) for human use. Nitrogen gas (N_2) is harmless and highly abundant in the Earth's atmosphere, making up 78% of every breath we take. A robust triple bond between two N atoms makes the N_2 molecule stable

and chemically unreactive. The reactive nitrogen (Nr) includes all other nitrogen forms, such as nitrogen oxides (NO_x), nitrous oxide (N₂O), ammonia (NH₃), and nitrate (NO₃⁻). Nr is essential for all biological systems ⁶. For example, nitric oxide (NO) is a crucial biological signaling compound, while ammonia (NH₃) is the foundation for amino acids, proteins, enzymes, and DNA. Nitrate (NO₃⁻) is a primary nitrogen nutrient form and essential for plant growth. Against these benefits, many types of Nr can also cause harmful impacts on the environment and human health. Nitric oxide (NO) and nitrogen dioxide (NO₂) are major air pollutants, which can decrease atmospheric visibility and air quality. Acute and chronic exposure to NO₂ induces severe respiratory and cardiovascular diseases ⁶. N₂O, as a greenhouse gas (GHG), is 300 times more potent than carbon dioxide. It also damages the stratospheric ozone and directly increases radiative forcing ⁵. In the hydrosphere, excess NH₄⁺ and NO₃⁻ cause eutrophication and affect biodiversity. Elevated NO₃⁻ level (>10 mg L⁻¹) in groundwater can pose a significant human health risk (e.g., bowel cancer and methemoglobinemia) via drinking water ^{7, 8}. Nevertheless, the transgression of the planetary boundary may substantially alter the ES functioning and is not conducive to planetary sustainable development.

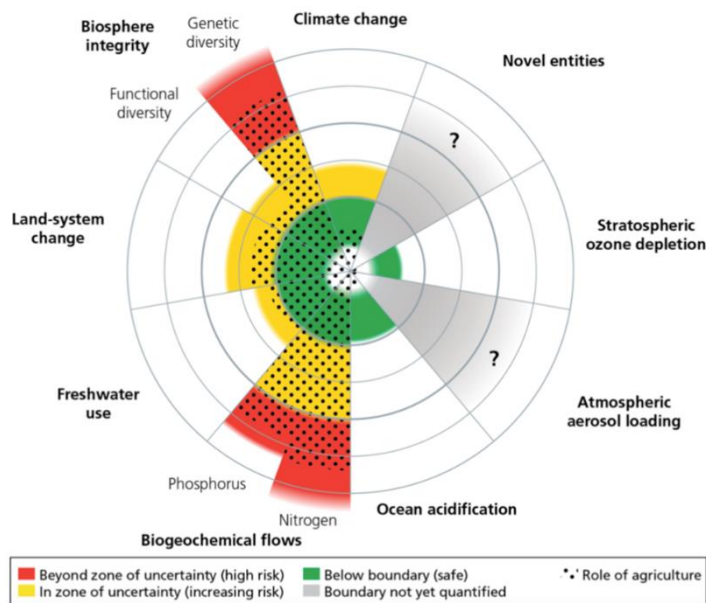
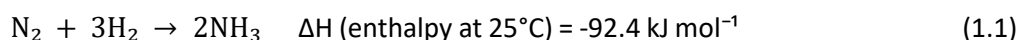


Figure 1.1: The status of the control variables for the nine planetary boundaries. Figure adapted from ¹.

1.2 Nitrogen fertilization in agriculture

The significant benefit of Nr compounds is to help produce food and animal feed. Until the end of the nineteenth century, the primary agricultural source of Nr was the fixation of N₂ by symbiotic bacteria in legumes planted and the limited amount of nitrogen in manure⁸. There was a concern of Nr-fertilizer shortage for food production due to a growing world population. To tackle this concern, the Haber– Bosch process of artificial nitrogen "fixation" came up in 1908, N₂ from the atmosphere and hydrogen (H₂O from water) gases are reacted over an iron catalyst (Fe³⁺), and aluminum oxide (Al₂O₃) and potassium oxide (K₂O) are used as promoters⁹. The reaction is carried out under 250 atmospheres (atm) and 450–500 °C (Reaction 1.1).



Haber– Bosch process allows the massive manufacture of Nr-fertilizers (e.g., ammonia, urea, and nitrate) on an industrial scale. Within one century, anthropogenic Nr production had more than doubled global rates of nitrogen fixation. Without Haber– Bosch process, around half of humanity would perish from hunger¹⁰. In general, three types of Nr are fed into agricultural cultivation systems: (i) biologically fixed nitrogen, (ii) synthetic Nr fertilizers from Haber– Bosch process, and (iii) organic fertilizers (e.g., crop residues, animal manure, and human waste^{11,12}). Among these three Nr sources, the first two are from inert N (N₂), and the third is from Nr of secondary sources.

For soil-based cultivation, all three Nr types mentioned above are applicable. The amount of Nr primarily determines the annual crop production added to the soil. On a global scale, about 120 million tons of new Nr and 50 million tons of previously created Nr (e.g., crop residue and animal manure) are added annually to cropland^{7,13}. The global cropland receives about 63% of the anthropogenic fixation of N₂ to Nr⁶.

However, due to the limited capacity of mineralization and nitrification in fertigation and hydroponic cultivation, only the inorganic Nr solutions (e.g., based on NO₃⁻-N) are applicable to higher plants' growth¹⁴. In a NO₃⁻-based nutrient solution, the presence of 5% to 10% of the N as NH₄⁺-N can enhance the uptake of NO₃⁻-N, while the excess

proportion of $\text{NH}_4^+\text{-N}$ may exhibit ammonium toxicity symptoms, such as breakdown of vascular tissue at the base of the plant, lesions on stems and leaves, and increased occurrence of blossom-end rot on fruit ¹⁵. To avoid the risk of ammonium toxicity, the formulas of some universal standard nutrient solutions (e.g., Hoagland nutrient solution and Steiner nutrient solution) exclude the $\text{NH}_4^+\text{-N}$ ¹⁶⁻¹⁹. Thus, farmers can directly choose liquid nitrate-based fertilizers.

Compared to soil-based agriculture, the modern hydroponic systems are water, nutrient, and space-efficient. Especially in closed or recirculation systems, 85-90% of irrigation water and 80-85% of fertilizer can be saved due to control over nutrient levels ²⁰. Besides, hydroponic cultivation can be more controllable to the root environment, timely nutrient feeding, nutrient content, and pH. Furthermore, in greenhouse-type operations, the light, temperature, humidity, and composition of the air can be manipulated ¹⁵. Therefore, it is possible to practice continuous production throughout the year in the controlled environment along the growing season ²¹.

Looking into the future, the amount of anthropogenic Nr input to the agroecosystems is expected to grow, with global food demand anticipated to increase 60% by 2050 from 2005 levels ²². Towards raising the Nr usage efficiency in fertilization, implementing controllable hydroponics can be one sustainable alternative to feed the world's growing population.

1.3 Nitrogen cascade

Nr can move along its biogeochemical pathway from one environmental system (e.g., terrestrial ecosystems, atmosphere, freshwater, and marine systems) to another ⁷. The sequential transfer of Nr through environmental systems is called the nitrogen cascade ²³.

The artificial nitrogen fixation via the Haber-Bosch process is primarily used to produce fertilizers. However, about half of Nr-fertilizers (e.g., ammonia, urea, and nitrates) applied to the global crop production is directly transferred to the atmosphere as NH_3 , N_2O , NO_x , or N_2 , or to the hydrosphere primarily as NO_3^- , or lost to the environment ^{7, 12}.

Furthermore, a final fertilizer-to-consumer efficiency of 11–22% N is achieved globally in the food supply chain^{12,24}. The massive loss of valuable nitrogen resources (i.e., 78-89%) represents the Nr pollution. The more Nr added to the crop agroecosystems, the more Nr is transferred to other systems along the N cascade. In general, agriculture contributes to approximately 95% of NH₃, 63% of N₂O, and 3% of NO_x emissions to the atmosphere, and 59% of Nr (primarily NO₃⁻) to the hydrosphere⁸. Besides, the domestic wastewater in some local areas is discharged directly after septic tank treatment (e.g., Flanders in Belgium with around 27% of Nr), making the domestic wastewater a nonnegligible point-source of Nr pollution to local water bodies. Altogether, the Nr cascade slowly erodes the Earth subsystem's resilience, making Nr one of the most critical pollution issues of the 21st century^{6,8}.

The UNEP 2014 Year Book emphasized the alarming consequence of excess Nr in the environment²⁵. The magnitude and complexity of the nitrogen cascade impede progress towards planetary sustainable development because the Nr pollution ranges from local (soil and water quality) and regional (air quality and biodiversity loss) to global scales (climate change and stratospheric ozone depletion)^{6,26}. In economic terms, to reduce the risk of Nr pollution, the global economy of €285-2850 billion is invested annually²⁷. As anthropogenic activities continue to pump out Nr pollution, it is essential to intervene the nitrogen cascade and make humanity return to the planetary nitrogen boundary over the coming century.

2. Nitrogen management in waste streams

There are two major categories of nitrogen emissions: non-point-source (NPS) and point source. The term "point source" means any discernible, confined, and discrete conveyance, including but not limited to any pipe, ditch, channel, tunnel, conduit, well, discrete fissure, container, rolling stock, concentrated animal feeding operation, or vessel or other floating craft, from which pollutants are or may be discharged²⁸. This term does not include agricultural stormwater discharges and return flows from irrigated agriculture. In contrast, the term "nonpoint source" is defined to mean any source of water pollution that does not meet the legal definition of "point source".

The NPS pollution generally results from land runoff, precipitation, atmospheric deposition, drainage, seepage, or hydrologic modification. Unlike industrial and sewage treatment plants, NPS pollution comes from many diffuse sources, making remediation efforts extremely complex and challenging²⁹. As mentioned in section 1.3 (**Chapter 1**), one of the major agricultural NPS pollutions is the excess fertilizer use on farmlands. Switching to the controlled hydroponic system could alleviate this type of NPS pollution due to its high nutrient-using efficiency and feasibility on waste solution collection²⁰.

In this thesis, only the point-source Nr waste streams were studied, because they are more easily identifiable and collectible to be managed. There are two approaches to manage the point-source Nr in the nitrogen cycle: (i) "Nr recovery (conversion)"— substituting a portion of new Nr production, (ii) "Nr removal"— converting Nr back to N_2 following Nr synthesis, namely 'recycling over the atmosphere' (Figure 1.2).

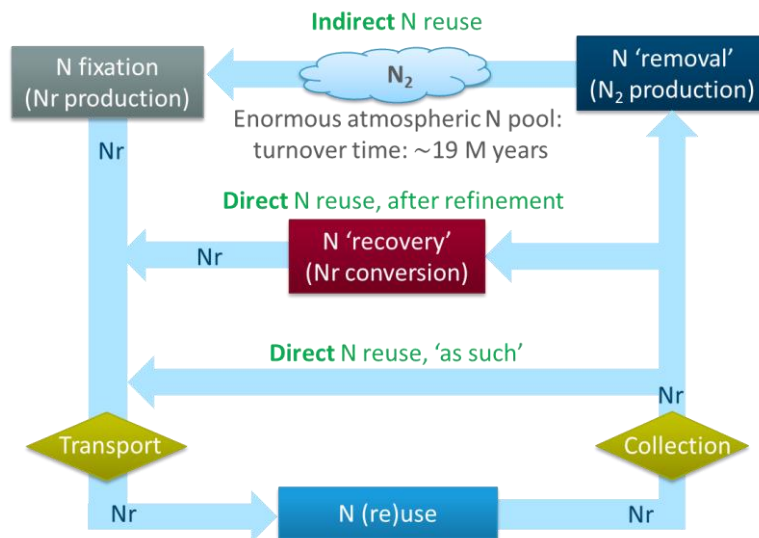


Figure 1.2: Waste streams: recycling routes for reactive nitrogen (Nr) species.

3. Nitrogen recovery

3.1 Collected and collectible waste streams containing Nr

Nitrogen recovery should be regarded as a solution to many current Nr pollution issues. The Circular Economy Package adopted by the European Union (EU) in 2015 aims to maximize resource-using efficiency in all the value chain steps, including production,

waste management, and recycling of secondary raw materials³⁰. The plan confirms the management and trade of waste-based fertilizers as key to recovering and recycling bio-nutrients, such as nitrogen and phosphorus, back in the EU's economy.

3.1.1 Inorganic Nr waste streams

The anthropogenic fixation of N₂ from the atmosphere is deemed a giant 'valve' that controls a massive flow of new Nr into the Earth. Inorganic Nr in waste streams exists mainly in the form of ammonia, nitrite, and nitrate. Ammonia is a primary inorganic Nr form; its separation from water is relatively easy based on its volatility and/or electrical mobility³¹. The collected and collectible ammonia exists in many different waste streams, mainly classified into three types (industrial, agricultural, and domestic) (Table 1.1). Most of the studies focused on ammonia from agriculture and domestic source.

On a global basis, 33 million tons Nr yr⁻¹ of grain is fed to animals, while around 85% of Nr is lost as manure and waste^{13, 32}. In the agricultural source, the anaerobically digested and undigested animal (e.g., pig and cattle) manures are the primary ammonia source, containing up to 5140 mg N L⁻¹. In the domestic source, the digestate of food waste³³, landfill leachate³⁴, and municipal sidestream sludge³⁵, raw domestic wastewater^{36, 37}, and hydrolyzed urine³⁸⁻⁴³ were covered. In many wastewater treatment plants (WWTPs), anaerobic digestion of municipal sludge is implemented to produce biogas and increase the dewaterability of the sludge. Digestate is the leftover of the anaerobic digestion, and reject water from digestate is the liquid phase left after the dewatering of anaerobically digested sludge⁴⁴. Reject water can contribute up to 30% of nitrogen load through recycling in the nitrogen treatment process⁴⁵. Compared to the reject water, human urine is not derived from the WWTPs. As the dominant Nr in urine, urea can be readily hydrolyzed to ammonia by the urease enzyme⁴⁶. Moreover, urine contributes 75–80% of the total nitrogen load in a WWTP, but only 1% of the total flow, making it a very concentrated stream for nitrogen recovery as well⁴⁷. Overall, except for the domestic wastewater, other waste streams, like anaerobically digested animal manures, hold ammonia in concentrations of several grams of nitrogen per liter, which are the most attractive for nitrogen recovery.

Table 1.1: Characteristics of collected and collectible waste streams containing $\text{NH}_4^+\text{-N}$, recovery technique, and results. N.A. represents data not available. TLR represents technology readiness levels ⁴⁸. Nr recovery (%) means the recovered mass of nitrogen divided by the total influent nitrogen mass.

| Source | Form | $\text{NH}_4^+\text{-N}$ (mg L^{-1}) | COD/ $\text{NH}_4^+\text{-N}$ ratio | Technique | Nr recovery (%) | Form of recovered Nr | Reference |
|-------------|--|--|---|--|--------------------|------------------------------|-----------|
| Industry | Ion exchange regeneration wastewater | 167 | 0.7 | Vacuum membrane distillation (TLR 3) | 100 | NH_4OH | 49 |
| | Anaerobic digestate of piggery wastewater | 1727 | | Struvite precipitation (TLR 5) | 100 | Struvite | 50 |
| Agriculture | Anaerobically digested & undigested cattle manure | 600-1100 | N.A. | Thermal stripping/ acid absorption (TLR 4) | 100 | | 51 |
| | Dairy manure digestate | 1620 | | Vacuum thermal stripping/acid absorption (TLR 7) | 100 | $(\text{NH}_4)_2\text{SO}_4$ | 33 |
| | Anaerobically digested swine wastewater | 1465-2097 | 0.7-1.4 | Gas permeable membrane (TLR 4) | 76-98 | | 52 |

Chapter 1

| | | | | | | | |
|-----------------|-------------------------------------|-----------|------|--|-------|---|----|
| Domestic | Food waste digestate | 1804-6400 | | | | | |
| | Retentate of landfill leachate | 5673-5760 | N.A. | Vacuum thermal stripping/acid absorption (TLR 6) | 100 | | 33 |
| | Municipal sludge digestate | 1093 | | | | | |
| | Reject water of sidestream at WWTPs | 1000 | 1.2 | Microbial electrolysis cell (MEC, TLR 3) | 100 | NH ₄ Cl | 35 |
| | Zeolite regeneration solution | 2400 | N.A. | Hollow fiber liquid-liquid membrane contactors (TLR 3) | 95-98 | NH ₄ NO ₃ & (NH ₄) ₂ HPO ₄ | 53 |
| | Landfill leachate | 4540 | 2.0 | MEC/ forward osmosis (FO, TLR 3) | 54 | (NH ₄) ₂ CO ₃ & (NH ₄) ₂ SO ₄ | 34 |
| | Raw domestic wastewater | 47 | 9.8 | Microbial electrolysis cell (TLR 3) | 62 | | 36 |
| | Hydrolyzed urine | 5490 | N.A. | Electrochemical cell/ stripping (TLR 3) | 68-87 | Struvite | 54 |

3.1.2 Organic Nr waste streams

Organic wastes containing significant amounts of organic carbon (C) and Nr can be categorized into agriculture, agro-food industry, and domestically sourced waste streams (Table 1.2 and 1.3).

The agricultural wastes rich in organic Nr chiefly take the form of crop residues (e.g., residual stalks, straw, leaves, roots, husks, shells) and raw animal wastes (e.g., manure)⁵⁵. For example, the vegetative parts of maize and soybean meal hold Nr of 6% and 7%, respectively (Table 1.2)^{56,57}. The chicken manure and pig slurry can contain 2.9% and 3.7% Nr, respectively^{56,58}. Besides, the organic carbon to Nr (C/Nr) ratio of crop residues is higher than animal waste.

The agro-food industry is divided into the food industry and the beverage industry⁵⁹. The food industry includes: the meat industry; fish, shellfish, and mollusk industry; dairy industry; manufacture of animal and vegetable oils and fats; fruit and vegetable industry; the making of grain, starches, and starchy products; animal feed production; and the preparation of sundry food products. The beverage industry includes the wine industry; the sundry alcoholic drinks industry; and the non-alcoholic drinks industry. The residues, by-products, and effluents are the agro-food industry waste rich in organic Nr. For example, the beet vinasse contains 2.0% to 3.0% of Nr with a C/Nr ratio of 6.0 (Table 1.2)⁶⁰. The horn and hoof of animal waste can hold 17% of Nr with a C/Nr ratio of 3.0⁶¹. Besides solid organic waste, the wastewater of the agro-food industry can contain organic Nr up to hundreds to thousands of milligrams per liter, such as distillery and sugar refinery wastewater (Table 1.3)⁶².

The domestic waste streams rich in organic Nr mainly include household waste, (unhydrolyzed) human urine, and (undigested) sewage sludge. Household is the most important source of food waste (53%)⁶³. Most kitchen waste has an Nr fraction of 1.1% to 5.4% and a C/Nr ratio between 8.9 and 35.1. Urine is a widely available, relatively concentrated source of Nr. The major proportion of Nr in fresh human urine is urea ($\text{CO}(\text{NH}_2)_2$), accounting for 88% to 99% of total Nr (TNr), with a relatively low organic C to organic Nr ratio (0.2-1.5)⁶⁴. Recently, source-separated urine has gained great interest

Table 1.2: Characteristics of collected and collectible solid waste streams containing organic Nr. C/Nr ratio means organic carbon to organic Nr ratio. N.A. represents data not available.

| Source | Waste | Dry matter (DM)% | Nr% (DM basis) | C/Nr ratio | Reference |
|---------------------------|---|------------------|----------------|------------|-----------|
| Agriculture | Wheat straw | 89.1 | 0.3 | 198.4 | 61 |
| | Alfalfa | N.A. | 2.3 | 20.0 | 56 |
| | Maize (vegetative parts) | N.A. | 6.0 | 80 | 56 |
| | Soybean meal | N.A. | 7.0 | 6.1 | 57 |
| | Cattle manure | N.A. | 1.65-2.9 | 16-29 | 56, 65 |
| | Pig slurry | N.A. | 3.7 | 11 | 56 |
| | Chicken manure | 21.8 | 2.9 | 7.5 | 58 |
| Agro-food industry | Sugar filter cake | 90.0 | 1.8 | 14.0 | 66 |
| | Beet vinasse | N.A. | 2.0-3.0 | 6.0 | 60 |
| | Grape marc | N.A. | 1.1-1.8 | 37.5 | 60 |
| | Horn and hoof | 84 | 17.0 | 3.0 | 61 |
| Domestic | Kitchen waste | 10-40 | 1.1-5.4 | 8.9-35.1 | 63 |
| | Mixed sewage sludge (primary and secondary) | N.A. | 7-12 | 4-7 | 67 |

Table 1.3: Composition of liquid waste streams from typical agro-food industry⁶² and domestic source⁶⁴. C/Nr ratio means organic carbon to Nr ratio. N.A. represents data not available. * The wide range is because of the calcareous soil particles in some scenarios.

| Source | Raw materials used for the production | Wastewater | | | | | |
|---------------------------|--|---|--|-------------------------------------|-----------------------------|------------|-----------|
| | | Suspended matter (mg L ⁻¹) | NH ₄ ⁺ -N (mg L ⁻¹) | Organic Nr (mg L ⁻¹) | Organic Nr % (TNr basis) | C/Nr ratio | |
| Agro- food industry | Sugar beet, molasses | 1100-11200* | 0-20 | 130-1250 | 87-100 | 11.5-16.9 | |
| | Distillery | Wheat | 1700 | 10 | 180 | 95 | 11.3 |
| | | Fruit | 11000 | 20 | 260 | 93 | 24.9 |
| | Sugar refinery | Sugar beet | 4100-362900* | 0-50 | 50-1040 | 75-100 | 10.6-46.8 |
| | Cannery | Vegetables | 1800-3800 | 160-180 | 150-290 | 48-62 | 6.2-6.7 |
| | Starch factory | Potato | 14500-16100 | 120-190 | 480-530 | 72-82 | 11.0-12.4 |
| | Winery | Grapes | 1500-6400 | 0-30 | 80-340 | 92-100 | 81.1-70.1 |
| Domestic | Fresh urine | Daily diet | N.A. | 125-600 | 4343-10881 | 88-99 | 0.2-1.5 |

as a valuable resource of nutrients, given its relatively high macronutrient concentration ($\sim 9 \text{ g N L}^{-1}$, 0.7 g P L^{-1} , and 2 g K L^{-1})⁶⁸. In the municipal wastewater treatment process, around 20% of N removal is assimilated in activated sludge¹², making the sewage sludge contain 7-12% of N_r with a C/N_r ratio of 4-7⁶⁷.

3.2 Recovery technologies

The recovery of nitrogen from the N_r-rich waste stream is expected to reduce or substitute the need for synthetic nitrogen fertilizers, the production of which is energy-intensive and fossil fuel-dependent^{12,69}. Meanwhile, this will further help to reduce the N_r cascade in the environment. Furthermore, the recovery of nitrogen to produce value-added and marketable products imply a significant economic opportunity towards a "nitrogen circular economy".

3.2.1 Inorganic N_r recovery

The anaerobic (co-) digestion of activated sludge or manure, and hydrolyzed urine results in ammonium release. The ammonium-rich liquid allows for ammonia recovery. According to the volatility and/or electrical mobility³¹, various methods have been reported to recover ammonia from waste streams (Table 1.1). The prevailing process can categorize ammonia recovery techniques as chemical, physical, biological, or combined (hybrid) processes.

The struvite precipitation with phosphate and magnesium is used as a common chemical technique^{50,70}. Struvite (i.e., magnesium ammonium phosphate) is a relatively insoluble crystalline precipitate that contains an approximately equimolar ratio of magnesium, phosphate, and ammonium ions. Its formation requires a tight pH range (i.e., 7-9) for optimal efficiency due to the potential volatilization of NH₃ at pH > 9.8^{71,72}.

Physical processes explored for ammonia recovery include membrane processes, stripping, and adsorption. Membrane processes are proven effective to strip ammonia from ammonium wastewaters, including membrane contactors⁵³, gas-permeable membrane⁷³⁻⁷⁵, and membrane distillation⁴⁹. The stripping process includes air⁷⁶, vacuum⁵¹, and thermal stripping³³ techniques. Sludge and manure are challenging to

recover by any technology other than stripping because the solid concentration tends to interfere with those techniques, especially those involving membranes. For the NH_3 emission capture, acid adsorption (e.g., sulfuric acid) has proved effective in converting NH_3 into non-volatile NH_4^+ salt fertilizer (e.g., ammonium sulfate). Alternatively, zeolite is a porous, naturally occurring mineral with preferential and reversible ammonium adsorption due to its high cation exchange capacity and selectivity⁵³.

Bio-electrochemical systems (BES) utilize electrochemically active microorganisms to catalyze reactions at either the anode or cathode of a cell to convert chemical energy to electrical energy (or vice versa)^{44, 77}. During electricity generation, NH_4^+ is transported from the anode to the cathode to maintain charge neutrality⁷⁸. The high pH of the catholyte due to reduction reactions converts NH_4^+ to NH_3 ⁷⁹. Various BES including microbial fuel cells (MFCs) and microbial electrolysis cells (MECs) have been studied to achieve ammonia recovery^{35, 36}. Compared to BESs, in electrochemical systems, all reactions are purely electrochemical, and no microorganisms are involved^{39, 40, 54}.

Overall, wastewater rich in NH_4^+ is a target stream for recovery by the aforementioned technologies, which can be a catch-all term for industrial wastewater, food waste, landfill leachate, etc. Finally, the recovered ammonia can be a potential nutrient for food production as fertilizers.

3.2.2 Organic Nr recovery

3.2.2.1 General recovery strategies

The streams rich in organic Nr (e.g., proteins and urea) should be more appropriately regarded as secondary raw materials, which can be inexpensive and relatively abundant feedstocks. Proper (e.g., physical and biological) treatments can make them into many value-added organic fertilizers.

The most common and basic technology to recover organic fertilizers is physical drying and pelletizing, applicable to most solid-based waste streams rich in organic Nr. Based on this technology, various commercial solid-based organic fertilizers are available, such as Alfalfa meal (2%-4% Nr), soybean meal (7% Nr), pelleted chicken manure (2%-4% Nr),

horn and hoof meal (17% Nr), vinasse based organic fertilizers (5%-7% Nr)^{61, 80, 81}. As the national legislation does not permit the direct application of municipal sewage sludge on arable land, indirect Nr recovery via coupling anaerobic digestion (for ammonium release) with inorganic Nr recovery technologies mentioned in section 2.2.1 can be an alternative strategy¹².

Composting is a reliable recovery technology of organic waste materials (e.g., green wastes, animal manures)⁸². Composting is a biological process that occurs under aerobic conditions, with adequate moisture (45-60%) and temperature (45-55°C), hygienically transforming organic wastes into a homogeneous and plant-available material (i.e., humus-like produce)⁸³. Compost is typically 1% to 2% N on a dry weight basis, less concentrated than commercial organic nitrogen fertilizers mentioned above⁸⁰. Compared to the conventional composting processes, vermicomposting is increasingly seen as a better viable eco-friendly technology. The vermicomposting process results in a better quality homogenous product with reduced mass, shorter process time, high humus content, reduced phytotoxicity, and more excellent fertilizer value in the microbiologically active manure, i.e., vermicompost^{84, 85}.

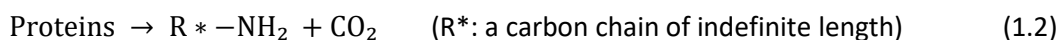
Recently, microbial protein production from agro-food industry wastewater has attracted broad interest. Effluents from potato processing and beer brewery are considered ideal grow media due to their relatively high carbon and nitrogen concentration (Table 1.3) but low contamination with pathogens and other harmful pollutants (e.g., heavy metals)^{86, 87}. The microbial biomass is ideally produced in high-rate systems (i.e., maximum production, high N content) at a short sludge retention time (SRT) to assimilate high nutrients levels, after which it is harvested and dried (down to around 10% moisture content)⁸⁸. It was found that SRT strongly influenced the N (protein) content, i.e., the shorter SRT, the higher the protein content⁸⁹. Spiller et al. (2020) explicitly described the processes and mass balances used to produce three metabolic types of microbial protein on potato wastewater, namely, a consortium of aerobic bacteria (CAB, or a 7% Nr), microalga (Spirulina, 8.6% Nr), and Purple Non-Sulfur Bacteria (PNSB, 8.5% Nr)⁹⁰. The high Nr content in those types of dried microbial biomass has

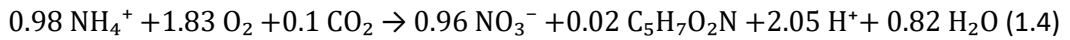
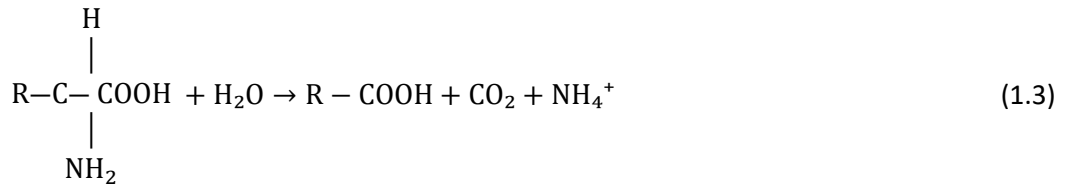
driven them into an emerging class of organic fertilizers — microbial fertilizers (MFs). The MFs can be applied to the soil or growing medium, where the microbiome mineralizes MFs into NO_3^- -N for plant growth^{88, 91}.

3.2.2.2 Application of organic fertilizers

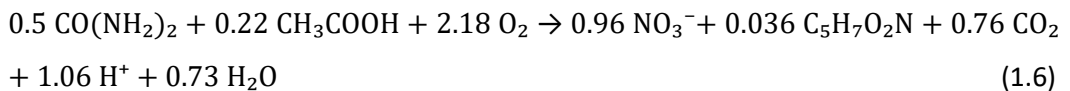
As we know, the recovered organic fertilizers, either in solid or liquid form, occur predominantly in the amino form (NH_2), which are applicable in soil-based cultivation. In contrast, only the liquid nutrient solutions are suitable for fertigation and hydroponic cultivation¹⁴. Unlike soil-based cultivation, there are no abundant microorganisms in hydroponic systems and thus limited biological conversion capacity to produce inorganic Nr (i.e., NH_4^+ -N and NO_3^- -N)^{15, 92, 93}. The plants in hydroponic systems require the preferable NO_3^- -N directly for their favorable growth⁹⁴. Considering the benefits of greenhouse hydroponic cultivation aforementioned in section 1.2, applying the recovered organic fertilizers into hydroponics can significantly promote the "nitrogen circular economy" development. Therefore, to upgrade those organic Nr fertilizers to the high-end nutrient (i.e., NO_3^- -N) for crops, biological conversion of organic nutrients (nitrogen mineralization and nitrification) is essential⁹⁵.

In the nitrogen mineralization process, microorganisms convert organic nitrogen (e.g., proteins) to inorganic form (i.e., ammonium) through hydrolysis (or aminization) and ammonification^{96, 97}. Hydrolysis (or aminization) is the first step of mineralization in which microorganisms break down complex proteins into simpler amino acids, amides, and amines (Reaction 1.2). Ammonification is the second step of mineralization. Ammonification refers to any chemical reaction (or hydrolysis reaction) in which NH_2 groups are converted into ammonia (NH_3) or ammonium (NH_4^+) as an end product (Reaction 1.3). During the nitrification process, NH_3 or NH_4^+ are oxidized to nitrite (NO_2^-) and then nitrate (NO_3^-) (Reaction 1.4).





Notably, the conversion of urea ($\text{CO}(\text{NH}_2)_2$) in the animal and human urine to NH_4^+ (Reaction 1.5) is an ammonification process, which is commonly called “urea hydrolysis”⁴⁶. The COD/N ratio of urine (i.e., around 1 g COD/g N) is equivalent to 0.22 mol acetic acid/mol N. Therefore, during the urine nitrification process, approximately 2.49 g CO_2 can be released when 1g NO_3^- -N is produced (Reaction 1.6).



Since organic carbon is one of the main constituents of organic fertilizers (Table 1.2 and 1.3), its mineralization occurs concomitantly with nitrogen mineralization^{82, 98}. During carbon mineralization, microorganisms (e.g., bacteria, archaea, and fungi) metabolize and release gaseous end products of heterotrophic respiration, i.e., CO_2 under aerobic conditions and CO_2 and CH_4 under anaerobic conditions. CO_2 is an essential component of photosynthesis, using light energy to convert CO_2 and water into sugars in green plants. It is well known that CO_2 supplementation within the greenhouse environment could remarkably improve plant growth and production⁹⁹. Except for burning carbon-based fuels such as natural gas, propane, kerosene, or directly from tanks of pure CO_2 , the CO_2 recovery during the mineralization of organic fertilizers can add extra value for nitrogen recovery.

4. Nitrogen removal

Anthropogenic activities have been intensifying the Nr cascade, eroding the resilience of the Earth subsystems, and making Nr a key pollutant to tackle from local to global scales¹⁰⁰. For this reason, the other choice for Nr intervention is to immediately convert

Nr to N_2 before it is distributed to the environment.

4.1 Nitrogen and carbon removal processes

The municipal wastewater treatment plants receive domestic and industrial wastewater, also rain and groundwater infiltrating into the sewer network¹². Most Nr in sewage is in reduced form as NH_4^+ -N and/or larger organic molecules (e.g., urea, amino acid, and protein). The Nr removal pathways generally start with NH_4^+ , which is released from the hydrolysis of larger organic molecules¹⁰¹. Biological wastewater treatment is carried out by microbial conversion processes. The following section will elaborate on those typical nitrogen transformations involved in the nitrogen cycle (Figure 1.3). With nitrogen treatment processes, organic carbon is oxidized to CO_2 in aerobic conditions (3.1.4) or anoxic conditions by denitrification (3.1.2).

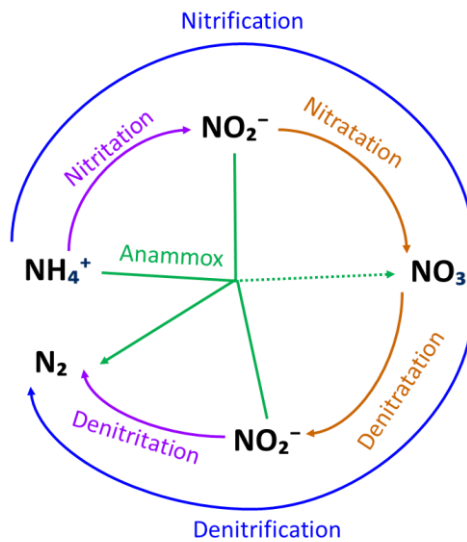


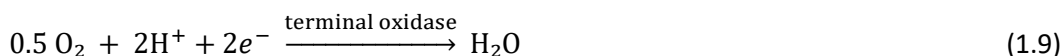
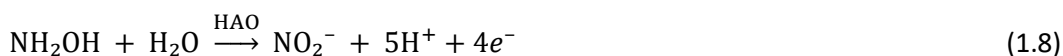
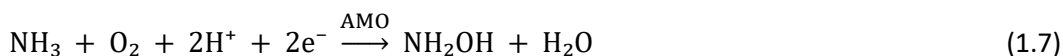
Figure 1.3: Typical nitrogen transformations in the nitrogen cycle regarding wastewater treatment.

4.1.1 Nitrification

Classical nitrification is a two-step process, where ammonia-oxidizing bacteria and archaea oxidize ammonia to nitrite (i.e., nitritation) and then nitrite-oxidizing bacteria convert to nitrate (i.e., nitrataion). Comammox means the complete conversion of ammonia into nitrate by a single microorganism. Only the classical two-stage nitrification is studied in this work.

4.1.1.1 Nitritation

As the first step of nitrification, nitritation denotes microbially mediating oxidation of ammonium to nitrite. Nitritation is deemed as a two-step metabolic process (Reaction 1.7-1.8). Firstly, ammonia is oxidized to hydroxylamine (NH₂OH) using the membrane-bound ammonia monooxygenase (AMO) enzyme. Secondly, NH₂OH is oxidized to nitrite, catalyzed by the periplasmic enzyme hydroxylamine oxidoreductase (HAO).



The total nitritation reaction:



Nitritation process is typically catalyzed by ammonium-oxidizing bacteria (AOB) from the genus *Nitrosomonas*, and to a lesser extent ammonium oxidizing archaea (AOA) from archaeal phylum of *Thaumarchaeota*^{101, 102}. Metabolically, AOA differ from AOB as they do not contain any HAO homologue, cytochrome c, or enzymes to detoxify hydroxylamine¹⁰³. Therefore, two hypothetical mechanisms were suggested for AOA metabolization: (i) the hydroxylamine produced by AMO, is oxidized to nitrite via a periplasmic multicopper oxidase (MCO) protein; (ii) AMO does not produce hydroxylamine but nitroxyl (HNO), which is subsequently oxidized via an MCO protein^{104, 105}.

Although ammonia (NH₃) is the actual substrate for AOB and AOA, it is in equilibrium with ammonium (NH₄⁺), a term commonly used to refer to AOB and AOA activity, as is done in this thesis. As autotrophic microorganisms, the central anabolic process in AOB and AOA is CO₂ fixation using the energy extracted from NH₄⁺ oxidation.

4.1.1.2 Nitratation

As the second step of nitrification, nitratation means oxidizing nitrite to nitrate by

autotrophic nitrite-oxidizing bacteria (NOB). The enzyme nitrite oxidoreductase (NXR) transfers the two produced electrons to a terminal oxidase for respiratory purposes (Reaction 1.11). Most of the NOB belong to the genera of *Nitrobacter*, *Nitrococcus*, and *Nitrotoga* (phylum *Proteobacteria*), the genus *Nitrospira* (phylum *Nitrospirae*), and the genus *Nitrospina* (phylum *Nitrospinae*)¹⁰⁶.

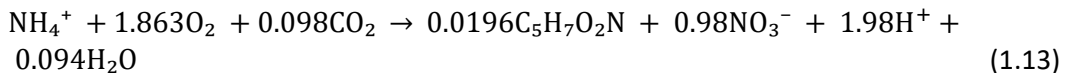


Combined with Reaction 1.9, the total nitrataion reaction:



4.1.1.3 Nitrification = nitritation + nitratation

In the complete nitrification stoichiometry (Reaction 1.13), 4.26 g of oxygen is consumed per gram of N, and 0.16 g of cells are produced¹⁰⁷. Besides dissolved oxygen (DO), nitrification also requires sufficient alkalinity of 7.14 g CaCO₃ g⁻¹ N¹⁰⁸.

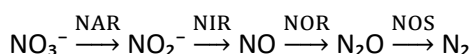


Several environmental factors can influence the nitrification process: pH, DO concentration, temperature, free ammonia (FA), and free nitrous acid (FNA). In general, the nitrification process in wastewater treatment plants is controlled between pH 7.0-7.2, although the optimum pH for nitrification ranges between 8 and 9¹⁰⁹. It was reported that outside the range of pH 7.0 to 9.8, less than 50% of the optimum nitrification rate occurs, and between pH 5 and 5.5, nitrification could even cease¹¹⁰. DO level above 2.0 mg L⁻¹ is recommended for nitrification¹¹¹. In natural habitats, nitrification occurs at a wide temperature range from mesophilic (5-35°C) to thermophilic (>45°C) but is typically limited to mesophilic conditions¹¹². The specific growth rate of nitrifiers showed an exponential increase between 5 and 30°C. The high concentration of FA and FNA, rather than total ammonia or nitrite ion, can inhibit the nitrification. In general, the tolerance of AOB on FA and FNA is stronger than NOB. The concentration ranges of FA that begin to inhibit the nitrifying organisms are 10 to 150 mg N L⁻¹ (*Nitrosomonas*, AOB) and 0.1 to 1.0 mg N L⁻¹ (*Nitrobacter*, NOB)¹¹³. The concentration ranges of FNA that initiate to inhibit

the nitrifying organisms are 0.22 to 2.8 mg N L⁻¹ (AOB) and 0.06 to 0.83 mg L⁻¹ (NOB) ¹¹⁴.

4.1.2 Denitrification

Denitrification is an anoxic respiration process in which nitrate is eventually reduced to nitrogen gas. The relevant enzymes are nitrate reductase (NAR), nitrite reductase (NIR), nitric oxide reductase (NOR), and nitrous oxide reductase (NOS) ¹¹⁵.



The denitrification rate is affected by pH and might be inhibited at values lower than 6.8 ¹¹⁶. Optimal pH conditions range from 6.8 to 8.2 ¹¹⁷, and the optimal temperature is about 35°C ¹¹⁸. Denitrification can be performed both heterotrophically and autotrophically (Table 1.4).

Table 1.4: Stoichiometries of typical denitrification reactions ¹¹⁹⁻¹²².

| Electron donor | Stoichiometric equation |
|-------------------------|--|
| Methanol | $1.08\text{CH}_3\text{OH} + \text{NO}_3^- + 0.24\text{H}_2\text{CO}_3 \rightarrow 0.056\text{C}_5\text{H}_7\text{O}_2\text{N} + 0.47\text{N}_2 + 1.68\text{H}_2\text{O} + \text{HCO}_3^-$ |
| Ethanol | $0.69\text{C}_2\text{H}_5\text{OH} + \text{NO}_3^- + \text{H}^+ \rightarrow 0.14\text{C}_5\text{H}_7\text{O}_2\text{N} + 0.43\text{N}_2 + 2.07\text{H}_2\text{O} + 0.67\text{CO}_2$ |
| Acetate | $0.846\text{CH}_3\text{COO}^- + \text{NO}_3^- \rightarrow 0.077\text{C}_5\text{H}_7\text{O}_2\text{N} + 0.462\text{N}_2 + 0.077\text{H}_2\text{O} + 1.308\text{CO}_2 + 1.846\text{OH}^-$ |
| Glucose | $\text{C}_6\text{H}_{12}\text{O}_6 + 2.8\text{NO}_3^- + 0.5\text{NH}_4^+ + 2.3\text{H}^+ \rightarrow 0.5\text{C}_5\text{H}_7\text{O}_2\text{N} + 1.4\text{N}_2 + 6.4\text{H}_2\text{O} + 3.5\text{CO}_2$ |
| Hydrogen sulfide | $0.421\text{H}_2\text{S} + 0.421\text{HS}^- + \text{NO}_3^- + 0.346\text{CO}_2 + 0.086\text{HCO}_3^- + 0.086\text{NH}_4^+ \rightarrow 0.086\text{C}_5\text{H}_7\text{O}_2\text{N} + 0.5\text{N}_2 + 0.842\text{SO}_4^{2-} + 0.434\text{H}_2\text{O} + 0.262\text{H}^+$ |
| Sulfur | $1.11\text{S}^0 + 1.06\text{NO}_3^- + 0.785\text{H}_2\text{O} + 0.3\text{CO}_2 \rightarrow 0.06\text{C}_5\text{H}_7\text{O}_2\text{N} + 0.5\text{N}_2 + 1.11\text{SO}_4^{2-} + 1.16\text{H}^+$ |
| Thiosulfate | $0.84\text{S}_2\text{O}_3^{2-} + \text{NO}_3^- + 0.43\text{H}_2\text{O} + 0.35\text{CO}_2 + 0.87\text{HCO}_3^- + 0.087\text{NH}_4^+ \rightarrow 0.087\text{C}_5\text{H}_7\text{O}_2\text{N} + 0.5\text{N}_2 + 1.69\text{SO}_4^{2-} + 0.7\text{H}^+$ |
| Hydrogen | $3.03\text{H}_2 + \text{NO}_3^- + \text{H}^+ + 0.23\text{CO}_2 \rightarrow 0.05\text{C}_5\text{H}_7\text{O}_2\text{N} + 0.48\text{N}_2 + 3.37\text{H}_2\text{O}$ |

Heterotrophic denitrification is a process that uses various organic carbon compounds as energy and electron sources. Stoichiometrically, 2.86g BOD is sufficient to reduce 1g nitrate (i.e., 2.86g O₂ g⁻¹ NO₃⁻-N) ¹²³. It is mediated by many bacterial genera, including *Pseudomonas*, *Paracoccus*, *Flavobacterium*, *Alcaligenes*, and *Bacillus spp* ^{120, 124}. Wastewater from the agro-food industry commonly contains significant amounts of organic carbon, favoring heterotrophic denitrification. However, for carbon-lean

wastewaters in industrial plants, such as mineral processing, electroplating, and power plants, additional carbon sources like methanol, acetate, and ethanol are required ¹²⁰.

Alternatively, autotrophic denitrification processes need inorganic electron donors such as sulfur and hydrogen gas. The elemental sulfur (S°) and inorganic sulfur compounds, including sulfide (S_2^-), thiosulfate ($S_2O_3^{2-}$), tetrathionate ($S_4O_6^{2-}$), and sulfite (SO_3^{2-}) were studied. Elemental sulfur (S°) was studied most extensively due to its low price and ease of handling ^{120, 125}. Sulfur-driven denitrification is known to be carried out typically by *Thiobacillus denitrificans* and *Sulfurimonas denitrificans* ^{126, 127}. Hydrogen is also a promising electron donor for autotrophic denitrification because of its high selectivity for nitrate removal and the lack of a harmful by-product (only N_2 and H_2O). Most of the hydrogen-driven denitrifiers belong to *Rhodopseudomonas sphaeroides*, *Paracoccus denitrificans*, *Alcaligenes eutrophus*, and *Pseudomonas pseudoflava* ¹²⁸.

In the absence of electron donors in the wastewater, autotrophic denitrification is considered superior to heterotrophic denitrification because of avoiding external carbon sources and lower sludge-handling costs ^{120, 129}. Autotrophic denitrification is characterized by lower sludge yields of $0.4\text{--}0.57\text{ g VSS g}^{-1}\text{ N}$ ^{120, 130} compared to heterotrophic denitrification ($0.8\text{--}1.2\text{ g VSS g}^{-1}\text{ N}$) ¹³¹. In addition, since the price of sulfur and hydrogen gas is much lower than the cost of carbon sources such as methanol, ethanol, and acetate, the operational cost of the denitrification process could be reduced (Table 1.5).

Table 1.5: Estimated costs of electron donors (i.e., substrates) for denitrification ¹²⁰.

| Electron donor | Price of substrate (€/kg) | Consumption of substrate ($\text{kg kg}^{-1}\text{ NO}_3^-$) | Substrate cost of denitrification ($\text{€ kg}^{-1}\text{ NO}_3^-$) | Nitrate removal rate ($\text{g N m}^{-3}\text{ day}^{-1}$) |
|----------------|---------------------------|--|--|--|
| Methanol | 0.78 | 2.08-3.98 | 1.52-3.03 | 1000-27000 |
| Ethanol | 0.93 | 2 | 1.85 | 400-1200 |
| Acetate | 1.41 | 2.7 | 3.68 | 600-1000 |
| Sulfur | 0.08 | 2.5 | 0.21 | 50-560 |
| Hydrogen | 1.85-2.61 | 0.43 | 0.8-1.1 | 500-2400 |

4.1.2.1 Denitrataion

Nitrate reduction to nitrite is termed denitrataion [122], although it was called "partial denitrification" in some studies. Several strategies have been investigated to achieve denitrataion.

Denitrifying communities usually contain bacteria with different nitrate and nitrite reductase activities. Some denitrifiers can only reduce nitrate to nitrite as the only product; some can only reduce nitrite to nitrogen gas; others can reduce nitrate and nitrite to nitrogen gas¹³². Thus, denitrifying communities that can only reduce nitrate to nitrite were selected to achieve denitrataion¹³³. Otherwise, denitrataion would rely on the maintained discrepancy of nitrate reductase activities upstream and nitrite reductase downstream¹³⁴. Several crucial factors for heterotrophic denitrataion were proposed, including types of carbon source, the ratio of chemical oxygen demand and nitrate (COD/NO₃⁻-N), and pH value. Among the well-investigated carbon sources, including sludge fermentation liquid, methanol, acetate, ethanol, and glucose, acetate is considered the most easily biodegradable carbon source to maintain a high nitrite accumulation efficiency of 90%¹³⁵⁻¹⁴⁰. The different denitrataion performance via various carbon sources could be related to how and where electrons are donated¹⁴¹. Nitrate reductase accepts electrons transferred through ubiquinone or cytochrome b in the upstream region of electron transfer chain. In contrast, nitrite reductase accepts electrons from cytochrome c in a more downstream region. Certain carbon sources (e.g., acetate) donate electrons in the upstream regions, while other sources (e.g., methanol) donate preferentially in the downstream region¹⁴¹.

Moreover, the COD/NO₃⁻-N ratio of 2.6–3.0 is usually selected to maintain denitrataion^{140, 142, 143}. Another critical factor is pH value. In general, a higher pH condition (e.g., pH 9) is taken, which can probably inhibit copper-type nitrite reductase (nirK) compared to pH 5.0 and 7.0¹⁴⁴.

For autotrophic denitrataion, sulfur-driven denitrataion processes using the reduced sulfur compounds (S₂⁻ and SO₃²⁻) and S⁰ were studied¹⁴⁵⁻¹⁴⁸. In the SO₃²⁻-driven denitrataion process, the SO₃²⁻-S/N ratio is crucial for controlling nitrite accumulation.

Nitrate could be entirely reduced to nitrogen gas without nitrite when the S/N ratio in the influent was higher than 4.3¹⁴⁹. Therefore, it was suggested the SO_3^{2-} -S/N ratio decreased to 1.5-2.0 would be favorable to maintain the denitrataion process^{147, 148}. In the S° -driven denitrataion process, pH conditions, the preference of electron acceptors, and the attached biofilm thickness could affect the denitrataion performance. Chen et al. (2018) showed pH 8.5 could be an optimal condition for denitrataion¹⁴⁵. Wang et al. (2019) specified the maximum specific substrate utilization rate of NO_3^- -N (3.54 g N g COD⁻¹·d⁻¹) was higher than that of NO_2^- -N (1.98 g N g COD⁻¹·d⁻¹), indicating the S° more preferentially reacts with NO_3^- -N to produce NO_2^- -N¹⁵⁰. Based on the substrate counter-diffusion model in the S° -driven denitrification process, the biofilm thickness could affect bulk NO_3^- -N diffusion and reduced sulfur species, creating an opportunity for denitrataion to occur¹⁵¹.

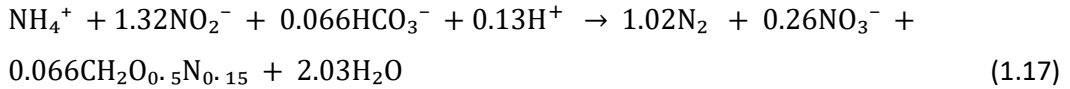
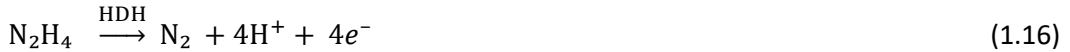
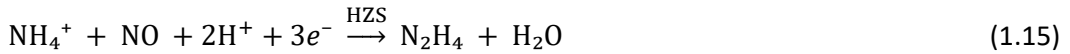
4.1.2.2 Denitritation

The reduction of nitrite to nitrogen gas is termed as denitritation¹⁵². As a shortcut in the denitrification process, denitritation initiates the reduction chain at nitrite instead of nitrate. Thus, it represents a cost-beneficial alternative for denitrification through a reduced biological sludge production of 40%, a minor carbon requirement of 40%, and the achievement of higher rates and thus smaller bioreactors (Fux and Siegrist, 2004).

4.1.3 Anammox

Anoxic ammonium oxidation (anammox) refers to anaerobically oxidize ammonium with nitrite as electron acceptor. Anammox bacteria complete this process in three steps: (i) NO_2^- is reduced to NO, catalyzed by the nitrite reductase (NIR) enzyme (Reaction 1.14); (ii) NO is combined with NH_4^+ to hydrazine (N_2H_4) by a hydrazine synthase enzyme (HZS) (Reaction 1.15)¹⁵³; (iii) N_2H_4 is oxidized by a hydrazine dehydrogenase (HDH) enzyme to N_2 gas (Reaction 1.16)¹⁵⁴. In addition, nitrite is oxidized to nitrate via an NXR enzyme during anammox anabolism, yielding extra electrons for CO_2 fixation and growth (Reaction 1.17)^{155, 156}.





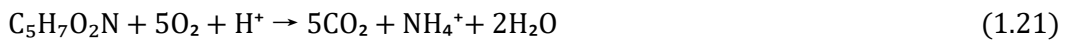
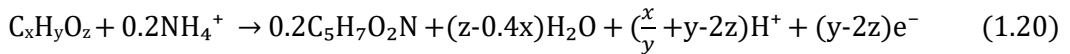
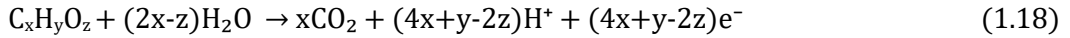
Anammox bacteria or AnAOB are exclusively affiliated with the phylum Planctomycetes, and five genera have been identified: *Brocadia*, *Kuenenia*, *Anammoxoglobus*, *Jettenia*, and *Scalindua*¹⁵⁷. The genus of *Scalindua* only thrives in marine or halophilic environments, whereas the other genera are geographically widespread in various ecosystem conditions¹⁵⁷. Anammox bacteria have an extremely slow overall growth rate with a doubling time of approximately two weeks¹⁵⁸. High FA (20-25 mg N L⁻¹) and FNA (0.5 µg L⁻¹) concentrations should be avoided to maintain the stable operation of anammox systems¹⁵⁹. A pH range of 6.5 and 9 is preferable for anammox bacteria, and an optimum pH of 8 is recommended¹⁶⁰. Nitrite concentrations above a range of 100 and 250 mg N L⁻¹ can inhibit the activity of anammox bacteria¹⁶⁰⁻¹⁶². Sufficient anoxic condition is critical to guarantee their activity¹¹⁴. Additionally, temperature also impacts the activity of anammox bacteria, and the optimum range is between 35 and 40 °C¹¹⁴.

4.1.4 Organic carbon removal

Nr waste streams usually contain organic carbon, such as proteins, amino acids, fatty acids, carbohydrates, polysaccharides, humic compounds¹⁰⁹. In the design and operation of treatment facilities and discharge legislation, organic compounds are often expressed by chemical oxygen demand (COD), indicating the amount of oxygen required to oxidize all organic matter in the wastewater and is expressed in mg O₂ L⁻¹.

Heterotrophic microorganisms use organic compounds as energy and carbon source for growth. Using a general formula for organic compounds (C_xH_yO_z), the stoichiometric reactions during organic carbon removal are represented by the following half-reactions. Firstly, C_xH_yO_z is partly oxidized to CO₂, protons, and electrons (Reaction 1.18). These electrons can use oxygen as the final electron acceptor and yield a proton motive force

to generate energy (Reaction 1.19) ¹¹⁵. Besides oxidation, part of $C_xH_yO_z$ is assimilated as biomass, usually represented by the empirical formula $C_5H_7O_2N$ (Reaction 1.20) ¹⁶³. The endogenous respiration of the cell material is shown as a simplified metabolic reaction (Reaction 1.21) ¹⁶⁴.



Besides oxygen, the aforementioned nitrate and nitrite are electron acceptors for COD removal during the denitrataion and denitritation processes. Hence, in anoxic conditions, the heterotrophic metabolism can shift from oxygen to nitrate or nitrite to remove organics. A broad range of heterotrophs can perform carbon removal. In wastewater treatment plants, *Proteobacteria* is the predominant phylum, of which *Betaproteobacteria* are the most abundant class. Following the phylum *Proteobacteria* in abundance are phylum *Bacteroidetes*, *Acidobacteria*, and *Chloroflexi* ¹¹⁵.

4.2 Processes for nitrogen (and organic carbon) removal

The separate oxidation and reduction processes to convert NH_4^+ -N to N_2 gas and COD to CO_2 can be combined in biotechnology for wastewater treatment. Typical nitrogen removal combinations start from NH_4^+ -N, including nitrification/denitrification (N/DN, section 3.2.1), nitritation/denitritation (section 3.2.2), and partial nitritation/anammox (PN/A, section 3.2.3), while denitrataion/anammox (section 3.2.4) acts on NO_3^- -N and NH_4^+ -N. Depending on the COD/N ratios in receiving water body, the COD and energy requirement will be different.

4.2.1 Nitrification/denitrification

Autotrophic nitrification and heterotrophic denitrification (N/DN) are the most commonly applied combination in wastewater treatment plants. The difference between nitrification (aerobic) and denitrification (anoxic) necessitates the implementation of

different conditions, separated in space or time, which can occur in a single-sludge or two-sludge configuration ¹¹⁵.

Separation in space can take place in two different ways, both of which create an aerobic zone for nitrification and an anoxic zone for denitrification. Firstly, space separation can be realized within the microbial flocs via simultaneous nitrification/denitrification. Secondly, space separation can occur in zones, where a baffle splits the anoxic and aerobic zone, or two individual reactors are used (2-stage). The position of the anoxic zone in the biological reactor, namely post-denitrification and pre-denitrification systems, significantly affects the denitrifying performance. For post-denitrification, an additional external carbon source is usually needed to achieve complete denitrification. In contrast, a pre-denitrification system can use influent organics as the carbon source for denitrification via recycling the nitrate-rich effluent of the aerobic nitrification reactor to the anoxic reactor. Separation in time typically implements in a sequencing batch reactor (SBR). Different phases of aeration and non-aeration are applied to enable nitrification and denitrification, with feeding in the anoxic phases.

For the denitrification process, sufficient carbon must be available to completely denitrify the nitrate formed during nitrification. For instance, according to the equation of glucose-based denitrification, 4.2 g COD g⁻¹ N is required for total nitrogen removal and assimilation ¹²². Considering a part of the COD in the N/DN process is oxidized by oxygen, the COD/N ratio required in practice should be higher, within a typical range of 5-10 g COD g⁻¹ N.

4.2.2 Nitritation/denitritation

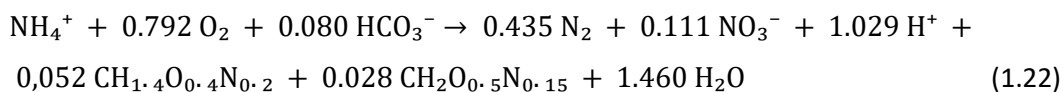
Nitritation/denitritation is a shortcut version of nitrification/denitrification, going over nitrite instead of nitrate. The same configuration choices as described for nitrification/denitrification apply to nitritation/denitritation.

Preventing the oxidation of nitrite to nitrate, namely the suppression of NOB, is vital to establish Nitritation/denitritation, and can be achieved by several control strategies.

Firstly, compared to AOB, the higher susceptibility of NOB towards FA and FNA opens up opportunities for NOB inhibition^{113, 114}. Secondly, the lower oxygen affinity of NOB facilitates the NOB out-selection at low DO concentrations (<1 mg L⁻¹)¹⁶⁵. An increase in AOB activity can be obtained by adjustment of the oxygen supply and level. Yet, care should be taken not to use DO concentrations above 0.5 mg L⁻¹ since this will favor the development of NOB¹¹⁴. Thirdly, the lower NOB growth rate at temperatures >20°C enables NOB washout by imposing a low sludge retention time (SRT)¹⁶⁶. Lastly, intermittent aeration patterns could outcompete NOB due to the NOB lag phase after the anoxic period¹⁶⁷.

4.2.3 Partial nitrification/anammox (PN/A)

In partial nitrification/anammox process, about half of the ammonium is aerobically oxidized to nitrite by aerobic ammonium-oxidizing bacteria (AerAOB), and the residual NH₄⁺ is further oxidized with the produced NO₂⁻ to generate nitrogen gas (N₂) by anoxic ammonium-oxidizing bacteria (AnAOB) (Reaction 1.17)¹¹⁴. The total PN/A reaction is shown as following (Reaction 1.22):



In PN/A systems, competitions occur between aerobic autotrophs (AerAOB and NOB), anoxic autotrophs (AnAOB), aerobic heterotrophs (COD conversion), and anoxic heterotrophs (denitrifiers). To minimize the competition, applying PN/A to carbon-lean streams with a biodegradable COD (bCOD)/N ratio < 2 is advisable¹⁶⁸. Furthermore, besides the necessity to inhibit NOB activity, an excellent PN/A performance relies on maximum sustaining of slow-growing AnAOB.

Over 100 full-scale PN/A processes have recently been installed globally, with more than 50% of them in SBR and 88% of all plants being operated as single-stage systems¹⁶⁹. Currently, it is primarily applied for the sidestream treatment of municipal wastewater. However, mainstream PN/A processes have been encountering unsatisfying nitrogen removal performance because some inherent features, e.g., low ammonium levels, low

temperatures, and fluctuant loading rate, make the out-selection of NOB immensely challenging¹⁷⁰⁻¹⁷².

4.2.4 Denitratation/anammox

There are two different application scenarios for denitratation/anammox. The first scenario is the typical municipal mainstream wastewater with ammonium as major Nr^{173, 174}. In this scenario, around half of ammonium is first nitrified to nitrate, then reduced to nitrite via denitratation; eventually, the produced nitrite is removed with the residual ammonium via anammox process (i.e., PN/denitratation/anammox). The second scenario is the wastewater directly containing both nitrate and ammonium like the effluents of mine and mill, and fertilizer factory^{146, 148}. However, nitrite produced by denitratation could also be reduced to nitrogen gas through denitratation. Therefore, to achieve stable and sufficient nitrite production for anammox, denitratation should be effectively maintained via the possible strategies mentioned in section 4.1.2.1.

Overall, based on the properties of four process types, the oxygen demand (i.e., aeration), COD consumption, and biomass yields were compared for nitrogen removal from wastewater with ammonium as primary Nr (Table 1.6). PN/A process consumes the least amount of oxygen and COD and produces the least amount of biomass. However, for wastewaters with a COD/N ratio higher than the N/DN requirement, DN based on the COD in wastewater is preferred; otherwise, COD requires energy for aerobic removal. Therefore, if sufficient COD is available in wastewaters, N/DN saves more oxygen than other processes (e.g., PN/A) plus additional aerobic carbon removal.

Table 1.6: Comparison between different processes. COD consumption was calculated using acetate as an example ^{173, 175}.

| Parameter | N/DN | nitritation/ denitritation | PN/A | denitrataion/anammox |
|---|------|-------------------------------|------|----------------------|
| Aeration (g O ₂ g ⁻¹ N removed) | 4.57 | 3.43 | 1.95 | 2.39 |
| COD consumption (g acetate COD g ⁻¹ N removed) | 3.81 | 1.71 | 0 | 1.67 |
| Biomass yield (g VSS g ⁻¹ N removed) | 0.86 | 0.39 | 0.14 | 0.29 |

5. Bioreactor configurations

This section outlines some of the commonly available bioreactor configurations used for Nr removal, also applicable for Nr recovery. Based on the growth mode or structural organization of microbes, biological processes are classified into suspended growth and attached growth. Two different aeration pathways (i.e., active and passive) can be implemented for the biological processes consuming oxygen according to the corresponding bioreactor configurations.

5.1 Growth mode

5.1.1 Suspended growth

In suspended growth systems, microbial cells grow as planktonic forms in bulk liquid medium without any support to the substratum, such as activated sludge (AS), aerated lagoons, and anaerobic sludge ¹⁷⁶.

A modified AS process is one of the most common biological processes used for carbon, nitrogen, and phosphorus removal/recovery. The AS is a brownish floc-like suspension ¹⁷⁷, comprised of approximately 80-90% bacteria and 10-20% higher organisms (protozoa, rotifers, and some higher forms of invertebrates) and non-biological mass ¹⁷⁸. These flocs are held together by naturally produced organic polymers and electrostatic forces ¹⁷⁹. In addition, some suspended non-biological materials become enmeshed inside the flocs, beneficially increasing the AS density. The floc morphology ranges from pin-point floc to

largely diffuse floc with high water content within the flocs ¹⁷⁸.

The suspended growth biomass systems are usually developed in the sequencing batch reactor (SBR) and continuous stirred-tank reactor (CSTR) with a settler. Good settleability, for instance, in the AS process, is crucial for efficient wastewater and sludge treatment. Otherwise, microbes can easily be 'washed out' from the reactor, influencing the wastewater treatment efficiency using suspended biomass. Furthermore, the settleability and nutrient removal efficiency are related to the density of flocs. Therefore, a selector based on biomass density is a practical application to enhance the AS process via returning the denser and more bioactive AS into the system ¹⁷⁹.

5.1.2 Attached growth

Most microorganisms in moist environments tend to proliferate on a biotic or abiotic substratum and develop a complex, three-dimensional, and resilient community called a biofilm ¹⁷⁶. The species in biofilms, such as bacteria, fungi, algae, and yeast, form microcolony clusters, which are enclosed within a self-produced glue-like extracellular polymeric substances (EPS) matrix. EPS have multiple functions, including promoting biofilm mechanical and chemical stability, acting as a natural absorbent and sequester of metals, and protecting against external physicochemical and biological stresses ¹⁷⁶.

There are several significant advantages of attached growth systems: (i) maintaining extremely robust environments to their colonizers against external stresses; (ii) quick adaptation to changes in the environment; (iii) providing a high active biomass concentration resulting in high removal rates at relatively short hydraulic retention times; (iv) automatic liquid and solid separation. The microbial biofilm reactors retain cells attached to fixed or moving carrying materials, except granular sludge systems. Over the last half-century, various types of biofilm reactors have been developed, mainly including trickling filter (TF), biological aerated filter (BAF), rotating biological contactor (RBC), moving bed biofilm reactor (MBBR), fluidized bed biofilm reactor (FBBR), membrane biofilm reactor (MBR), and granular sludge system.

A trickling filter (TF) is a fixed bed biofilm reactor where microorganisms grow on carrier

materials (e.g., rocks and plastic materials) as biofilm¹⁸⁰. Oxygen is provided in the TF system either by natural ventilation or forced aeration (using fan and blower), creating the aerobic condition for the biochemical conversion processes¹⁸¹. When influent wastewater is sprayed from the top of the TF reactor, it percolates downward over the biofilm surface, where microorganisms degrade the organic substances and nitrogen from the liquid phase. The effluent drained out of the bottom of the reactor is usually recirculated to ensure complete biological conversion of carbon and/or nitrogen¹⁸⁰.

A biological aerated filter (BAF) contains packing granular media that provide a large surface area per unit volume for biofilm development. Opposite to TF reactors, the BAF is a submerged filter and can incorporate suspended solids removal¹⁸².

In a conventional rotating biological contactor (RBC), multiple circular discs are fixed on a horizontal shaft continuously rotated by a motor¹⁸³. The packed-cage RBC is a rotating porous cage filled with carrier materials¹⁸⁴. The disc and carriers support the growth of microorganisms as biofilm. The oxygen diffusion is achieved by directly exposing the biofilm to the atmospheric air. The bulk DO level can be controlled by the rotation speed¹⁸⁵ and the immersion level of the discs or cage¹⁸⁶.

The moving bed biofilm reactor (MBBR) incorporates the edges of both suspended and attached growth, where microorganisms grow on plastic carriers as biofilm¹⁸⁷. The biofilm carriers are moved either by the agitation produced by aeration (aerobic process) or mechanical stirrers (anoxic/anaerobic process)^{187, 188}. Like the MBBR, the fluidized bed biofilm reactor (FBBR) utilizes small, fluidized media for carrier immobilization and retention. In the concept of FBBR, wastewater passes up through a packed bed of particles at a velocity sufficient to impart motion to or fluidize the particles¹⁸⁹.

A membrane biofilm reactor (MBR) employs a gas-permeable membrane that delivers a gaseous substrate (e.g., oxygen, hydrogen, methane) to a biofilm formed on the outer surface of the membrane^{180, 190}. Unlike other biofilm technologies, the electron donor and acceptor substrates in MBR adopt the counter-gradient diffusion mode^{191, 192}. A membrane-aerated biofilm reactor (MABR) is one type of MBRs, where the air or oxygen

acts as the electron donor. Compared to the oxygen transfer efficiency (OTE) of the conventional AS process (15–40%), MABR with closed-end operation allows almost 100% OTE, significantly saving aeration energy ¹⁸⁰.

Granular sludge is the result of three-dimensional aggregate expansion by microbial growth based on species-specific physiology (e.g., DO affinity or inhibition) combined with globular surface erosion by hydrodynamic shear ¹⁹³. Granular sludge is usually well compacted, forming different layers comprised of various functional bacteria. Compared to the suspended growth process, granular sludge shows excellent settleability ¹⁷⁹. Granules can establish gradients of substrates, creating specialized niches where microorganisms with different metabolic functions can co-exist. For example, mature PN/A granules contain AerAOB in the aerobic rim and AnAOB in the anoxic core ¹⁹³.

Besides, some hybrid growth systems involving both suspended and attached growth processes in one reactor have been developed. For example, integrated fixed-film activated sludge (IFAS) is a typical hybrid growth system. In the IFAS system, solid media (e.g., suspended plastic carriers) are added to the suspended growth environment to provide attaching surface for biofilm, thereby increasing the microbial concentrations and contaminant degradation rates ¹⁹⁴. For instance, the attached biofilm carriers in the IFAS can enrich the slow-growing autotrophs (e.g., AerAOB and AnAOB) central to nitrogen removal in wastewater treatment, thus improving the nitrogen removal capacity without building new reactors ^{172, 195}.

5.2 Aeration approach

Aerobic processes can occur either with active or passive aeration. Active aeration systems require additional energy consumption of forced aeration, while in passive aeration processes, the oxygen transferred to the biomass is provided naturally by diffusion from the air ¹⁹⁶. Among all the bioreactor configurations described in section 4.1, only the trickling filter (TF) and rotating biological contactor (RBC) can be implemented with passive aeration. Based on the configuration of several typical bioreactors, the overall costs, area requirement, ease of DO control, sludge content, ease of biomass retention, low hydraulic retention time (HRT) feasibility, the risk for

mechanical failure and clogging, and the operational complexity are qualitatively compared (Table 1.7) ¹¹⁴. Thereinto, the feasibility of low HRT is vital for treating wastewaters with low nitrogen levels (e.g., mainstream), in the order of hours and hence about 24 times lower than for side stream treatment ¹¹⁴. Applying low HRT can vastly increase the required settling time or settler volume for SBR and CSTR and the necessary number of membranes for MBR. In contrast, TF reactors have low HRT feasibility, passive aeration, and low operational complexity, rendering low overall costs. Therefore, TF reactors are interesting configurations used to explore the nitrogen recovery and removal.

Table 1.7: Qualitative comparison of typical reactor configurations (advantages indicated in the shade) ¹¹⁴.

| Biomass growth | Suspended (flocs) | | | | Attached (biofilm) | | |
|-----------------------------|-----------------------|--------|-------------------|---------|-----------------------|-------------------------------|--------|
| | Reactor configuration | SBR | CSTR with settler | TF | RBC (fixed or moving) | Bed reactor (fixed or moving) | MBR |
| Overall costs | Medium | Medium | Low | Low | Medium | High | Medium |
| Area requirement | Medium | High | Medium | High | Medium | Medium | Low |
| Aeration | Active | Active | Passive | Passive | Active | Active | Active |
| Ease of DO control | High | High | Low | Medium | Medium/High | High | High |
| Sludge content | Low | Low | Medium | Medium | Medium | High | High |
| Ease of biomass retention | Low | Low | Medium | Medium | Medium | High | Low |
| Low HRT feasibility | No | No | Yes | Yes | Yes | No | Yes |
| Risk for mechanical failure | Low | Low | Medium | High | Low | Medium | Low |
| Risk for clogging | Low | Low | High | Low | High/Low | High | Low |
| Operational complexity | High | Medium | Low | Low | Medium | High | Medium |

6. Research outline

The reactive nitrogen (Nr) has surpassed the planetary boundary three times in the past decades. The severe transgression of the safety level is not conducive to planetary sustainable development. As human activities keep generating Nr pollution, it is vital to sustainably manage the Nr on the Earth and restore humanity to the Nr boundary. In this thesis, both "Nr recovery (conversion)" and "Nr removal" were investigated to manage the point-source Nr in the nitrogen cycle.

This Ph.D. thesis aimed to develop different bioreactor strategies for Nr recovery, conversion, and removal from various waste streams. The Nr recovery and conversion was investigated on high-strength Nr waste streams towards fertigation and hydroponic application, while the Nr removal was studied on the low to medium strength Nr waste streams. Figure 1.4 depicts a structural overview of all research chapters.

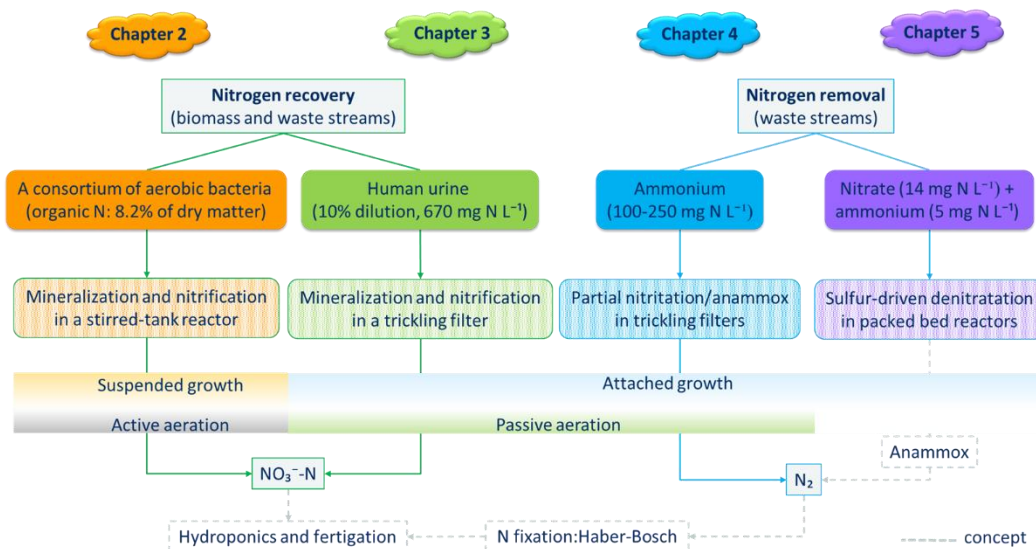


Figure 1.4: Overview of the research chapters in this thesis.

In **Chapter 2**, a concept of a novel controlled mineralization and nitrification system was proposed, which can be integrated into hydroponics systems. This system is suitable for the $\text{NO}_3^- \text{-N}$ recovery from solid organic fertilizers. The research was carried out in 4 steps. Firstly, batch tests were implemented to determine the optimal temperature and DO conditions for the mineralization of solid organic fertilizers. Then, informed by the batch

tests, the optimal operating conditions were applied to a controlled mineralization and nitrification bioreactor to convert a type of microbial fertilizer to a nitrate-rich nutrient solution. Furthermore, nutrient balancing strategies were proposed to make the produced solutions match a universal standard nutrient solution. Finally, the economic assessment of nutrient production from the bioreactor systems was compared to commercially available inorganic fertilizers.

Chapter 3 investigated Nr recovery from diluted urine (around 670 mg N L⁻¹) by controlled nitrification in a packed-bed trickling filter. In this concept, the TF, as a passively aerated configuration for nitrification, was proposed to produce nutrient solutions on-site for hydroponic or fertigation systems. Firstly, synthetic urine was fed to the trickling filter. Then, after the stable complete nitrification performance was reached, the influent was switched to real human urine for feasibility and stability tests. Finally, based on the nutrient supplementing strategy proposed in **Chapter 2**, the NO₃⁻-N-rich nutrient solution obtained from the trickling filter was balanced to a standard nutrient solution. Calcium hydroxide was used as a urine alkalization, nitrification pH control, and nutrient supplementation chemical. The optimal hydraulic loading rate (HLR) on nitrification performance and the electrical energy consumption were investigated.

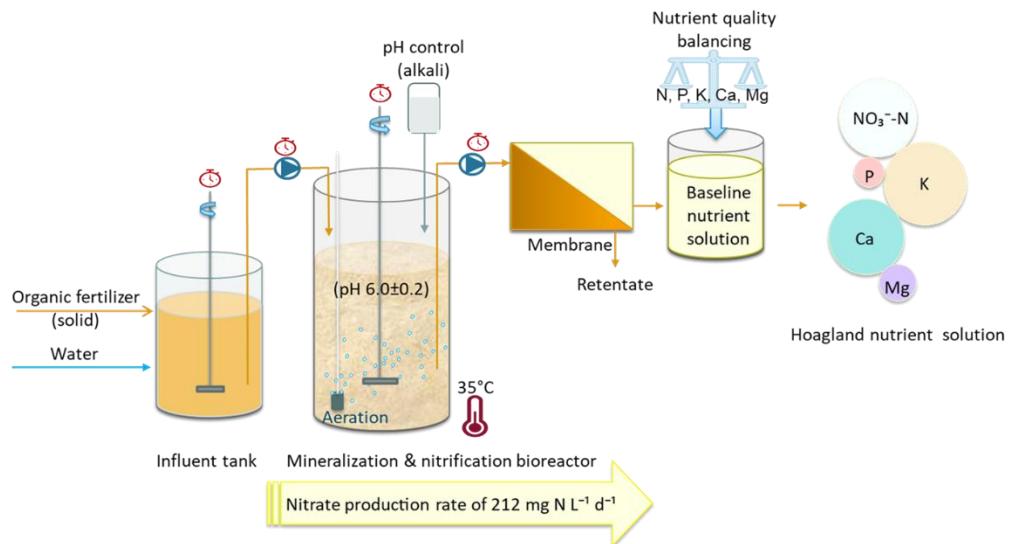
In **Chapter 4**, packed-bed trickling filters were employed to explore the feasibility of Nr removal via the PN/A process. Synthetic wastewater containing 100-250 mg NH₄⁺-N L⁻¹ was tested to simulate household waste streams after carbon removal. Three types of carrier materials with different surface areas were tested in parallel. Towards a balanced PN/A process, the influence of passive ventilation approaches (top only vs. top and bottom) and hydraulic loading rate (HLR, 0.4 – 2.2 m³ m⁻² h⁻¹) were examined. The vertical activity stratification of functional bacteria in the trickling filters was compared. Besides, the optimal HLR and carrier materials on PN/A performance and energy consumption were investigated as well.

For the underdeveloped mainstream PN/A process, the effluent commonly contains above 10 mg L⁻¹ NO₃⁻-N and some residual ammonium. In **Chapter 5**, a secondary effluent polishing concept via sulfur-driven denitrification/anammox was proposed. The goal of

this research was to investigate the feasibility and stability of sulfur-driven denitrification in long-term operation. Parameters affecting the nitrite accumulation like pH setpoint, residual NO_3^- -N level, and biomass-specific NO_3^- -N loading rate were tested. The composition evolution of the microbial community in the biofilm was monitored as well.

Chapter 2

A bioreactor and nutrient balancing approach for the conversion of solid organic fertilizers to liquid nitrate-rich fertilizers: Mineralization and nitrification performance complemented with economic aspects



This chapter has been redrafted after:

Xie, Y.; Spiller, M.; Vlaeminck, S. E., A bioreactor and nutrient balancing approach for the conversion of solid organic fertilizers to liquid nitrate-rich fertilizers: Mineralization and nitrification performance complemented with economic aspects. *Science of The Total Environment*, 2021: 150415.

Abstract

Due to the high water- and nutrient-use efficiency, hydroponic cultivation is increasingly vital in progressing to environment-friendly food production. To further alleviate the environmental impacts of synthetic fertilizer production, the use of recovered nutrients should be encouraged in horticulture and agriculture at large. Solid organic fertilizers can largely contribute to this, yet their physical and chemical nature impedes application in hydroponics. This study proposes a bioreactor for mineralization and nitrification followed by a supplementation step for limiting macronutrients to produce nitrate-based solutions from solid fertilizers, here based on a novel microbial fertilizer. Batch tests showed that aerobic conversions at 35 °C could realize a nitrate (NO_3^- -N) production efficiency above 90% and a maximum rate of 59 mg N L⁻¹ d⁻¹. In the subsequent bioreactor test, nitrate production efficiencies were lower (44–51%), yet rates were higher (175–212 mg N L⁻¹ d⁻¹). Calcium and magnesium hydroxide were compared to control the bioreactor pH at 6.0 ± 0.2 , while also providing macronutrients for plant production. A mass balance estimation to mimic the Hoagland nutrient solution showed that 92.7% of the NO_3^- -N in the $\text{Ca}(\text{OH})_2$ scenario could be organically sourced, while only 37.4% in the $\text{Mg}(\text{OH})_2$ scenario. Besides, carbon dioxide (CO_2) generated in the bioreactor can be used for greenhouse carbon fertilization to save costs of nitrate-rich liquid fertilizer production. An estimation of the total cost showed that producing a nutrient solution from solid organic fertilizers can be cost-competitive compared to using commercially available liquid inorganic fertilizer solutions.

1. Introduction

Agriculture and food production take a major share in the consumption of global resources, with for instance about 90% of global freshwater ¹⁹⁷ and > 80% of global ammonia produced through the Haber-Bosch process ¹⁹⁸. However, during the artificial nitrogen fixation from N₂ to ammonia (NH₃) via the Haber-Bosch process, greenhouse gas and NH₃ emissions, and PM2.5 (particulate matter with a diameter less than 2.5 μm) formation can aggravate the global climate change and the air pollution, and thus threaten human health ¹⁹⁹. Therefore, efficient use of nutrients and water is essential to progress towards an environmentally friendly agricultural system. Hydroponics in greenhouses is among the most water- and nutrient-use efficient agricultural systems, with up to 90% water and 85% nutrient saving ²⁰. However, current hydroponic systems rely entirely on inorganic nitrogen supplied by the Harber-Bosch process, dosed as liquid fertilizers ^{14, 94}. An alternative strategy is to increase the share of recovered nutrients in horticulture, and agriculture at large, to reduce the demand for synthetic fertilizers. Use of recovered nitrogen can reduce the amount of new N fertilizer synthesis via the Haber-Bosch process. Therefore, reusing nitrogen and other nutrients derived from by-products or residues from the agro-food industry can further reduce the environmental impact of greenhouse hydroponic systems, and other crop production systems relying on liquid fertilizers or fertigation.

Solid organic fertilizers are conventionally produced from plant- and animal-based sidestreams from the agro-food industry, and the majority of their nitrogen content is organically bound. Decreasing the consumption of animal products was suggested to have a considerably beneficial impact on the environment (e.g., greenhouse gas emission) ²⁰⁰; thus, plant-based fertilizers could be more environmentally friendly than animal-based fertilizers. However, microbial fertilizers are considered a novel type of organic fertilizers, which can be produced on effluents from the food and beverage industry, for instance, on potato industry wastewater ^{88, 90}. Resource recovery here typically occurs through the production and drying of microbial biomass, which can be based on several groups of microbes, such as microalgae, purple non-sulfur bacteria, and a consortium of

aerobic bacteria (CAB).

Given the physical (solid) and chemical (organic) nature of nitrogen in solid organic fertilizers, these are not directly usable in hydroponics and fertigation applications, where there is a demand for liquid and nitrate-based fertilizers. Indeed, the primary nitrogen form utilized by plants is nitrate (NO_3^- -N)^{15, 201}. For organic nitrogen to become available for crops, the biomass must undergo a mineralization and nitrification process²⁰². In the mineralization process, microorganisms convert organic nitrogen (e.g., proteins) to an inorganic form (i.e., ammoniacal nitrogen) through hydrolysis and ammonification^{96, 97}. Parameters such as temperature and dissolved oxygen (DO) affect the hydrolysis of organic nitrogen^{203, 204}. The hydrolysis rate of biowaste was shown to increase at higher temperatures²⁰⁵. Some studies suggested limited aeration (i.e., micro-aeration) could significantly enhance the hydrolysis of proteins^{204, 206}. However, micro-aeration could induce denitrification risk, resulting in the loss of NO_3^- -N²⁰⁷. In the nitrogen mineralization process, hydrolysis is considered the rate-limiting step²⁰⁸. Therefore, it is indispensable to explore the optimal hydrolysis conditions (e.g., temperature and DO) of organic fertilizers to promote their mineralization performance.

Obtaining mineralization and nitrification within hydroponic systems poses several challenges hindering the use of organic nitrogen. Besides the practical difficulty of dosing solid fertilizer to the root zone over the whole production season, the release pattern of the macronutrients cannot really be controlled. The direct dosing of organic fertilizers in hydroponic systems was shown to limit plant growth due to the deficiency of NO_3^- -N^{201, 209}. When using organic growing media for the plants, pre-dosing organic fertilizers is sometimes practiced, yet it is challenging to control the bioconversion rates, even though a proper selection of the growing media constituents influences these^{15, 210}. Shinohara et al. (2011) proposed directly dosing organic fertilizers into a hydroponic pot and introducing inoculum with continuous aeration to bioconvert organic fertilizers²¹¹. However, this technique cannot easily manage the solution quality (e.g., composition and concentration) in the rhizosphere immediately and flexibly, especially for large-scale hydroponic cultivation¹⁵. Furthermore, direct dosing could stimulate heterotrophic

pathogens, increasing the competition for oxygen in the root environment and creating food safety concerns^{14, 212}. Disinfection of the fertigation water loop is typically in place, for instance, using ultraviolet radiation to control the proliferation of fungal and bacterial pathogens such as *Fusarium spp.* and *Escherichia coli*^{15, 213, 214}.

This study proposes a novel pH-controlled bioreactor system for mineralization and nitrification of solid organic fertilizers, followed by a chemical supplementation step to achieve a well-balanced hydroponic nutrient solution (Figure 2.1). This concept has the advantage of accurately tuning the composition and concentration of a more sustainable liquid nitrate-based fertilizer to match the plant needs (Figure 2.1a), while avoiding the entry of organic carbon, oxygen demand, and stimulation of microbial risks in the hydroponic system. Besides, carbon dioxide (CO₂) generated during the organic fertilizer mineralization can also be used for CO₂ fertilization in the greenhouse. The proposed concept for the controlled mineralization and nitrification system comprises four parts: (i) an influent tank to mix the solid organic fertilizer with water; (ii) a bioreactor for mineralization and nitrification with pH control (base addition); (iii) a membrane module (e.g., microfiltration) to remove the solids and yield a baseline nutrient solution (BNS); and (iv) a nutrient balancing step to further tune the BNS macronutrient composition to the plant's needs.

This research aims at a proof of concept for the bioreactor conversion performance and economic estimation of the overall concept. The specific objectives are to (i) optimize the mineralization performance by defining the best-operating conditions, (ii) realize the liquid nitrate-rich fertilizer production from solid organic fertilizer in a mineralization and nitrification bioreactor, where various pH control reagents were tested, (iii) investigate the microbial community in the bioreactor, (iv) model the nutrient balancing according to plant needs, and (v) assess the economic feasibility of the concept by comparing the costs for producing the nutrient solution from the bioreactor with that of inorganic fertilizer nutrient solutions.

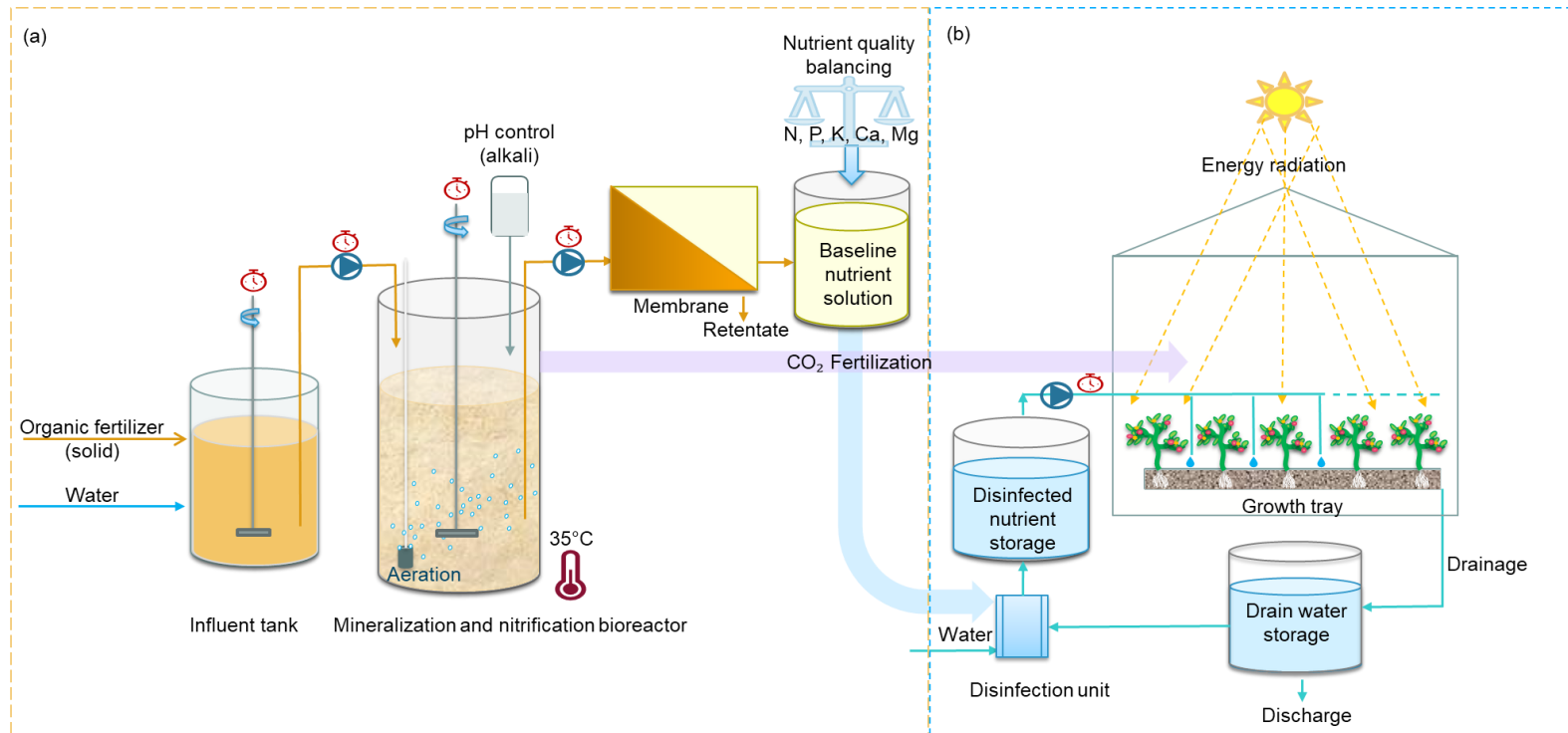


Figure 2.1: Concept of a novel hydroponic nutrient supply system: (a) mineralization and nitrification of organic fertilizer to provide the suitable nutrient solution for (b) hydroponic cultivation in a greenhouse. The timers could automatically control the operation sequence and duration in each cycle.

2. Material and methods

The research was carried out in 4 steps. Initially, batch tests were implemented to determine the optimal conditions (i.e., temperature and DO) for nitrogen mineralization (Section 2.2). Informed by the batch tests, the operating conditions were applied to a mineralization and nitrification bioreactor, which is fully aerated as well as pH and temperature-controlled (Section 2.3). Furthermore, a nutrient balancing strategy for the BNS was developed (Section 2.5). Finally, the economics of the nutrient solution produced from organic fertilizers was compared to commercially available inorganic fertilizer nutrient solutions (Section 2.5).

2.1 Organic fertilizers

BioAgenasol[®] profigreen (BAPN) (AGRANA group, Austria) and CAB were tested in this study. BAPN represents a class of commercially available plant-based fertilizers and is a by-product of bioethanol production. The CAB represents a class of novel microbial fertilizers obtained from the company Avecom (Wondelgem, Belgium). CAB was produced through a patented aerobic fermentation process based on diluted process streams of food processing companies. Based on the dry weight, the total nitrogen (TN) content of BAPN and CAB are 4.8% and 8.2%, respectively. No inorganic nitrogen (i.e., $\text{NH}_4^+\text{-N}$, $\text{NO}_2^-\text{-N}$, and $\text{NO}_3^-\text{-N}$) could be detected in TN.

2.2 Batch tests

Batch tests were carried out in both anaerobic and aerobic conditions. Anaerobic digestion sludge (ADS) and nitrifying activated sludge (AS) were used as inocula for the anaerobic and aerobic tests, respectively. They were sampled from a municipal wastewater treatment plant (Aquafin Antwerpen-Zuid, Belgium). The inoculum of 0.4 g volatile suspended solids (VSS) L^{-1} was added to 2L of tap water and mixed continuously by a magnetic stirrer. For anaerobic tests, the ADS inoculum was flushed with N_2 gas for 30 mins to eliminate the residual DO in tap water. No aeration was provided during the whole batch period, resulting in a DO of around 0 $\text{mg O}_2 \text{L}^{-1}$ in the anaerobic tests. To explore the effect of DO on nitrogen mineralization, the aerobic tests were implemented in open glass flasks with the AS as an inoculum. The DO level in the aerobic test was

controlled at 3 ± 0.5 mg O₂ L⁻¹ via air pumps (Tetra TEC APS 150). Two different reaction temperatures of 20°C and 35°C were implemented in anaerobic and aerobic tests.

An initial TN (i.e., organic nitrogen) concentration of 370 mg N L⁻¹ was set for all the batch tests. This concentration was determined according to the weight proportion of TN in BAPN and CAB in the dry biomass (section 2.1). The concentration of 370 mg N L⁻¹ was based firstly on the typical values in growing media (240-530 mg N L⁻¹)⁸⁸ and secondly on the TN requirements in hydroponic nutrient solutions (140-300 mg N L⁻¹)¹⁵, while accounting for a potentially incomplete N mineralization. The pH in the reactors was continuously monitored by a pH probe (SP11X, Consort) and controlled at 7.0 ± 0.2 via dosing hydrochloric acid (HCl) or potassium hydroxide (KOH) by a multi-parameter controller (R3610, Consort). To monitor the mineralization performance of each batch test, samples were taken periodically, filtered via 0.2 µm syringe filters (CHROMAFIL Xtra PVDF), and stored at 4°C until analysis.

2.3 Nitrate conversion in a controlled mineralization and nitrification bioreactor

A controlled bioreactor system for converting solid organic fertilizers to liquid nitrate-rich fertilizers is shown in Figure 2.1a. The solid organic fertilizer was mixed in an influent tank with water before a mineralization and nitrification bioreactor. The system was equipped with timer-controlled influent and effluent pumps (Seko peristaltic pumps, PR7) and overhead stirrers (ES Overhead Stirrer, Velp Scientifica). The bioreactor was operated with a cycle time of 8 h, including 2 min feeding, 446 min reaction, 30 min settling, and 2 min decanting. The settling phase was only kept for a short period (day 0-42) to retain as much biomass as possible in the bioreactor. Following day 42 until the end of the experiments on day 170, the bioreactor was run with continuous mixing without settling due to the poor settleability of sludge, which meant the sludge retention time (SRT) was equal to the HRT.

Based on the batch test results, CAB was used in this step, and aerobic bioconversion at 3 ± 0.5 mg O₂ L⁻¹ and 35°C was implemented in the bioreactor. The inoculum was taken from the aerobic batch test and added into the 3 L bioreactor with an initial concentration

of 0.4 g VSS L⁻¹. The influent TN concentration increased from 500 to 3000 mg N L⁻¹ and the loading rate from 100 to 400 mg N L⁻¹ d⁻¹, resulting in a volume exchange ratio of 4.4-6.67% and a hydraulic retention time (HRT) of 5.5-7.5 days. The pH of the bioreactor was initially controlled at 7.0±0.2 (day 0-133), and then at 6.0±0.2 (day 134-170), which was directly consistent with the optimum pH range of most nutrient solutions (5.5-6.5)¹⁴. To explore the optimal pH control reagent according to the nutrient composition and concentration for plant needs, various pH control reagents including KOH, sodium hydroxide (NaOH), calcium hydroxide (Ca(OH)₂), and magnesium hydroxide (Mg(OH)₂) were tested. The operational parameters are detailed in the top table of Figure 2.4. To monitor the performance of the bioreactor, samples were taken periodically from the influent and effluent.

2.4 Physicochemical water, biomass, and microbiome analyses

The NH₄⁺-N, NO₂⁻-N, NO₃⁻-N, and phosphate (PO₄³⁻) were measured with the San++ Automated Wet Chemistry Analyzer. The TN, total phosphorus (TP), total chemical oxygen demand (TCOD), soluble chemical oxygen demand (SCOD) were photometrically determined using NANOCOLOR test tubes (Macherey-Nagel, Germany). The VSS was measured using standard methods²¹⁵. Elements of potassium (K), calcium (Ca), magnesium (Mg), and sodium (Na) were measured by inductively coupled plasma mass spectrometry (Thermo Scientific™ iCAP Q, Thermo Fisher Scientific).

To understand the microbial community working in the bioreactor, biomass samples were collected for microbiome analysis during the operation period. According to the manufacturer's instructions, DNA was extracted using a PowerFecal® DNA isolation kit (QIAGEN, Germany). The DNA extracts were sent to Novogene (UK) Co., Ltd for microbial amplicon-based metagenomics sequencing (Illumina Novaseq6000 PE250, Q30≥75%). 16S rRNA genes of 16S V3-V4 were amplified using specific primers 341F (CCTAYGGGRBGCASCAG) and 806R (GGACTACNNGGTATCTAAT). All PCR reactions were carried out with Phusion® High-Fidelity PCR Master Mix (New England Biolabs). For each representative sequence, Mothur software was performed against the SSUrRNA database of SILVA Database (see details <http://www.arb-silva.de/>) for species annotation

²¹⁶. The alpha diversity (Shannon's) and beta diversity (Bray-Curtis dissimilarity) were analyzed in each sample and between different samples.

2.5 Nutrient balancing strategy and economic assessment

The effluent of the bioreactor was filtered through the 0.2 μm filters to simulate the function of a membrane module. The filtrate was regarded as the BNS. Hoagland nutrient solution (HNS) is considered one universal nutrient solution for plant growth in hydroponics. The concentration of major elements in HNS is 210 mg NO_3^- -N L^{-1} , 31 mg P L^{-1} , 235 mg K L^{-1} , 200mg Ca L^{-1} , and 48 mg Mg L^{-1} ¹⁵. To model the nutrient balancing according to the HNS recipe, a nutrient balancing strategy was illustrated in Figure 2.2. The water of low salinity ($< 0.75 \text{ mS cm}^{-1}$) is recommended in the dilution step ²¹⁷. Commonly used chemical compounds for making nutrient solutions such as calcium nitrate ($\text{Ca}(\text{NO}_3)_2$), magnesium nitrate ($\text{Mg}(\text{NO}_3)_2$), magnesium sulfate (MgSO_4), calcium sulfate (CaSO_4), potassium sulfate (K_2SO_4) and dipotassium phosphate (K_2HPO_4) were selected to supplement relevant nutrients to the BNS (SI Table S2.1). The market reference prices of chemicals were obtained from two large global suppliers (i.e., <https://www.alibaba.com/> and <https://www.ec21.com/>). The selection of compounds followed two major principles: firstly, the dosage of each compound should not exceed water solubility after the final dilution to HNS; secondly, the cheaper compounds according to the indicative market price should always be selected in priority, only using the relative expensive chemicals once other nutrient elements in the cheaper chemicals reached the required level. Based on the three types of pH control reagents used in phase VII, VIII, and IX, the nutrient balancing strategy was applied to three organic scenarios (i.e., NaOH, $\text{Ca}(\text{OH})_2$, and $\text{Mg}(\text{OH})_2$). Subsequently, the concentration of nonessential element sodium (Na) and the electric conductivity (EC) in balanced organic scenarios were checked.

Following the strategy to prepare HNS from the BNS organic scenarios, two types of commercially available inorganic fertilizers, YaraTera Kristalon Scarlet and Floraflex B1™/B2™ (composition and price in SI Table S2.2), were used to design the HNS as commercial scenarios for the convenience of further cost comparison with organic

scenarios. Besides, HNS composed of individual chemical compounds was set as a benchmark scenario.

The costs of nitrate-rich liquid fertilizer production were calculated based on the cost of CAB, commercial hydroponic fertilizers, supplemented chemical compounds, the aeration for COD removal and nitrification, the saved cost of CO₂ production for CO₂ fertilization, and the cost of membrane filtration. The price for CAB was 1 € g⁻¹ dry matter, communicated by the company Avecom. The O₂ consumption for complete nitrification was assumed to be 4.57 g g⁻¹ NO₃⁻-N¹⁰⁹. The average O₂ transfer efficiency and electricity cost were taken as 2kg kWh⁻¹ and 0.117€ kWh⁻¹^{218, 219}. The heat produced via electricity generation was assumed to be recovered during the operation of combined heat and power (CHP) configurations in farms^{220, 221}. Thus, reactor heating was considered for free. The cost of a membrane module was assumed in a range of 0.36-1.25 € m⁻³, based on total project costs, annual operation, and maintenance costs^{222, 223}.

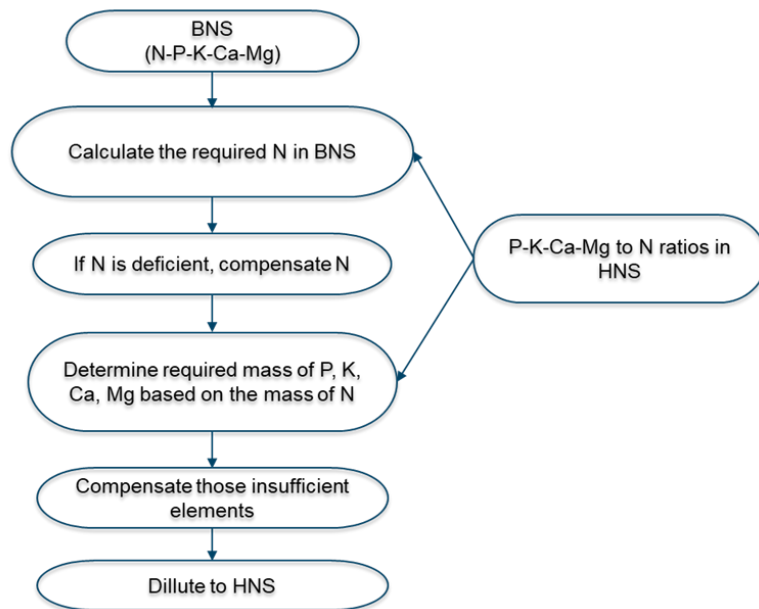


Figure 2.2: Flow diagram of the methodology to carry out the mass balance of the baseline nutrient solution (BNS) according to the elemental composition and concentration in Hoagland nutrient solution (HNS).

3. Results and discussion

3.1 Batch test screen for optimal mineralization conditions

In the batch tests, the performance of inorganic nitrogen (i.e., $\text{NH}_4^+\text{-N}$, $\text{NO}_2^-\text{-N}$, and $\text{NO}_3^-\text{-N}$) release was employed to indicate the mineralization and nitrification of BAPN and CAB (Figure 2.3). The first-order kinetics fitted the total inorganic nitrogen (TIN) releasing performance in all the batch tests ($R^2 \geq 0.92$), and k is the kinetic rate constant. In the anaerobic tests, only $\text{NH}_4^+\text{-N}$ was detected as TIN. The mineralization performance of both BAPN and CAB at 35°C was better than at 20°C with higher rate constants and efficiencies (Figure 2.3a and 2.3b). In the anaerobic tests at 35°C, the TIN releasing efficiency of CAB reached 43% in two days, which was much higher than BAPN, with only 9% released at day 2. Like the anaerobic tests, aerobic tests at 35°C showed higher rate constants than at 20°C (SI Figure S2.1) for BAPN and CAB. Compared to the anaerobic tests at 35°C, the improvement of mineralization in the BAPN batch was negligible (Figure 2.3c). By contrast, the aerobic incubation further improved the mineralization efficiency of CAB to 91% and stabilized in 9 days. Therefore, CAB was more promising than BAPN as organic fertilizer in the bioconversion process. Figure 2.3d showed the dynamic changes of $\text{NH}_4^+\text{-N}$, $\text{NO}_2^-\text{-N}$, and $\text{NO}_3^-\text{-N}$ during the aerobic batch test of CAB. There was no $\text{NO}_2^-\text{-N}$ detected during the whole batch period. $\text{NH}_4^+\text{-N}$ was seen in the first 5 days. Since day 6, only $\text{NO}_3^-\text{-N}$ could be detected in the reactor, indicating the nitrification process could be completed under aerobic mineralization. Moreover, the maximum and average nitrification rates of the CAB aerobic test were calculated based on the increase in TIN concentrations over the corresponding periods (the first 4 and 9 days), which were 59 and 38 $\text{mg N L}^{-1} \text{d}^{-1}$, respectively.

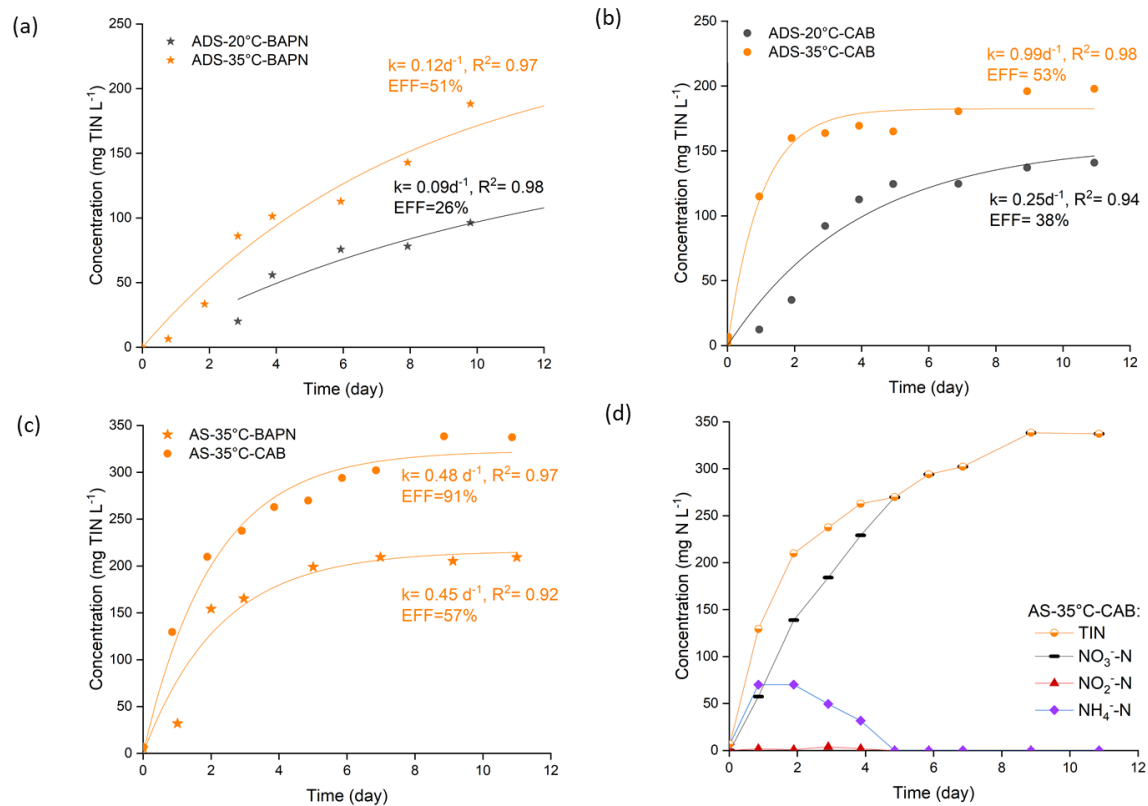


Figure 2.3: Performance evaluation of batch tests; anaerobic mineralization with ADS at 20 °C and 35 °C (a) BAPN and (b) CAB; (c) aerobic mineralization with AS at 35 °C on BAPN and CAB; (d) dynamic changes of specific inorganic nitrogen during "AS-35 °C-CAB" test. "k" is the kinetic rate constant. "EFF" means the mineralization efficiency.

The poor mineralization performance of BAPN could be attributed to some intrinsic characteristics, such as the potential hydrolysis inhibition by tannins in plants^{224, 225} or by cellobiose from cellulose degradation²²⁶. Besides the improvement via increasing temperature to 35°C, sufficient aeration could break the bottleneck of CAB hydrolysis. In our batch study, aerobic mineralization at 3 ± 0.5 g O₂ L⁻¹ substantially improved the NH₄⁺-N released and completely converted the NH₄⁺-N to NO₃⁻-N. Spanoghe et al. (2020) showed more than 70% of the organic nitrogen mineralized from CAB into ammonium and nitrate in 77 days⁸⁸. This prolonged mineralization process should be attributed to the poor incubation conditions via blending CAB with a commercial organic growing medium and storing it at a relative humidity of 75% and temperature of 16 °C.

3.2 Nitrate production in the mineralization and nitrification bioreactor

In the influent tank, TIN only accounted for 3±1% of TN (SI Figure S2.2). The performance of NO₃⁻-N production in the bioreactor was divided into nine phases (I to IX, Figure 2.4a). A new phase started when a parameter was changed to improve the performance of NO₃⁻-N production or balance the nutrient quality in BNS. In the bioreactor, the accumulation of NH₄⁺-N and NO₂⁻-N was detected only for short periods at the beginning of phases I, III, and IV (Figure 2.4a).

3.2.1 Performance of nitrate production under various controlling parameters

The bioreactor was started with an influent loading rate of 100 mg TN L⁻¹ d⁻¹ in phase I. The concentration of NO₃⁻-N in the bioreactor gradually increased and stabilized at 275±8 mg N L⁻¹ with a conversion efficiency of 55±2% after three rounds of HRT (i.e., 15 days) (Figure 2.4a). Under the same operational condition, doubling the loading rate to 200 mg TN L⁻¹ d⁻¹ in phase II (via increasing the influent concentration) further increased the NO₃⁻-N concentration. In this phase, the bioreactor obtained a stable NO₃⁻-N conversion efficiency of 54±2% after three rounds of HRT again, with 540±16 mg NO₃⁻-N L⁻¹. Due to the poor settleability of sludge with 6.5g VSS L⁻¹ in phase II, the 30 min settling was discontinued at day 42. Afterward, the HRT was always equal to the SRT.

In phase III, the TN loading rate was further increased to 400 mg TN L⁻¹ d⁻¹. The

bioreactor overflowed twice due to a foaming issue on day 49 and 61, resulting in a temporary TIN decrease in the bioreactor (Figure 2.4a). To tackle this foaming problem, Antifoam SE-15 (Sigma-Aldrich), as a typical active silicon antifoam, was applied to the reactor with the dosage of 0.1% (v/v of influent)²²⁷. By the end of this phase, nitrate concentrations stabilized at $1060 \pm 26 \text{ mg N L}^{-1}$ with its production efficiency of $53 \pm 1\%$ and rate of $212 \pm 6 \text{ mg N L}^{-1} \text{ d}^{-1}$. Since the potassium (K) concentration of bioreactor effluent was $3428 \pm 40 \text{ mg L}^{-1}$, the K to NO_3^- -N ratio reached around 3.2. The influent K content of $1581 \pm 49 \text{ mg L}^{-1}$ could obtain a K to NO_3^- -N ratio of about 1.5 in the bioreactor, which was already 1.3 times higher than that in HNS. Thus, to avoid the excessive K supplement to the BNS, KOH was replaced by NaOH as a pH control reagent in phase V. In phase IV and V, prolonging the HRT to 7.5 days under the loading of $400 \text{ mg TN L}^{-1} \text{ d}^{-1}$ could achieve $1301 \pm 45 \text{ mg NO}_3^- \text{ L}^{-1}$. Still, the TIN conversion efficiency only reached 46% without further improvement. Starting at phase VI, the HRT was decreased back to 5 days. Subsequently, the nitrate concentration was stable at $874 \pm 23 \text{ mg N L}^{-1}$ with a conversion efficiency of $44 \pm 1\%$ and conversion rate of $175 \pm 5 \text{ mg N L}^{-1} \text{ d}^{-1}$ in phase VI to IX.

Starting in phase VII, the pH of the bioreactor was lowered to 6.0 ± 0.2 to meet the optimum pH range of most nutrient solutions. Compared to Phase VI, decreasing the pH to 6.0 ± 0.2 had no negative impact on the TIN conversion. Due to the deficiency of the elements Ca (around 42 mg L^{-1}) and Mg (about 46 mg L^{-1}) in the influent and subsequently in the BNS of phase VI and VII, Ca(OH)_2 and Mg(OH)_2 were used as pH control reagents in phase VIII and IX, respectively. In phase VIII of day 152, the dosage of Ca(OH)_2 could significantly increase the element Ca to 752 mg L^{-1} , but the PO_4^{3-} concentration dropped to 19 mg P L^{-1} (Figure 2.4b). The P recovery efficiency in the effluent was less than 10%, and therefore lower than previous phases with around 50% recovery. Presumably, the loss of PO_4^{3-} could be attributed to the chemical precipitation of calcium phosphates such as dicalcium phosphate (CaHPO_4) and tricalcium phosphate ($\text{Ca}_3(\text{PO}_4)_2$) at high calcium concentration²²⁸. After replacing Ca(OH)_2 with Mg(OH)_2 as a pH control reagent, the PO_4^{3-} concentration in effluent gradually increased to $106 \pm 5 \text{ mg P L}^{-1}$, and its recovery efficiency reached around 50% again (Figure 2.4b).

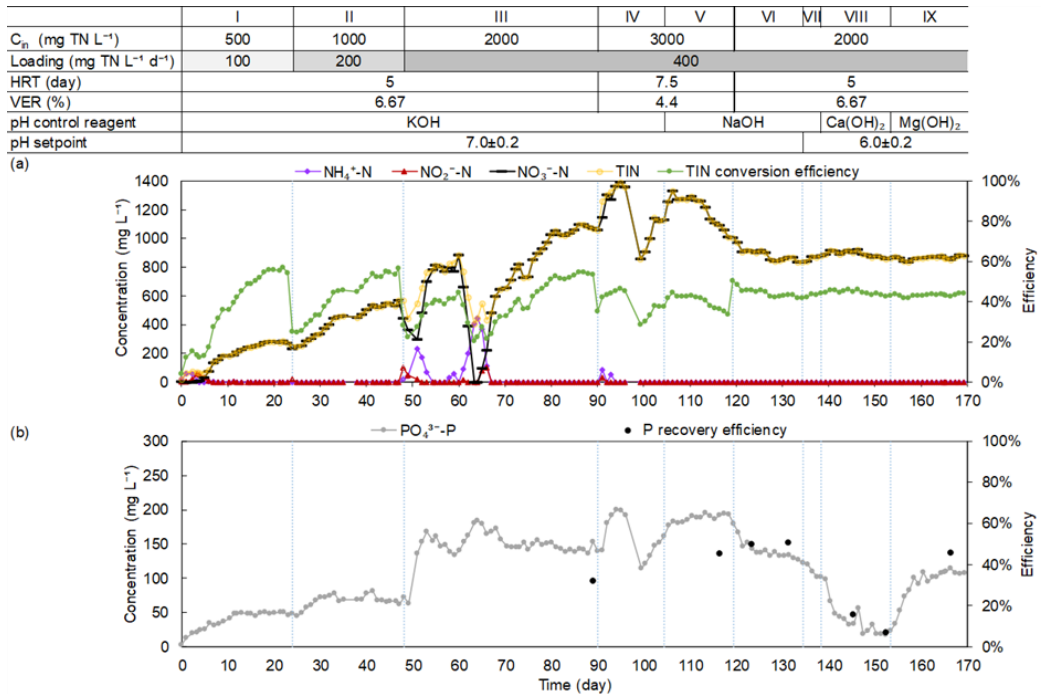


Figure 2.4: The profile of the inorganic nitrogen conversion (a) and phosphate recovery (b) in the effluent of mineralization and nitrification bioreactor from day 0 to day 170. The major variables are shown on top. TIN conversion efficiency and P recovery efficiency represent the concentration ratios of TIN and $\text{PO}_4^{3-}\text{-P}$ in the effluent to TN and TP in the influent, respectively.

From phase I to III, stepwise increasing the TN loading rate could always obtain over 50% TIN production. The decreased $\text{NO}_3^- \text{-N}$ concentration and TIN releasing efficiency (phase V, day 112-119) compared to phase IV (day 90-96) were probably related to the influence of cations (i.e., K^+ and Na^+ from pH reagents) on microbial activity and community. The nitrogen mineralization was suggested to be less tolerant to Na^+ than K^+ ²²⁹. Hence, the decreasing trend of $\text{NO}_3^- \text{-N}$ concentration in phase V was probably due to the switching of pH reagent from KOH to NaOH.

Nevertheless, under the influent loading rate of $400 \text{ mg TN L}^{-1} \text{ d}^{-1}$ at 5-day HRT and SRT, $\text{NO}_3^- \text{-N}$ production efficiency and rate could stabilize in a range of 44-53% and 175-212 $\text{mg N L}^{-1} \text{ d}^{-1}$, respectively. The $\text{NO}_3^- \text{-N}$ production rate in the bioreactor was significantly improved over the long-term operation, compared to the CAB aerobic batch test of 59 $\text{mg N L}^{-1} \text{ d}^{-1}$ (section 3.1). By contrast, mineralization rates of organic fertilizers in soils or growing media were considerably slower (SI Table S2.4). Laboratory incubation of

common organic fertilizers (e.g., thermally-dried biosolids, manures, and composts) in soils only obtained nitrogen mineralization rates in a range of 0.13-1.88 mg N L⁻¹ d⁻¹)²³⁰⁻²³². In most cases, even under these low rates, complete nitrification could not be guaranteed. Previous mineralization tests for CAB realized complete nitrification only at a rate of 5.12 mg N L⁻¹ d⁻¹ in organic growing media⁸⁸. These slow nitrogen transformation rates should mainly be attributed to the relatively low incubation temperature (16-25°C) as well as water and oxygen availability^{233, 234}. Similarly, the carbon mineralization rates in soil incubations were only 36-158 mg CO₂-C L⁻¹ d⁻¹^{235, 236}. Assuming the microbial cell formula is C₅H₇O₂N, the corresponding carbon mineralization rates of CAB were 750-909 mg CO₂-C L⁻¹ d⁻¹ during the NO₃⁻-N production²³⁷. Therefore, the proposed well-controlled bioreactor approach produced liquid nitrate-rich fertilizer more rapidly than was realized in soils. Additionally, the performance of SCOD removal was excellent over the whole operation period, especially the phase V-IX with above 90% removal (SI Figure S2.3), which could benefit the hydroponic cultivation by decreasing the risk of the proliferation of heterotrophic pathogens and biofilms^{213, 238}.

3.2.2 The microbial community in the bioreactor

Three bioreactor samples from days 86, 133, and 161 (i.e., phase III, VI, and IX) were analyzed to identify the active microbial community working on nitrogen mineralization and nitrification (Figure 2.5). The influent CAB sample was regarded as a control group. In all samples, the most predominant genera were aerobic hydrolysis and fermentative bacteria, including *Thermomonas*, *Permianibacter*, and *Acinetobacter*. The relative abundance of these hydrolysis and fermentative bacteria stepwise decreased from 42% of day 86 to 17% of day 161, mainly related to the constant operating conditions (e.g., substrate and DO). The Shannon index of each bioreactor sample decreased from day 86 to 161, indicating that the number of genera decreased during the bioreactor operation. The abundance of *Thermomonas* increased from 4% of day 86 to 14.7% of day 161, while *Permianibacter* and *Acinetobacter* decreased from 28.8% and 9.6% of day 86 to 0.9% and 1.3% of day 161, respectively (Figure 2.5). Yang et al. (2011) revealed that the Shannon index was positively related to the number of utilizable carbon sources²³⁹. Hence, the

observed decreasing species diversity could be related to the unitary organic carbon source (i.e., CAB) provided throughout the 170-day bioreactor operation. Furthermore, the Bray-Curtis dissimilarity between the first sample (day 86) and the following two samples (day 133 and 161) increased from 0.39 to 0.69. Thus, a community shift occurred during the experiment, indicating the inoculum structure may not be as decisive as the operating conditions in shaping the community. The decrease in diversity in bioreactors has been observed previously due to the acclimatization of inoculum to stable and optimized operating conditions^{240, 241}. The decreased abundance of hydrolysis and fermentative bacteria resulted in a slight decrease in nitrogen mineralization efficiency (phase VI-IX) compared to phase III.

The relative abundance of microorganisms correlated with nitrification was relatively low in all bioreactor samples. The total abundance of ammonium oxidizing microbes, including *Nitrosomonas*, *Nitrospira*, and *Candidatus Nitrocosmicus*²⁴², was always less than 1% (Figure 2.5). Only two types of nitrite-oxidizing bacteria (NOB), i.e., *Nitrospira* and *Nitrolancea*, were detected in this study. The relative abundance of NOB in all three bioreactor samples was lower than 0.1%. Besides autotrophic nitrifying microbes, some identified heterotrophic nitrifying bacteria (HNB) were found in this study as well, mainly *Pseudomonas*, *Bacillus*, and *Ochrobactrum*^{243, 244}. Some studies suggested *Acinetobacter* could act as HNB as well^{245, 246}; in this case, the total relative abundance of HNB would reach around 2% to 11%. Over the bioreactor operation, the total relative abundance of these HNB was at around 1%. Among the nitrifying microbes, the autotrophic nitrifying genera failed to occupy a dominant position, probably due to the inhibition effect of high COD concentration²⁴³.

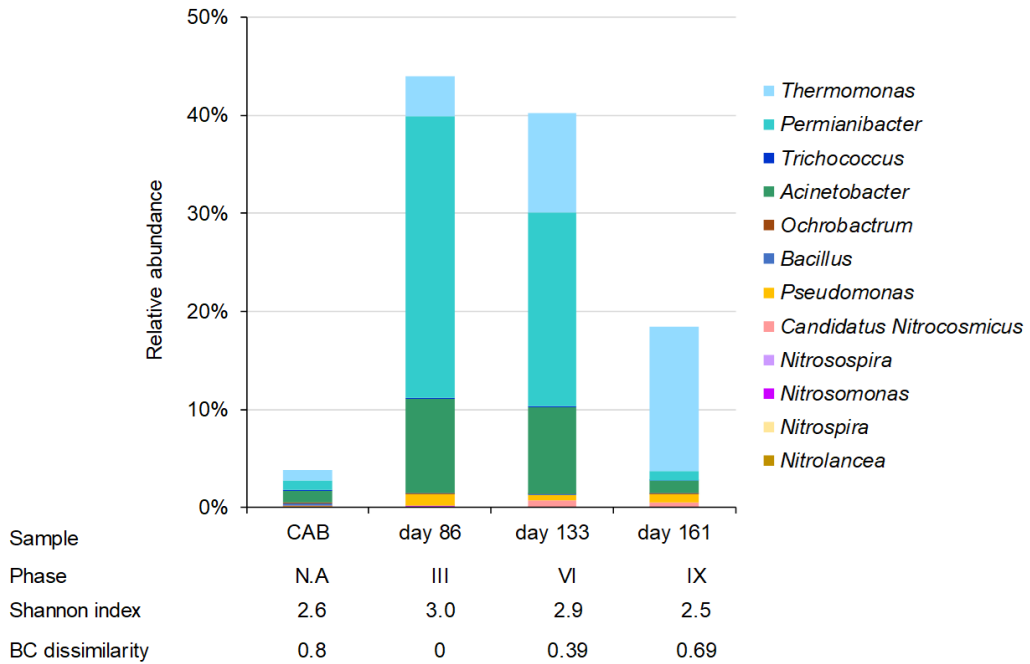


Figure 2.5: The relative abundance of microbes in the mineralization and nitrification bioreactor at genus levels. CAB means the influent composed of CAB. BC dissimilarity represents the Bray-Curtis dissimilarity between day 86 and each other sample.

3.3 Nutrient quality balancing and economic analysis

The nutrient quality balancing was modeled in each BNS organic scenario (i.e., NaOH, $\text{Ca}(\text{OH})_2$, and $\text{Mg}(\text{OH})_2$) according to the proposed balancing strategy (Figure 2.2). Consequently, the sodium concentration of HNS reached 332, 74, and 28 mg Na L⁻¹ in NaOH, $\text{Ca}(\text{OH})_2$, and $\text{Mg}(\text{OH})_2$ scenario, respectively, and the salinity of HNS was 4.4, 3.0, and 2.8 mS cm⁻¹. Since the allowable nonessential element sodium and the salinity should not exceed 180 mg Na L⁻¹ and 4 mS cm⁻¹ ^{15, 247}, the NaOH scenario was evidently out of the ranges.

The Sankey diagrams based on the nutrient mass flow in each section of the $\text{Ca}(\text{OH})_2$ and $\text{Mg}(\text{OH})_2$ organic scenarios are shown in Figure 2.6a and 2.6b. In the bioreactor section, the observed accumulative dosing of $\text{Ca}(\text{OH})_2$ and $\text{Mg}(\text{OH})_2$ until the sampling time (around 14 days) introduced 1656 mg Ca and 552 mg Mg into 1 L bioreactor content, respectively. As a result of the membrane filtration, nutrients are separated into liquid and solid fractions. A share of 57.5% or 1150 mg TN was retained in the solid fraction (i.e.,

retentate), which can be applied to land as a fertilizer. According to the typical microfiltration process, the volume ratio of permeate and primary flow was assumed to be 0.98¹⁰⁹. After the membrane section, soluble nutrients could be recovered in 0.98 L permeate as the BNS. In the nutrient balancing section, element K was the limiting factor of Ca(OH)₂ scenario, and extra NO₃⁻-N (67 mg), P (117 mg), Ca (136 mg), and Mg (164 mg) should be supplemented into the BNS tank (Figure 2.6a). Eventually, after 4.5 times of dilution by H₂O, 4.38 L HNS could be obtained in the Ca(OH)₂ scenario, and the NO₃⁻-N sourced from CAB mineralization accounted for 92.7% of NO₃⁻-N in HNS. While in the Mg(OH)₂ scenario, element Mg was the limiting factor, and the additional NO₃⁻-N (1427 mg), P (231 mg), K (1524 mg), and Ca (2129 mg) were supplemented (Figure 2.6b). After 11.1 times dilution, 10.88L HNS could be obtained for the Mg(OH)₂ scenario. Compared to the Ca(OH)₂ scenario, the proportion of organic-sourced NO₃⁻-N (i.e., NO₃⁻-N_{OG}) in HNS of Mg(OH)₂ scenario was much lower (only 37.4%).

Chapter 2

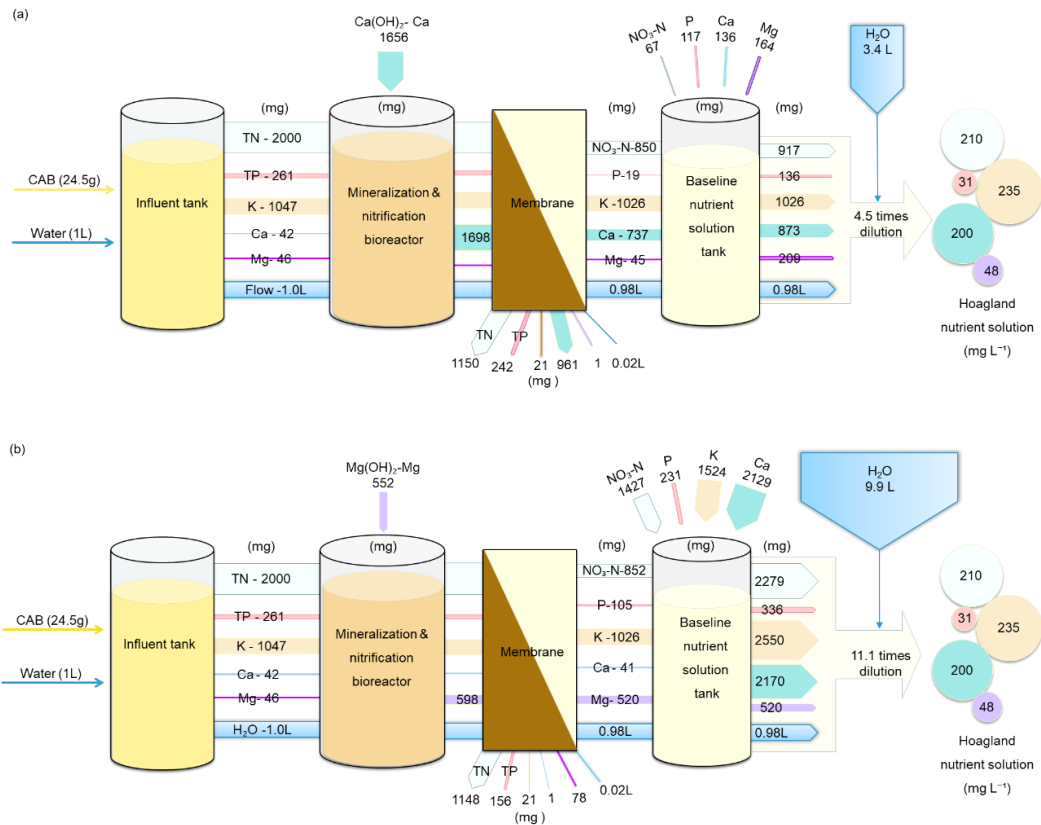


Figure 2.6: Sankey diagram based on the mass of nutrients in different sections of (a) $\text{Ca}(\text{OH})_2$ scenario and (b) $\text{Mg}(\text{OH})_2$ scenario. TN, TP, and HNS mean the total nitrogen, total phosphorus, and Hoagland nutrient solution, respectively.

The costs of nitrate-rich liquid fertilizer production are shown in Table 2.1. All the expenditure was expressed as euro cubic meter of HNS. According to the Sankey diagram in Figure 2.6, approximately 25 g CAB was needed to obtain 1 L BNS. In the $\text{Ca}(\text{OH})_2$ organic scenario, there was roughly 0.19 g NO_3^- - N_{OG} in HNS. Calculated from the stoichiometry of nitrification (i.e., $4.57 \text{ g O}_2 \text{ g}^{-1} \text{ N}$), $0.9 \text{ g O}_2 \text{ L}^{-1}$ HNS was needed. Besides, the O_2 consumption for TCOD removal was around $14.9 \text{ g O}_2 \text{ L}^{-1}$ BNS (SI Figure S2.3), namely $3.3 \text{ g O}_2 \text{ L}^{-1}$ HNS. Based on the average O_2 transfer efficiency and electricity cost, the total aeration cost of 0.25 € m^{-3} HNS could be calculated. According to the microbial cell formula of $\text{C}_5\text{H}_7\text{O}_2\text{N}$, the aerobic mineralization of CAB was assumed to release CO_2 of $15.71 \text{ g g}^{-1} \text{ NO}_3^-$ - N_{OG} ²³⁷. Therefore, around $3.1 \text{ g CO}_2 \text{ L}^{-1}$ HNS could be produced in the $\text{Ca}(\text{OH})_2$ scenario. Since the market price of liquid CO_2 is in a range of 0.08 - 0.15 € kg^{-1} ²⁴⁸,

the HNS produced in the $\text{Ca}(\text{OH})_2$ scenario could save a maximum of 0.46 € m^{-3} for the CO_2 fertilization. As a result of the lower NO_3^- - N_{OG} concentration in the $\text{Mg}(\text{OH})_2$ organic scenario (around 0.08 g L^{-1} HNS), the total aeration cost and CO_2 fertilization saving were only 0.1 and 0.18 € m^{-3} HNS, respectively. In addition, assuming 1 m^{-3} bioreactor effluent delivered to the membrane module (0.36 - 1.25 € m^{-3}) can cost at least 0.37 € m^{-3} HNS, after final dilution, the cost of HNS would be 0.08 and 0.03 € m^{-3} for $\text{Ca}(\text{OH})_2$ and $\text{Mg}(\text{OH})_2$ scenario, respectively.

Among the three cost categories, the cost of CAB dominated the total costs of the organic scenarios, while chemical costs were four to seven orders of magnitude lower than that of fertilizers for either of the suppliers investigated (SI Table S2.3). The total expenses of commercial scenarios only included the costs of fertilizer and supplemented compounds. As a result, the costs of YaraTrea and FloraFlex scenarios were 1 and 34 € m^{-3} HNS, respectively. The cost of the chemicals-only blending scenario was the lowest ($0.000\ 017$ or $0.000\ 018 \text{ € m}^{-3}$ HNS), highlighting that the cost of the organic fertilizer dominates the total costs of the proposed concept.

In Table 2.1, the total costs of the $\text{Ca}(\text{OH})_2$ scenario were 2.5-fold the $\text{Mg}(\text{OH})_2$ scenario, due to its higher NO_3^- - N_{OG} proportion. Compared to the commercial scenarios, the total costs of the $\text{Ca}(\text{OH})_2$ scenario was 5.5-fold of the YaraTera scenario, but only 0.16-fold the FloraFlex scenario, indicating its potential to be cost-competitive in hydroponic fertilization.

Table 2.1: The cost categories for preparing Hoagland nutrient solution (HNS). “BNS” means the baseline nutrient solution. “N.A.” means the operation was not applicable. The costs of chemical compound supplementation were based on the market reference prices from two global suppliers (i.e., Alibaba or EC21, details in SI Table S2.3).

| Cost category | | Ca(OH) ₂ organic scenario | Mg(OH) ₂ organic scenario | YaraTera | FloraFlex | Blending chemicals only scenario |
|-----------------------------------|---|--------------------------------------|--------------------------------------|----------------------------|------------------------|----------------------------------|
| CAB or commercial fertilizer | g CAB L ⁻¹ BNS | 25.0 | 25.0 | | N.A. | |
| | € m ⁻³ HNS | 5.6 | 2.3 | 1.0 | 34 | N.A. |
| Aeration | g NO ₃ ⁻ -N _{OG} L ⁻¹ HNS | 0.19 | 0.08 | | | |
| | g O ₂ L ⁻¹ HNS (nitrification) | 0.9 | 0.4 | | | |
| | g O ₂ L ⁻¹ HNS (COD removal) | 3.3 | 1.3 | | N.A. | |
| | € m ⁻³ HNS | 0.25 | 0.1 | | | |
| CO ₂ production | g CO ₂ L ⁻¹ HNS | 3.1 | 1.2 | | | |
| | € m ⁻³ HNS (CO ₂ fertilization) | -0.46 | -0.18 | | | |
| Chemical compound supplementation | € m ⁻³ HNS | 0.000 066 or 0.000 011 | 0.000 15 or 0.000 14 | 0.000 005 9 or 0.000 006 8 | 0.000 003 or 0.000 004 | 0.000 018 or 0.000 017 |
| Membrane module | € m ⁻³ HNS | 0.08 | 0.03 | | N.A. | |
| Total costs | € m ⁻³ HNS | 5.48 | 2.23 | 1.0 | 34 | 0.000 018 or 0.000 017 |

4. Conclusion

This study delivered a proof of concept for an approach based mainly on a bioreactor and a nutrient balancing step to produce a nitrate-rich liquid fertilizer from a solid organic fertilizer. In all the batch tests, CAB mineralization performance outcompeted that of BAPN. The higher temperature (35°C) could always result in higher mineralization rates. Aerobic conditions could achieve higher mineralization efficiency compared to anaerobic tests. The nitrification performance of the microbial fertilizer at 35°C could reach an efficiency above 90% and a maximum rate of $59 \text{ mg N L}^{-1} \text{ d}^{-1}$, while completely oxidizing the released $\text{NH}_4^+\text{-N}$ to $\text{NO}_3^-\text{-N}$. Subsequently, 35°C was chosen to operate a bioreactor, reaching a nitrate production rate of $212 \text{ mg N L}^{-1} \text{ d}^{-1}$, yet at a lower efficiency of 51%. According to nutrient balance estimation to simulate the Hoagland nutrient solution, the Ca(OH)_2 scenario was recommended due to a higher proportion of organically sourced $\text{NO}_3^-\text{-N}$ (92.7%) than Mg(OH)_2 scenario. The CO_2 generated in the bioreactor can be used for greenhouse CO_2 fertilization and lower the total costs. The Hoagland solution produced from the microbial fertilizer is potentially cost-competitive compared to the commercially available inorganic fertilizer nutrient solution (5.48 or 2.23 versus 34 € m^{-3} in total costs).

5. Supplementary information

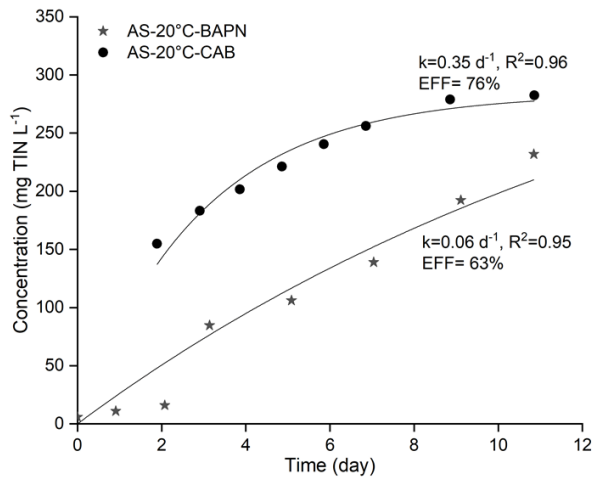


Figure S2.1: Performance evaluation of batch tests: aerobic mineralization with AS at 20 °C on BAPN and CAB; “k” is the kinetic rate constant. “EFF” means the mineralization efficiency.

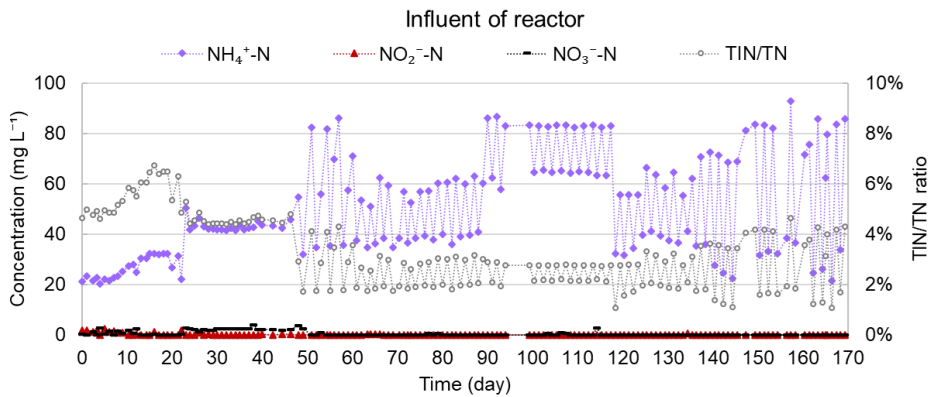


Figure S2.2: Inorganic nitrogen species in the influent of the bioreactor. TIN/TN represents the ratio of the total inorganic nitrogen and the total nitrogen of influent.

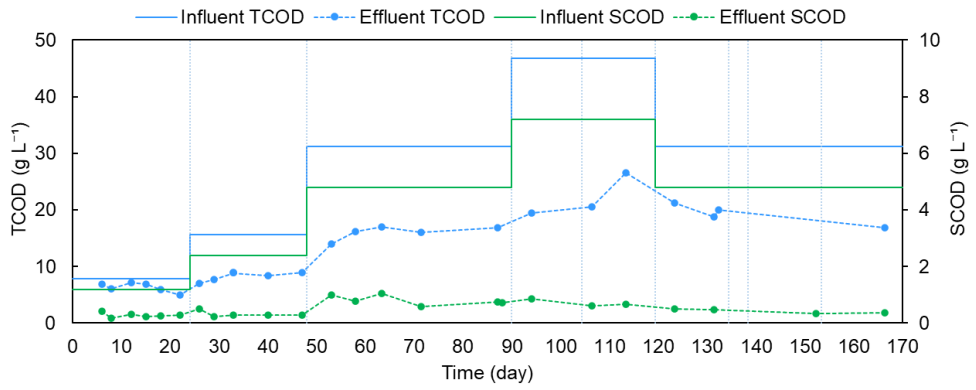


Figure S2.3: The profile of COD in the influent and effluent of the bioreactor.

Table S2.1: Reagents, formula, representative market price, and water solubility of commonly used compounds for making nutrient solutions.

| Chemical candidates | | Market reference price (excl. VAT) | | Price for calculation | Solubility in water ²⁴⁹ |
|---|--|------------------------------------|------------|-----------------------|------------------------------------|
| | | (alibaba.com) | (ec21.com) | (Alibaba/ EC21) | (20°C) |
| Reagent | Chemical formula | (€ ton ⁻¹) | | (€ kg ⁻¹) | (g L ⁻¹) |
| Potassium Hydroxide | KOH | 294-882 | 336-1386 | 0.29/ 0.34 | 1120 |
| Sodium Hydroxide | NaOH | 195-326 | 244-672 | 0.20/ 0.24 | 1110 |
| Magnesium Hydroxide | Mg(OH) ₂ | 462-840 | 424-509 | 0.46/ 0.42 | 8.2 |
| Calcium Hydroxide | Ca(OH) ₂ | 50-84 | 85-186 | 0.05/ 0.09 | 1.73 |
| Magnesium Sulphate heptahydrate | MgSO ₄ ·7H ₂ O | 42-126 | 59-109 | 0.04/ 0.06 | 1130 |
| Calcium Sulfate | CaSO ₄ | 185-420 | 280-424 | 0.19/ 0.28 | 2 |
| Potassium Sulfate | K ₂ SO ₄ | 336-378 | 395-412 | 0.34/ 0.40 | 111 |
| Monopotassium Phosphate | KH ₂ PO ₄ | 503-924 | 672-1047 | 0.50/ 0.67 | 226 |
| Dipotassium phosphate | K ₂ HPO ₄ | 672-1008 | 848-1310 | 0.67/ 0.85 | 1493 |
| Calcium Dihydrogen Phosphate | Ca(H ₂ PO ₄) ₂ | 254-381 | 983-1000 | 0.25/ 0.98 | 20 |
| Magnesium hydrogen phosphate trihydrate | MgHPO ₄ ·3 H ₂ O | 1271-2543 | 1270-1700 | 1.27/ 1.27 | 0.25 |
| Calcium Nitrate Tetrahydrate | Ca(NO ₃) ₂ ·4H ₂ O | 168-252 | 210-218 | 0.17/ 0.21 | 1290 |
| Magnesium Nitrate hexahydrate | Mg(NO ₃) ₂ ·6H ₂ O | 242-305 | 168-210 | 0.24/ 0.17 | 733 |
| Potassium Nitrate | KNO ₃ | 551-661 | 294-672 | 0.55/ 0.29 | 316 |
| Ammonium Nitrate | NH ₄ NO ₃ | 178-220 | 203-338 | 0.18/ 0.20 | 1900 |

| | | | | | |
|-------------------------|-------------------|--------|---------|------------|-----|
| Calcium Chloride | CaCl ₂ | 76-126 | 101-126 | 0.08/ 0.10 | 745 |
|-------------------------|-------------------|--------|---------|------------|-----|

Table S2.2: Nutrient composition and price of commercial inorganic fertilizers.

| Commercial inorganic fertilizers | Nutrient Composition (g kg ⁻¹) | | | | | | Price (€ kg ⁻¹ , excl VAT) | Website |
|-------------------------------------|--|-----|-----|-----|----|----------------------------------|--|---|
| | NO ₃ ⁻ -N | P | K | Ca | Mg | SO ₄ ²⁻ -S | | |
| YaraTera Kristalon Scarlet | 75 | 52 | 299 | 0 | 27 | 40 | 1.72 | https://www.yara.co.uk/crop-nutrition/fertiliser/soluble/yaratera-kristalon-scarlet/ |
| Floraflex B1™/B2™ | B1™ | 135 | 0 | 183 | 70 | 0 | 25 | https://floraflex.com/product/bloom-nutrients-combo-b1-b2/ |
| | B2™ | 0 | 122 | 149 | 0 | 70 | 110 | |

Table S2.3: Compound-supplementation design and cost calculation of different scenarios in stable periods.

| Control scenario | | NO₃⁻-N | P | K | Ca | Mg | Remark |
|---|---------------------------------------|--|--|---|---------------------------------|--------------------------------|--|
| HNS | (mg L ⁻¹ H ₂ O) | 210 | 31 | 235 | 200 | 48 | Element Na and EC in SNS: <ul style="list-style-type: none"> • 41 mg Na L⁻¹, v • EC: 3.0 mS cm⁻¹, v |
| Compounds for making HNS | | Ca(NO ₃) ₂ ·4H ₂ O | Mg(NO ₃) ₂ ·6H ₂ O | KNO ₃ | K ₂ HPO ₄ | K ₂ SO ₄ | |
| | (mg L ⁻¹ H ₂ O) | 1180.0 | 512.0 | 101.1 | 174.2 | 263.2 | |
| Cost (€) | | 3.6×10 ⁻⁹ / ₉ | 1.9×10 ⁻⁹ / ₉ | 5.5×10 ⁻⁹ / ₉ / 2.9×10 ⁻⁹ | 3.9×10 ⁻⁹ / / | 2.9×10 ⁻⁹ / / | |
| | | 4.5×10 ⁻⁹ / ₉ | 1.3×10 ⁻⁹ / ₉ | | 4.9×10 ⁻⁹ | 3.4×10 ⁻⁹ | |
| Cost (€ m⁻³ HNS) | | 0.000 018/ 0.000 017 | | | | | |
| YaraTera Kristalon Scarlet | | NO₃⁻-N | P | K | Ca | Mg | Nutrient cost (Scarlet 1 kg m⁻³)* |
| Concentration | (mg L ⁻¹ H ₂ O) | 75 | 52 | 299 | 0 | 27 | * Optimal concentration to minimize extra supplementation. Element Na and EC after dilution: <ul style="list-style-type: none"> • 41 mg Na L⁻¹, v • EC: 2.7 mS cm⁻¹, v |
| Compounds as supplementation | | Ca(NO ₃) ₂ ·4H ₂ O | Mg(NO ₃) ₂ ·6H ₂ O | MgSO ₄ ·7 H ₂ O | K ₂ SO ₄ | | |
| | (mg L ⁻¹ H ₂ O) | 1994 | 396 | 174 | 220 | | |
| Cost (€ m ⁻³ H ₂ O) | | 6.0×10 ⁻⁶ / ₆ | 1.5×10 ⁻⁶ / ₆ | 1.2×10 ⁻⁷ / ₆ / 1.7×10 ⁻⁷ | 2.4×10 ⁻⁶ / / | 2.9×10 ⁻⁶ | 1.7 |
| Diluting time(s) | (to HNS) | 1.7 | | | | | |
| Cost (€ m⁻³ HNS) | | 1.0/ 1.0 | | | | | |
| FloraFlex B1+B2 | | NO₃⁻-N | P | K | Ca | Mg | Nutrient cost (1.1 kg B1+ 0.3 kg B2 m⁻³)** |
| Concentration | (mg L ⁻¹ H ₂ O) | 145.8 | 31.0 | 235.0 | 75.6 | 17.8 | ** Optimal combination to minimize extra supplementation. |
| | | | | | | | Element Na and EC after |

Chapter 2

| | | | | | | | | | |
|--|------------------------------------|--|---------------------------------------|---|--------------------------------------|--------------------------------------|---|--|--|
| Compounds as supplementation | | Ca(NO ₃) ₂ ·4H ₂ O | CaSO ₄ | MgSO ₄ ·7H ₂ O | | | | | dilution: |
| (mg L ⁻¹ H ₂ O) | | 541 | 111 | 310 | | | | | <ul style="list-style-type: none"> • 41 mg Na L⁻¹, v • EC: 2.7 mS cm⁻¹, v |
| Cost (€ m ⁻³ H ₂ O) | | 1.6×10 ⁻⁶ / ₆ | 1.1×10 ⁻⁶ / ₆ | 2.2×10 ⁻⁷ / _{3.0×10⁻⁷} | | | 34.1 | | |
| Diluting time(s) | (to HNS) | | | 1.0 | | | | | |
| | Cost (€ m⁻³ HNS) | | | | | | 34.1/ 34.1 | | |
| NaOH organic scenario (day 135-137) | | NO₃⁻-N | P | K | Ca | Mg | Cumulative dosage of base | Nutrient cost (kg CAB m⁻³) | |
| Concentration | (mg L ⁻¹ BNS) | 863 | 111 | 1047 | 42 | 46 | | | Element Na and EC after dilution: |
| Compounds as supplementation | | Ca(NO ₃) ₂ ·4H ₂ O | CaSO ₄ | Ca(H ₂ PO ₄) ₂ | CaCl ₂ | MgSO ₄ ·7H ₂ O | NaOH | | <ul style="list-style-type: none"> • 332 mg Na L⁻¹, X • EC: 4.4 mS cm⁻¹, X |
| (mg L ⁻¹ BNS) | | 615 | 2094 | 103 | 309 | 1721 | 2005 | | |
| Cost (€ m ⁻³ BNS) | | 1.9×10 ⁻⁶ / ₆ | 2.1×10 ⁻⁵ / ₅ | 4.8×10 ⁻⁷ / _{1.8×10⁻⁶} | 1.9×10 ⁻⁶ / _/ | 1.2×10 ⁻⁶ / _/ | 2.4×10 ⁻⁴ / _{3.1×10⁻⁴} | 25 | |
| Diluting time(s) | (to HNS) | | | 4.5 | | | | | |
| | Cost (€ m⁻³ HNS) | | | | | | 5.6/ 5.6 | | |
| Ca(OH)₂ organic scenario (day 150-152) | | NO₃⁻-N | P | K | Ca | Mg | | Nutrient cost (kg CAB m⁻³) | |
| Concentration | (mg L ⁻¹ BNS) | 867 | 19 | 1047 | 752 | 46 | | | Element Na and EC after dilution: |
| Compounds as supplementation | | Ca(NO ₃) ₂ ·4H ₂ O | MgHPO ₄ ·3H ₂ O | CaSO ₄ | MgSO ₄ ·7H ₂ O | | Ca(OH) ₂ | | <ul style="list-style-type: none"> • 74 mg Na L⁻¹, v • EC: 3.0 mS cm⁻¹, v |
| (mg L ⁻¹ BNS) | | 575 | 671 | 140 | 772 | | 28866 | | |
| Cost (€ m ⁻³ BNS) | | 1.7×10 ⁻⁶ / ₆ | 2.8×10 ⁻⁵ / ₅ | 1.4×10 ⁻⁶ / _{2.1×10⁻⁶} | 5.4×10 ⁻⁷ / _/ | | 2.6×10 ⁻⁴ / _{4.5×10⁻⁴} | 25 | |

Chapter 2

| | | | | | | | | |
|--|------------------------------------|--|--|--|--|-----------|--|---|
| | | 2.2×10^{-6} | 2.8×10^{-5} | | 7.5×10^{-7} | | | |
| Diluting time(s) | (to HNS) | | | | | | | 4.5 |
| | Cost (€ m⁻³ HNS) | | | | | | | 5.6/ 5.6 |
| Mg(OH)₂ organic scenario (day 163-165) | | NO₃⁻-N | P | K | Ca | Mg | | Nutrient cost (kg CAB m⁻³) |
| Concentration | (mg L ⁻¹ BNS) | 869 | 107 | 1047 | 42 | 531 | | Element Na and EC after dilution: |
| Compounds as supplementation | | Ca(NO ₃) ₂ ·4H ₂ O | K ₂ HPO ₄ | K ₂ SO ₄ | CaSO ₄ | | Mg(OH) ₂ | <ul style="list-style-type: none"> • 28 mg Na L⁻¹, v • EC: 2.8 mS cm⁻¹, v |
| | (mg L ⁻¹ BNS) | 12274 | 1326 | 2143 | 312 | | 11159 | |
| | Cost (€ m ⁻³ BNS) | 3.7×10^{-5} / 4.6×10^{-5} | 2.9×10^{-5} / 3.7×10^{-5} | 2.4×10^{-5} / 2.8×10^{-5} | 3.1×10^{-6} / 4.7×10^{-6} | | 1.5×10^{-3} / 1.4×10^{-3} | 25 |
| Diluting time(s) | (to HNS) | | | | | | | 11.1 |
| | Cost (€ m⁻³ HNS) | | | | | | | 2.3/ 2.3 |

Table S2.4 The nitrogen and carbon mineralization performance of organic fertilizers in literature and this study. “N.A.” means data are not available.

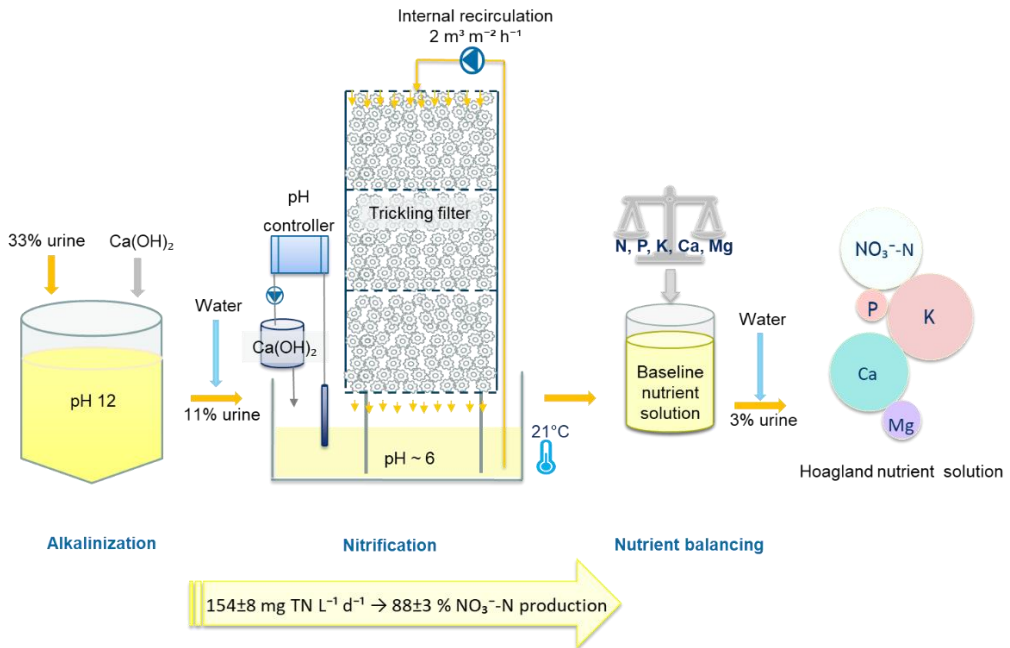
| Bioconversion | Scenario | Organic fertilizer type | Incubation temperature (°C) | Incubation water-holding capacity (%) | Mineralization rate (average, mg L ⁻¹ d ⁻¹) | Reference |
|-----------------|------------------------|--|-----------------------------|---------------------------------------|---|----------------|
| Nitrogen | Soil | Thermally-dried biosolids | 25 | N.A. | 0.63-1.88 (NO ₃ ⁻ -N) | ²³⁰ |
| | | cattle manure, compost, green manure | 20 | 55 | 0.47-1.37 (NH ₄ ⁺ -N & NO ₃ ⁻ -N) | ²³¹ |
| | | Plant/ manure composts, granular fertilizers | 23 | 60 | 0.13-1.46 (NH ₄ ⁺ -N & NO ₃ ⁻ -N) | ²³² |
| | Organic growing medium | Microbial fertilizer (CAB) | 16±2.7 | N.A. | 5.12±0.81 (NO ₃ ⁻ -N) | ⁸⁸ |
| | Controlled bioreactor | CAB | 35 | Liquid | 175-212 (NO ₃ ⁻ -N) | This study |
| Carbon | Soil | Compost, hen manure | 25 | 60 | 36-87 (CO ₂ -C) | ²³⁵ |
| | | Cattle manure | 25 | 60 | 158 (CO ₂ -C) | ²³⁶ |
| | Controlled bioreactor | CAB | 35 | Liquid | 750-909 (CO ₂ -C) | This study |

6. Acknowledgments

This work was supported by the China Scholarship Council (File No. CSC201706130131). The authors would like to thank: (i) company Avecom (Wondelgem, Belgium) for the CAB supply, (ii) Veerle Van Malderen for her insightful discussions, (iii) dr. Tim Van Winckel (University of Antwerp), dr. Pieter Joos (Water-link; University of Antwerp) and Els Van Meenen (Water-link) for their help with metal measurements via ICPMS in the Water-link laboratory (Rumst, Belgium), and (iv) dr. Wannes Van Beeck for his assistance with DNA extraction.

Chapter 3

A nitrification trickling filter as key to produce hydroponic nutrient solutions from real urine



Publication of a redrafted version of this chapter is intended:

Xie, Y.; Jia, M.; Timmer, M. J.; De Paepe, J.; Spiller, M.; Vlaeminck, S. E., A nitrification trickling filter as key to produce hydroponic nutrient solutions from real urine. (In preparation)

Abstract

As a major stream of nitrogen mass flow in domestic wastewater, urine is widely available and rich in valuable nutrient resources for agricultural plant production. In this study, a novel concept consisting of urine collection, alkalization, nitrate (NO_3^- -N) production, and further nutrient supplementation to completely fulfill plant requirements was proposed as meaningful progress towards sustainable agriculture. The NO_3^- -N production from real human urine was explored in a trickling filter (TF) for the first time. The full nitrification of alkalized real urine to nitrate was realized in the pH-controlled TF by calcium hydroxide ($\text{Ca}(\text{OH})_2$) at around pH 6 and 21°C. The TF could handle different urine collection batches and maintain relatively stable nitrification performance, with NO_3^- -N production efficiency and rate of $88\pm 3\%$ and $136\pm 4 \text{ mg N L}^{-1} \text{ d}^{-1}$, respectively. The optimal hydraulic loading rate to realize this nitrification performance was $2 \text{ m}^3 \text{ m}^{-2} \text{ h}^{-1}$, with an estimated electricity consumption of $1.8 \text{ kWh kg}^{-1} \text{ NO}_3^-$ -N. Ammonium oxidation was the rate-limiting process. Additionally, high COD removal efficiency ($\geq 94\pm 3\%$) was always realized in the nitrification TF. This work showcases the triple advantages of $\text{Ca}(\text{OH})_2$ in urine alkalization, full nitrification, and macronutrient supplementation.

1. Introduction

Increasing resource use efficiency is a primary step towards sustainable agriculture. Compared to conventional soil-based agriculture, the greenhouse hydroponic system could realize up to 90% water and 85% nutrient saving²⁰. Nitrogen (N), as a key nutrient element for crop growth, mainly comes from synthetic chemical fertilizers via the Haber-Bosch process¹⁹⁸. However, in the past decades, the massive manufacture of artificial N fertilizers has aggravated air pollution and global climate change, and further threatened human health¹⁹⁹. Therefore, substituting less-damaging N nutrients for synthetic N becomes another effort to develop sustainable agriculture²⁵⁰.

Urine is widely available on the Earth, containing the majority of nutrients present in human excreta: 80–90% of the nitrogen (N), 55-67% of phosphorus (P), and 50–80% of potassium (K)²⁵¹. As a relatively concentrated solution (i.e., up to 9 g N L⁻¹, 0.7 g P L⁻¹, and 2 g K L⁻¹), urine contributes for 70-80% of N, 40-56% of P, and 60-63% of K load in domestic wastewater, but less than 1% of volume^{252, 253}. Therefore, recovering those nutrients from urine may shorten nutrient cycles on the Earth, lessen the ecological burden of fertilizer production, and lower the nutrient loads and costs of domestic wastewater treatment^{251, 254}.

Separating urine at the source is a practical approach to recover nutrients from wastewater²⁵⁵. Urea, as a dominant nitrogen form in fresh urine, can be readily hydrolyzed into ammonia (NH₃) or ammonium (NH₄⁺) and bicarbonate (HCO₃⁻) by bacterial urease, causing a pH increase²⁵⁶. Consequently, during the storage, transport, and application of urine, nitrogen can volatilize as free ammonia (FA), causing significant N losses and environmental and health concerns^{257, 258}. On the other hand, since nitrate (NO₃⁻-N) is the preferent N nutrient for most plants¹⁶, the direct use of hydrolyzed urine as a medium for hydroponic plant production is phytotoxic due to its high ammonia concentration²⁰¹. Moreover, control strategies, such as heat treatment, UV radiation, and membrane filtration, are commonly used to avoid nuisances of fungal and bacterial pathogens such as *Fusarium spp.* and *Escherichia coli*^{213, 214}. Thus, the nitrification capacity of hydroponic systems could be pretty limited. Overall, the direct use of

hydrolyzed urine in hydroponic systems would limit plant growth due to the deficiency of NO_3^- -N.

All the challenges mentioned above indicate the necessity for urine treatment before applying to hydroponics. To this end, urine alkalization is considered a practical approach to prevent N loss via urea hydrolysis during storage and transport ²⁵⁹. The corresponding pH increase could even inactivate the potential viruses and pathogens in urine ²⁵⁹. Subsequently, urine nitrification can be used to transform NH_4^+ -N (from urea urease) to bioavailable NO_3^- -N for plants. During the urine nitrification process, alkalinity is needed to counteract the proton released by nitritation (about 2 mol alkalinity per mol NH_4^+ -N) ²⁶⁰. However, urea hydrolysis only releases 1 mol alkalinity per mol NH_4^+ -N, allowing only half nitrification without base addition. Therefore, both urine alkalization and nitrification require base addition. As a common base, sodium hydroxide (NaOH , about 0.61 € kg^{-1} OH^-) was employed in most studies (Table 3.1). Although dosing NaOH could facilitate reactor operation at stable pH, sodium (Na), as a nonessential element for plant growth, can only increase the salinity of the produced nutrient solution ¹⁵. In contrast, calcium hydroxide ($\text{Ca}(\text{OH})_2$), as a cheap base (about 0.37 € kg^{-1} OH^-), could provide calcium that is also a critical macronutrient for plant growth ¹⁵, while effectively stabilize fresh urine in a pH range of 11 and 13 ²⁵⁹.

Urine nitrification has been implemented in various bioreactors under different urine types, total nitrogen (TN) loading, pH, temperature, and hydraulic retention time (HRT) conditions (Table 3.1). Compared to the suspended growth systems (e.g., SBR), the attached growth (biofilm) systems, such as moving bed biofilm reactor (MBBR), and membrane-aerated biofilm reactor (MABR), were preferred in most literature, probably due to the advantages of easy biomass retention, high HRT feasibility, and the robustness against external physicochemical and biological stresses ¹⁷⁶. Besides those primary advantages, trickling filters (TFs) commonly require lower operational complexity and maintenance compared to other biofilm systems. More importantly, the passive aeration approach of TFs could avoid energy consumption by aeration pumps in other nitrification systems. Bornemann et al. (2015) and Bornemann et al. (2018) investigated the

nitrification process of unhydrolyzed synthetic urine in TFs, applying pumice grains as the filter material and mussel shells as a buffer^{261, 262}. However, the high temperature (about 30°C) and long HRT (23-128 d) could not guarantee high final nitrification efficiency. Additionally, the extremely low pH of nitrified urine (around pH 3) cannot satisfy the requirement of plant growth in practice (pH 5.5-6.5)²⁶³. Compared to synthetic urine, the composition of the real urine is complex and fluctuant, depending on individuals and their daily diet⁶⁴, and may thus induce different nitrification behaviors. Nevertheless, to our best knowledge, nitrification tests using real urine in TFs have not been reported yet.

This study proposed a novel concept of a controlled urine nitrification TF that can be in-situ integrated into hydroponic systems (Figure 3.1). The proposed concept consists of three sections: (i) fresh urine alkalinization, (ii) urine nitrification in TF for producing nitrate-rich nutrient solution, (iii) nutrients balancing for direct application in hydroponic systems. Since the suggested pH range for most hydroponic solutions is between 5.8 and 6.5¹⁵, the pH of the TF was controlled at around 6 to sustain nitrification while minimizing the need for further pH adjustment. The phosphate ($\text{PO}_4^{3-}\text{-P}$) recovery, chemical oxygen demand (COD) removal, and optimal hydraulic loading rate (HLR) during the urine nitrification were studied as well.

Table 3.1: Overview of typical urine nitrification processes tested in the literature. SBR: sequencing batch reactor, MBR: membrane bioreactor, MBBR: moving bed biofilm reactor, MABR: membrane-aerated biofilm reactor, MEC: microbial electrolysis cell, PBBR: packed-bed bioreactor, TF: trickling filter, N.A.: not available. HR-urine: hydrolyzed real urine; UR-urine: unhydrolyzed real urine; US-urine: unhydrolyzed synthetic urine.

| Reactor | | | Influent | | | Effluent | | | Reference |
|---------------------|---------------|-----------|----------|-----------------------------|---|--|-------------------|--------------------|----------------|
| Growth mode | Type | pH | Type | TN (mg L ⁻¹) | Loading (mg N L ⁻¹ d ⁻¹) | Product | Nitrification (%) | COD removal (%) | |
| Suspended growth | SBR | 7.3-7.6 | HR-urine | 1500 | 1100 | NaNO ₃ | 99.6±0.2 | 89.2±1.1 | ²⁶⁴ |
| | MBR | 6.9 - 7.1 | | 6300 | 225 ± 33 | NaNO ₃ | 95 | 96 | ²⁶⁵ |
| | MBBR | 6.7-6.8 | | 1080 & 2160 | 215 | NaNO ₃ | 92 | 92 | ²⁶⁶ |
| Attached growth | MEC & MABR | 6.85 | UR-urine | 760 & 1850 | 129 & 247 | NaNO ₃ | 100 | 85 | ²⁶⁷ |
| | PBBR | 8 | US-urine | 650 | 46.5 | NaNO ₃ | 94.9±1 | N.A. | ²⁶⁸ |
| | TF | 3-8 | | 520 & 1555 | 93 & 229 | CaNO ₃ | 90 & 81 | N.A. | ²⁶¹ |
| | TF | 3-9 | | 3110-7780 | 304-409 | CaNO ₃ & NH ₄ NO ₃ | 59-97 | N.A. | ²⁶² |
| | TF | 7-6 | | UR- & US-urine | 685±38 | 50-176 | CaNO ₃ | 80-98.7 | 94-98 |

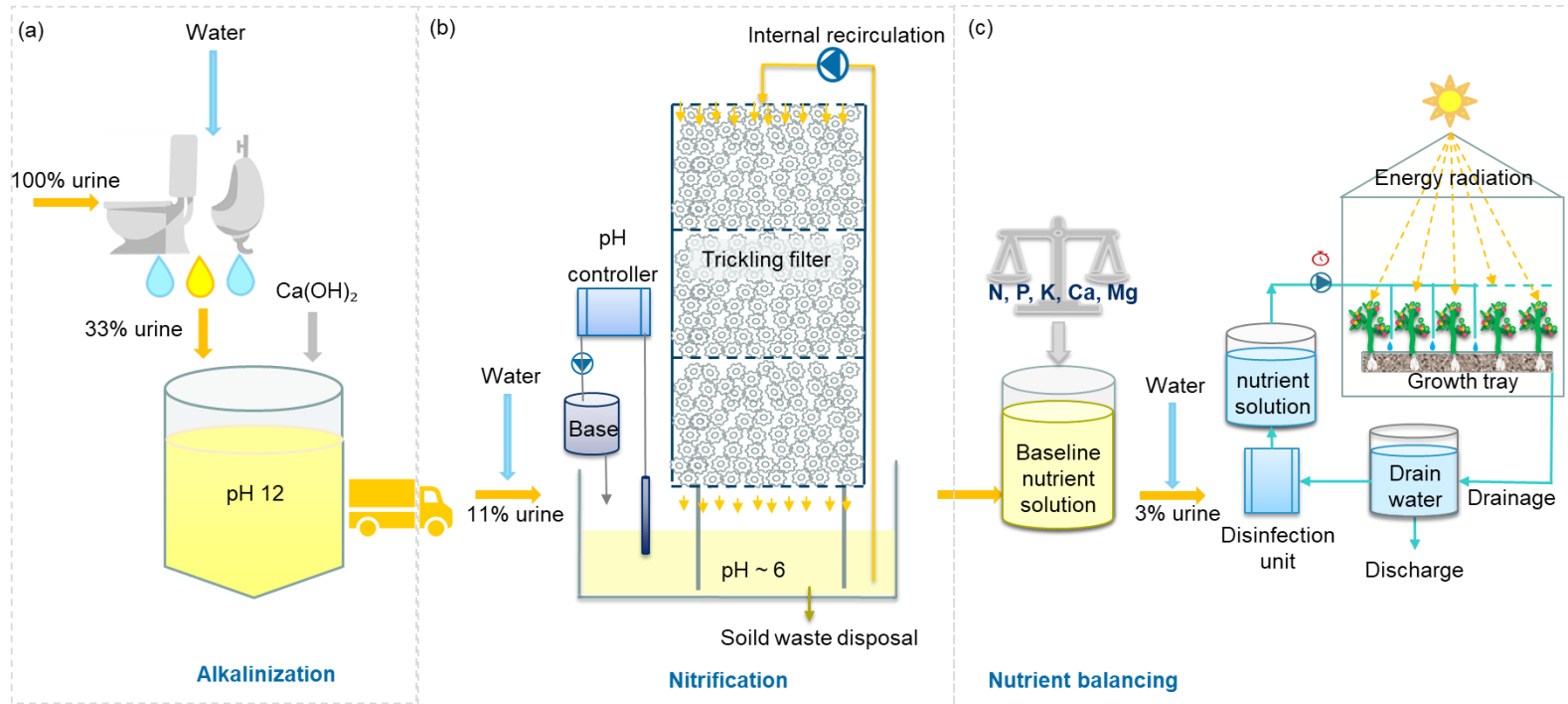


Figure 3.1: A concept of nutrient recovery from urine to a nitrate-rich fertilizer solution: (a) fresh urine collection and alkalization, (b) nitrate-rich (i.e., baseline) nutrient solution production from trickling filter system, (c) suitable fertilizer solution for hydroponic cultivation in a greenhouse. “X%” urine means the urine volume in a water-diluted solution.

2. Materials and methods

2.1 Urine collection and alkalization

Fresh urine from healthy male donors was collected using 0.8 L polyethylene buckets and stored for a maximum of 12h at 4°C to prevent urea hydrolysis before the alkalization treatment. Urine collection was approved by the Ethical Committee of the University of Antwerp (registration number B3002021000034). The urine was diluted with tap water (33.3 vol% urine; 66.6 vol% water), simulating the diluting effect of flush water in urine-diverting toilets ²⁶⁹. The 3-fold diluted urine was further alkalized with 1.4 ± 0.2 g $\text{Ca}(\text{OH})_2 \text{ L}^{-1}$, resulting in a pH increase to around 12 (20°C). The alkalized urine was then stored at 4°C before being fed into the TF. After urine alkalization, precipitation occurred, attributed to the calcium and magnesium salts triggered by pH increase ²⁵⁹. Ten collection batches (NO.1-10) were obtained, and key components of each batch were shown in SI Figure S3.2.

2.2 Bioreactor setup

The bioreactor system consists of an influent tank and a TF reactor. The precipitates triggered by the alkalization treatment were homogenized in the influent tank and fed into the reactor.

2.2.1 Reactor operation

The TF was built from polyvinyl chloride cylinders with an inner diameter of 10.4 cm. The TF was 156 cm in height and consisted of three separate compartments, each 52 cm in height. The total volume of the TF was 13.2 L. The TF was filled with Kaldnes K1 carriers, which had a high specific surface of $950 \text{ m}^2 \text{ m}^{-3}$ and porosity of 84%. At the top of the TF, a 6-channel dripping system was installed to distribute the urine homogeneously over the carrier material. At the bottom of the TF, a 5 L reservoir was installed. The urine was recycled from the reservoir to the top of the TF.

The TF system was operated in a temperature-controlled room at 21 ± 1 °C and equipped with timer-controlled influent and effluent pumps (Seko peristaltic pumps, PR7). The reactor was run in 12 cycles d^{-1} , including 8-25 min continuous feeding and 4 min decanting in each cycle. The flow rate of the influent pump was fixed at 10 ml min^{-1} limited

by the pump capacity. When the TN loading rate increased, the feeding time was prolonged to minimize the pH peak caused by the high pH of the influent (i.e., pH 12). Around 16.5 ml cycle⁻¹ of deionized water was added into the reservoir to compensate for water evaporation (about 220 ml d⁻¹) in the TF system.

The HLR was determined by the flow rate of continuous recirculation pumps and the sectional area of the TF, expressed as 'm³ m⁻² h⁻¹'. During the reactor operation, the DO concentration in the TF was indirectly controlled by adjusting the HLR. A portable digital oxygen meter HQ30d (Hach Lange, Germany) was used to measure the DO in the reservoir. The turbid liquid of 1.5 M Ca(OH)₂ was used to provide additional alkalinity for full nitrification (i.e., complete ammonium conversion to nitrate without nitrite accumulation) and control the bulk pH at around 6. Acid dosing (i.e., 1M HCl) was barely used over the whole experiment unless the bulk solution exceeded pH 7 (SI Figure S3.1). The pH in the reservoir was continuously monitored by a pH controller (Consort R3610, Consort, Belgium). The electrical conductivity (EC) was measured using a conductivity meter (Hanna edge® HI-2030 edge, USA).

2.2.2 Reactor inoculation and start-up

The inoculum was a mixture of sewage-activated sludge (74% volatile suspended solid (VSS), Aquafin Antwerpen-Zuid, Belgium) and industrial activated sludge (26% VSS, PB Leiner, Belgium). The inoculum sludge was recirculated in the TF for 48 h, and then 4.9 g VSS L⁻¹ TF was retained.

In the start-up period, the TF was run with synthetic urine solution. The synthetic urine was prepared by dissolving 1.37g urea and 0.15g ammonium sulfate ((NH₄)₂SO₄) as N source (a total of 670 mg N), 0.98g sodium acetate, 0.5g potassium chloride (KCl), 0.32g monopotassium phosphate (KH₂PO₄), 0.05g calcium chloride (CaCl₂), and 0.05 g magnesium sulfate (MgSO₄) in 1 L tap water. Then, 0.97g L⁻¹ of Ca(OH)₂ was added into the synthetic urine, increasing the pH to 12. The TN loading rate was initiated from 50 mg N L⁻¹ d⁻¹ and finally reached 100 mg N L⁻¹ d⁻¹. During this period, the HLR increased from 1.5 to 2.0 m³ m⁻² h⁻¹ (in the top table of Figure 3.2).

2.2.3 Reactor operation with real urine

After full nitrification was achieved with synthetic urine at $100 \text{ mg N L}^{-1} \text{ d}^{-1}$, the alkalized real urine was fed to the TF. To be consistent with the synthetic urine influent, the real urine was diluted to around 670 mg TN L^{-1} , and extra Ca(OH)_2 of $1.0 \pm 0.1 \text{ g L}^{-1}$ was added to maintain pH 12. In this stage, the TN loading rate increased up to $176 \text{ mg N L}^{-1} \text{ d}^{-1}$. Meanwhile, the HLR increased to $2.5 \text{ m}^3 \text{ m}^{-2} \text{ h}^{-1}$ (in the top table of Figure 3.2). One bioaugmentation ($1 \text{ g VSS L}^{-1} \text{ TF}$) was implemented on day 126, with the same sewage-activated sludge used for reactor start-up.

Since the urine composition may fluctuate depending on the donators and their daily activity, the impact of different collection batches on the stability nitrification performance was tested. Among the urine collection batches (NO.1-10), three batches, named as batch A, B, and C, were selected over the whole collection timespan of 38 days, i.e., beginning (NO.1- A), middle (NO.6- B), and end (NO.10- C) (SI Figure S3.2).

2.3 Sampling and analytical methods

Influent and effluent samples were taken periodically, filtered through $0.22 \text{ }\mu\text{m}$ Chromafil® Xtra filters (Macherey-Nagel, USA), and stored at 4°C before analysis. The $\text{NH}_4^+\text{-N}$ was determined by the Nessler method²⁷⁰. The nitrite ($\text{NO}_2^-\text{-N}$), $\text{NO}_3^-\text{-N}$, $\text{PO}_4^{3-}\text{-P}$, potassium (K^+), calcium (Ca^{2+}), magnesium (Mg^{2+}), and sodium (Na^+) were determined on ion chromatography (Eco IC, Metrohm, Switzerland).

The TN, total phosphorus (TP), COD of influent samples are measurements of unfiltered urine with precipitates. The TN, TP, and COD of effluent samples are filtered over the $0.22 \text{ }\mu\text{m}$ Chromafil® Xtra filters to avoid the interference of biomass in the TF reservoir. The TN and COD concentrations were measured with the Nanocolor® tube test kits (TN220 and COD1500, MachereyNagel, USA). The total phosphorus (TP) was measured with the Spectroquant® phosphate cell test (Merck KGaA, Germany).

2.4 Calculation of the element supplementation for nutrient balancing

The TF effluent was filtered through the $0.2 \text{ }\mu\text{m}$ filters here to simulate the function of a membrane module. The filtrate was regarded as the baseline nutrient solution (BNS).

The Hoagland nutrient solution (HNS) is considered one universal nutrient solution for plant growth in hydroponics¹⁵. The concentration of major elements in HNS is 210 mg NO_3^- -N L^{-1} , 31 mg P L^{-1} , 235 mg K L^{-1} , 200 mg Ca L^{-1} , and 48 mg Mg L^{-1} . Based on the standard ratio of P, K, Ca, and Mg to NO_3^- -N in HNS, the corresponding elements shortage in the BNS should be compensated by common compounds, such as calcium nitrate ($\text{Ca}(\text{NO}_3)_2$), dipotassium phosphate (K_2HPO_4), calcium sulfate (CaSO_4), and MgSO_4 . Detailed nutrient balancing strategy can be found in section 2.5 of **Chapter 2**. The water of low salinity ($< 0.75 \text{ mS cm}^{-1}$) is recommended for the final dilution of the balanced BNS to HNS²¹⁷.

3. Results and discussion

As shown in Figure 3.1, the proposed concept illustrates the complete process from human urine collection to nutrient solution application in hydroponic systems. The urine is assumed to be collected from water-flush toilets, resulting in diluted urine (around 33vol% urine, Figure 3.1 a). After the immediate alkalization by $\text{Ca}(\text{OH})_2$ to pH 12, the urine is transported to a TF beside a hydroponic greenhouse. The TF is fed with further diluted urine (around 11vol% urine). Due to the nitrification process, extra alkalinity will be required to avoid reactor pH dropping below 6 (Figure 3.1 b). The solid waste accumulated in the reservoir was mainly biomass and phosphorus precipitate, which can be applied to land as a fertilizer. After the nutrient balancing for the BNS, the diluted nitrate-based standard solution mainly from around 3 vol% urine is directly applied to the hydroponic system (Figure 3.1 c). This concept allows the urine-sourced standard nutrient solution produced by TFs to directly supply to hydroponic systems.

3.1 Reactor start-up and nitrification performance on synthetic urine

In the start-up stage, the TF was fed with the $\text{Ca}(\text{OH})_2$ alkalized synthetic urine. The synthetic urine contained $662 \pm 12 \text{ mg TN L}^{-1}$, more specifically, negligible NO_2^- -N and NO_3^- -N, but $31 \pm 2 \text{ mg NH}_4^+$ -N L^{-1} (SI Figure S3.3). The TN loading rate was initiated with $50 \pm 1 \text{ mg N L}^{-1} \text{ d}^{-1}$, and complete nitrification was achieved after 4 days (Figure 3.2a), indicating a sufficient nitrification capacity of the inoculum at the initial loading strength. When the TN loading rate was increased to $106 \pm 1 \text{ mg N L}^{-1} \text{ d}^{-1}$ on day 23, NH_4^+ -N

immediately emerged and stabilized at $135 \pm 24 \text{ mg N L}^{-1}$. To avoid this incomplete nitrification, the TN loading rate was decreased to $75 \pm 1 \text{ mg N L}^{-1} \text{ d}^{-1}$. After this intermediate loading rate, it took around 26 days to get the full nitrification at a loading rate of $100 \pm 2 \text{ mg N L}^{-1} \text{ d}^{-1}$.

In the synthetic urine stage, the NO_3^- -N production efficiency increased from $80 \pm 1\%$ to $95 \pm 3\%$ (Figure 3.2b), indicating an increase of nitrifiers and a decrease of denitrifiers in the TF. The nitrifiers could get promoted due to the high DO level (above $6 \text{ mg O}_2 \text{ L}^{-1}$) in most cases (SI Figure S3.4), while the denitrifiers were suppressed and probably washed out.

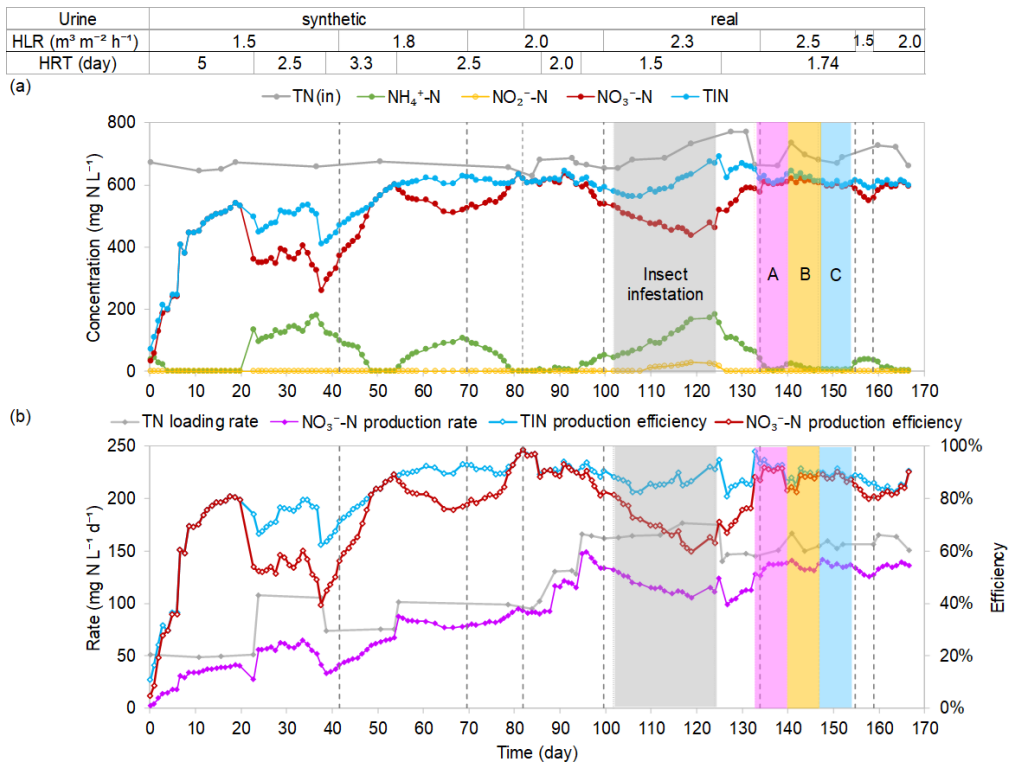


Figure 3.2: The profile of nitrogen (N) conversion from urine. The urine types and hydraulic loading rate (HLR) are shown on top. (a) concentrations of total nitrogen of influent (TN(in)), NH_4^+ -N, NO_2^- -N, NO_3^- -N, and total inorganic nitrogen (TIN) in the effluent. (b) volumetric TN loading rate, NO_3^- -N production rate, TIN production efficiency, and NO_3^- -N production efficiency. Both efficiencies are based on the concentration of TN(in). TN(in) includes both organic nitrogen (mainly urea) and inorganic nitrogen, while TIN in effluent contains NH_4^+ -N, NO_2^- -N, NO_3^- -N. The color shading “A”, “B” and “C” mean three different urine collection batches.

3.2 Nitrification performance on real urine

From day 81 onwards, the alkalized real urine substituted for the alkalized synthetic urine as the TF influent. The TN in the influent was relatively stable at $695 \pm 40 \text{ mg N L}^{-1}$, with $58 \pm 7 \text{ mg NH}_4^+\text{-N L}^{-1}$ but negligible $\text{NO}_2^-\text{-N}$ and $\text{NO}_3^-\text{-N}$ (SI Figure S3.3).

3.2.1 Nitrification performance after switching to real urine

After switching from synthetic to real urine, the TN loading rate of $100 \pm 2 \text{ mg N L}^{-1} \text{ d}^{-1}$ was maintained for another 6 days. The full nitrification was not affected in this period, with the $\text{NO}_3^-\text{-N}$ production efficiency and rate of $94 \pm 6\%$ and $92 \pm 1 \text{ mg N L}^{-1} \text{ d}^{-1}$, respectively (Figure 3.2b). Increasing the TN loading rate to $130 \pm 2 \text{ mg N L}^{-1} \text{ d}^{-1}$ could keep the full nitrification performance, and the $\text{NO}_3^-\text{-N}$ production rate increased to $118 \pm 3 \text{ mg N L}^{-1} \text{ d}^{-1}$. However, further increase of TN loading rate to $166 \pm 5 \text{ mg N L}^{-1} \text{ d}^{-1}$ immediately led to $\text{NH}_4^+\text{-N}$ accumulation, revealing the insufficient nitrification capacity of TF.

From day 102 to day 124, insect infestation was observed in the TF. The insects were speculated as water springtails from a subclass of *Collembola*²⁷¹. It was suspected that the insect infestation impaired the TIN release via urine hydrolysis and exacerbated the incomplete urine nitrification (Figure 3.2). Chemical control via dosing insecticide into the TF effectively eliminated this insect problem.

Increasing the TN loading rate could always trigger the $\text{NH}_4^+\text{-N}$ accumulation, but not affected the $\text{NO}_2^-\text{-N}$ accumulation and TIN production via urine hydrolysis (Figure 3.2a). Therefore, nitrification (i.e., $\text{NH}_4^+\text{-N} \rightarrow \text{NO}_2^-\text{-N}$) should be the bottleneck of urine nitrification in this system. It was suggested the optimum pH for ammonium-oxidizing bacteria (AOB) and nitrite oxidizing bacteria (NOB) is neutral and slightly alkaline²⁷². Acidic pH could limit the nitrification, and $\text{NH}_4^+\text{-N}$ oxidation could be wholly inhibited at pH 5¹¹⁰. Nevertheless, the whole experiment was still operated under the faintly acidic pH (around 6) to directly satisfy the pH requirement for hydroponic cultivation¹⁵ and avoid further pH down-regulation. Moreover, maintaining the faintly acidic pH could favor the release of macronutrients (i.e., P, Ca, and Mg) in urine precipitate during the nitrification process²⁷³. Although nitrification was the bottleneck, it was suggested that nitrification rate (AOB activity) was barely affected at low EC ($< 58 \text{ mS cm}^{-1}$). Furthermore,

the electrical conductivity (EC) of the effluent ($6.2 \pm 0.2 \text{ mS cm}^{-1}$, SI Figure S3.1) was within the EC threshold of 9.5 mS cm^{-1} for full nitrification²⁷⁴, suggesting no adverse effect. In addition, the FA level in the effluent was much lower ($0\text{-}1 \text{ mg N L}^{-1}$) to suppress AOB activity (FA $8\text{-}120 \text{ mg N L}^{-1}$)¹¹⁴.

The reported maximum TN loading rate of attached growth systems for urine nitrification was $409 \text{ mg N L}^{-1} \text{ d}^{-1}$ in Table 3.1²⁶². They fed the TFs with undiluted synthetic urine of $7780 \text{ mg TN L}^{-1}$ and operated the TFs with HRT up to 128 days under a broad pH range ($9.0\text{-}3.0$). The low NO_3^- -N production efficiency (59%) obtained after this long HRT could be attributed to the high urine concentration (i.e., high salinity) and the harmful pH ($< \text{pH } 5$), as high salinity and low pH could impair and even cease the nitrification process^{110, 266}. Additionally, an adequate acclimation period was needed for nitrifying communities to adapt to a high ionic environment²⁶⁶. Since the nitrified urine is aimed to use as liquid fertilizer for plant growth eventually, and dilution is inevitable, the urine nitrification process started with diluted urine (around 11% dilution in this study) could be more efficient in NO_3^- -N recovery. A previous study showed that lower TN concentration (520 mg N L^{-1}) and loading rate ($96 \text{ mg N L}^{-1} \text{ d}^{-1}$) could result in a NO_3^- -N production efficiency of 90% with an HRT of 27 days²⁶¹. Their slow full nitrification process could still result from poor pH control (pH $3\text{-}8$). Compared to the mussel shells (CaCO_3 content: $70\text{-}80\%$) used in TFs^{261, 262}, the turbid liquid of $\text{Ca}(\text{OH})_2$ employed in this study could control the bulk pH more timely and accurately.

As a whole, there was little difference in NO_3^- -N production efficiencies between synthetic and real urine when full nitrification was achieved, which was consistent with the literature studies summarized in Table 3.1. The high nitrate production efficiency ($80\text{-}98.7\%$) makes urine an ideal nitrogen recovering source, probably due to the easily hydrolyzable urea and low COD to N ratio (0.88 ± 0.06 in this study). Similarly, the COD removal efficiencies of synthetic and real urine were quite close, with $98 \pm 2\%$ and $94 \pm 3\%$ (Figure 3.3), respectively. The COD source of synthetic urine in this study was urea and sodium acetate, while that of real urine was relatively complex, including urea, creatinine, uric acid, citrate, and some other organic compounds²⁷⁵. Taken together with the

relatively higher COD level of synthetic urine than real urine (730 ± 29 versus $604\pm 38\text{mg L}^{-1}$) and lower COD removal efficiency with real urine, COD removal in real urine seemed more challenging. Nevertheless, the excellent COD removal efficiency could eliminate the odor nuisance and benefit hydroponic plant production by lowering the proliferation risk of heterotrophic pathogens and insects^{213, 238}.

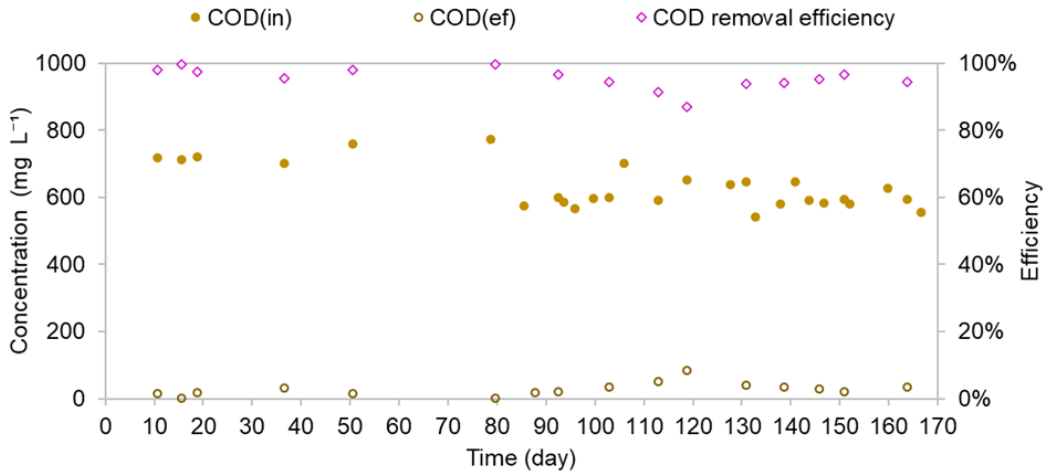


Figure 3.3: The COD concentration and removal efficiency. COD(in) means the COD concentration of unfiltered influent. COD(ef) means the COD concentration of filtered effluent. The COD removal efficiency is based on the COD(in) and COD(ef).

3.2.2 Nitrification performance stability under different collection batches

The composition of human urine varies between and within individuals due to diet, health, environmental conditions, and daily activities⁶⁴. Among the characterized urine batches collected over a month, the relative concentration of COD, TP, and major ions (NH_4^+ , K^+ , Ca^{2+} , Mg^{2+} , Na^+ , SO_4^{2-} , and Cl^-) to TN showed visible differences (SI Figure S3.2). Three different batches of A, B, and C were selected over the whole collection period. The major differences of batch A, B and C were the relative concentration of COD (0.81, 0.97, and 0.89 mg mg^{-1} TN), Ca^{2+} (0.39, 0.33, 0.31 mg mg^{-1} TN), K^+ (0.25, 0.28, 0.31 mg mg^{-1} TN), Na^+ (0.38, 0.34, and 0.29 mg mg^{-1} TN), and Cl^- (0.67, 0.61, 0.55 mg mg^{-1} TN). These batches were tested from day 133 to day 154 under the TN concentration and loading rate of $687\pm 30\text{ mg N L}^{-1}$ and $154\pm 8\text{ mg N L}^{-1}\text{ d}^{-1}$. As shown in Fig 2, the NO_3^- -N

concentration, production efficiency, and rate during the stability tests were constant at $604 \pm 11 \text{ mg N L}^{-1}$, $88 \pm 3\%$, and $136 \pm 4 \text{ mg N L}^{-1} \text{ d}^{-1}$. Therefore, the nitrification performance in the TF was relatively stable and scarcely affected by the difference in urine batches, probably due to the little difference in concentrations of all the major compositions between each collection batch.

During this batch stability test, the total Ca(OH)_2 dosage as alkalization and pH control reagent for urine storage and nitrification was recorded (SI Figure S3.5). The molar ratio of total hydroxide ion (OH^-) supplementation and NO_3^- -N production is around 1.0, consistent with the half alkalinity required for urine full nitrification²⁶⁰. Thus, the function of Ca(OH)_2 as alkalinity supplier was proved for urine full nitrification in TF.

3.2.3 Impact of hydraulic loading rate on urine nitrification and electrical energy consumption

Before day 155, the HLR was raised along with the increase of the TN loading rate. It was suggested that the typical HLR in TFs to keep the carrier material moist is between 1 to $3 \text{ m}^3 \text{ m}^{-2} \text{ h}^{-1}$ ²⁷⁶. The HLR tested in this study (1.5 to $2.5 \text{ m}^3 \text{ m}^{-2} \text{ h}^{-1}$) is in the recommended range.

After increasing the TN loading rate from 50 ± 1 to $106 \pm 1 \text{ mg N L}^{-1} \text{ d}^{-1}$, the lower bound of DO (DO(min)) in each operating cycle decreased from 8.1 ± 0.3 to $3.0 \pm 0.3 \text{ mg O}_2 \text{ L}^{-1}$, but increased to $6.6 \pm 0.3 \text{ mg O}_2 \text{ L}^{-1}$ after increasing HLR from 1.5 to $1.75 \text{ m}^3 \text{ m}^{-2} \text{ h}^{-1}$ (SI Figure S3.4), indicating that raising HLR could increase the DO level in the TF. Controlling the DO in the biofilm was difficult as it was not directly measured in the TF. Only the DO in the reservoir was measured and considered a combined result of oxygen dissolved into the reservoir, ventilated into the TF, and consumed by nitrifiers and other aerobic microorganisms. The HLR control was related to the DO in the carrier biofilm. Presumably, increasing the HLR could induce more oxygen sucked into the reactor^{277, 278}. The nitrifying bacteria cannot grow if the oxygen content falls below $0.5 \text{ mg O}_2 \text{ L}^{-1}$ in stream waters²⁷⁹. A minimum oxygen level of $2 \text{ mg O}_2 \text{ L}^{-1}$ was recommended in aquaculture nitrification reactors²⁸⁰. Therefore, over the whole experiment period, the DO(min) in the reservoir was consistently above $2 \text{ mg O}_2 \text{ L}^{-1}$ via controlling HLR and TN loading rates. Additionally,

the DO in the reservoir was always about $0.6 \text{ mg O}_2 \text{ L}^{-1}$ lower than that in the drops from the bottom compartment, indicating the extra oxygen-consuming microorganisms (e.g., nitrifiers and aerobic heterotrophs) existed in the reservoir.

Besides controlling moisture and DO, HLR could also manage the contact time between urine and biofilm in the TF. The HLR of $2.5 \text{ m}^3 \text{ m}^{-2} \text{ h}^{-1}$ with a recirculation flow rate (Q_{rec}) of 21.6 L h^{-1} made the total 5 L urine circulate 8.5 times through the TF in each cycle (i.e., 2 h). In comparison, the HLR of 2.0 and $1.5 \text{ m}^3 \text{ m}^{-2} \text{ h}^{-1}$ with Q_{rec} of 17.1 and 12.7 L h^{-1} could only circulate the urine 7.1 and 5.2 times, respectively. Thus, after decreasing the HLR from 2.5 to $1.5 \text{ m}^3 \text{ m}^{-2} \text{ h}^{-1}$, the $\text{NH}_4^+\text{-N}$ accumulation emerged and increased to $38 \pm 2 \text{ mg L}^{-1}$, while raising the HLR from 1.5 to $2.0 \text{ m}^3 \text{ m}^{-2} \text{ h}^{-1}$ effectively eliminated the $\text{NH}_4^+\text{-N}$ accumulation and recovered the full nitrification of urine. Thus, under the TN loading rate of $152 \pm 7 \text{ mg TN L}^{-1} \text{ d}^{-1}$, the HLR of $1.5 \text{ m}^3 \text{ m}^{-2} \text{ h}^{-1}$ could guarantee enough DO for full nitrification but not provide sufficient contact times between urine and biofilm. Although HLR of 2.0 and $2.5 \text{ m}^3 \text{ m}^{-2} \text{ h}^{-1}$ could realize the full nitrification, from the perspective of electrical energy consumption, lower HLR means lower power consumption from recirculation pumps.

In contrast to the active aeration in other nitrification systems, the recirculation pump is the major energy-consuming item in TFs. To estimate its energy consumption, several operating parameters were assumed, including a daily nitrogen production per capita (person) of 3.7 g N d^{-1} ²⁸¹, reactor height of 156 cm, pump depth in the reservoir of 20 cm, a pipe head loss of 0.33 m m^{-1} pipe and pump efficiency of 80%²⁸². The calculated electrical energy consumption was $1.8 \text{ kWh kg}^{-1} \text{ NO}_3^-\text{-N}$ production under the $\text{NO}_3^-\text{-N}$ production rate of $0.136 \text{ kg N m}^{-3} \text{ d}^{-1}$ (details in SI Table S3.1). At this stage, the $\text{NO}_3^-\text{-N}$ production rate could be further improved due to the high level of residual DO ($4.1 \pm 0.1 \text{ mg O}_2 \text{ L}^{-1}$) in the reservoir (SI Figure S3.4). The energy consumption can still be further reduced by increasing the potential $\text{NO}_3^-\text{-N}$ production rate in the TF.

3.3 Nutrient quality balancing for direct application in hydroponic systems

In the proposed concept, urine stabilization by dosing Ca(OH)_2 increased the pH to 12 and triggered salt precipitation, e.g., hydroxyapatite ($(\text{Ca})_{10}(\text{PO}_4)_6(\text{OH})_2$) and struvite

($\text{NH}_4\text{MgPO}_4 \cdot 6\text{H}_2\text{O}$), resulting in reduced concentrations of PO_4^{3-} ^{259, 283}. As shown in Figure 3.4, the influent $\text{PO}_4^{3-}\text{-P}$ concentration was 0 in most cases. In the effluent of the TF, $\text{PO}_4^{3-}\text{-P}$ could be detected again, especially from day 132 to 151, which stabilized at $34 \pm 3 \text{ mg P L}^{-1}$ with a $\text{PO}_4^{3-}\text{-P}$ recovery efficiency of $73 \pm 5\%$. Over the whole experiment, the effluent $\text{PO}_4^{3-}\text{-P}$ concentration and recovery efficiency fluctuated in a range of 2% to 91%, probably related to the effluent pH (pH(min)) in the TF system (SI Figure S3.1). Spearman's correlation analysis over the whole experiment period showed the association between the effluent $\text{PO}_4^{3-}\text{-P}$ concentration and pH(min) was moderate negative ($\rho = 0.57$, $p < 0.01$). It indicated lower bulk pH could benefit the $\text{PO}_4^{3-}\text{-P}$ release from the precipitate, reducing the clogging risk of TF in the long term.

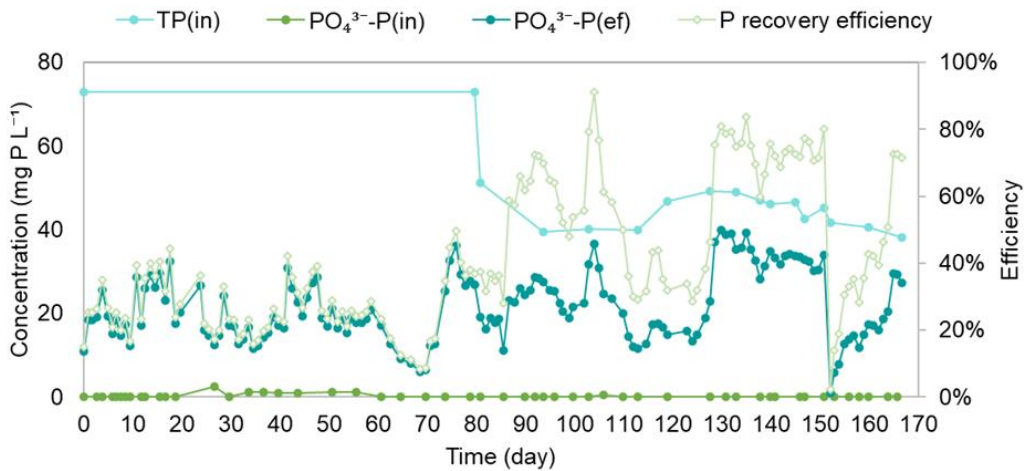


Figure 3.4: Phosphorus concentration and recovery efficiency during urine nitrification process in TF. TP(in) means the total phosphorus concentration in the unfiltered influent. $\text{PO}_4^{3-}\text{-P(in)}$ and $\text{PO}_4^{3-}\text{-P(ef)}$ represent $\text{PO}_4^{3-}\text{-P}$ concentration in filtered influent and effluent, respectively. P recovery efficiency is calculated from the ratio of $\text{PO}_4^{3-}\text{-P(ef)}$ and TP(in).

According to the proposed balancing strategy in section 2.5 (Chapter 2), the nutrient quality balancing was modeled for the filtered TF effluent. The Sankey diagram based on the nutrient mass flow in each section of the proposed concept is shown in Figure 3.5. In the influent section, the diluted urine (about 11% v/v) was alkalized by dosing Ca(OH)_2 , introducing 528 mg Ca into 1 L urine flow. In the urine nitrification section, the bulk pH control with Ca(OH)_2 added 396 mg Ca into the flow. In this trickling filter and membrane

section, the TN loss of 70 mg may be attributed to the microorganism assimilation and the potential denitrification in some anoxic zone inside the TF; the 14 mg TP, 158 mg Ca, and 3 mg Mg loss could be due to the microorganism assimilation and precipitation. In the nutrient balancing section, element Ca was the limiting factor, and extra NO_3^- -N (220 mg), PO_4^{3-} -P (89 mg), K^+ (742 mg), and Mg (173 mg) should be supplemented into the BNS tank (Figure 3.5). The corresponding chemical compounds used to complete the HNS were shown in SI Table S3.2, referring to the principle in section 2.5 (**Chapter 2**). Eventually, after further dilution, 3.94 L HNS could be obtained, and the urine-sourced NO_3^- -N accounted for 73.3% of the NO_3^- -N in the HNS. Combined with the electricity cost of HLR control, the total cost of urine-sourced HNS was 0.033 € m^{-3} HNS (SI Table S3.2).

To minimize the external NO_3^- -N supplementation, the overdosed element Ca coming from the $\text{Ca}(\text{OH})_2$ as a pH-control reagent can be substituted by other bases that contain major nutrients. Since 91% of Mg was compensated in the end, a mixed pH control reagent of $\text{Mg}(\text{OH})_2$ and $\text{Ca}(\text{OH})_2$ could be an alternative.

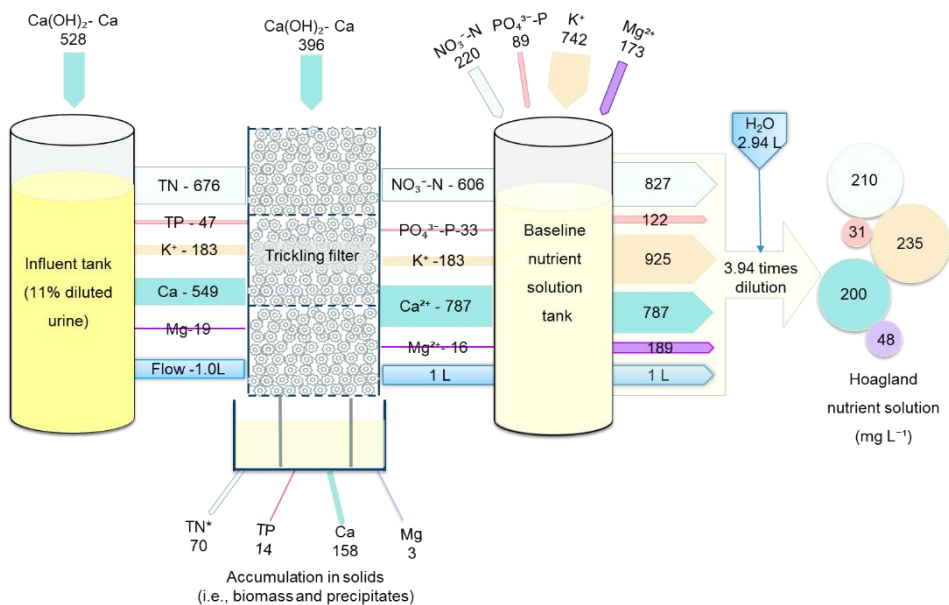


Figure 3.5: The Sankey diagram is based on the mass (mg) of nutrients in different sections. The nutrient quality balancing step and dilution step are according to the elemental composition and concentration in Hoagland nutrient solution (HNS). TN* loss includes the N accumulation in solids and potential denitrification.

4. Conclusion

A new concept for nutrients recovery from human urine for hydroponic cultivation was proposed in this study. Full nitrification of real urine in a TF was realized, with a high NO_3^- -N production efficiency of $88\pm 3\%$ and a stable production rate of $136\pm 4 \text{ mg NO}_3^- \text{-N L}^{-1} \text{ d}^{-1}$. Similar nitrification and COD removal efficiencies were obtained after switching from synthetic urine to real urine. Relatively stable nitrification performance was maintained with different batches of real urine of variant compositions, further highlighting the stability of TF in treating real urine. The HLR control in TF could positively affect the nitrification performance via increasing DO level and the contact time between substrate and biofilm. The HLR of $2 \text{ m}^3 \text{ m}^{-2} \text{ h}^{-1}$ was the optimal condition to realize full nitrification under the TN loading rate of $152\pm 7 \text{ mg TN L}^{-1} \text{ d}^{-1}$ with an electrical energy consumption of $1.8 \text{ kWh kg}^{-1} \text{ NO}_3^- \text{-N production}$. The triple benefits of Ca(OH)_2 in urine alkalization, full nitrification, and macronutrient supplementation were proved for the proposed concept. After nutrient balancing, the urine-sourced $\text{NO}_3^- \text{-N}$ accounted for around 73% of the $\text{NO}_3^- \text{-N}$ in the HNS for hydroponic plant production.

5. Supplementary information

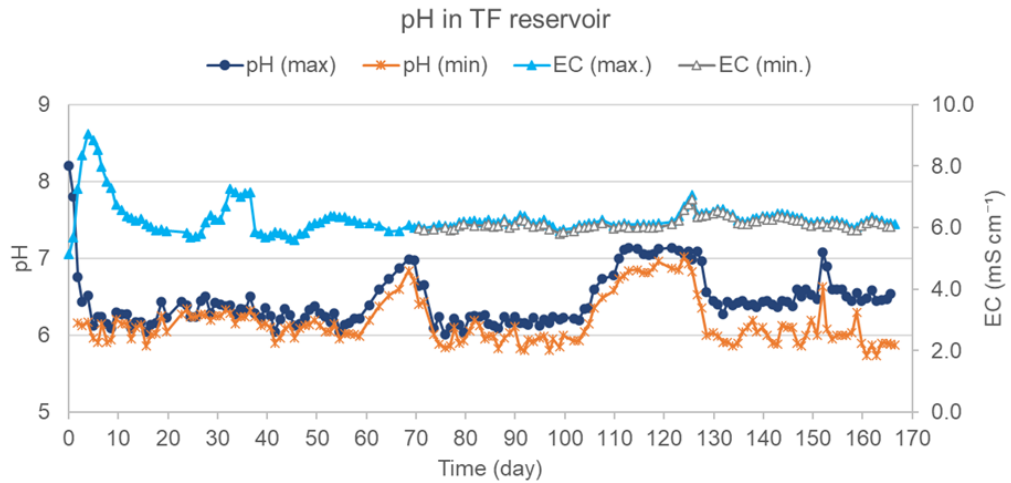


Figure S3.1: The profile of pH and electrical conductivity (EC) in TF reservoir. The pH(max) and pH(min) mean the pH threshold values in an operating cycle. pH(min) is the effluent pH of the trickling filter as well.

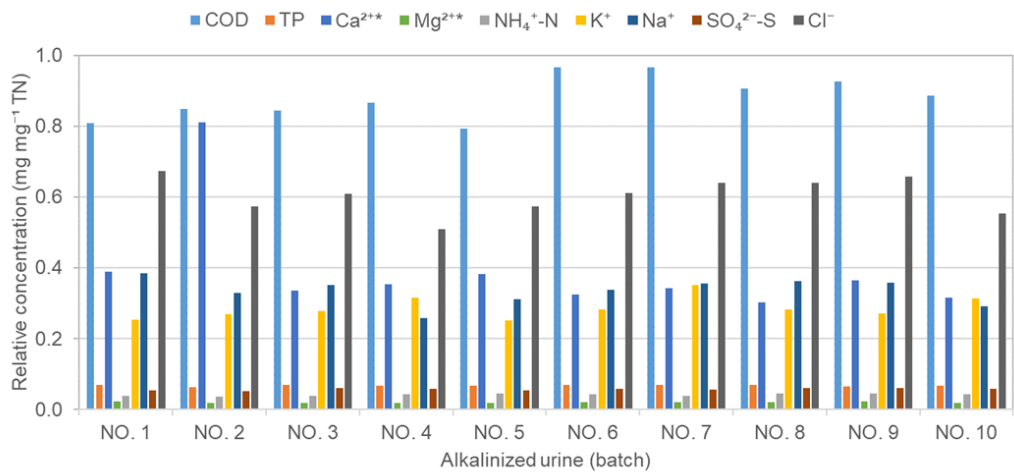


Figure S3.2: The relative concentration of chemical oxygen demand (COD), total phosphorus (TP), and major ions to total nitrogen (TN) in each collection batch and their average values. The COD, TP, and TN are measured from unfiltered urine with precipitates. The Ca^{2+} and Mg^{2+} were measured after acidifying the unfiltered urine to pH <1 to ensure all the precipitates were dissolved.

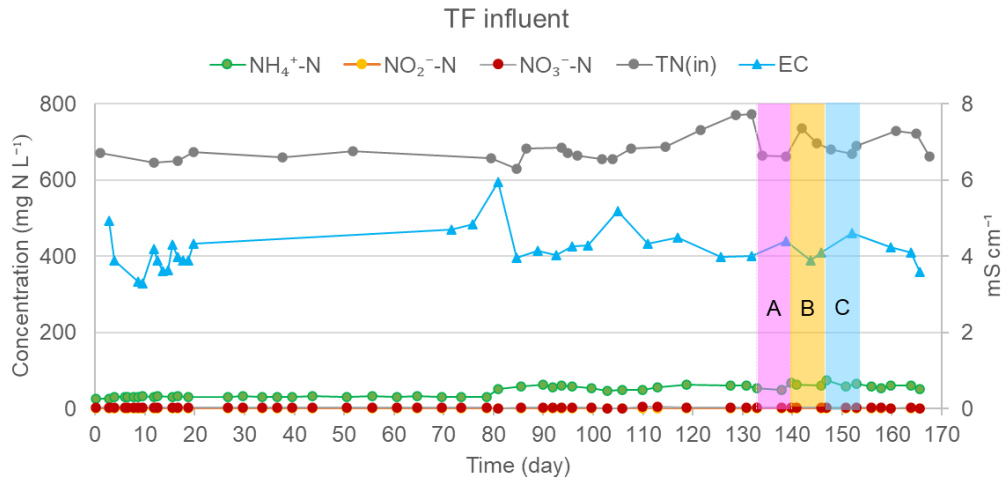


Figure S3.3: Nitrogen profile and EC in influent.

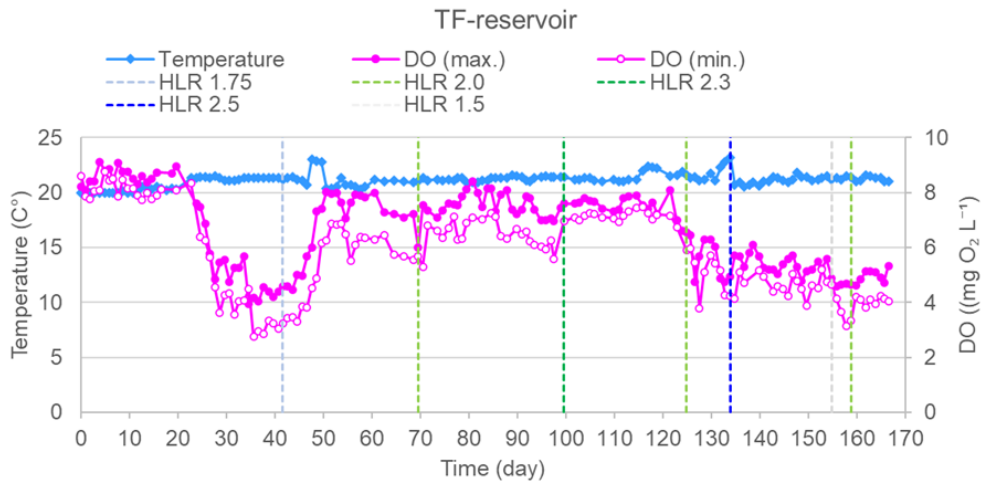


Figure S3.4: The temperature and dissolved oxygen (DO) monitoring during different hydraulic loading rates (HLR, $\text{m}^3 \text{m}^{-2} \text{h}^{-1}$). DO(max) and DO(min) mean the DO threshold values in an operating cycle.

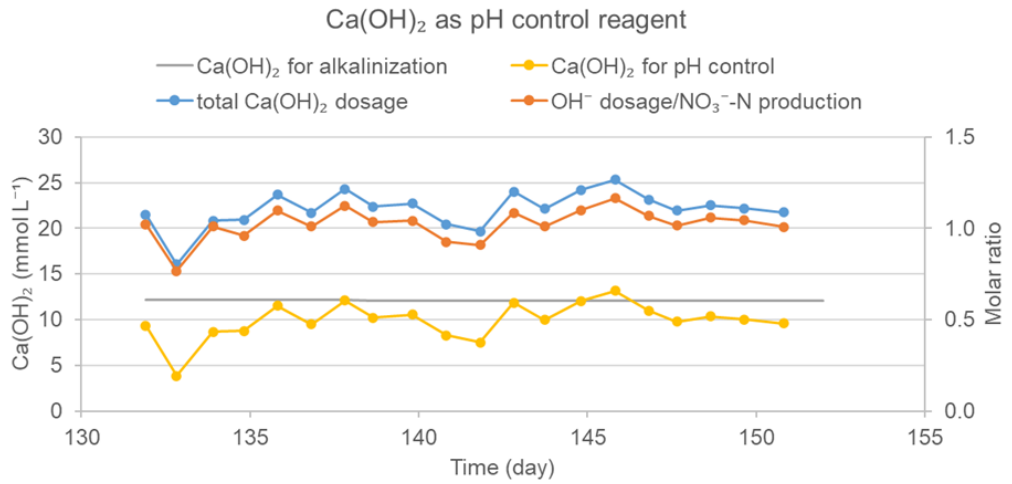


Figure S3.5: Ca(OH)₂ as alkalization and pH control reagent for urine storage and nitrification.

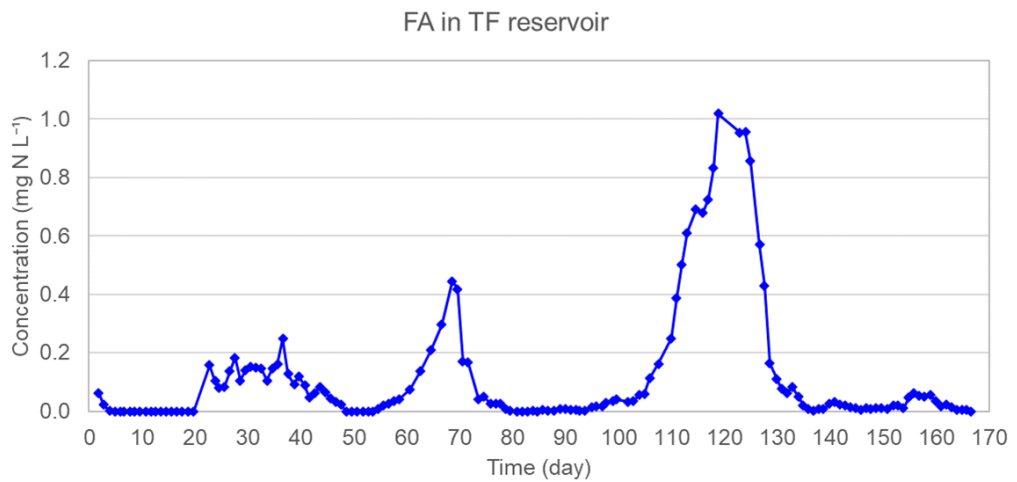


Figure S3.6: FA level over the whole operation period, calculated based on the NH₄⁺-N level of effluent.

Table S3.1: Electrical energy estimation of TF. The equation of pump power ($P(W_{el}) = \rho * g * h * Q / \eta$, $\rho = 1000 \text{ kg m}^{-3}$, $g = 9.807 \text{ m s}^{-2}$, pump efficiency (η) = 80%. The calculated values are **in bold**.

| Hydraulic load ($\text{m}^3 \text{ m}^{-2} \text{ h}^{-1}$) | Volumetric production rate ($\text{kg m}^{-3} \text{ d}^{-1}$) | Per capita (person) (kg N d^{-1}) | Height of filter (m) | Section area (m^2) | Flow rate (Q) ($\text{m}^3 \text{ s}^{-1}$) |
|---|--|--|----------------------|--|---|
| 2 | 0.136 | 0.0037 | 1.56 | 0.017 | 0.00001 |
| Depth of pump (m) | Head loss pipes (m m^{-1} pipe) | Total height (m) | Power of pump (kW) | Designed NO_3^- -N production rate (kg N h^{-1}) | Energy consumption ($\text{kwh kg}^{-1} \text{ NO}_3^-$ -N production) |
| 0.2 | 0.33 | 2.341 | 0.00028 | 0.00015 | 1.80 |

Table S3.2: OPEX estimation on the production of urine-sourced Hoagland nutrient solution (HNS). BNS means the baseline nutrient solution. The price of chemical compound supplementation refers to SI Table S2.1.

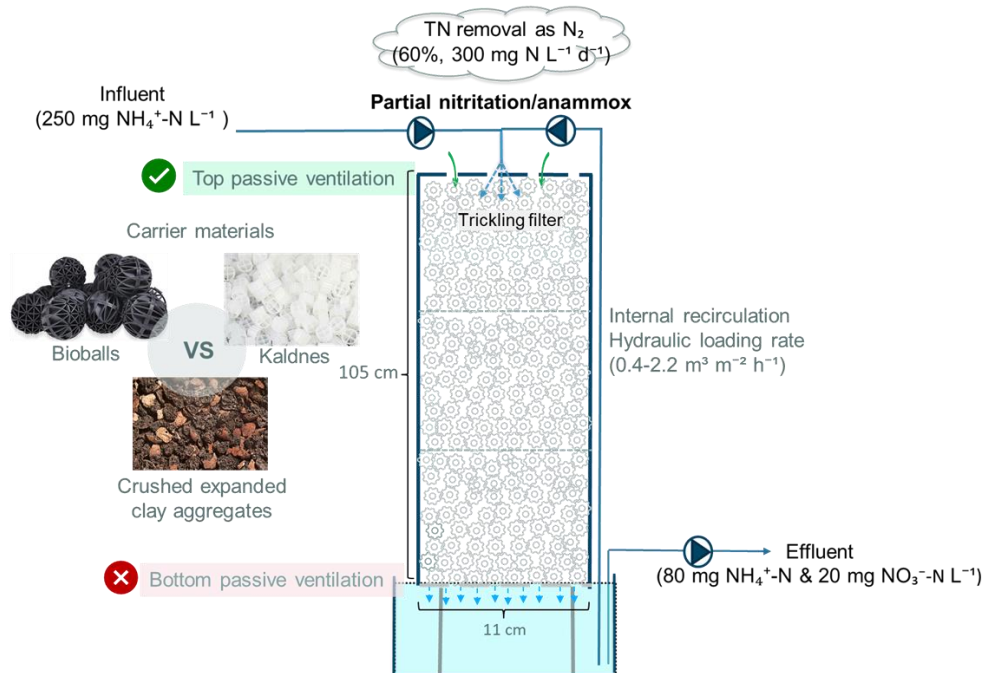
| | | NO_3^--N | P | K | Ca | Mg |
|------------------------------|---|--|----------------|--------------------------|-------------------------|--------------------------|
| Permeate content | (mg L^{-1} BNS) | 606 | 33 | 183 | 787 | 16 |
| Compounds as supplementation | | $\text{Mg}(\text{NO}_3)_2 \cdot 6\text{H}_2\text{O}$ | KNO_3 | K_2HPO_4 | K_2SO_4 | $\text{Ca}(\text{OH})_2$ |
| | (mg L^{-1} BNS) | 1845 | 137 | 501 | 1037 | 1633 |
| | (€ m^{-3} BNS) | 0.0000064 | 0.000012 | 0.000011 | 0.000019 | 0.00005 |
| Diluting time(s) | (to HNS) | | | 3.94 | | |
| Electricity consumption | ($\text{kwh kg}^{-1} \text{ NO}_3^-$ -N production) | | | 1.80 | | |
| | (kg NO_3^- -N _{urine} L ⁻¹ HNS) | | | 0.00015 | | |
| | (kwh L^{-1} HNS production) | | | 0.00028 | | |
| | (€ m^{-3} HNS) | | | 0.032 | | |
| Total cost | (€ m^{-3} HNS) | | | 0.033 | | |

6. Acknowledgments

This work was supported by the China Scholarship Council (File No. CSC201706130131). The authors would like to thank Olivier Voet and Karolien De Wael for their help in cation measurement via ion chromatography.

Chapter 4

Feasibility of a trickling filter for partial nitritation/anammox: Effects of carrier material, passive ventilation and hydraulic loading rate at lab scale



Publication of a redrafted version of this chapter is intended:

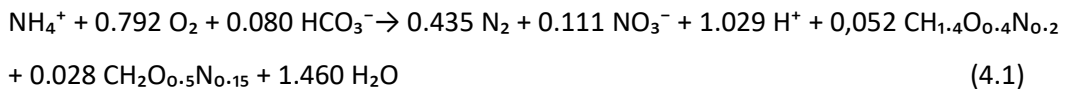
Xie, Y.; Jia, M.; De Wilde F.; Daeninck, K.; De Clippeleir, H.; Verstraete, W.; Vlaeminck, S. E., Feasibility of a trickling filter for partial nitritation/anammox: Effects of carrier material, passive ventilation and hydraulic loading rate at lab scale. (In preparation)

Abstract

Partial nitrification/anammox (PN/A) is a resource- and cost-effective technology for biological nitrogen removal from wastewater low in organic carbon. As a passively aerated biofilm reactor, trickling filters (TF) can further reduce the energy demand associated with aeration. With the goal of extreme power-efficient nitrogen removal, the feasibility of a TF for one-stage PN/A was tested with synthetic wastewater containing 100-250 mg $\text{NH}_4^+\text{-N L}^{-1}$. Three parallel systems were each packed with other carrier materials of different specific surface areas. Passive ventilation approaches (top only vs. top and bottom) and hydraulic loading rates (HLR, $0.4\text{-}2.2 \text{ m}^3 \text{ m}^{-2} \text{ h}^{-1}$) were investigated. Interestingly, the cheap carrier based on expanded clay achieved similar rates as commercially used plastic carrier materials. The top-only ventilation combined with an optimum HLR of $1.8 \text{ m}^3 \text{ m}^{-2} \text{ h}^{-1}$ could reach approximately 60% total nitrogen (TN) removal at a rate of $300 \text{ mg N L}^{-1} \text{ d}^{-1}$. A relatively low $\text{NO}_3^-\text{-N}$ production (13%) was achieved for the first time via PN/A in TFs. Most of the TN removal took place in the top compartment, where anammox activity was highest. The results provide proof of the feasibility of a TF for one-stage PN/A. Estimated electricity consumption of $0.78 \text{ kWh kg}^{-1} \text{ N}$ was 35% more energy-efficient than an actively aerating reactor, suggesting the proposed process could be a suitable low-energy alternative for nitrogen removal.

1. Introduction

Minimizing energy consumption, greenhouse gas emissions, and sludge production are critical for progress towards sustainable wastewater treatment. Compared to conventional nitrification/denitrification, partial nitrification/anammox (PN/A) consumes almost 60% less oxygen associated with aeration energy, 100% less organic carbon, and saves 90% of the sludge handling and transport for nitrogen removal from waters low in biodegradable organics²⁸⁴. In PN/A process, about half of the ammonium (NH_4^+) is aerobically oxidized to nitrite (NO_2^-) by aerobic ammonium-oxidizing bacteria (AerAOB), and the residual NH_4^+ is oxidized with the produced NO_2^- to generate nitrogen gas (N_2) by anoxic ammonium-oxidizing bacteria (AnAOB) (Reaction 4.1)¹¹⁴.



Two typical variations of the PN/A process are related to distinct microbial aggregates: (i) suspended growth and (ii) attached growth (e.g., biofilm). Different reactor configurations determine the way biomass is retained in the system. In one-stage PN/A, high biomass retention is a prerequisite of high process stability. Biofilm reactor technologies are conceived to be easier to retain the slow-growing AnAOB than suspended growth systems like sequencing batch reactors (SBR) containing suspended biomass and continuous stirred-tank reactors^{114, 285}. Various types of PN/A biofilm reactors have been established, including rotating biological contactor (RBC)^{183, 286}, membrane-aerated biofilm reactor (MABR)^{287, 288}, moving bed biofilm reactor (MBBR)^{289, 290}, biological aerated filter (BAF)^{291, 292}, and granular sludge reactor^{293, 294} (Table 4.1). In these systems, cells grow in biofilms attached to the added inert carrier materials, except for granular sludge. Among these biofilm-based technologies, the MBBR, BAF, and granular sludge belong to submerged reactors and rely on active bubble-aeration for oxygen supply, while RBC is a partially emerged reactor that alternately exposes a proportion of biofilm to atmospheric oxygen, passively providing aeration¹⁸⁶. Commonly, passively aerated reactors such as RBC and trickling filters (TFs) consume less energy and are more robust and less complex to operate^{295, 296}. Furthermore, TFs have been

suggested to have lower area requirements than RBC ¹¹⁴. In practice, TFs are used as a post-treatment step of anaerobic sewage treatment, especially in developing countries ²⁹⁷. In this case, TFs are typically designed for carbon oxidation and nitrification ²⁹⁸, allowing them to achieve high ammonium removal but not necessarily total nitrogen (TN) removal. Therefore, implementing PN/A in TFs would greatly expand their applications and offer a cost-effective alternative for TN removal. Yet, the feasibility of PN/A in TFs has only been limitedly examined.

The complex dissolved oxygen (DO) control could be one major challenge for PN/A implementation in TFs, where the vertical flow of air through the filter media is induced by air draft. DO plays a vital role in balancing the PN/A process as sufficient oxygen is required for nitritation, whereas nitratation should be suppressed to allow good anammox activity ¹⁸⁶. The feasibility of PN/A in TFs has only been tested in two studies using down-flow hanging sponge (DHS) reactors as TFs, with horizontally layered polyurethane sponge slabs as filter media ^{299, 300}. In these DHS- TFs, each sponge sheet was supported by a perforated aluminum plate, and the natural air convection was realized through lateral openings above each sponge layer. The complicated strategies of DO via manipulating the influent DO and the lateral openings are unpractical in bigger-scale applications. Compared to the DHS-TFs, solid packed bed TFs without lateral openings are more straightforward in structure and installation and thus more attractive for applications ³⁰¹. Nevertheless, the feasibility of single-stage PN/A in the simpler packed-bed TFs has not been tested so far.

To the best of our knowledge, the implementation of single-stage PN/A in an uncomplicated packed-bed TF has not been tested yet. Three types of carrier materials with different surface areas were tested in three parallel TFs. The PN/A process was tested in the long term with medium-strength synthetic NH_4^+ wastewater (100-250 mg N L^{-1}) devoid of organic carbon to mimic household waste streams after carbon removal. Besides the proper DO control, an optimal hydraulic condition is another prerequisite of a balanced PN/A process ¹¹⁴. It was suggested that the hydraulic loading rate (HLR) of TFs could affect carrier humidity and the amount of oxygen sucked into the reactor ²⁷⁶⁻²⁷⁸.

Hence, the effects of passive ventilation (top only vs. top and bottom) and HLR (0.4- 2.2 $\text{m}^3 \text{m}^{-2} \text{h}^{-1}$) were explored. Besides, the vertical activity stratification in the TFs was investigated as well.

Table 4.1: Overview of typical operating conditions and nitrogen conversion performance in existing biofilm reactors for one-step PN/A processes and this study. N.A. means data are not available.

| Reactor type | T | Aeration | COD | Influent concentration | N loading rate | HRT | N removal efficiency | NO ₃ ⁻ -N production efficiency | Reference |
|------------------------|------|----------|-----------------------|---|---|-----------|----------------------|---|-----------|
| | (°C) | | (mg L ⁻¹) | (mg NH ₄ ⁺ -N L ⁻¹) | (mg N L ⁻¹ day ⁻¹) | (day) | (%) | (%) | |
| RBC | 29 | passive | N.A. | 60 | 850 | 0.08 | 54 | 7 | 286 |
| RBC | 25 | passive | N.A. | 66- 537 | 840 | 0.08-0.67 | 51-79 | 13-31 | 183 |
| MABR | 31 | active | N.A. | 50-100 | 50-100 | 1 | 69-84 | 19-34 | 287 |
| MABR | 20 | active | 7-230 | 31-120 | 74 | 0.3-1.2 | 89-97 | 10-26 | 288 |
| MBBR | 25 | active | 56-404 | 108-884 | 138-358 | 0.78-2.45 | 44-86 | 8-45 | 289 |
| MBBR | 25 | active | 210 | 568 | 500-700 | 1-0.67 | 62 | 7 | 290 |
| BAF | 20 | active | N.A. | 400 | 2622 | 0.04 | 80 | 13 | 292 |
| BAF | 20 | active | N.A. | 300 | 1467 | 0.04 | 75 | 12 | 291 |
| Granular sludge | 35 | active | N.A. | 200 | 300 | 1 | 82 | 11 | 293 |
| Granular sludge | 32 | active | N.A. | 84 | 2000 | 0.04 | 60 | 11 | 294 |

Chapter 4

| | | | | | | | | | |
|-----------------|----|---------|------|-----|----------|-----------|-------|-------|------------|
| TF (DHS) | 30 | passive | N.A. | 100 | 950-1680 | 0.07-0.12 | 52-54 | 25-34 | 299 |
| TF (DHS) | 30 | passive | N.A. | 100 | 550 | 0.15 | 43 | 48 | 300 |
| TF-A | 30 | passive | N.A. | 255 | 514 | 0.1 | 54 | 13 | This study |
| TF-B | 30 | passive | N.A. | 260 | 508 | 0.1 | 60 | 15 | This study |
| TF-K | 30 | passive | N.A. | 254 | 460 | 0.1 | 57 | 19 | This study |

2. Materials and methods

2.1 Trickling filter configuration

Three trickling filters (TFs) with the same dimension and configuration were built for this study. Each TF was constructed from polyvinyl chloride cylinders with a diameter of 11 cm and a height of 105 cm, consisting of three separate compartments (each 35 cm in height) (Fig. 1). The volume of each TF was 10 L. Each TF cap was evenly opened with 20 small holes (0.5cm in diameter) to let the airflow draw through. A spaying apparatus was installed at the top of each TF to ensure that water was distributed homogeneously over the packed carriers. At the bottom of each TF, there was a 2 L reservoir. Water was recycled from the reservoir to the top of the TFs.

Each trickling filter (TF) was filled with a different carrier material: Argex crushed expanded clay aggregates (Argex, Belgium) as TF-A, polypropylene Bioball as TF-B, and polyethylene Kaldnes K1 as TF-K. The characteristics of the three carrier materials are shown in Table 4.2.

2.2 Influent composition

Synthetic wastewater was used as the influent, consisting of $(\text{NH}_4)_2\text{SO}_4$, NaHCO_3 , KH_2PO_4 (10 mg P L⁻¹), and 2 mL L⁻¹ trace element solution³⁰². The initial influent nitrogen concentration was approximately 100 mg NH₄⁺-N L⁻¹, with a dosage of 18 mg NaHCO₃ mg⁻¹ N. After day 158, their compositions increased to around 250 mg NH₄⁺-N L⁻¹ and 24 mg NaHCO₃ mg⁻¹ N.

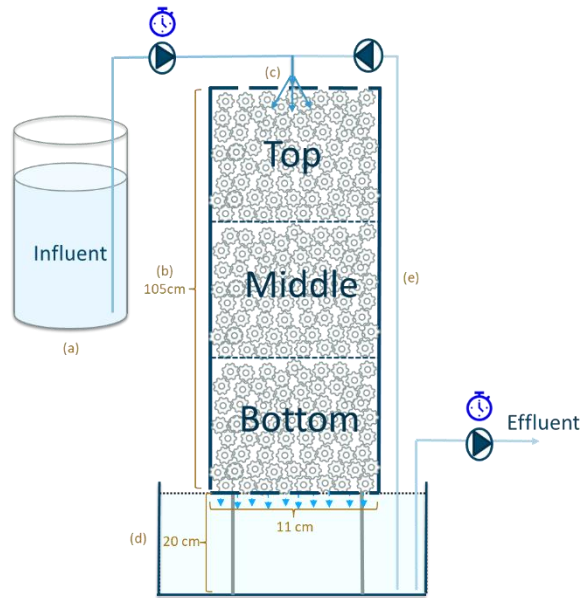


Figure 4.1: Schematic diagram of the packed-bed TF system: (a) influent tank; (b) trickling filter, consisted of three separate compartments (top, middle, and bottom); (c) spaying apparatus; (d) reservoir; (e) recirculation flow.

Table 4.2: Characteristics of the carrier materials used in the TFs.

| Carrier material | Argex (TF-A) | Bioball (TF-B) | Kaldnes (TF-K) |
|--|--------------|----------------|----------------|
| Diameter (mm) | 4-8 | 42 | 9 |
| Specific surface area ($\text{m}^2 \text{m}^{-3}$) | 500-1000 | 340 | 800 |
| Porosity (%) | 88 | 78 | 84 |
| Cost (€ m^{-3} , indicative) | 42 | 1983 | 1590 |

2.3 Trickling filter operation

A mixture of PN/A biofilm taken from a pilot-scale¹⁸⁵ and lab-scale RBC¹⁸⁶ was used as inoculum for all the three TFs. The TFs were operated in a temperature-controlled room at 30 ± 1 °C. Influent was sprayed semi-continuously over the top of the filter (1.25 min on, 8.75 min off), with a flow rate of 22 ± 2 L d⁻¹. The hydraulic loading rate (HLR) was determined by the flow rate of continuous recirculation pumps and the sectional area of

the TF, expressed as $\text{m}^3 \text{m}^{-2} \text{h}^{-1}$.

The whole operation period was divided into nine phases (I-IX). A new phase started when a parameter was changed to improve the performance of the PN/A process. Every operational parameter change, including influent nitrogen concentration, HLR, passive ventilation, and pH, was simultaneously applied in these three TFs. The pH was measured by a portable, digital pH meter C833 (Consort, Belgium). The DO was measured by a portable digital oxygen meter HQ30d (Hach Lange, Germany). The DO concentration was indirectly controlled by adjusting the HLR, passive ventilation approaches (top only, top and bottom), or aeration in the reservoir. When no passive ventilation was carried out, the bottom of the TF was submerged in the reservoir, while the holes on the top cap were sealed entirely with tapes. Active aeration was only implemented in phase V via aeration pumps to introduce oxygen into the recirculation flow. The pH and DO in the reservoir were measured daily. The parallel operating conditions for all the three TFs are detailed in the top table of Figure 4.2.

The influent and effluent samples were taken periodically from the influent vessel and the reservoir, respectively. The samples were immediately filtered with $0.45 \mu\text{m}$ filters and stored at $4 \text{ }^\circ\text{C}$ until $\text{NH}_4^+\text{-N}$, $\text{NO}_2^-\text{-N}$, and $\text{NO}_3^-\text{-N}$ concentration analysis.

2.4 Determination of microbial activity in each compartment

Microbial activity in three compartments of each TF was determined on day 259 (phase IX) via three rounds of batch tests. Before each round of batch tests, the recirculation pump of a TF was turned off. The columns were left to stand for 30 mins to drain the water out. The reservoir at the bottom of a TF was then filled with 2 L of tap water containing $100 \text{ mg NH}_4^+\text{-N L}^{-1}$ and $24 \text{ mg NaHCO}_3 \text{ mg}^{-1} \text{ N}$ as a buffer to keep the pH at around 7.5. The recirculation pump was then turned on again with the same HLR as in phase IX (i.e., $1.8 \text{ m}^3 \text{m}^{-2} \text{h}^{-1}$). The first-round batch test was first carried out for the integrated reactor. In the second round, the bottom compartment was taken down, and the two upper compartments were kept for the activity test. Finally, the third-round batch test was performed only in the top compartment. The batch test in every round lasted for 180 mins and samples were taken from the reservoir every 30 mins.

2.5 Physicochemical water analyses and microbial activity calculations

$\text{NH}_4^+\text{-N}$ was determined according to the standard Nessler method ²⁷⁰. $\text{NO}_2^-\text{-N}$, and $\text{NO}_3^-\text{-N}$ were determined on a 761 compact ion chromatograph equipped with a conductivity detector (Metrohm, Switzerland).

The microbial activities of the AerAOB, AnAOB, and NOB in the TFs were calculated based on the anammox stoichiometry (Strous et al., 1998) and mass balance of the nitrogen compounds (Eq. 4.1, 4.2, and 4.3) ^{114, 156}. Heterotrophic denitrification was assumed to be neglectable as no COD dosage was added into the influent. The AerAOB activity was determined as the sum of the individual contributions of $\text{NO}_2^-\text{-N}$ consumed by the NOB, $\text{NO}_2^-\text{-N}$ consumed by AnAOB, and residual $\text{NO}_2^-\text{-N}$ production ($P_{\text{NO}_2^-\text{-N}}$). The AnAOB activity was determined by the TN removal (R_{TN} , i.e., complete conversion to N_2) and the 11% $\text{NO}_3^-\text{-N}$ production by AnAOB (Reaction 4.1)). Finally, NOB activity was obtained from total $\text{NO}_3^-\text{-N}$ production ($P_{\text{NO}_3^-\text{-N}}$) subtracted by the $\text{NO}_3^-\text{-N}$ production by AnAOB.

$$\text{AerAOB activity (mg N L}^{-1}\text{ d}^{-1}\text{)} = (P_{\text{NO}_2^-\text{-N}}) + (P_{\text{NO}_3^-\text{-N}} - \frac{0.11}{0.89} * R_{\text{TN}}) + (\frac{1.32}{2.32} * (R_{\text{TN}} + \frac{0.11}{0.89} * R_{\text{TN}})) \quad (4.1)$$

$$\text{AnAOB activity (mg N L}^{-1}\text{ d}^{-1}\text{)} = R_{\text{TN}} + \frac{0.11}{0.89} * R_{\text{TN}} \quad (4.2)$$

$$\text{NOB activity (mg N L}^{-1}\text{ d}^{-1}\text{)} = P_{\text{NO}_3^-\text{-N}} - \frac{0.11}{0.89} * R_{\text{TN}} \quad (4.3)$$

3. Results and discussion

The performances of TF-A, TF-B, and TF-K were divided into nine phases (I to IX, Figure 4.2 and 4.3) based on the changes of operation parameters. The observed DO levels in each reservoir are shown in the top tables of Figure 4.2 and 4.3. Since the overall trend of performance in TF-B and TF-K reactor was similar to TF-A, the results of TF-A were highlighted. More details about the TF-B and TF-K can be found in SI Figure S4.1 and S4.2.

3.1 Startup periods: nitrate accumulation

Phase I and II are considered startup periods when ventilation was allowed only from

the top of TFs. The bulk solution was recirculated continuously with a hydraulic loading rate (HLR) of $0.8 \text{ m}^3 \text{ m}^{-2} \text{ h}^{-1}$ in phase I. The $\text{NH}_4^+\text{-N}$ removal efficiencies were around 54% in all the three TFs (Figure 4.2b0, while the TN removal efficiency was much lower ($17\pm 4\%$, $19\pm 2\%$, and $12\pm 6\%$), mainly due to the high $\text{NO}_3^-\text{-N}$ production (relative to the removed $\text{NH}_4^+\text{-N}$ corrected for the $\text{NO}_2^-\text{-N}$ accumulation) of $71\pm 6\%$, $54\pm 3\%$, and $64\pm 15\%$ in TF-A, TF-B, and TF-K, respectively. The $\text{NO}_3^-\text{-N}$ production was significantly above the optimal level of 11% for the PN/A process¹⁵⁶, which could be attributed to NOB activity. The $\text{NO}_2^-\text{-N}$ accumulation of around 60% (relative to the removed $\text{NH}_4^+\text{-N}$) was initially observed in all the three TFs, indicating that NOB and AnAOB were both limited initially. Over time, $\text{NO}_2^-\text{-N}$ accumulation gradually decreased in phase I, and NOB won the competition for $\text{NO}_2^-\text{-N}$ over anammox due to the relatively high DO ($0.6\text{-}1.1 \text{ mg L}^{-1}$, top tables of Figure 4.2 and 4.3).

In phase II, under a lower HLR of $0.4 \text{ m}^3 \text{ m}^{-2} \text{ h}^{-1}$, the $\text{NO}_3^-\text{-N}$ production efficiency decreased to $30\pm 2\%$, $44\pm 2\%$, and $40\pm 2\%$ in TF-A, TF-B, and TF-K, respectively. Combined with the further increase of $\text{NH}_4^+\text{-N}$ removal and decrease of $\text{NO}_2^-\text{-N}$ accumulation, the TN removal efficiency increased to $51\pm 3\%$, $31\pm 2\%$, and $31\pm 2\%$ for TF-A, TF-B, and TF-K, respectively. By the end of phase II, the TN removal rates stabilized at 132 ± 12 , 75 ± 5 , and $64\pm 7 \text{ mg N L}^{-1} \text{ d}^{-1}$ in TF-A, TF-B, and TF-K, respectively.

The improved TN removal performance from phase I to II was related to the activity shift of functional bacteria (i.e., AerAOB, AnAOB, and NOB, Figure 4.2d), likely due to the decreased DO concentration in the reactors via reducing the HLR. Presumably, decreasing the HLR could induce less oxygen sucked into the reactor^{277, 278}. AerAOB have a higher oxygen affinity than NOB, with the half-saturation constant K_s of 0.6 and $2.2 \text{ mg O}_2 \text{ L}^{-1}$, respectively³⁰³. Thus, at low DO concentrations ($< 1 \text{ mg O}_2 \text{ L}^{-1}$), the oxygen would preferentially go to AerAOB, limiting the NOB activity. Another possible explanation could be the increased biofilm thickness over time, which created more anoxic zones that promoted the AnAOB activity^{193, 304}. Consequently, less $\text{NO}_2^-\text{-N}$ was available for NOB. Nevertheless, controlling the DO level in TFs was difficult as it was not directly measured. Only the DO in the reservoir was measured, which was a combined result of the oxygen

dissolved into the reservoir, ventilated into the TF, and consumed by AerAOB and NOB.

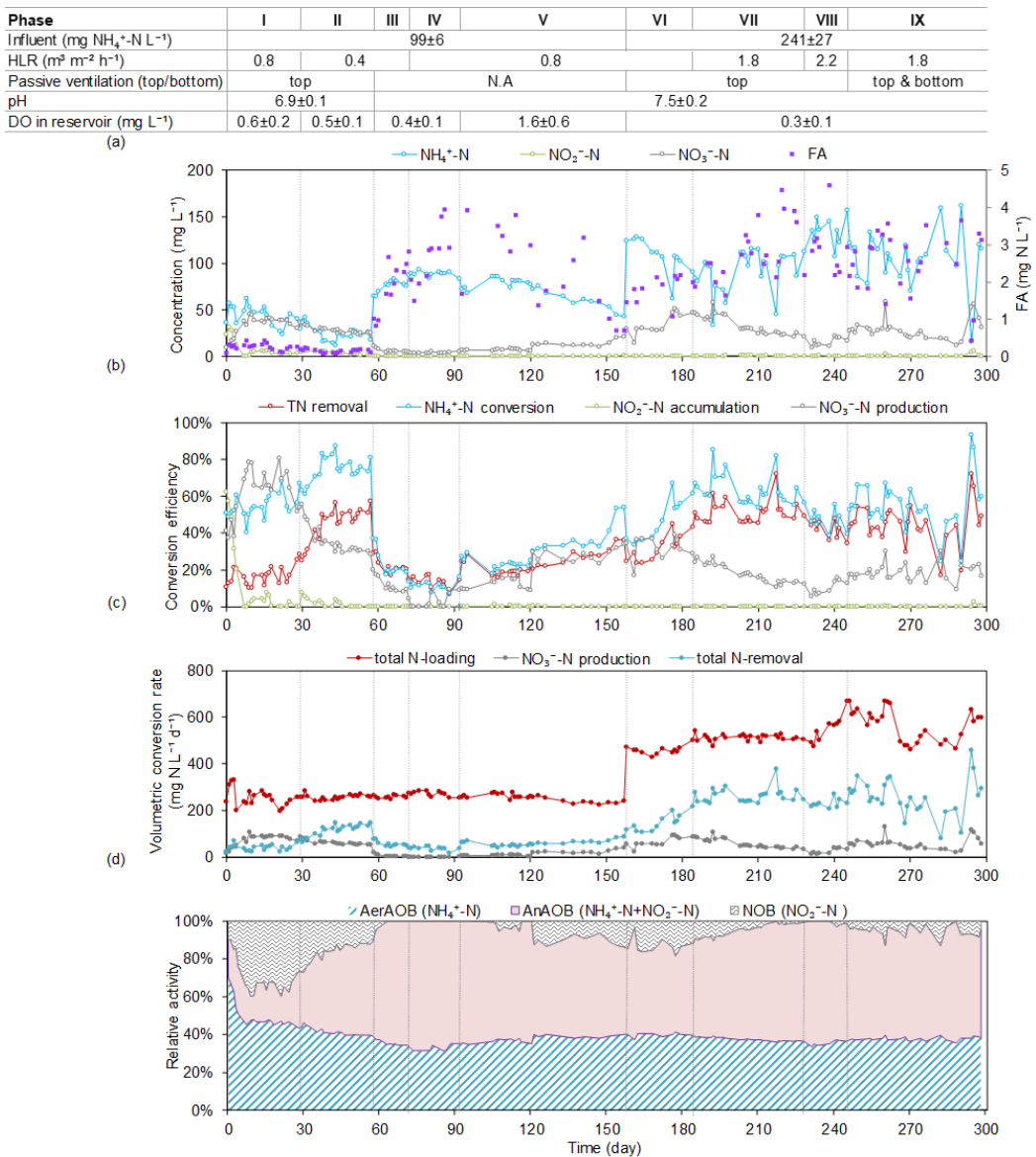


Figure 4.2: Performance overview of TF-A in phase I-IX (day 0-300): (a) effluent concentration and FA level, (b) nitrogen conversion efficiency, (c) volumetric loading and conversion rate, and (d) relative activity of AerAOB, AnAOB, and NOB. The main variables per phase are shown on the top.

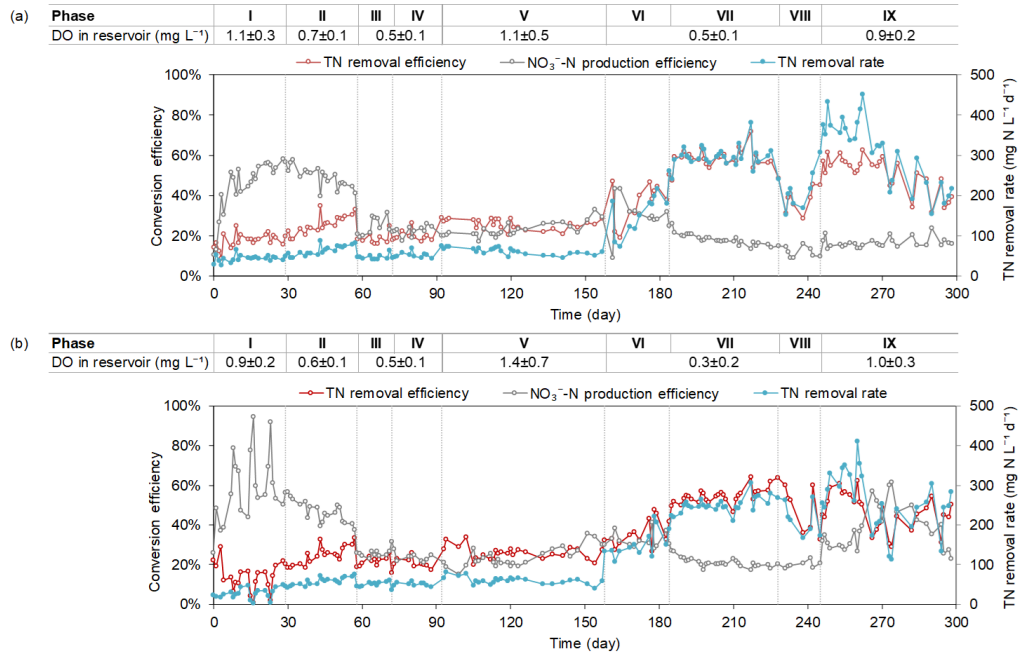


Figure 4.3: Performance overview of (a) TF-B and (b) TF-K in phase I-IX (day 0-300), including TN removal efficiency, NO_3^- -N production efficiency, and TN removal rate.

3.2 Effect of the top passive ventilation and TN loading rate

The top ventilation was stopped in phase III to further decrease the NO_3^- -N production via reducing the DO in TFs. The NO_3^- -N production significantly decreased to $12 \pm 4\%$, $25 \pm 5\%$, and $25 \pm 1\%$ in TF-A, TF-B, and TF-K, respectively (Figure 4.2b and 4.3). No NO_2^- -N accumulation was observed in any TF. However, stopping the top ventilation caused the decrease of NH_4^+ -N removal efficiency to around 24% in all the TFs, probably attributed to the insufficient oxygen for AerAOB. The sharply steep drop of NH_4^+ -N removal efficiency offset the decrease of NO_3^- -N production, causing the TN removal efficiency to drop to around 20% in all TFs (Figure 4.2b and Figure 4.3).

In phase IV, the HLR was recovered to $0.8 \text{ m}^3 \text{ m}^{-2} \text{ h}^{-1}$ again, aiming to raise the DO and, consequently, the NH_4^+ -N oxidation in TFs. However, only increasing HLR failed to achieve these goals (e.g., Figure 4.2). Since the TFs were completely closed, no air could be sucked in, and the only DO source was the oxygen dissolved into the reservoir. Therefore, in phase V, aeration pumps were installed in the reservoir to actively introduce more DO into the recirculation stream. The active aeration successfully promoted the NH_4^+ -N

oxidation in all the TFs, particularly in TF-A (from $11\pm 2\%$ to $50\pm 7\%$), indicating low oxygen concentration was the limiting factor.

In phase VI, the top passive ventilation replaced the active aeration in the reservoir. Meanwhile, the influent concentration was increased to about $250 \text{ mg NH}_4^+\text{-N L}^{-1}$. These two actions increased the $\text{NH}_4^+\text{-N}$ removal efficiency to around 60% in all the TFs. Compared with phase I at the same HLR, phase VI got similar $\text{NH}_4^+\text{-N}$ conversion efficiency but lower $\text{NO}_3^-\text{-N}$ production efficiency of around 32% (Figure 4.2b and 4.3). As a result, the TN removal efficiency increased to approximately 42% in TFs. Furthermore, due to the influent loading rate, the TN removal rate increased to about $184 \text{ mg N L}^{-1} \text{ d}^{-1}$ compared to $40 \text{ mg N L}^{-1} \text{ d}^{-1}$ in phase I for all the TFs (Figure 4.2c and Figure 4.3).

The highest $\text{NO}_3^-\text{-N}$ production observed during the startup periods indicated the most potent NOB activity. When the top passive ventilation was stopped, $\text{NO}_3^-\text{-N}$ production and $\text{NH}_4^+\text{-N}$ removal drastically dropped as limited amount of DO was introduced into TFs. Meanwhile, an increase in pH from around 7.0 to 7.5 was observed due to fewer protons (H^+) production. With the rise of residual $\text{NH}_4^+\text{-N}$ and pH, the FA level in all the TFs increased from around $0.3 \text{ mg NH}_3\text{-N L}^{-1}$ to above $1.3 \text{ mg NH}_3\text{-N L}^{-1}$ in phase III and IV (e.g., Figure 4.2a). Since NOB are sensitive to FA¹¹⁴, FA inhibition could be another reason for the almost vanished NOB activity in phase III and IV (e.g., Figure 4.2d). Nevertheless, passive ventilation was necessary to get enough oxygen into the reactors for partial nitrification.

Compared to the performance of period I, the increase of TN removal efficiency and the decrease of $\text{NO}_3^-\text{-N}$ production efficiency in phase VI indicated that AnAOB activity increased at the expense of NOB activity. Additionally, the higher loading rate promoted the $\text{NH}_4^+\text{-N}$ removal rate and intensified the DO consumption in TFs, as evidenced by the decreased DO concentration in the reservoirs (to around 0.3 mg L^{-1}). Consequently, AerAOB may have a competitive advantage for oxygen over NOB³⁰⁵, and thus the NOB activity decreased.

3.3 Effect of hydraulic loading rate

In phases VII and VIII, the impact of HLR was investigated under the top passive ventilation condition. The HLR was increased to $1.8 \text{ m}^3 \text{ m}^{-2} \text{ h}^{-1}$ and $2.2 \text{ m}^3 \text{ m}^{-2} \text{ h}^{-1}$ in phases VII and VIII, respectively. In phase VII, $\text{NH}_4^+\text{-N}$ conversion was improved further, while the $\text{NO}_3^-\text{-N}$ production kept decreasing, especially in TF-A, with $64\pm 8\%$ and $13\pm 1\%$, respectively. As a result, the TN removal efficiency increased to $52\pm 7\%$, $59\pm 4\%$, and $55\pm 3\%$, and the TN removal rate reached 269 ± 34 , 300 ± 23 and $251\pm 19 \text{ N L}^{-1} \text{ d}^{-1}$, in TF-A, TF-B, and TF-K, respectively (Figure 4.2c and 4.3). In phase VIII, after increasing the HLR to $2.2 \text{ m}^3 \text{ m}^{-2} \text{ h}^{-1}$, no further improvements of the $\text{NH}_4^+\text{-N}$ conversion and TN removal were observed. Since the higher HLR means more electrical energy consumption by recirculation pumps, the best HLR was considered $1.8 \text{ m}^3 \text{ m}^{-2} \text{ h}^{-1}$.

It was suggested the typical HLR in TFs to keep the carrier material moist is between 1 to $3 \text{ m}^3 \text{ m}^{-2} \text{ h}^{-1}$ ²⁷⁶. The best HLR found in this study, i.e., $1.8 \text{ m}^3 \text{ m}^{-2} \text{ h}^{-1}$, was within this recommended range. Thus, the higher TN removal efficiency at $1.8 \text{ m}^3 \text{ m}^{-2} \text{ h}^{-1}$ could be partly because the carriers were more completely wetted, while a lower HLR could not make the bulk solution reach the carrier, resulting in some dry zones and substrate diffusion limitations. Besides, the relatively high FA level in phase VII, especially in TF-A ($3.2\pm 0.7 \text{ mg N L}^{-1}$, Figure 4.2a), could be another reason for the decreased NOB activity and improved PN/A performance.

3.4 Effect of top and bottom ventilation

In phase IX, the bottom of the TFs emerged from the water of reservoirs; hence, the passive ventilation was carried out via the top and bottom of TFs. Compared to phase VII (same HLR but only via top ventilation), the TN removal efficiency and rate were roughly stable for all the three TFs in phase IX.

Allowing passive ventilation from the bottom resulted in the reservoir DO increase to $1.0 \text{ mg O}_2 \text{ L}^{-1}$ in TF-B and TF-K, probably related to the porosity of carrier materials (Table 4.2). The high porosity of Argex in TF-A probably allowed more oxygen to reach the bottom compartment with only the top ventilation. Consequently, after further allowing the bottom ventilation, less oxygen was sucked in in TF-A than in the other two TFs. This

hypothesis was consistent with the relatively constant $\text{NH}_4^+\text{-N}$ and $\text{NO}_3^-\text{-N}$ conversion performance in TF-A (Figure 4.2) before and after allowing ventilation from the bottom. The FA level was relatively constant ($2.3 \pm 0.7 \text{ mg N L}^{-1}$) in TF-B but decreased to $0.7 \pm 0.3 \text{ mg N L}^{-1}$ in TF-K from phase VII to IX (SI Figure S4.2). Compared to the lower $\text{NO}_3^-\text{-N}$ production efficiency in TF-B, the rise of $\text{NO}_3^-\text{-N}$ production efficiency in TF-K could be related to the decreased FA level. Nevertheless, the TN removal performance was comparable to that in phase VII for all the three TFs, without regard to the increased $\text{NO}_3^-\text{-N}$ production in TF-K (Figure 4.2 and 4.3)). Therefore, it could be concluded that passive ventilation via the top and bottom of TFs could not facilitate TN removal and was unnecessary.

3.5 Vertical activity stratification in trickling filters

The TFs used in this study consisted of three vertical compartments (top, middle, and bottom). Batch tests were carried out on day 259 to quantify the microbial activity of AerAOB, AnAOB, and NOB in each compartment (Eq. 4.1, 4.2, and 4.3, section 2.5).

In TF-A, the AerAOB activity increased from the top of $290 \text{ mg N L}^{-1} \text{ d}^{-1}$ to the bottom compartment of $461 \text{ mg N L}^{-1} \text{ d}^{-1}$ (Figure 4.4). The AnAOB activity was highest in the top compartment and accounted for about 65% of total AnAOB activity. The NOB activity decreased from bottom to top, with 46% activity in the bottom compartment. In TF-B, the AerAOB and AnAOB activities were highest in the top compartment with 291 and 403 $\text{mg N L}^{-1} \text{ d}^{-1}$, respectively. The AnAOB activity in the bottom compartment was almost zero. The NOB activity was low and approximately equal in all compartments with $45 \pm 9 \text{ mg N L}^{-1} \text{ d}^{-1}$. Similarly to TF-A, the highest AerAOB and AnAOB activities were in the top compartment of TF-K, while the highest NOB activity was in the bottom, accounted for 46%.

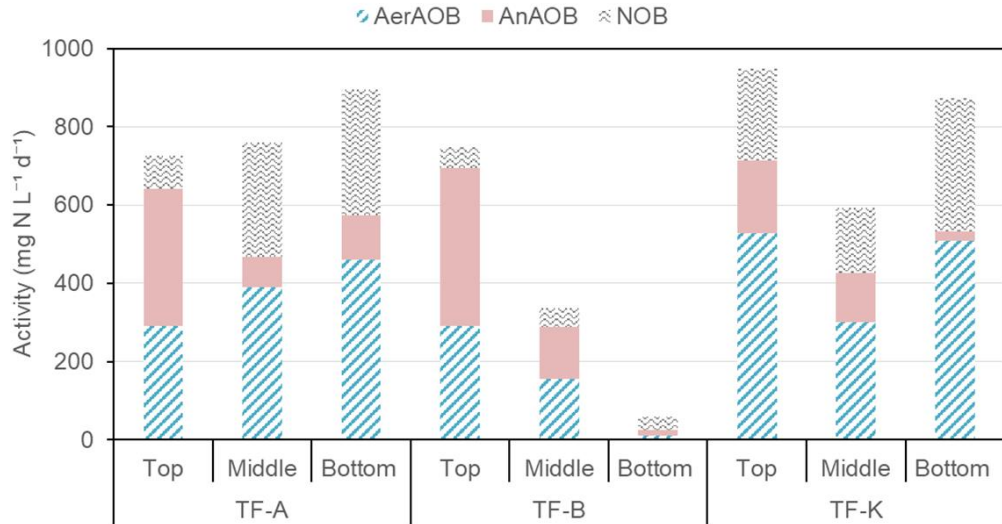


Figure 4.4: The microbial activities of AerAOB, AnAOB, and NOB in each compartment of the TFs on day 259, phase IX.

In TF-A, the increasing AerAOB activity from top to bottom could be the combined effects of the DO and AnAOB availability. Presumably, the high porosity had resulted in relatively homogeneous ventilation in TF-A, but allowing the bottom ventilation further intensified the DO level in the bottom compartment, favored the prosperity of AerAOB. Besides, the lower AnAOB activity in the middle and bottom compartments resulted in less competition over AerAOB for $\text{NH}_4^+\text{-N}$. The lower AnAOB activity in the bottom compartment of TF-A resulted in less competition with NOB for $\text{NO}_2^-\text{-N}$, and thus the proliferation of NOB activity (around 50%) (Figure 4.4). In TF-B, it was striking that the microbial activities in the bottom compartment were much lower than in the other TFs (Figure 4.4). It was likely due to the washout of biomass from the bottom compartment. The low specific surface area of TF-B (Table 4.2) was suggested to grow ticker biofilms³⁰⁶, which are much less stable and easier to be removed by the water flow³⁰⁷. In TF-K, the AerAOB and NOB activity decreased in the middle compartment but increased again in the bottom compartment (Figure 4.4). The increased AerAOB and NOB activity in the bottom compartment might benefit from the bottom ventilation, which increased the oxygen concentration there.

3.6 Carrier materials and electrical energy consumption

Since oxygen is a crucial parameter for the microbial balance between AerAOB, AnAOB, and NOB, the thickness of biofilm and thus the oxygen penetration depth are crucial^{308, 309}. The thickness of the biofilm is partly determined by the structure and shape of the carrier material. The lower the specific surface area, the less biomass can be exposed to oxygen per reactor volume. In the compartment activity tests, the total AerAOB activity in TF increased following TF-B < TF-A < TF-K. The lowest AerAOB activity in TF-B could be related to the lowest specific surface area of Bioballs ($340 \text{ m}^2 \text{ m}^{-3}$, Table 4.2).

From another perspective, owing to the smaller specific surface of TF-B, the chance was greater to form thicker biofilms and thus more anoxic zones for AnAOB. In contrast to the Bioballs in TF-B, the Kaldnes K1 in TF-K, with a higher specific surface area of $800 \text{ m}^2 \text{ m}^{-3}$, showed a higher NOB activity. Nevertheless, the available specific surface area and tiny pores of Argex in TF-A could still provide sufficient anoxic zones to guarantee AnAOB activity. Therefore, it is concluded that a larger specific surface area is not necessarily preferable for higher PN/A performance.

For all the three TFs, the highest TN removal efficiency of 60% and TN removal rate of $300 \text{ mg N L}^{-1} \text{ d}^{-1}$ were achieved in phase VII, with the top ventilation and the best HLR ($1.8 \text{ m}^3 \text{ m}^{-2} \text{ h}^{-1}$) (Figure 4.2 and 4.3). Notably, a relatively low NO_3^- -N production of 13% was achieved for the first time for PN/A in TF-A. The TN removal rate was moderate among those (35 to $2130 \text{ mg N L}^{-1} \text{ d}^{-1}$) obtained in other PN/A biofilm reactors according to their TN loading rate and removal efficiency (Table 4.1). Compared to those two PN/A studies in DHS-TFs, the higher TN removal efficiency and lower NO_3^- -N production efficiency were achieved in this study. Although the difference in TN removal performance by the three carrier materials in this study was negligible, the lowest price makes Argex economically attractive among these three carrier materials to achieve PN/A in a TF (Table 4.2).

In the designed TFs, oxygen is passively introduced into the reactor. Instead of the energy-consuming active aeration, the recirculation pump becomes the energy-consuming item. To calculate its electrical energy consumption, several parameters were

assumed, including a daily nitrogen production per inhabitant equivalent of 1.5 g N d^{-1} ³¹⁰, reactor height of 105 cm, pump depth in the reservoir of 20 cm, a pipe head loss of 0.33 m m^{-1} pipe and a high pump efficiency of 80%²⁸². The estimated electricity consumption was $0.78 \text{ kWh kg}^{-1} \text{ N}$ removal under the operation scenario of phase VII, which was 1.95-fold of an RBC ($0.4 \text{ kWh kg}^{-1} \text{ N}$)³¹¹, but 35% more energy-efficient than an SBR ($1.2 \text{ kWh kg}^{-1} \text{ N}$)³¹².

To realize a more economical PN/A process in TFs, further improving the TN removal efficiency is necessary. The $\text{NH}_4^+\text{-N}$ conversion efficiency was below 90% in most cases and around 70% in phase VII, indicating the overloading in TFs. Hence, a proper decrease in the TN loading rate may help the improvement of TN removal efficiency. Additionally, since most TN removal capacity was distributed in the top two compartments, reducing the height of TF may further increase the TN removal efficiency and cut the capital expenditure, which requires further demonstration in the future.

4. Conclusions

This study demonstrated the feasibility of packed-bed TFs for one-stage PN/A. The tests on ventilation approaches showed that the top passive ventilation was sufficient to supply oxygen for PN/A. For all the three TFs, more than 56% of the AnAOB activity was found in the top compartment. Under the optimal HLR of $1.8 \text{ m}^3 \text{ m}^{-2} \text{ h}^{-1}$, a TN removal efficiency of 60% and a rate of $300 \text{ mg N L}^{-1} \text{ d}^{-1}$ were achieved. A relatively ideal $\text{NO}_3^- \text{-N}$ production (13%) was performed in the TF-PN/A process. Moreover, the cheap carrier based on expanded clay was recommended due to the similar TN removal rates as commercially used plastic carrier materials. The estimated electricity consumption of PN/A in TFs was 35% lower than an actively aerating reactor, making it a potentially economical alternative for nitrogen removal.

5. Supplementary information

| Phase | I | II | III | IV | V | VI | VII | VIII | IX |
|--|---------|-----|-------|----|-----|---------|-----|--------------|-----|
| Influent ($\text{mg NH}_4^+\text{-N L}^{-1}$) | | | 100±6 | | | | | 243±28 | |
| HLR ($\text{m}^3 \text{m}^{-2} \text{h}^{-1}$) | 0.8 | 0.4 | | | 0.8 | | 1.8 | 2.2 | 1.8 |
| Passive ventilation (top/bottom) | top | | N.A. | | | top | | top & bottom | |
| pH | 7.0±0.1 | | | | | 7.5±0.2 | | | |

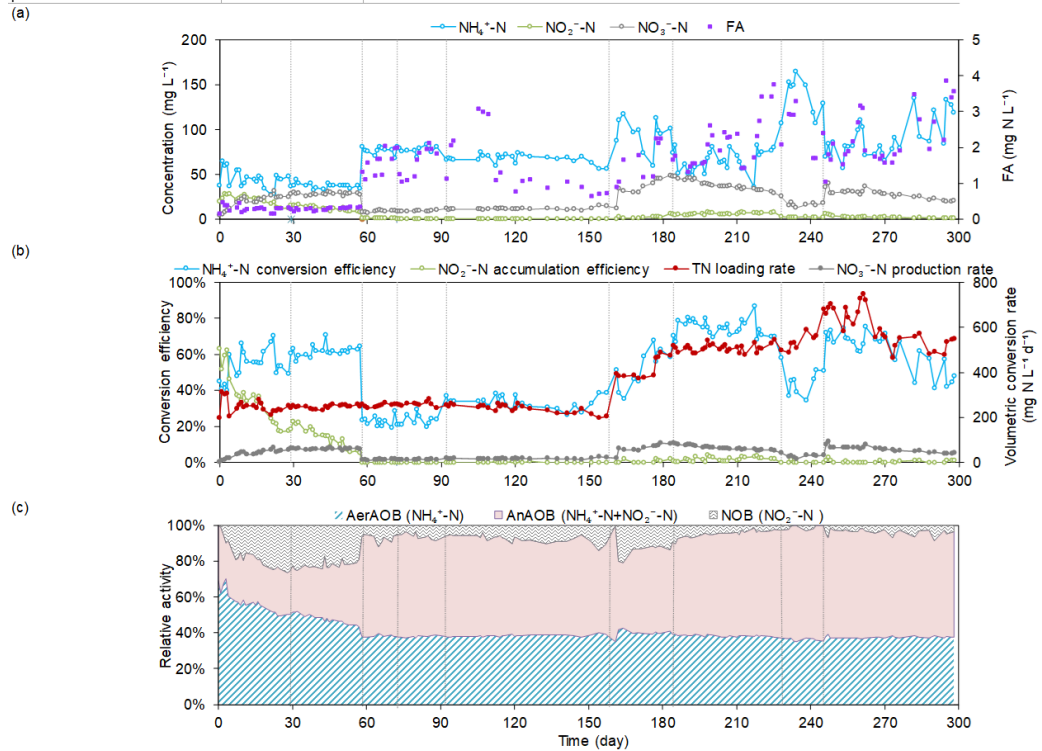


Figure S4.1: Performance overview of TF-B in phase I-IX (day 0-300): (a) effluent concentration and FA level, (b) $\text{NH}_4^+\text{-N}$ conversion efficiency, $\text{NO}_2^-\text{-N}$ accumulation efficiency, TN volumetric loading rate, and $\text{NO}_3^-\text{-N}$ production rate, and (d) relative activity of AerAOB, AnAOB, and NOB. The main variables per phase are shown at the top.

Chapter 4

| Phase | I | II | III | IV | V | VI | VII | VIII | IX |
|--|---------|-----|------|----|-----|---------|-----|--------------|-----|
| Influent ($\text{mg NH}_4^+\text{-N L}^{-1}$) | | | 99±6 | | | | | 248±33 | |
| HLR ($\text{m}^3 \text{m}^{-2} \text{h}^{-1}$) | 0.8 | 0.4 | | | 0.8 | | 1.8 | 2.2 | 1.8 |
| Passive ventilation (top/bottom) | top | | N.A | | | top | | top & bottom | |
| pH | 7.0±0.1 | | | | | 7.4±0.2 | | | |

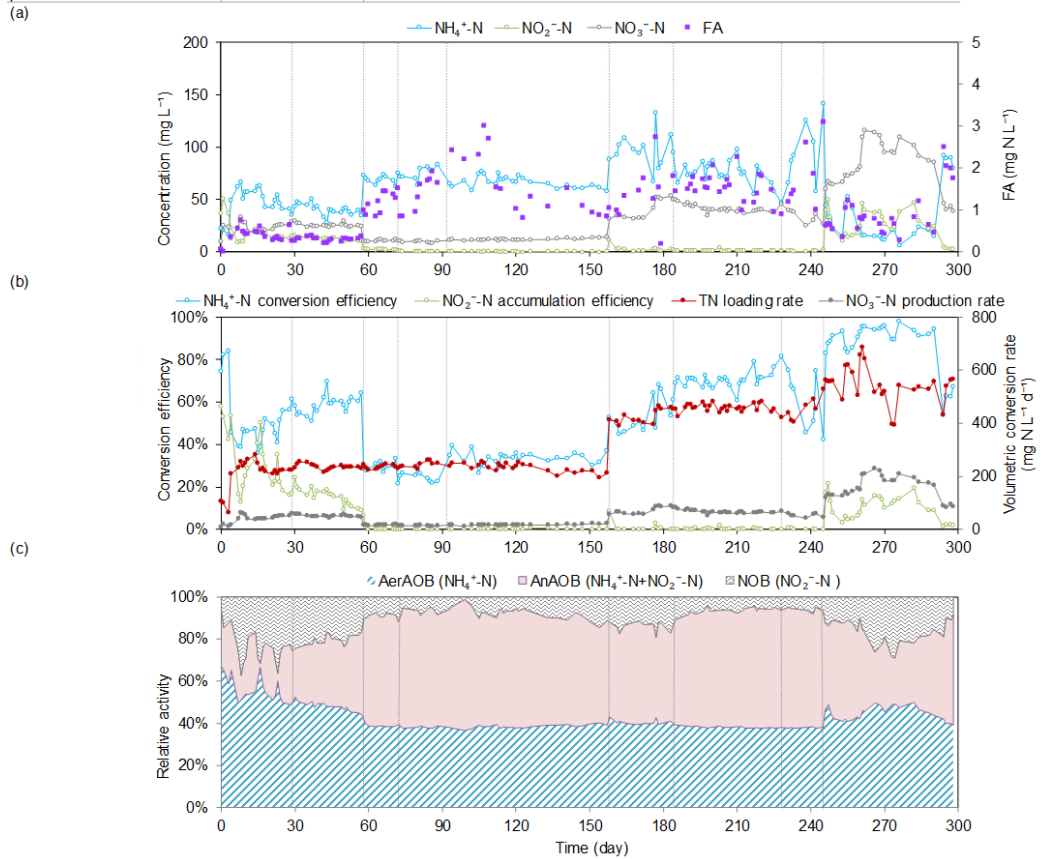


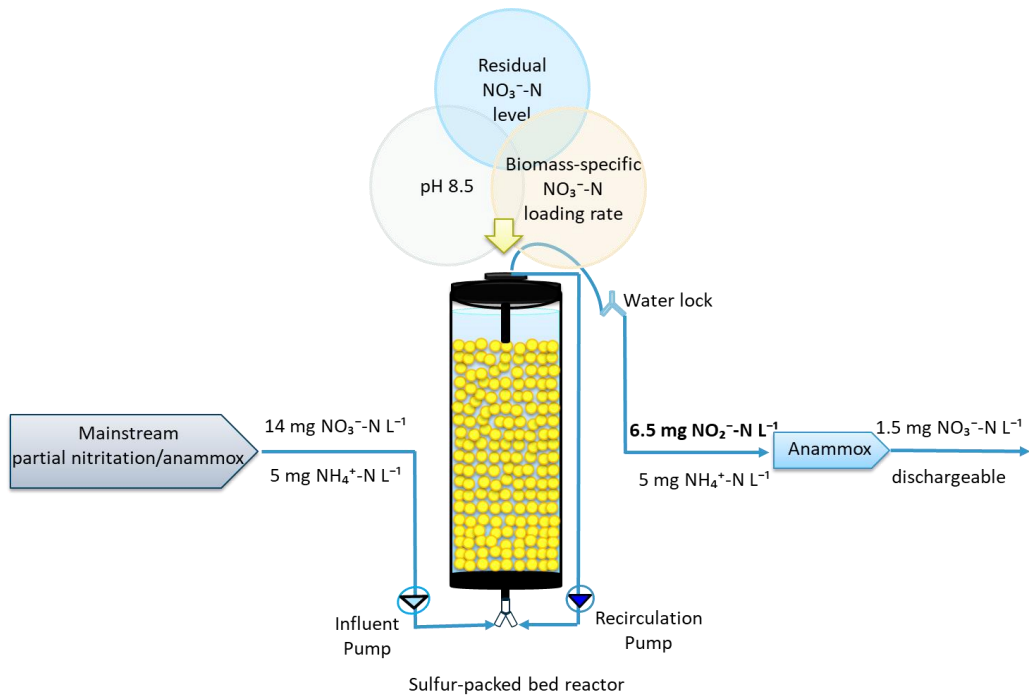
Figure S4.2: Performance overview of TF-K in phase I-IX (day 0-300): (a) effluent concentration and FA level, (b) $\text{NH}_4^+\text{-N}$ conversion efficiency, $\text{NO}_2^-\text{-N}$ accumulation efficiency, TN volumetric loading rate, and $\text{NO}_3^-\text{-N}$ production rate, and (d) relative activity of AerAOB, AnAOB, and NOB. The main variables per phase are shown at the top.

6. Acknowledgments

The authors would like to acknowledge the financial support for S.E.V. through a postdoctoral fellowship from the Research Foundation - Flanders (FWO) and for Y.X. from the China Scholarship Council (File no. CSC201706130131).

Chapter 5

Autotrophic nitrogen polishing of secondary effluents: Challenges in obtaining sulfur-driven denitratation for downstream anammox treatment



Publication of a redrafted version of this chapter is intended:

Xie, Y.; Van Tendeloo, M.; Zhu, W.; Peng, L.; Vlaeminck, S. E., Autotrophic nitrogen polishing of secondary effluents: Challenges in obtaining sulfur-driven denitratation for downstream anammox treatment. (In preparation)

Abstract

Energy-positive sewage treatments, such as mainstream partial nitrification/anammox, are often confronted with effluent issues of accumulated nitrate (NO_3^-) and residual ammonium. This study proposed a novel polishing strategy by coupling sulfur-driven denitrification with anammox. To simulate the effluent quality of the mainstream PN/A, low-strength synthetic wastewater was applied in two sulfur-packed bed reactors. To explore the feasibility of sufficient and stable nitrite (NO_2^-) accumulation in the long term, the effects of pH setpoints, residual nitrate level, and biomass-specific nitrate loading rate (BSNLR) were investigated. Alternating the pH setpoints between 7.0 and 8.5 could temporarily stimulate nitrite accumulation. Both the residual nitrate level and the BSNLR showed highly positive correlations with the nitrite accumulation efficiency. Under the control of pH 8.5, $1.0 \pm 0.8 \text{ mg NO}_3^- \text{-N L}^{-1}$ and $150 \pm 42 \text{ mg NO}_3^- \text{-N g}^{-1} \text{ VSS d}^{-1}$, sulfur-driven denitrification could produce $6.4 \pm 1.0 \text{ mg NO}_2^- \text{-N L}^{-1}$ over 30 days. *Thiobacillus* members may play a crucial role in managing the $\text{NO}_2^- \text{-N}$ accumulation, but their abundance reduction and possible adaptation significantly impaired the efficacy of control strategies in the long run. Probably, additional control tools need to be investigated for longer-lasting nitrite accumulation.

1. Introduction

Partial nitrification/anammox (PN/A) is considered a resource- and cost-effective technology for autotrophic nitrogen removal from wastewater¹¹⁴. However, mainstream PN/A processes have faced effluent issues containing nitrate above 10 mg N L⁻¹. Several inherent features of the mainstream, e.g., low ammonium (NH₄⁺) levels, low temperatures, and fluctuant loading rate, make the out-selection of nitrite-oxidizing bacteria (NOB) quite challenging¹⁷⁰⁻¹⁷². Besides, to provide kinetic superiority for aerobic and anoxic ammonium-oxidizing bacteria over NOB, some residual NH₄⁺ (e.g., around 5 mg N L⁻¹) is required in the mainstream PN/A system³¹³. Therefore, to meet a stringent discharge limit of total nitrogen concentrations (<10 mg N L⁻¹)³¹⁴, an additional polishing step is essential to remove both NH₄⁺ and NO₃⁻ in mainstream PN/A effluent. Recently, an innovative denitrification /anammox (DN/A) technology has been proposed, where the nitrite (NO₂⁻) anoxically reduced from NO₃⁻ would be removed together with NH₄⁺ via anammox. Depending on the electron donor sources for denitrification, the technology can be classified as heterotrophic (i.e., COD-driven)³¹⁵⁻³¹⁷ and autotrophic DN/A processes^{146, 148, 318}. Sufficient and stable NO₂⁻ accumulation via DN process is the crucial prerequisite for desirable polishing performance, as anammox process could be readily steered as long as NO₂⁻ is available^{137, 319}.

Heterotrophic DN has been explored with various carbon sources such as acetate, ethanol, and methanol^{136, 137, 320}. Although these electron donors could successfully realize DN performance, they are costly to apply to the effluent polishing scenario. Besides the cost of external carbon, their sludge yields (0.4-0.9 g cell g⁻¹ NO₃⁻-N) are higher than autotrophic DN (0.4-0.5 g cell g⁻¹ NO₃⁻-N)^{109, 130}. Thus, autotrophic DN should be advocated as a more promising alternative.

Elemental sulfur (S⁰) could be an appealing electron donor for DN. It is more sustainable and cheaper than those carbon sources and can even serve as a biomass carrier^{120, 321}. Since S⁰ is poorly soluble in water, three possible mechanisms of electron donor production for NO₃⁻ reduction were proposed: (i) some sulfur-oxidizing bacteria (SOB) with membrane-bound enzymes can obtain electrons via direct contact with the S⁰

surface^{322, 323}; (ii) some SOB producing extracellular enzymes can convert S^0 into soluble polysulfides (S_n^{2-}), which can then diffuse into the biofilm as electron donors^{150, 324}; (iii) the produced S_n^{2-} could be further converted to biologically produced S^0 , which can be used as electron donors as well¹⁴⁶.

In the autotrophic denitrification process, few studies investigated the effects of pH setpoints on the nitrite accumulation efficiency (NAE), representing the ratio of accumulated NO_2^- -N to reduced NO_3^- -N. Chen et al. (2018) proposed that the optimum pH values for NO_3^- and NO_2^- reduction were 8.5 and 7.0 in the sulfur autotrophic denitrification process, as the nitrate reductase activity could outcompete that of nitrite reductase for electrons at alkaline condition¹⁴⁵. They found the effective NO_2^- -N accumulation (NAE > 80%) by setting pH at 8.5 in the short term (45 days). However, the long-term effects of pH control strategy on NAE and the associated microbial community structure have not yet been reported.

The kinetics of S^0 based reduction of NO_3^- and NO_2^- has been investigated in several studies. It was found that the maximum specific substrate utilization rate of nitrate is around 1.8 times higher than that of nitrite¹⁵⁰. Thus, when NO_3^- is reduced in the S^0 attached biofilm, NO_2^- may accumulate and diffuse to the bulk liquid. It was found that bulk nitrate level could affect the extent of nitrite accumulation; namely, nitrite would be reduced once nitrate has been significantly or entirely converted^{150, 151, 325, 326}. Therefore, using the residual nitrate control to realize the sulfur-driven denitrification (SDN) would be possible.

Wang et al. (2016) proposed a substrate counter-diffusion model in the sulfur denitrifying process¹⁵¹. The soluble sulfur species diffuse from the S^0 surface into the attached biofilm, while NO_3^- diffuses from the bulk liquid into the biofilm. As the nitrate reductase has a greater affinity for reduced electron carriers (e.g., NADH) than the nitrite reductase³²⁷, the diffusion extent of nitrate and reduced electron carriers in biofilm may influence nitrite accumulation. However, it is rarely feasible to maintain the desired thickness because of biofilm growth, detachment, and predation over time¹⁵⁰. The specific nitrate loading rate based on biomass could be a more accessible alternative to

manipulate the substrate counter-diffusion, consequently to the nitrite accumulation.

According to our knowledge, there is no study looking into the feasibility of SDN for stable nitrite accumulation in long-term operation. The long-term feasibility of pH setpoints (7.0 and 8.5), residual nitrate level (0 to 15 mg N L⁻¹), and biomass-specific nitrate loading rate (BSNLR, 113 to 507 mg N g⁻¹ VSS L⁻¹) were comprehensively investigated to realize stable SDN for the downstream anammox process. The correlations between the control strategies (residual nitrate level and BSNLR) and NAE were analyzed. In addition, the evolution of microbial community composition in the biofilm was studied.

2. Material and methods

2.1 Reactor setup

Two packed bed reactors (R-1 and R-2) were set up independently as duplicates in this study. Each reactor had a total volume of 1 L (inner diameter 6.4 cm and height 23.3 cm) but a bed volume of 0.8 L (including void volume), packed with pure S⁰ particles of 3-4 mm diameter. The reactors were operated in up-flow mode. During the long-term operation, the continuous influent flowrates were 43 and 86 L d⁻¹, using peristaltic pumps (Seko Peristaltic Pumps, PR7). The flow rate of 86 L d⁻¹ was only imposed for short periods: day 0-44 and 75-101 in R-1, and day 109-124 and 165-177 in R-2. Thus, two HRT settings (i.e., 6 and 12 min) were used in this research, based on the S⁰ void volume and free reactor volume (tubing volume and upper space of S⁰ bed). In addition, a recirculation rate of 1382 L d⁻¹ was imposed to give entirely mixed conditions with a recirculation ratio (i.e., the ratio of recirculation flow to influent flow) of 16 and 32 via peristaltic pumps (Etatron BH3-V Peristaltic Pump).

2.2 Chemicals and influent

The synthetic influent contained 5.6±0.7 mg NH₄⁺-N L⁻¹ and 13.8±1.4 mg NO₃⁻-N L⁻¹ to mimic the poor-quality effluent of the mainstream PN/A process. During the operation of the second reactor (R-2), the concentration of nitrate once increased to 17.7±0.1 mg NO₃⁻-N L⁻¹ (day 81-88) and 22.4±1.0 mg NO₃⁻-N L⁻¹ (day 89-94). Bicarbonate (130 mg HCO₃⁻ L⁻¹), phosphate (1 mg P L⁻¹), and 0.1 mL L⁻¹ of trace element solutions A and B ³²⁸

were added into influent to mimic the general secondary effluent and avoid the limitation of microbial growth. To simulate the anoxic condition of PN/A effluent, the influent tanks in this study were sealed, and the influent was maintained anoxic by regularly sparging with nitrogen gas (N_2).

2.3 Reactor operation

The reactors were inoculated with 1 g VSS L^{-1} activated sludge from a municipal wastewater treatment plant (Aquafin Antwerpen-Zuid, Belgium). The reactors were operated in a temperature-controlled room at $21\pm 1\text{ }^\circ\text{C}$ and continuously fed with anoxic influent (except day 0-45 of R-1 without dissolved oxygen control). Thus, the reactors could maintain the anoxic condition and suppress the consumption of $\text{NH}_4^+\text{-N}$ via aerobic ammonium-oxidizing bacteria (AerAOB).

Sodium hydroxide was added into the influent to indirectly maintain the reactor pH at 7.0 ± 0.2 or 8.5 ± 0.1 in different operating phases. The pH in the reactors was periodically monitored with a Hanna Edge pH meter (HI2002-02) equipped with a Hanna pH electrode (HI-12301).

To explore the parameter of BSNLR (representing the ratio of the volumetric nitrate loading rate and biomass concentration in the reactor) and residual nitrate level on SDN performance, nitrate concentrations ($13.8\text{-}22.4\text{ mg NO}_3^-\text{-N L}^{-1}$), and flow rate of influent (43 and 86 L d^{-1}) were adjusted as mentioned in 2.1 and 2.2.

Biomass control was implemented via washing off the biofilm attached to S^0 particles using N_2 purged influent. To suppress toxic sulfide formation, the waste biomass was preserved at 4°C and supplied with nitrate (100 mg N L^{-1})¹¹⁴. Biomass renewal was performed on two occasions for the R-1 by replacing 33% of reactor biomass with an equal amount of stock biomass from biomass wasting, as indicated in Figure 5.1a.

2.4 Analytical methods

To monitor the system performance, influent and effluent samples were collected periodically, filtered using $0.2\text{ }\mu\text{m}$ filters (CHROMAFIL Xtra PVDF), and stored at 4°C until analysis. $\text{NH}_4^+\text{-N}$, $\text{NO}_2^-\text{-N}$, and $\text{NO}_3^-\text{-N}$ were measured with the San++ Automated Wet

Chemistry Analyzer. Biomass in the reactor was sampled periodically from the mixed-well S^0 bed material via taking 5ml biofilm-growing S^0 and collecting the biomass based on the aforementioned biomass-control process. Biomass level in reactor was measured based on volatile suspended solids (VSS) using standard methods³²⁹.

When appropriate, Spearman's correlation was analyzed (IBM® SPSS® Statistics 26) to explore the correlation of control parameters (BSNLR and residual nitrate level) with NAE (i.e., the concentration ratio of nitrite accumulation and nitrate removal). Statistical significance was defined as a p-value of less than 0.05.

2.5 Microbiome Analysis

To assess the evolution of microbial community composition, biomass samples were collected from each reactor for microbiome analysis during the operation period. Samples were stored at $-20\text{ }^{\circ}\text{C}$ before DNA extraction. According to the manufacturer's instructions, DNA was extracted using a PowerFecal® DNA isolation kit (QIAGEN, Germany). The DNA extracts were sent to Novogene (UK) Co., Ltd for microbial amplicon-based metagenomics sequencing (Illumina Novaseq6000 PE250, Q30 \geq 75%). 16S rRNA genes of 16S V3 were amplified used specific primers 338F (5'- ACT CCT ACG GGA GGC AGC AG -3') and 518R (5'- ATT ACC GCG GCT GCT GG -3'). All PCR reactions were carried out with Phusion® High-Fidelity PCR Master Mix (New England Biolabs). For each representative sequence, Mothur software was performed against the SSUrRNA database of SILVA Database (see details <http://www.arb-silva.de/>) for species annotation²¹⁶. In addition, the alpha diversity (Shannon's) and beta diversity (Bray-Curtis dissimilarity) were analyzed in every sample and between different samples to characterize the variation in the microbial community, respectively.

3. Results and discussion

The SDN process was carried out in two sulfur-packed bed reactors independently. The overviews of reactor performance in R-1 and R-2 are shown in Figure 5.1 and 5.2, respectively. The NAE is always below 1, indicating that the complete sulfur-driven denitrification (i.e., $\text{NO}_3^- - \text{N} \rightarrow \text{N}_2$) existed during the whole experiment. Due to the anoxic condition in the reactors (except day 0-45 of R-1), $\text{NH}_4^+ - \text{N}$ loss was negligible ($2\pm 2\%$, in SI

Figure S5.1).

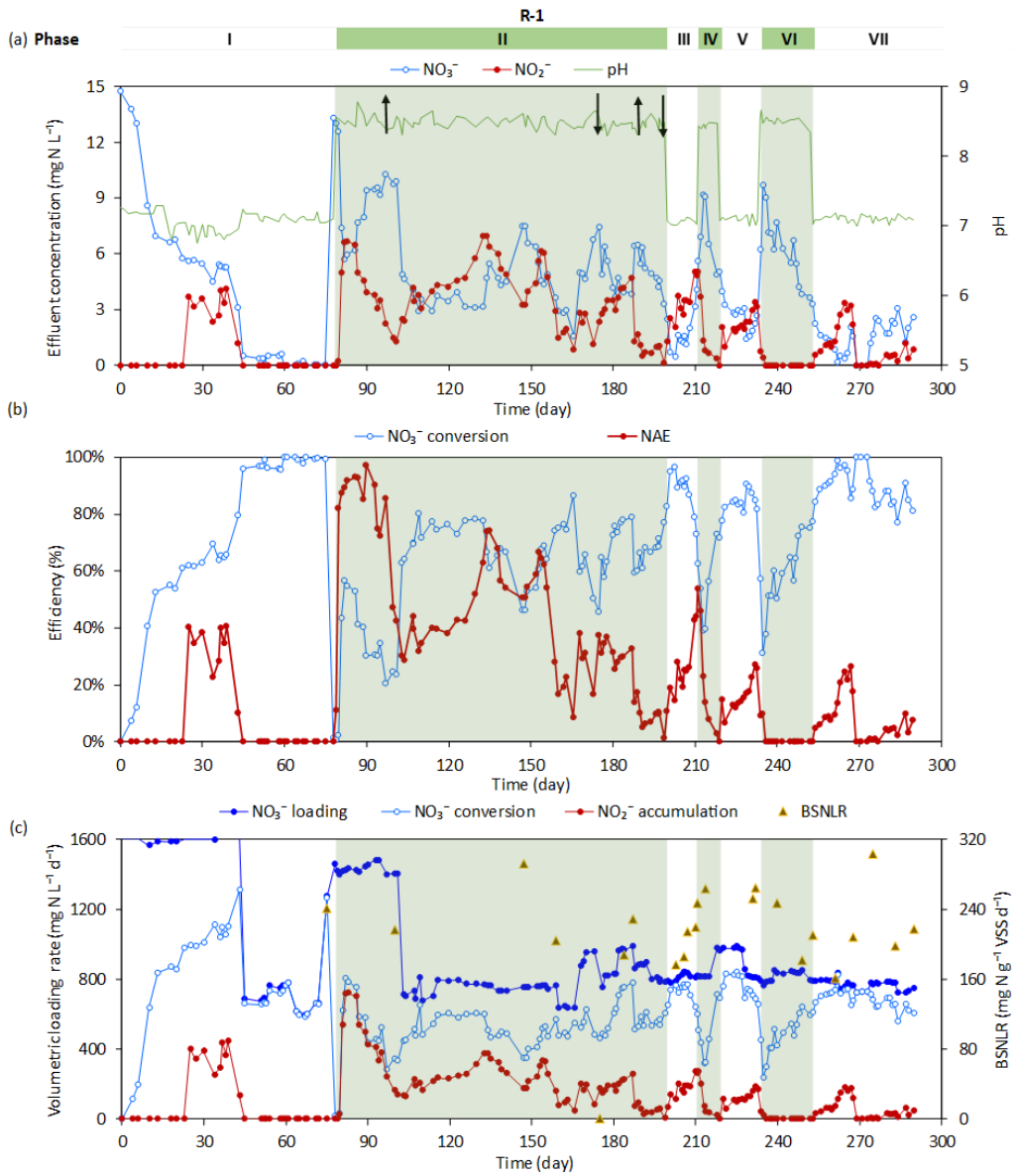


Figure 5.1: Overview of the reactor performance of R-1 from day 0 to day 290. Phases I to VII on top are divided based on different pH setpoints in the reactor. The green shadings in phases II, IV, and VI mean pH control at around 8.5. "↑" means the implementation of the biomass wasting process, "↓" means the biomass renewal.

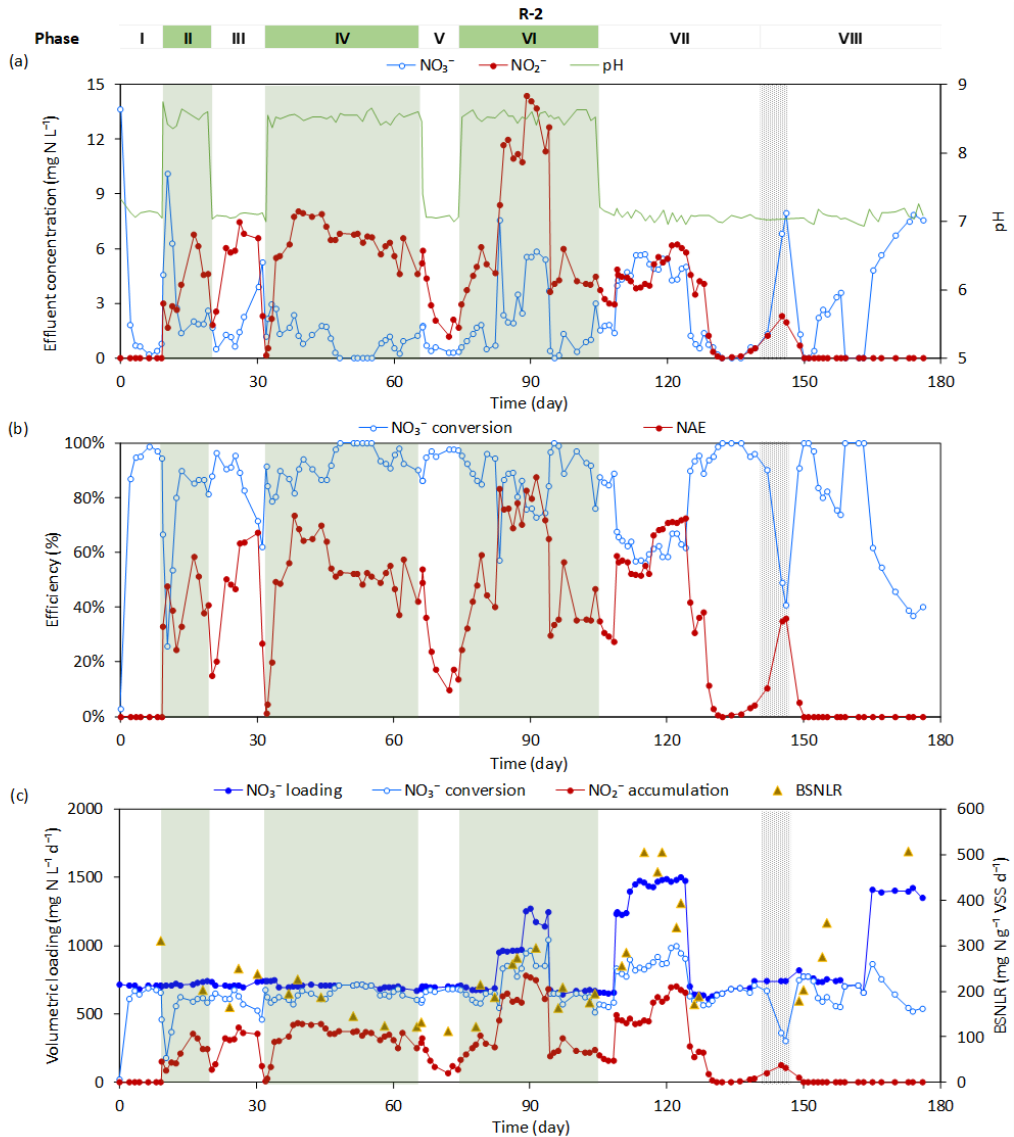


Figure 5.2: Overview of the reactor performance of R-2 from day 0 to day 177. Phases I to VII on top are divided based on different pH setpoints in the reactor. The green shadings in phases II, IV, and VI mean pH control at around 8.5. The black shading in phase VIII represents a technical issue.

3.1 Effects of the pH control strategy

The pH control strategy was implemented in both reactors via switching two pH setpoints (7.0 and 8.5) over the whole operation period. Both R-1 and R-2 were started running at pH 7.0. After the nitrogen conversion performance stabilized under anoxic conditions, reactor pH was switched to 8.5 for the first time.

In R-1, after the switchover to 8.5, the nitrite accumulation appeared immediately and momentarily reached $6.0 \pm 0.9 \text{ mg N L}^{-1}$ with NAE of $91 \pm 2\%$ as shown in phase II of Figure 5.1a and 5.1b. The subsequent decrease of nitrate removal efficiency and nitrite concentration was suspected due to substrate-diffusion limitation. Some black biomass was observed in the reactor, probably due to an excessive amount of biomass clogging or diffusion limitation and subsequent anaerobic biomass decay³³⁰. A biomass control process was implemented on day 97 to avoid the risk of fouling and short-circuiting. After the biomass wasting, the biomass level decreased from 6.5 to 2.3 g VSS L^{-1} , and the nitrate removal efficiency and nitrite concentration successively recovered. With the increase of nitrite accumulation concentration and efficiency, the nitrite accumulation rate could maintain at $262 \pm 63 \text{ mg N L}^{-1} \text{ d}^{-1}$ from day 107 to day 156. Subsequently, the performance of nitrite accumulation deteriorated with its concentration dropping from 6.2 mg N L^{-1} on day 153 to only 1.2 mg N L^{-1} on day 173 (Figure 5.1b). The biomass renewal was implemented twice (i.e., on day 174 and 198). After the first biomass renewal, the performance of nitrite accumulation visibly improved. Interestingly, when around 33% of biomass was taken out on day 189, the performance of nitrite accumulation got impaired immediately. It indicated the reactor biomass before renewal either got community shifted or adapted to pH 8.5. In the following phases III, V, and VII, operation at pH 7.0 instead of 8.5 could successfully stimulate the nitrite accumulation. However, switching from pH 7.0 to 8.5 could not further promote the nitrite accumulation but interrupt its accumulation in phases IV and VI.

Like R-1, switching to pH 8.5 successfully stimulated the nitrite accumulation in phase II of R-2 (Figure 5.2). The nitrite concentration gradually increased to 6.8 mg N L^{-1} , then decreased. In phase III, switching the pH back to 7.0 could immediately revive the nitrite accumulation and make it stable at $6.4 \pm 0.4 \text{ mg N L}^{-1}$. The ratio of accumulated NO_2^- -N and NH_4^+ -N in reactor effluent was close to the ideal NO_2^- -N/ NH_4^+ -N ratio of 1.3 for the anammox process¹¹⁴. However, this ideal SDN performance was unstable. In phase IV, the performance of nitrite accumulation could quickly recover from the shock of pH 8.5 on day 32 and maintain at $6.4 \pm 1.0 \text{ mg N L}^{-1}$ with a relatively stable NAE of $54 \pm 9\%$ over 30

days. However, the slightly declining trend in phase IV was accelerated by switching to pH 7.0 in phase V, but changing back to pH 8.5 in phase VI effectively reversed the decreasing trend.

It was proposed that nitrite could accumulate at high pH (e.g., 8.5 in this study) because nitrate reductase activity could outcompete that of nitrite reductase for electrons^{145, 331}. Meijer et al. (1979) suggested that the protons (H^+) required for nitrate reduction come from inside the cytoplasmic membrane, whereas nitrite reductase receives the H^+ from outside of the cytoplasmic membrane³³². At pH 8.5, H^+ could be relatively scarce outside the cytoplasmic membrane, inhibiting nitrite reduction but not nitrate reduction³³³. This theory supports the results in phase II of R-1 and phase II, IV, VI of R-2 but is not applicable for phase IV and VI of R-1. Nevertheless, nitrate reduction was still affected by pH 8.5, especially at the beginning of each pH-8.5 period in both reactors, resulting in a transient decrease of nitrate conversion efficiency. In this study, it seemed that the nitrate reductase could quickly adapt to the alkaline circumstance, whereas nitrite reductase was slower to get acclimated. In the long term, once the nitrite reductase got adapted, the performance of nitrite accumulation would start vanishing, which might explain the weaker effect of pH 8.5 on the nitrite accumulation in the later phase II of R-1 (day 156-173) and phase IV of R2. When the effect of pH 8.5 got weaker with NAE less than 15% in R-1 and the phase II of R-2, switching to pH 7.0 successfully stimulated the NAE. It is assumed the alkaline pH may inhibit both the nitrate and nitrite reductase activity, once recovering to neutral pH, the inhibition on these reductases could be relieved, but the relieving speed of nitrate reductase is faster than nitrite reductase. Yet, the conjectural microbial conversion mechanisms of pH alternation from 8.5 to 7.0 require to be confirmed in future study.

The effects of pH alternation on SDN also depended on the performance of nitrite accumulation itself. When the performance of nitrite accumulation deteriorated, the pH alternation could stimulate its accumulation; if the ongoing accumulation performance was still adequate, the pH alternation would interrupt it (phase IV and VI of R-1 and phase V of R-2). The SDN interruption in phase IV and VI of R-1 was probably attributed to

microbial community adaptation to the alkaline pH during phase II, which consequently cannot be stimulated to get nitrite accumulation by neutral pH. However, the reason for SDN interruption in phase V of R-2 was unclear yet.

To obtain stable nitrite accumulation at around 6.5 mg N L^{-1} for subsequent anammox process, alternation of pH setpoints should be considered once the decreasing trend of NAE occurs. In this study, alternating pH setpoints between 7.0 and 8.5 could temporarily stimulate the nitrite accumulation, but this ongoing performance could be interrupted by the pH switching as well. The mechanism of pH alternation on behaviors of nitrite accumulation requires further investigation and demonstration in future studies.

3.2 Effects of residual nitrate level control

The residual nitrate concentration in the reactors was controlled via the volumetric nitrate loading rate, as shown in Figure 5.1c and Figure 5.2c. The dynamic changes of nitrite concentration with residual nitrate level were relatively distinct in R-2. The nitrite concentration increased to $11.9 \pm 1.7 \text{ mg N L}^{-1}$ under $4.2 \pm 1.9 \text{ mg N L}^{-1}$ of residual nitrate in phase VI (day 83-94), but dramatically dropped to $4.3 \pm 0.8 \text{ mg N L}^{-1}$ when residual nitrate decreased to $0.6 \pm 0.5 \text{ mg N L}^{-1}$. Lowering the residual nitrate level weakened the nitrite accumulation, consistent with the past S^0 driven denitrification studies^{150, 326}. However, in phase VII of R-2 (day 109-124), under a similar residual nitrate level of $4.9 \pm 0.6 \text{ mg N L}^{-1}$, the nitrite concentration was only kept at $4.9 \pm 0.8 \text{ mg N L}^{-1}$, indicating the nitrite accumulation in phase VI was further reinforced by alkaline pH of 8.5. Actually, the performance of nitrite accumulation was not always affected by the residual nitrate level. In phase IV of R-2 (day 48-55), an ideal nitrite level of $6.7 \pm 0.2 \text{ mg N L}^{-1}$ could still obtain even no residual nitrate existed in the reactor, also mainly attributed to the effect of pH 8.5. Nevertheless, in whole phase IV, the relative ideal ratio of $\text{NO}_2^- \text{-N}$ to $\text{NH}_4^+ \text{-N}$ (around for 1.3) for anammox (in SI Figure S5.2) together with the residual nitrate of $1.0 \pm 0.8 \text{ mg N L}^{-1}$ could theoretically get the final effluent with only nitrate of $2.5 \pm 0.8 \text{ mg N L}^{-1}$.

At the beginning of phase VIII, the reactor recirculation was terminated accidentally, leading to the heterogeneous delivery of substrate and the subsequent biofilm decay and

sloughing from S^0 particles³³⁰. Since then, even increasing the residual nitrate above $5.5 \pm 0.2 \text{ mg N L}^{-1}$ could never accumulate any nitrite. Compared to the nitrite accumulation under $5.5 \pm 0.2 \text{ mg NO}_3^- \text{ N L}^{-1}$ in phase VII, it was deduced that the technical issues perturbed the microbial community structure in R-2.

To further understand the relationship between residual nitrate level and NAE, Spearman's correlation analysis was implemented in the whole and individual phases (Table 5.1). In R-1, the correlation coefficient of the entire periods (I-VII) was moderate positive ($\rho = 0.41$, $p < 0.0001$), that of phase II to III was stronger with ρ of 0.55; further zooming in on phase III, the correlation was much more substantial with ρ of 0.64 in Table 5.1a. In R-2, the difference of correlation in the long and short term was more prominent. Compared to the weak correlation of phase I to VIII, there were very strong positive correlations between residual nitrate level and NAE in phase VI ($\rho = 0.87$, $p < 0.0001$) and VII ($\rho = 0.80$, $p < 0.0001$). Due to the influence of different pH setpoints and uncertainty in the microbial community in the long run, there were stronger correlations in the short period but weaker in the long term. Besides the interference from pH setpoints, the primary influence was suspected from the microbial community adaptation and/or shift in long-term operation.

Table 5.1: Correlation analysis of residual NO_3^- -N and NO_2^- -N accumulation efficiency in R-1 (a) and R-2 (b) during different operational phases. P-values and Spearman's rho are reported.

(a)

| Phase | I | II | III | IV | V | VI | VII | I-VII | II-III |
|---------|------|-------------------|-------------|------|-------|------|-------|-------------------|-------------------|
| p-value | 0.08 | <0.0001 | 0.04 | 0.62 | 0.01 | 0.33 | 0.34 | <0.0001 | <0.0001 |
| rho | 0.28 | 0.52 | 0.64 | 0.26 | -0.69 | 0.28 | -0.19 | 0.41 | 0.55 |

(b)

| Phase | I | II | III | IV | V | VI | VII | VIII | I-VIII | IV-VII |
|---------|------|------|------|-------------|------|--------------------|--------------------|------|---------------|--------------------|
| p-value | 0.31 | 0.38 | 0.20 | 0.05 | 0.07 | < 0.0001 | < 0.0001 | 0.19 | 0.0002 | < 0.0001 |
| rho | 0.41 | 0.33 | 0.44 | 0.39 | 0.77 | 0.87 | 0.80 | 0.30 | 0.31 | 0.68 |

3.3 Effects of the BSNLR control

For both reactors, the dynamic changes of BSNLR were monitored periodically, as shown in Figure 5.1c and Figure 5.2c, respectively. The volumetric nitrate loading rate and biomass level could affect the BSNLR. The biomass concentration in R-1 and R-2 was 3.9 ± 1.0 and 3.8 ± 1.0 g VSS L⁻¹, respectively (details in SI Figure S5.3). As shown in Figure 5.2c, the ideal nitrite accumulation of 6.4 ± 1.0 mg N L⁻¹ for anammox was achieved at BSNLR of 150 ± 42 mg N g⁻¹ VSS d⁻¹ in phase IV of R-2. To understand the association between BSNLR and the corresponding NAE more explicitly, Spearman's correlation coefficients were obtained in both the long and short periods (Table 5.2). There were very strong positive correlations between the BSNLR and NAE in phase II-III of R-1 ($\rho=0.81$, $p=0.003$) and phase II-VII of R-2 ($\rho=0.73$, $p<0.0001$). There was even a very strong positive correlation between the BSNLR and NO₂⁻-N accumulation concentration in phase II-VII of R-2 ($\rho=0.83$, $p<0.0001$). The strong positive correlation indicated that increasing the strength of nitrate imposing on the biofilm could significantly promote the nitrite accumulation performance. According to the counter-diffusion theory, increasing the BSNLR means the nitrate penetration was intensified via the nitrate loading and/or biofilm thickness¹⁵¹. Since the slow S⁰ oxidation rates could result in the insufficient supply of electron donors, the greater electron affinity of nitrate reductase could facilitate the nitrite accumulation³²⁷. However, the long-term correlation between BSNLR and NAE was relatively negligible. It was deduced that the potential microbial community shift in the long-term operation affected the SDN process. It is noted that there was a very high positive correlation between BSNLR and residual nitrate level ($\rho=0.83$, $p<0.0001$) in R-2 as well. Hence, increasing the BSNLR has the potential to cause the high residual nitrate level if the capacity of nitrate conversion is insufficient.

Table 5.2: Correlation analysis of BSNLR and NAE in R-1 and R-2. P-values and Spearman's rho are reported. The correlations of BSNLR with corresponding NO_2^- -N accumulation and residual NO_3^- -N concentration are also shown.

| | | R-1 | | R-2 | |
|--|---------|--------|--------------|--------------------|--------------------|
| Phase | | I- VII | II- III | I- VIII | II- VII |
| BSNLR & NAE | p-value | 0.52 | 0.003 | 0.06 | < 0.0001 |
| | rho | 0.14 | 0.81 | 0.31 | 0.73 |
| BSNLR & NO_2^--N | p-value | 0.67 | 0.09 | 0.96 | < 0.0001 |
| | rho | 0.10 | 0.54 | 0.01 | 0.83 |
| BSNLR & Residual NO_3^--N | p-value | 0.27 | 0.10 | < 0.0001 | < 0.0001 |
| | rho | 0.24 | 0.53 | 0.75 | 0.83 |

3.4 Evolution of the microbial community in the long term

The microbiome in R-1 and R-2 was analyzed to assess their contribution to SDN during the long-term operation. Based on the Bray-Curtis dissimilarity analysis, the variation in the microbial community between the first sample and each subsequent sample became more significant over time, indicated the community shift during the experiment (Figure 5.3).

In R-1, the Shannon index ranged from 1.1 to 1.7 and showed a decreasing trend as a whole, meaning richness and diversity reduced over the long-term operation. Among all the putative sulfurotrophs shown in Figure 5.3a, *Thiobacillus*, *Caldimonas*, *Chlorobi_bacterium_OLB5* were the three most abundant members. *Thiobacillus* is one of the most common genera in sulfur autotrophic denitrification system³³⁴, using element sulfur (S^0) or sulfide (S^{2-}) as electron donors to convert both NO_3^- and NO_2^- ^{335, 336}. Compared to day 75 of phase I, day 141 showed a significant increase in the abundance of *Thiobacillus* (from 4.7% to 29.9), which was probably attributed to the relative ideal anoxic condition for autotrophic denitrifying bacterial community compared to the first 45 days in phase I. From day 141 to day 249, the relative abundance of *Thiobacillus* decreased stepwise from 29.9% to 4.3% (Figure 5.3a). According to Spearman's correlation analysis between the relative abundance of *Thiobacillus* and nitrogen (i.e., NO_3^- -N and NO_2^- -N) conversion performance (in SI Table S5.1), there was a very high positive correlation between its relative abundance and NAE ($\rho=0.878$, $p=0.004$). Thus, the reduction of *Thiobacillus* abundance probably affected the nitrite accumulation in the reactor. *Thiobacillus* could be the critical community to control the nitrite accumulation, and further demonstrations such as SDN study with pure *Thiobacillus* microbes are necessary in the future. pH was considered a decisive factor for the survival of bacteria. There are two identified autotrophic denitrifying species in the genus *Thiobacillus*, i.e., *Thiobacillus denitrificans* and *Thiobacillus thiophilus*, and the growth pH are 6.8-7.4 and 6.3-8.7, respectively¹²⁷. The long-term operation out of the growth pH of *Thiobacillus denitrificans* could cause the shrinkage of relative abundance of genus *Thiobacillus*. To our knowledge, the long-term effects of pH on microbial

community shift in SDN are barely reported in the past.

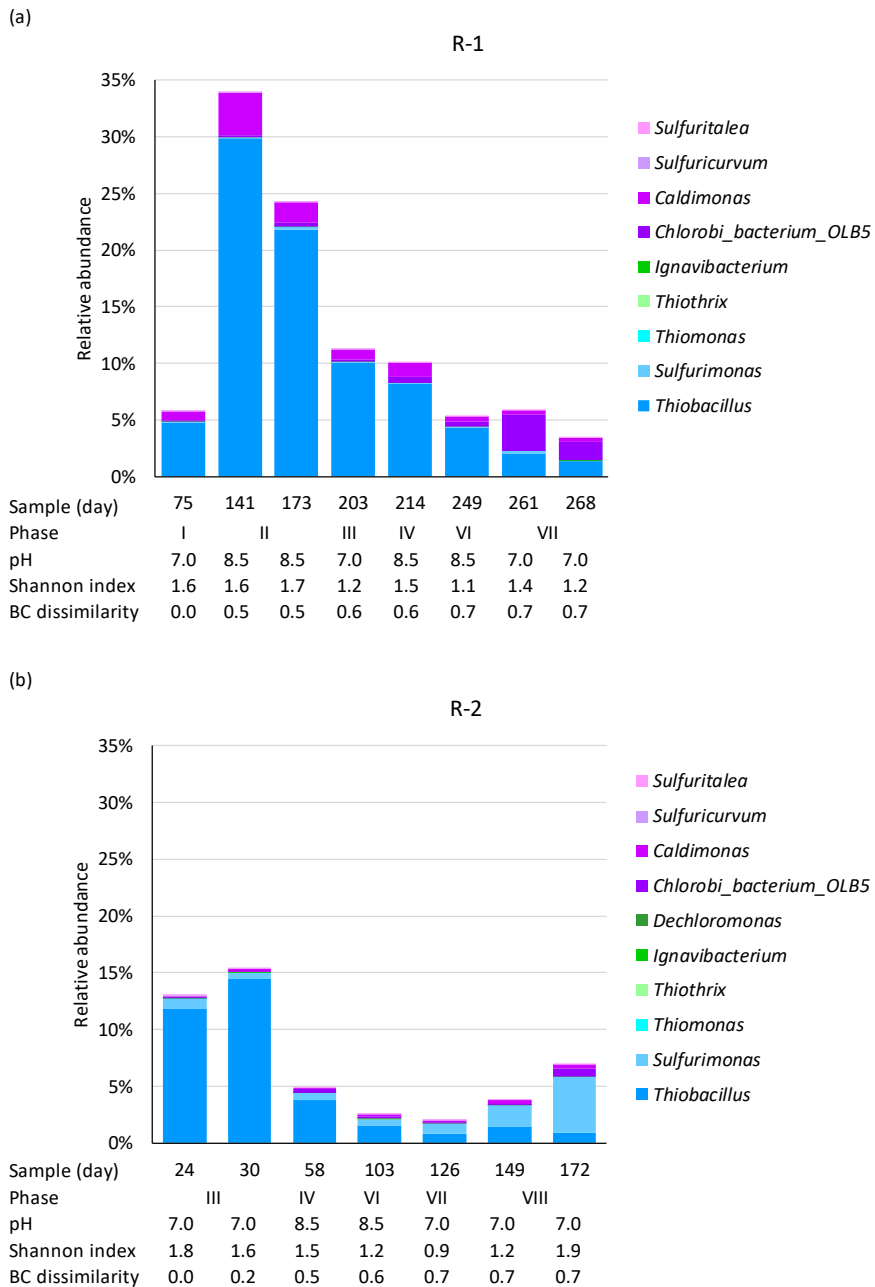


Figure 5.3: The relative abundance of the sulfurotrophic community at genus levels in R-1 (a) and R-2 (b) during the experiment. BC dissimilarity represents the Bray-Curtis dissimilarity between the first and each subsequent sample.

In R-2, compared to the relatively high abundance in phase III (14.4% of day 30),

Thiobacillus in phase IV (day 58) and VI (day 103) decreased to 3.8% and 1.5%, respectively, which could be ascribed to the adverse effect of pH 8.5 on its proliferation. The abundance increase of *Thiobacillus* from day 24 to day 30 revealed its possibility of enrichment at pH 7.0. However, in phase VIII, the relative abundance of day 149 and 172 did not recover to the high level like phase III, with only 1.5% and 0.9%, respectively. Instead of *Thiobacillus*, *Sulfurimonas* showed visible prosperity. *Sulfurimonas* are the most commonly reported sulfur-based autotrophic denitrifiers as well ^{126, 127, 337}. They competed with *Thiobacillus* for substrate and then became the dominant genera in phases VII and VIII. Like R-1, the relative abundance of *Thiobacillus* was positively correlated with NAE ($\rho=0.857$, $p=0.014$). It is interesting to discover the highly negative correlation between the relative abundance of *Sulfurimonas* and NAE. This distinct community shift could support the speculation about the failure of nitrite accumulation under the residual nitrate level and BSNLR control in section 3.2 and 3.3.

Compared to the successful nitrite accumulation control in phase VI of R-2, the failure in phase VI of R-1 with a higher relative abundance of *Thiobacillus* could be attributed to bacteria adaptation to pH 8.5. The relative abundance of *Thiobacillus* in phase IV (3.8%) and VI (1.5%) of R-2 were much lower than that in phase II (29.8%) of R-1 (Figure 5.3). Still, the performance of nitrite accumulation was comparable to phase II of R-1. Therefore, it is speculated that only a limited amount of *Thiobacillus* was effectively working on SDN, and the residual *Thiobacillus* might be adapted to pH 8.5 in phase II of R-1. This conjecture could be supported by the subsequent worse performance of phase IV and VI in R-1 with high *Thiobacillus* abundance.

Overall, *Thiobacillus* could be the critical community to realize the nitrite accumulation under three control parameters. However, the inhibition effect of pH 8.5 might be the main reason for the stepwise reduction of *Thiobacillus* abundance in this study. In the long term, the adaptation effect and community shift would invalidate these control strategies on SDN. Thus, bioaugmentation with the new inoculum abundant in *Thiobacillus* could be a “renascent” strategy. In the full-scale application as a polishing step, the effective biomass that could realize high nitrite accumulation could be

appropriately collected and stored in low temperature, e.g., 4°C under nitrate preservation. Updating the reactor with the effective biomass should be a possible backup when the efficacy of control strategies gets weak. Nevertheless, more extra technologies that can maintain a stable SDN process for the downstream anammox treatment are needed to be explored in future studies.

4. Conclusions

This study investigated the feasibility of sulfur-driven denitritation of secondary effluents for downstream anammox treatment via three control strategies (pH, residual nitrate, and BSNLR) in long-term operation. Alternating pH setpoints between 7.0 and 8.5 could temporarily stimulate nitrite accumulation. Both the residual nitrate level and BSNLR were strongly and positively correlated with NAE. Under the conditions of pH 8.5, $1.0 \pm 0.8 \text{ mg NO}_3^- \text{-N L}^{-1}$ and $150 \pm 42 \text{ mg NO}_3^- \text{-N g}^{-1} \text{ VSS d}^{-1}$, sulfur-driven denitritation could produce $6.4 \pm 1.0 \text{ mg NO}_2^- \text{-N L}^{-1}$ over 30 days. *Thiobacillus* might play a key role in nitrite accumulation. However, the effects of control strategies could be impaired by community adaptation and shift. It is hard to maintain stable nitrite accumulation only depending on these three strategies in the long term, and additional control tools need to be explored.

5. Supplementary information

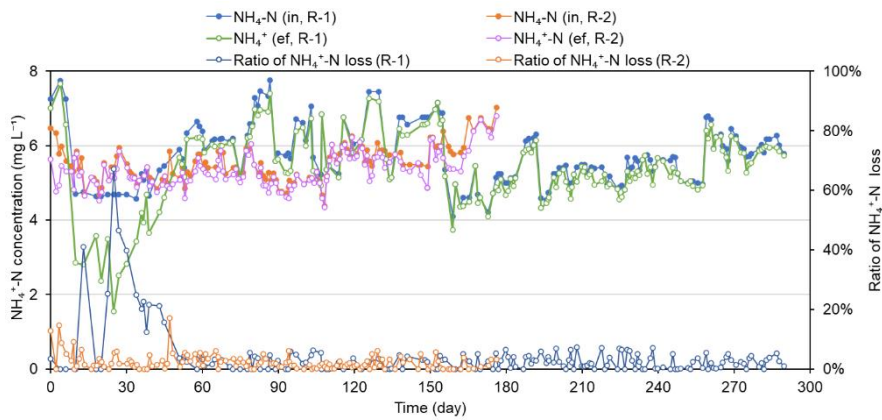


Figure S5.1: NH₄⁺-N concentration in sulfur-driven denitratation (SDN) influent (“in”), effluent (“ef”), and the ratio of NH₄⁺-N loss to influent NH₄⁺-N concentration during the whole operation period of R-1 and R-2.

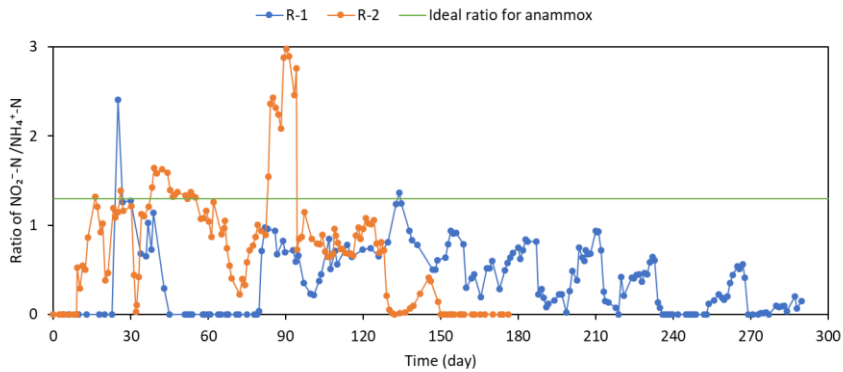


Figure S5.2: The ratio of accumulated NO₂⁻-N to NH₄⁺-N in reactor effluent during the whole operation period of R-1 and R-2. The ideal ratio for anammox is 1.3.

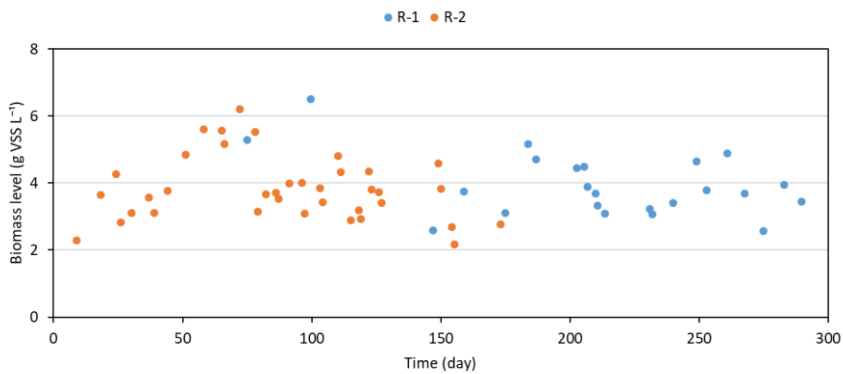


Figure S5.3: The biomass level monitoring during the whole operation period of R-1 and R-2.

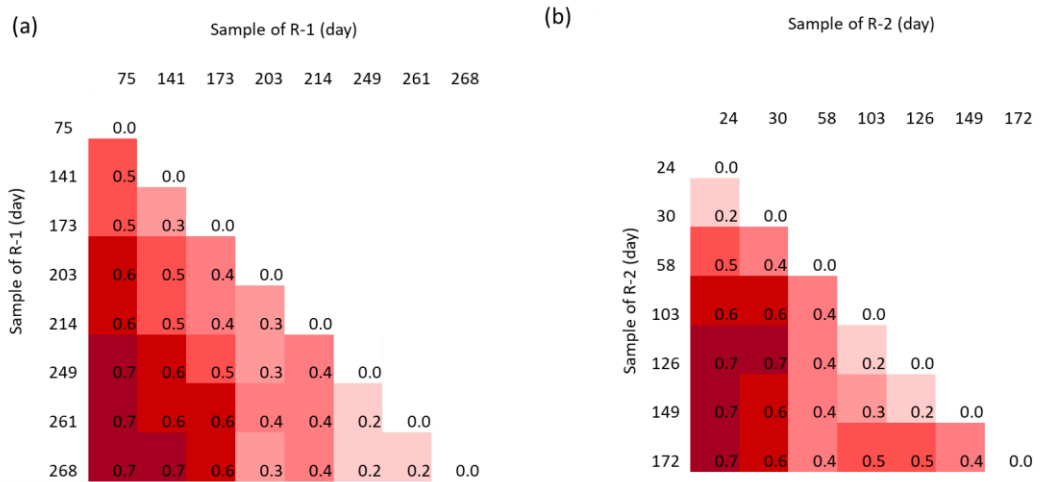


Figure S5.4: Bray-Curtis dissimilarity of R-1 (a) and R-2 (b) analysis for every two samples at genus level; the gradation of color represents the dissimilarity.

Table S5.1: Correlation analysis of the relative abundance of *Thiobacillus* and *Sulfurimonas* with corresponding NO_3^- -N removal efficiency (NRE) and NO_2^- -N accumulation efficiency (NAE) in R-1 and R-2. P-values and Spearman’s rho are reported.

| | R-1 | | | | R-2 | | | |
|---------|--------------------------------|--------------------------------|--------------------------------|--------------------------------|--------------------------------|--------------------------------|--------------------------------|--------------------------------|
| | <i>Thiobacill</i> <i>us</i> | <i>Thiobacill</i> <i>us</i> | <i>Sulfurimon</i> <i>as</i> | <i>Sulfurimon</i> <i>as</i> | <i>Thiobacill</i> <i>us</i> | <i>Thiobacill</i> <i>us</i> | <i>Sulfurimon</i> <i>as</i> | <i>Sulfurimon</i> <i>as</i> |
| | & NRE | & NAE | & NRE | & NAE | & NRE | & NAE | & NRE | & NAE |
| p-value | 0.12 | 0.004 | 0.26 | 0.307 | 0.645 | 0.014 | 0.482 | 0.036 |
| rho | -0.595 | 0.878 | -0.452 | 0.415 | -0.214 | 0.857 | -0.321 | -0.786 |

6. Acknowledgments

Y. X. and W. Z. were supported by the China Scholarship Council (File No. CSC201706130131 and CSC201709370063). M.V.T. was supported by a Ph.D. SB Fellowship from the Research Foundation - Flanders (FWO-Vlaanderen, 1S^o 3218N). The authors would like to thank Dr. Wannes Van Beeck for his guidance on microbial DNA extraction.

Chapter 6

General discussion and outlook

1. Main research outcomes

The purpose of this Ph.D. thesis was to investigate different bioreactor strategies for Nr recovery and removal depending on the strength and form of Nr in the waste streams. The work can be divided into two major parts. In the first part, the focus goes to the NO_3^- -N recovery from microbial fertilizer via aerated suspended growth bioreactor (**Chapter 2**) and human urine via a trickling filter (**Chapter 3**). The second part was to develop Nr removal techniques for low to medium strength wastewater, including PN/A in trickling filters (**Chapter 4**) and sulfur-driven denitrification (**Chapter 5**). Here, the major findings are recapitulated chapter by chapter:

In **Chapter 2**, a novel controlled mineralization and nitrification system was developed, converting organic fertilizers to hydroponic nutrient solutions. Based on batch test results, an aerated bioreactor running with CAB could obtain a NO_3^- -N production efficiency of 51% under the TN loading rate of $400 \text{ mg L}^{-1} \text{ d}^{-1}$ at a 5-day HRT and 35°C . To control the pH of the bioreactor, both $\text{Ca}(\text{OH})_2$ and $\text{Mg}(\text{OH})_2$ were tested, which could provide nutrient elements (Ca and Mg) in the baseline nutrient solution as well. Nutrient balancing strategies derived from the Hoagland nutrient solution (HNS) were used to polish the baseline nutrient solutions. The HNS derived from the $\text{Ca}(\text{OH})_2$ organic scenario contained a higher proportion of organic-sourced NO_3^- -N than the $\text{Mg}(\text{OH})_2$ scenario. Compared to the commercial inorganic fertilizers, the operational expenditure of the $\text{Ca}(\text{OH})_2$ scenario has the potential to be cost-competitive in hydroponic fertilization.

In **Chapter 3**, human urine, a widely available Nr waste with a much lower COD/Nr ratio than the solid CAB used in **Chapter 2**, was investigated for nitrate conversion in a trickling filter. Full nitrification of real urine in the TF was realized, with NO_3^- -N production at the high efficiency of $88\pm 3\%$ and a stable rate of $136\pm 4 \text{ mg NO}_3^- \text{-N L}^{-1} \text{ d}^{-1}$. There was little difference in nitrification and COD removal efficiency between synthetic and real urine. The TF could maintain relatively stable nitrification performance under different urine collection batches, which differed in major ion concentrations. The HLR control in the TF could positively affect the nitrification performance via increasing the contact time between substrate and biofilm. The HLR of $2 \text{ m}^3 \text{ m}^{-2} \text{ h}^{-1}$ was proved to be the optimal

condition to realize full nitrification of urine under the TN loading rate of 152 ± 7 mg TN $L^{-1} d^{-1}$, with electricity consumption estimation of 1.8 kWh $kg^{-1} NO_3^-$ -N production. Besides, the triple benefits of $Ca(OH)_2$ in urine alkalization, full nitrification, and macronutrient supplementation were demonstrated for the proposed nutrient recovery and use concept.

Chapter 2 and **Chapter 3** focused on the nitrate recovery from organic Nr-rich streams. Instead of those high-strength streams, **Chapter 4** investigated the feasibility of low to medium strength Nr (i.e., NH_4^+ -N) removal via the PN/A process in trickling filters. The DO control via top passive ventilation was proved reliable in the DO supply for the partial nitrification (PN) process. Around 60% of TN removal at a removal rate of 300 mg N $L^{-1} d^{-1}$ was achieved with a proper HLR of 1.8 $m^3 m^{-2} h^{-1}$. The crushed expanded clay aggregates were recommended for a low cost among three types of tested carrier materials. In addition, the electricity consumption estimation of PN/A in TFs was 35% lower than in suspended growth SBR mode, making it a potentially economically viable option for nitrogen removal.

To remove Nr from low-strength wastewater containing nitrate and ammonium, a concept of sulfur-driven denitrification/anammox process was proposed in **Chapter 5**. Concretely, the goal was to demonstrate the feasibility of sulfur-driven denitrification for stable nitrite accumulation in the long term. All three control strategies, namely, pH, residual NO_3^- -N, and high biomass-specific nitrate loading rate, could realize the stable NO_2^- -N accumulation in the short term. In the view of the microbial community, *Thiobacillus* members may play a crucial role in denitrification. However, the effects of control strategies could be impaired by microbial community adaptation and shift in long-term operation. Therefore, it is tricky to maintain stable NO_2^- -N accumulation in the long term only depending on these three strategies. Additional control tools need to be investigated for higher and longer-lasting nitrite accumulation.

2. Nitrogen management to make the N cycle more sustainable

Nitrogen as an essential element for agriculture is primarily produced by the Haber-Bosch process based on the consumption of fossil fuels in modern society. However, since

anthropogenic activities keep making reactive nitrogen (Nr), the nitrogen level has three times surpassed the safe boundary of the Earth system. To relieve the Nr pollution during the nitrogen cascade and the consequent harm on planetary sustainability, nitrogen recovery and removal from waste streams are two major approaches. Therefore, there are two routes to make Nr available for farming: (i) direct Nr recovery and conversion into a reusable form (e.g., ammonia and nitrate); (ii) Nr conversion into N_2 plus the Haber-Bosch process (i.e., 'recycling over the atmosphere')³³⁸. However, only very limited knowledge is available to decide the proper pathway (removal or recovery) benefitting the sustainable nitrogen cycle. In this section, nitrogen management was discussed from three aspects: the process sustainability (environment, human health, and economy), the nitrogen strength of waste streams, and the technology performance and feasibility.

2.1 Sustainability

“Sustainability means transforming our ways of living to maximize the chances that environmental and social conditions will indefinitely support human security, well-being and health.”

—McMichael, et al.³³⁹

2.1.1 Environmental sustainability

Environmental sustainability is the responsibility to conserve natural resources and protect global ecosystems to support health and wellbeing, now and in the future. Environmental sustainability covers a wide range of issues starting from a specific location to global. Global issues comprise concerns about GHG mitigation, climate change, and renewable energy, while the location-specific issues are soil erosion, water management, soil quality, and air and water pollution³⁴⁰. The environmental sustainability of nitrogen management should be considered in the proposed concepts.

In **Chapter 2**, a consortium of aerobic bacteria (CAB) as a novel organic fertilizer was used to produce NO_3^- -N nutrient solution in a novel hydroponic concept. Primarily, the ecosystem impacts of CAB production should be taken into account in terms of environmental sustainability. According to the life cycle assessment (LCA), CAB production caused lower ecosystem impacts (species/year) of 28% than the soybean

meal (as a type of plant-based fertilizer)⁹⁰. The main contributors to ecosystem impacts are climate change (mainly due to GHG emissions) and agricultural land occupation. The production of soybean meal shows a three times higher contribution in the farmland occupation than CAB. From this perspective, CAB is a sustainable alternative to soybean meal as a type of organic fertilizer. During the mineralization and nitrification process, CAB can release $15.7 \text{ kg CO}_2 \text{ kg}^{-1} \text{ NO}_3^- \text{-N}$ according to the empirical formula $\text{C}_5\text{H}_7\text{O}_2\text{N}$ of CAB (Reaction 1.19 and 1.11 in **Chapter 1**). Direct CO_2 emission into the atmosphere is adverse to the control of the greenhouse effect. After the proper collection, the produced CO_2 can be supplied to the greenhouse to stimulate the plant photosynthesis, reducing the cost of CO_2 supplementation by burning carbon-based fuels or directly from the liquid CO_2 tanks⁹⁹. In addition, the waste sludge obtained from the membrane filter could still be applied to arable land as a slow-release fertilizer, replacing a proportion of synthetic N fertilizers.

In **Chapter 3**, the Nr in source-separated urine was recovered via a trickling filter through urea hydrolysis and nitrification processes. Since urine is a major nitrogen contributor (75-80%) in municipal wastewater⁴⁷, urine nitrogen removal in municipal wastewater streams could increase the nutrient loads of WWTPs and the risk of the corresponding GHG releases, like nitrous oxide (N_2O , up to 2.6% of total nitrogen load)³⁴¹. By contrast, the nitrate recovery in Chapter 3 could relieve the burden of WWTPs and reduce the N_2O production due to complete nitrification³⁴². Compared to the high COD/N ratio of solid CAB (around 16) used in **Chapter 2**, human urine with a much lower COD/N ratio (about 1.0) requires less O_2 for COD removal, which is more suitable to be treated in passively aerated apparatuses, like trickling filters. Besides, the liquid urine and the less waste sludge yield later can result in a lower clogging risk and less burden of sludge disposal. According to the urine nitrification stoichiometry (Reaction 1.6 in **Chapter 1**), the CO_2 emission is assumed to be $2.49 \text{ kg kg}^{-1} \text{ NO}_3^- \text{-N}$ production, only around 16% of that during CAB mineralization. Hence, if no additional CO_2 collection is implemented, the environmental impact of urine-sourced N recovery is less than the CAB-sourced N recovery process.

Currently, the removal of low to medium-strength $\text{NH}_4^+\text{-N}$ in WWTPs is dominated by the nitrification/heterotrophic denitrification (N/HDN) process. Depending on the COD/N ratio of the influent, the requirement of external carbon sources is determined for the N/HDN process. Anyhow, this conventional N/HDN route causes high global warming potential and accelerates ozone layer depletion due to high CO_2 emission (173-347 g CO_2 m^{-3} wastewater)^{343, 344}. Towards an energy-autarkic wastewater treatment process, avoiding external COD dosing and converting internal COD to CH_4 as recovered energy is much more environment-friendly. The subsequent $\text{NH}_4^+\text{-N}$ removal could be completed by the PN/A process. In **Chapter 4**, the feasibility of PN/A process was tested in trickling filters, which could convert approximately 60% of $\text{NH}_4^+\text{-N}$ to inert N_2 . In some developing countries like Brazil, trickling filters are typically used to remove carbon and ammonium²⁹⁷. There is no restriction on $\text{NO}_3^-\text{-N}$ and TN in their discharge standards³⁴⁵. The realization of PN/A in trickling filters could be significant progress to their wastewater treatment process. While in European countries, the discharge limitation of TN in municipal wastewater treatment plants is more strict, with a TN less than 10-15 mg L^{-1} ³¹⁴. Mainstream PN/A processes are not mature in the current state due to the unsatisfying effluent quality with residual $\text{NH}_4^+\text{-N}$ and $\text{NO}_3^-\text{-N}$. Therefore, a polishing concept for the effluent of mainstream PN/A was proposed in **Chapter 5**. The autotrophic denitrification driven by element sulfur was investigated rather than the heterotrophic denitrification to avoid the external organic carbon addition and excess sludge production.

Besides the possible emissions of GHG during the nitrogen removal process in WWTPs, the industrial nitrogen fixation via the Haber-Bosch process can emit a considerable amount of CO_2 (1.93-4.29 kg CO_2 kg^{-1} $\text{NH}_3\text{-N}$)³⁴⁶. Thus, if the CO_2 produced during the N_r removal plus industrial nitrogen fixation cannot be captured for CO_2 fertilization in greenhouse plant production, the in-situ CO_2 recovery during the $\text{NO}_3^-\text{-N}$ recovery from CAB and urine could be more sustainable in the view of environmental sustainability. However, the quantitative monitoring of CO_2 and other possible gas emissions (e.g., N_2O and nitrogen oxides) was not implemented in this thesis. Therefore, further study about this aspect is required in the future.

2.1.2 Human health and sustainability

The concept of human health is understood in a broader context than health as the absence of disease³⁴⁷. Human health is part of the social dynamics of social organization, lifestyles, and consumption patterns, influenced by the biophysical environment. Many health and sustainability problems emerge due to society's appropriation of natural resources and the overexploitation of environmental services. In other words, many public health and environmental issues are caused by the increased intensification of agriculture and food production. There is a growing recognition that food security is an essential dimension of healthy life³⁴⁸. Besides, the current climate change has been bringing focus on the relationship between sustainability and health³⁴⁹.

In **Chapter 2**, a type of microbial fertilizer (CAB) was employed as an organic example to test a novel concept of converting organic fertilizers to hydroponic nutrient solutions. When considering CAB as organic fertilizer in the concept, crop and consumer safety are crucial. Spiller et al. (2020) found that CAB caused lower impacts than soybean meal on human health, with only 52% soybean meal⁹⁰. The impacts of CAB production on human health are mainly a function of climate change indicators. Muys et al. (2020) systematically screened the safety of dried CAB biomass from full-scale activated sludge plants from 25 companies in the food sector³⁵⁰. According to the EU limits for heavy metals in organic fertilizers³⁵¹, most CAB samples were safe. CAB biomass contamination with pathogens was not considered because the waste streams used to produce CAB typically exclude sanitary waste³⁵⁰. Otherwise, those cultivated microorganisms cannot be blindly accepted as fertilizer due to the potentially elevated risk of pathogens and other contaminations in the biomass. In **Chapter 2**, the heavy metal levels in the filtered effluent of the CAB bioreactor were all below the EU limits for heavy metals in inorganic fertilizer (Table 6.1).

Table 6.1 Contaminants in CAB and urine-sourced Hoagland nutrient solution. Limit values of contaminants expressed in mg, in relation to the total micronutrient content (boron (B), cobalt (Co), copper (Cu), iron (Fe), manganese (Mn), molybdenum (Mo), and zinc (Zn)) expressed in kg. "N.D." means not detected.

| Contaminant | mg kg ⁻¹ of total micronutrient content | | |
|--------------|--|---------------|-------------|
| | CAB-sourced | Urine-sourced | Limit value |
| Arsenic (As) | 150 | 201 | 1000 |
| Cadmium (Cd) | 17 | 11 | 200 |
| Lead (Pb) | 14 | 2 | 600 |
| Nickel (Ni) | 839 | 1152 | 2000 |
| Mercury (Hg) | N.D. | N.D. | 100 |

Some studies found the heavy metal concentrations of urine are lower than animal manure and industrial fertilizers^{352, 353}. In **Chapter 3**, the heavy metal concentrations in urine-sourced Hoagland nutrient solution were all lower than the EU limits for heavy metals in inorganic fertilizer (Table 6.1). Concerning the hygienic issues, the urine is sterile in the bladder of a healthy individual. When the urine is transported out of the body, some dermal bacteria can be picked up, and the freshly excreted urine typically contains less than 10,000 bacteria mL⁻¹³⁵⁴. Thus, the pathogens transmitted through urine are rarely sufficient and common to constitute a significant public health problem. Storage (e.g., 20°C for ≥6 months) is an easy method for urine disinfection in case of any contamination³⁵⁴. To shorten the time of pathogen inactivation, dosing Ca(OH)₂ to increase urine pH (≥11.5) was suggested with an exposure time of less than 1 h^{259, 355}. In **Chapter 3**, the urine stabilization by Ca(OH)₂ at pH 12 was employed to disinfect urine and prevent enzymatic urea hydrolysis. Besides the heavy metal and pathogen issues, the possible existence of various pharmaceutical residues could be another potential risk, which is not involved in this study. Knowledge of their presence in urine and their behavior from urine nitrification to plant uptake is still limited. Some researchers claimed that many pharmaceuticals, especially antibiotics, are biodegradable³⁵³ and photodegradable³⁵⁶. Although some pharmaceuticals (e.g., carbamazepine) can accumulate in the plants, the amounts are so small that it has not been regarded as a

health risk³⁵⁷. Anyhow, pharmaceuticals in urine can be a limiting factor for fertilizer use if found in large amounts or if any evident accumulation or other disturbance in edible plant parts occurs. Further study about the existence, level, and behavior of pharmaceuticals is necessary during using urine-sourced nutrients in agriculture. In principle, with proper treatment, there will be fewer restraints from the quality point of view to accept urine-sourced nutrients as a type of fertilizer.

For the Nr removal processes (**Chapter 4 and 5**), the final purpose is to convert Nr to inert N₂, which is harmless and chemically unreactive. The potential air pollution caused by GHG (e.g., CO₂, N₂O, and nitrogen oxides) emission may affect human health.

Overall, from the angle of heavy metal, pathogen, and pharmaceutical contamination, the nitrogen recovery from CAB and urine can satisfy the contamination limitation of inorganic fertilizer and subsequently cause no risk to human health. For the 'nitrogen recycling over the atmosphere', the air pollution should be adequately managed to mitigate its potential on human health.

2.1.3 Economic sustainability

Ideally, we should minimize the capital expenditures and OPEX to recover the fraction of Nr suitable for fertilizers and then remove the residual fraction. Energy (actually exergy) is as essential to the functioning of the global economic system as gasoline is to a car or electricity to a light bulb³⁵⁸. Therefore, one of the critical indicators of economic sustainability is the energy requirement of a specific process. Although energy considerations cannot completely represent the whole capital consumption, the energy consumption in the form of electricity and fuel is one of the key indicators to evaluate Nr management processes.

In **Chapter 2**, the major energy consumption is from aeration (electricity) and heating (fuel) in the bioreactor. We assume that the heat produced via electricity generation could be recovered during the operation of combined heat and power (CHP) configurations in farms^{220, 221}. Therefore, we considered heating is for free. The oxygen supplementation via aeration is mainly consumed by nitrification and the COD removal

process. The O_2 consumption for complete nitrification is $4.57 \text{ kg kg}^{-1} \text{ NO}_3^- \text{-N}$ production. Based on the $\text{NO}_3^- \text{-N}$ production performance in Ca(OH)_2 and Mg(OH)_2 scenarios, the O_2 requirement for COD removal is around $16.8 \text{ kg kg}^{-1} \text{ NO}_3^- \text{-N}$ production. Assuming the average O_2 transfer efficiency was 2 kg kWh^{-1} ²¹⁸, the electrical energy consumption by aeration is at least $10.7 \text{ kWh kg}^{-1} \text{ NO}_3^- \text{-N}$ (equal to $38.5 \text{ MJ kg}^{-1} \text{ NO}_3^- \text{-N}$).

Besides the CAB mineralization and nitrification process, the energy consumption during the CAB production should also be considered to elevate the economic sustainability of the concept proposed in **Chapter 2**. According to the energy balance during the CAB production, the electrical (el) and thermal (th) energy demand is 6.48 and 32.76 MJ kg^{-1} crude protein⁹⁰. Apparently, the heat demand significantly exceeds the electrical energy demand and is dominated by the drying process. With an N-to-protein conversion factor of 5.5, the electrical and thermal energy demand is 35.64 and $180.18 \text{ MJ kg}^{-1} \text{ N}$ ³⁵⁰. Based on the nitrification efficiency in Ca(OH)_2 and Mg(OH)_2 scenarios (around 50%), the electrical and thermal energy demand is 71.28 and $360.36 \text{ MJ kg}^{-1} \text{ NO}_3^- \text{-N}$. With the energy consumption by aeration, the total energy demand is $470.14 \text{ MJ kg}^{-1} \text{ NO}_3^- \text{-N}$ production. Unexpectedly, the heat demand is the dominant energy sink, with around 77% total energy consumption. Future research should further explore the energy-saving strategies in heat demand. One possible pathway to tackle energy-related issues in CAB production is to employ currently unused waste heat, such as the waste heat of refrigerator systems in food industries³⁵⁹.

Compared to the CAB producing system, microalgae-CAB (MaB) cultivation systems are more energy-efficient due to a bidirectional product/substrate (i.e., O_2/CO_2) exchange between photolithoautotrophic microalgae and CAB³⁶⁰. The biomass growth in the MaB system is partially autotrophic, and nitrogen is incorporated in microalgal biomass without COD demand. Therefore, compared to the CAB cultivation system, more COD can be anaerobically digested to obtain biogas, and energy is produced, with a positive generation of 792 MJ (el) and $1030 \text{ MJ (th)} \text{ kg}^{-1} \text{ N}$ ^{90, 361}. Therefore, if CAB is replaced with energetically MaB in **Chapter 2**, the aeration energy consumption can be fully covered, and economic sustainability should be remarkably improved.

Several techniques of Nr recovery from urine have been explored in both full-sale and

lab-scale bases, such as struvite formation, ammonia stripping, and thermal volume reduction³³⁸. In many cases, the analysis of different N_r recovery and removal techniques in urine has shown that recovery is energetically more efficient than removal plus new-production via the Haber-Bosch process. For example, struvite production, stripping with air plus (NH₄)₂SO₄ production, and eliminating 90% water of stabilized urine with vapor compression require 81, 32, and 18 MJ kg N recovery, respectively³³⁸. Suppose only the operating electricity, chemical, and fossil energy requirements are considered for the N removal and fertilizer production. In that case, the following specific energy requirements can be calculated: 87 MJ kg⁻¹ N for N/HDN with methanol as substrate and 43 MJ kg⁻¹ N for N-fertiliser production. Suppose the anthropogenic produced NH₃ is used to generate NO₃⁻-N, the aeration for nitrification is around 8.2 MJ kg⁻¹ N. In that case, the energy consumption from anthropogenic nitrogen fixation to nitrate production can be 51.2 MJ kg⁻¹ NO₃⁻-N. Therefore, the total energy demand of N_r removal plus new production (138.2 MJ kg⁻¹ N) is higher than the values derived for the recovery techniques mentioned above.

In **Chapter 3**, a novel concept of urine-based NO₃⁻-N production from a TF was proposed. The primary energy requirement is the recirculation pump, as no active aeration was needed. Based on the NO₃⁻-N production rate achieved and the operating conditions, the energy demand is 6.49 MJ kg⁻¹ NO₃⁻-N production, which can be further reduced via increasing the NO₃⁻-N production rate. It should be noted that the energy cost of urine transport was not taken into account for nitrate production here. The transportation cost was related to the collected urine volume and the distance between the collection location and the hydroponic farm. The collection should follow the principle of proximity. The concentration of collected urine (33% urine v/v) in this thesis tripled the transport cost. Installing water-saving urinals (e.g., vacuum urinals) in the collection area will further cut the cost of urine transport.

The conventional N/HDN process is generally used for low to medium strength NH₄⁺-N wastewater. If the COD/N ratio of wastewater (< 5-10) cannot satisfy the HDN process, an external carbon source would be required¹²². Thus, the PN/A process is usually employed in treating waste streams with a COD/N ratio lower than 1, consuming 100%

less organic carbon and almost 60% less oxygen than the conventional N/HDN pathway¹¹⁴. The energy demand of some PN/A processes has been estimated, with 4.32 and 1.44 MJ kg⁻¹ N removed in SRB and RBC reactors, respectively^{311, 312}. The large difference in the energy demand between SBR and RBC is mainly a function of the aeration approaches, i.e., active aeration in SBR and passive aeration in RBC.

In **Chapter 4**, the typical packed-bed trickling filters were employed to investigate the feasibility of the PN/A process. Since the trickling filters rely on passive aeration, the recirculation pumps are installed to control the DO level and wettability. Based on the nitrogen removal performance achieved in phase VII, the electricity consumption estimation was 2.8 MJ kg⁻¹ N removed, which was 1.9 times higher than the RBC, but 35% more energy-efficient than the SBR. Nevertheless, based on the performance in **Chapter 4**, the total energy demand (Nr removal plus NO₃⁻-N production via the Haber-Bosch process) can be at least 54 MJ kg⁻¹ N. Compared to the energy demand for direct NO₃⁻-N production in a trickling filter (i.e., 6.49 MJ kg⁻¹ NO₃⁻-N production) in **Chapter 3**, the indirect NO₃⁻-N production here via Nr removal plus the Haber-Bosch process consumes over 8-fold of energy. Therefore, from the angle of energy demand, the economic sustainability of Nr recovery via trickling filter is much more significant than Nr removal plus new production. Notably, the energy consumption for artificial NO₃⁻-N production accounts for the major energy-consuming proportion.

The performance of the sulfur-driven partial denitrataion process investigated in **Chapter 5** was not stable, and the subsequent combination with anammox process in long-term operation is still quite challenging. Thus, the energy demand analysis of this concept is not implemented.

Besides the energy consumption, the rough costs for nitrogen management with nitrate-based nutrients for agricultural fertilization were estimated. The preparation of Hoagland nutrient solution (HNS) was regarded as a uniform objective, and two types of commercial inorganic fertilizers were set as control. Only the costs of waste streams, supplemented chemicals, electricity consumption, and membrane filtration (Chapter 2) were involved in the total cost calculation (Table 6.2). For the biomass-based HNS production in Chapter 2, the cost-saving of CO₂ fertilization was considered as well.

Without regard to the transport cost of biomass, human urine, and commercial fertilizers, the total costs of urine-based HNS production were the lowest, while that of biomass-based HNS was higher than commercial YaraTera fertilizer, mainly attributed to the cost of CAB biomass. As mentioned above, further lowering the energy consumption during the CAB production and recovery could decrease its total costs.

Table 6.2 The costs of Hoagland nutrient solution (HNS) prepared from the waste streams studied in this thesis. The expenses of microbial fertilizer and commercial inorganic fertilizers refer to Table 2.1. N.A. means the process is not applicable.

| (€ m ⁻³ HNS) | Nr recovery & conversion | | Commercial inorganic fertilizer | |
|--|--------------------------|-------------------------|---------------------------------|-----------|
| | Biomass (CAB, Chapter 2) | Human urine (Chapter 3) | YaraTera | FloraFlex |
| CAB/urine/ commercial fertilizer | 5.6 | N.A. | 1.0 | 34.1 |
| Chemical compounds | 0.000 066 | 0.000 013 | 0.000 005 9 | 0.000 003 |
| Electricity (i.e., aeration, recirculation pumps) | 0.25 | 0.032 | | |
| Membrane module | 0.08 | N.A. | | N.A. |
| CO₂ fertilization saving | 0.46 | 0.031 | | |
| Total cost | 5.48 | 0.0019 | 1.0 | 34.1 |

To evaluate the economic sustainability, this section mainly analyzed the energy consumption of Nr management, which can directly affect the costs of HNS production for fertilization. The scalability of techniques and the capital expenditures contained in hardware such as reactors and pumps are outside our scope. Given the limited scope of this analysis and the distinct characterization of each process, there may be unforeseen economic aspects, including energy, resources, and processing costs. This research has attempted to estimate the economic sustainability of Nr recovery and removal with energy consumption as an indicator, but the data are not robust. Future work should further assess each technique in their pilot-scale installations and operations.

2.2 Nitrogen strength of waste streams

In practice, the nitrogen strength of waste streams can be a reference for nitrogen

management, closely related to the feasibility. Roughly three nitrogen concentration ranges can be distinguished: high ($>1 \text{ g L}^{-1}$), medium ($0.1\text{-}1 \text{ g L}^{-1}$), and low ($<0.1 \text{ g L}^{-1}$) strength.

Like source-separated urine and reject water from digestate, high-strength waste streams can contain pure or highly concentrated Nr (e.g., urea and $\text{NH}_4^+\text{-N}$) streams (Table 1.1 and 1.3) and should be considered targeted streams for nitrogen recovery. In principle, recovering the high-strength $\text{NH}_4^+\text{-N}$ stream is feasible via physical or chemical methods: stripping, adsorption, or struvite precipitation^{362, 363}. Most studies focus on nitrogen recovery in ammonia, but this thesis investigated nitrate recovery directly for hydroponic or fertigation applications. Therefore, the well-stabilized urine with concentrated urea was treated by biological method to get $\text{NO}_3^-\text{-N}$ nutrient in **Chapter 3**.

The medium-strength waste streams preferred biological treatments no matter via recovery or removal²⁸⁴. Some waste streams from the agro-food industry (e.g., potato-processing and brewery wastewater) contain medium-strength Nr (e.g., $0.1\text{-}0.5 \text{ g L}^{-1}$). Besides, these waste streams can also contain high concentrations of carbon (e.g., $4\text{-}15 \text{ g COD L}^{-1}$) and other nutrients ($0.04\text{-}0.08 \text{ g P L}^{-1}$), which have been recommended for Nr recovery via microbial fertilizer production³⁵⁰. The produced microbial fertilizers can either be directly applied to the soil-based plant production or further biologically converted to $\text{NO}_3^-\text{-N}$ solution for hydroponic or fertigation application in **Chapter 2**. Some municipal wastewater with low to medium Nr strength is preferred to apply the nitrogen removal strategies (**Chapter 4**) due to complex contamination (e.g., viruses, pathogens, heavy metals, and polyaromatic hydrocarbons).

In general, the low-strength wastewater with Nr, less than 0.1 g L^{-1} , is suggested to be removed biologically as N_2 based on the large volume of water and the cost-effectiveness^{284, 364}. Most of the municipal wastewater is within this low Nr strength range. Recovering Nr from low-concentration wastewater requires high-cost and high-energy consumption³⁶⁵. Pre-concentrating via membrane technology or capacitor deionization technology (CDI) could be a possible route. Still, the high cost of membrane materials and the size limitation of CDI electrodes significantly impede this route^{364, 366}. Therefore, biological

removal is still recommended considering the large water volume and low Nr level. According to different treatment processes used in global WWTPs, wastewater varies in nitrogen types (e.g., $\text{NH}_4^+\text{-N}$, $\text{NO}_3^-\text{-N}$) and concentrations, requiring targeted technologies (e.g., PN/A in **Chapter 4**, and denitrification/anammox in **Chapter 5**).

2.3 Technology performance and feasibility

The bioreactor strategies proposed in this thesis were used to manage Nr in various Physical (solid and liquid) and chemical (organic and inorganic) forms. The technology performance (on Nr recovery, conversion, or removal) and feasibility are two fundamental factors to decide the sustainable nitrogen cycle.

The technology proposed in **Chapter 2** is used for the Nr recovery and conversion from the solid organic waste streams (e.g., microbial biomass powder) via a suspended growth bioreactor. For the $\text{NO}_3^-\text{-N}$ production from CAB in a mineralization and nitrification reactor, the $\text{NO}_3^-\text{-N}$ production rate achieved at approximately $200 \text{ mg L}^{-1} \text{ d}^{-1}$ at a 5-day HRT (35°C), while the maximum $\text{NO}_3^-\text{-N}$ conversion efficiency only reached 51%. Compared to the higher $\text{NO}_3^-\text{-N}$ conversion efficiency (around 91%) in the batch test, doubling the HRT to 10 days could further elevate the efficiency. A trade-off between efficiency and production rate was made in this experiment. However, the further disposal of waste sludge containing the other half of nitrogen would still be challenging due to the large volume and transporting costs. One ideal disposal pathway is applying the sludge on the arable land as a slow-release fertilizer. Therefore, in practice, depending on the requirements of farmers, the specific trade-off between $\text{NO}_3^-\text{-N}$ production efficiency and rate should be made via controlling the HRT.

The concept of **Chapter 2** can be implemented in three steps: (i) mixing the solid organic fertilizers with water (e.g., tap water and rainwater) in an influent tank, (ii) bioconversion including ammonification and nitrification in a stirred-tank reactor, (iii) solid-liquid separation by microfiltration or ultrafiltration modules to obtain the $\text{NO}_3^-\text{-N}$ solution. The second step requires several parameter controls (i.e., temperature, pH, and DO), which can be realized by automatic control panels. Therefore, this recovery concept is relatively feasible for farmers.

The technology proposed in **Chapter 3** is used for the Nr recovery and conversion from liquid waste streams (e.g., sourced-separated urine) via a trickling filter. The rate and efficiency of urine-sourced NO_3^- -N production depends on the microbial activity, DO level, and HLR in the trickling filter. The obtained NO_3^- -N production efficiency and rate were $88\pm 3\%$ and $136\pm 4 \text{ mg NO}_3^- \text{-N L}^{-1} \text{ d}^{-1}$, respectively, at the hydraulic loading rate (HLR) of $2 \text{ m}^3 \text{ m}^{-2} \text{ h}^{-1}$ (21°C). Since the reservoir DO was still above 4 mg L^{-1} , as long as the DO is above 2 mg L^{-1} via controlling the HLR, the NO_3^- -N production rate can be further increased. The functional microorganisms, such as urease-positive bacteria, AOB, and NOB can be inoculated from municipal and industrial activated sludge. During the reactor operation, the biomass level increased over time, and several parameters (e.g., pH, temperature, salinity, inorganic carbon, and DO) could affect their activity. Since both the top and bottom ventilation were allowed, the DO level in the carrier biofilm was determined by the HLR and the Nr loading rate. Without increasing the HLR, increase the Nr loading rate would lead to the DO decrease. Full nitrification would not be achieved once the DO drops below 2 mg L^{-1} ³⁶⁷.

Similar to **Chapter 2**, the concept of **Chapter 3** can be implemented in two steps: (i) influent pretreatment (optional, e.g., urine alkalization) and (ii) Nr conversion in trickling filter. Due to the non-detectable TSS and VSS level in the effluent of trickling filter, purifying the nitrate-rich solution by microfiltration or ultrafiltration modules was unnecessary. The trickling filter used in the second step is low in maintenance and simple in operation. As a biofilm system, the trickling filter can be relatively robust in protecting against external physicochemical and biological stresses (**Chapter 1**, section 4.1). One typical disadvantage of trickling filters is the clogging issue during the long-term operation, especially for waste streams with high COD content. In fact, some pretreatment (e.g., anaerobic digestion) for the high COD waste streams can be considered, which can recover additional valuable products (e.g., methane). In **Chapter 3**, the COD content is relatively low, with a COD/N ratio of around 1. Thus, no clogging issue occurred during the whole operation period. The other problem that might arise in trickling filters is insect infestation, which could severely impair the nitrification process.

Nevertheless, chemical control via dosing insecticides can easily relieve this crisis.

The technology proposed in **Chapter 4** is used to remove Nr from liquid waste streams (e.g., domestic wastewater) via a trickling filter. For the medium-strength Nr (i.e., 250 mg $\text{NH}_4^+\text{-N L}^{-1}$) removal by the PN/A process, the TN removal rate could stabilize at 300 mg $\text{N L}^{-1} \text{d}^{-1}$ under the TN loading rate of 500 mg $\text{N L}^{-1} \text{d}^{-1}$ (30 °C). The $\text{NH}_4^+\text{-N}$ conversion efficiency seldomly exceeded 90%, indicating the TN overloading in TFs. Besides decreasing the TN loading rate, lowering the produced $\text{NO}_3^-\text{-N}$ level is necessary as well. By controlling the passive ventilation and hydraulic loading rate, the activity of NOB was excellently suppressed, with the $\text{NO}_3^-\text{-N}$ production efficiency of 13%, which is close to the ideal stoichiometric value of the anammox process. To further lower the $\text{NO}_3^-\text{-N}$ level in the effluent, some additional techniques should be considered, such as involving autotrophic denitrification in the PN/A trickling filters via mixing some sulfur particles with the carrier materials.

In **Chapter 4**, the feasibility of nitrogen removal via the PN/A process was demonstrated in trickling filters. As a biofilm system, trickling filter can effectively retain the slow-growth anammox biomass in biofilms. The major difficulty here is to balancing oxygen supply with nitrogen load. Although the structure of the trickling filter cannot allow flexible and accurate DO control like suspended growth systems, adjusting the ventilation openings (i.e., top and bottom) and the HLR can still realize adequate DO control. The top passive ventilation combined with a proper HLR (e.g., $1.8 \text{ m}^3 \text{ m}^{-2} \text{ h}^{-1}$) effectively realized PN/A in trickling filters.

The technology proposed in **Chapter 5** is used to polish secondary effluents (e.g., mainstream PN/A effluent) via coupling autotrophic denitrification in a sulfur-packed bed reactor with the downstream anammox. The performance of sulfur-driven denitrification is fluctuant, and the stable $\text{NO}_2^-\text{-N}$ accumulation could only be maintained in a short period. In the long-term operation, the $\text{NO}_2^-\text{-N}$ accumulation vanished, and only the complete denitrification existed. Based on the microbial community analysis, the *Thiobacillus* members might play a key role in managing the denitrification, but its abundance reduced, and adaptation occurred under the controlling strategies in the long

run.

Three controlling parameters were investigated in **Chapter 5**: pH setpoints, residual NO_3^- -N level, and biomass-specific NO_3^- -N loading rate. The pH setpoints of pH 7 and 8.5 in the reactor were realized by adjusting the influent pH. The residual NO_3^- -N level was controlled via the TN loading rate. The biomass-specific NO_3^- -N loading rate control was related to both TN loading rate and biomass level in the reactor. However, it is challenging to maintain a stable NO_2^- -N accumulation in the long term, only depending on these three strategies. Probably, additional control tools should be investigated.

Table 6.3 gives the advantages and challenges for Nr management via each bioreactor strategy in a qualitative way, which should always be interpreted according to case-specific requirements. In general, the performance and feasibility of nitrogen recovery and conversion from organic waste streams are relatively high, according to the concepts proposed in this thesis. Applying the cost-effective nitrogen removal process (i.e., PN/A) in trickling filters is medium-feasible with moderate performance. In contrast, implementing the autotrophic nitrogen polishing of secondary effluents via sulfur-driven denitrification is still quite challenging.

Table 6.3 Qualitative comparison of Nr management via the bioreactor strategies studied in this thesis ((advantages indicated in the green shading).

| | Nr management | Nr recovery & conversion | | Nr removal | |
|--------------------|-----------------------------|-------------------------------------|---------------------------------|---|---|
| | Reactor strategy | Stirred-tank reactor (Chapter 2) | Trickling filter (Chapter 3) | Trickling filter (Chapter 4) | Packed-bed reactor (Chapter 5) |
| | Substrate | Solid (microbial biomass) | Liquid (human urine) | Liquid (medium-strength NH ₄ ⁺) | Liquid (low-strength NH ₄ ⁺ & NO ₃ ⁻) |
| Performance | Efficiency | Medium | High | Medium | Medium |
| | Rate | Medium | Medium | Medium | Medium |
| | Stability | High | High | High | Low |
| | Ease of DO control | High | Medium | Low | High |
| | Ease of pH control | High | Medium | Medium | Medium |
| Feasibility | Ease of biomass retention | Low | Medium | Medium | Medium |
| | Risk for mechanical failure | Low | Low | Low | Low |
| | Risk for clogging | Low | Medium | Medium | High |
| | Risk for insect infestation | Low | Medium | Low | Low |
| | Operational complexity | Medium | Low | Low | High |

3. Overall conclusions and outlook

This thesis explored different bioreactor strategies for nitrogen recovery, conversion or removal based on mineralization, nitrification, anammox and/or autotrophic denitrification. The bioreactor strategies vary with the waste stream types, including solid via suspended growth reactor (**Chapter 2**) and liquid via attached growth reactors (**Chapter 3, 4, and 5**). Among these Nr management concepts, the recovery and conversion concepts are mainly for high-strength Nr streams like biomass (**Chapter 2**) and urine (**Chapter 3**); the removal concepts are for low- to medium-strength Nr streams (**Chapter 4 and 5**). Behind these concepts, sustainability (incl. environment, human health, and economy) is the primary decision-maker. The Nr management direction should be based on specific cases with the best sustainability, like the high concentrations are more likely to be recovered sustainably, while the low concentrations are preferred to be removed sustainably. Besides, the technology performance and feasibility are two basic decision-makers. In this thesis, the performance and feasibility of the NO_3^- -N recovery concepts (**Chapter 2 and 3**) and the TN removal concept (**Chapter 4**) are relatively promising, except for **Chapter 5**.

In the future, the Nr management concepts should be further improved to make the nitrogen cycle more sustainable with higher resource use efficiency and less Nr emissions to the environment. The sustainability of microbial fertilizer production from waste streams, especially for the energy required for biomass drying, is crucial for promoting the concept proposed in **Chapter 2**. Although the PN/A process for mainstream wastewater treatment is an attractive concept, the effluent issue is still a major barrier. A polishing strategy was proposed in **Chapter 5** via coupling the sulfur-driven denitrification and anammox, which is potentially sustainable. Additional strategies to achieve stable nitrite production for long-term operation require further exploration.

Overall, the proposed Nr management (i.e., recovery, conversion, and removal) concepts in this dissertation open up more opportunities for a sustainable nitrogen cycle. Furthermore, sustainable Nr management will help the Nr back to the safe boundary in the long run.

Bibliography

1. Steffen, W.; Richardson, K.; Rockstrom, J.; Cornell, S. E.; Fetzer, I.; Bennett, E. M.; Biggs, R.; Carpenter, S. R.; De Vries, W.; De Wit, C. A.; Folke, C.; Gerten, D.; Heinke, J.; Mace, G. M.; Persson, L. M.; Ramanathan, V.; Reyers, B.; Sorlin, S., Planetary boundaries: Guiding human development on a changing planet. *Science* **2015**, *347*, (6223), 1259855-1259855.
2. Steffen, W.; Crutzen, P. J.; McNeill, J. R., The Anthropocene: are humans now overwhelming the great forces of nature. *AMBIO: A Journal of the Human Environment* **2007**, *36*, (8), 614-621.
3. Crutzen, P. J., Geology of mankind. In *Paul J. Crutzen: A Pioneer on Atmospheric Chemistry and Climate Change in the Anthropocene*, Springer: 2016; pp 211-215.
4. Steffen, W.; Sanderson, R. A.; Tyson, P. D.; Jäger, J.; Matson, P. A.; Moore III, B.; Oldfield, F.; Richardson, K.; Schellnhuber, H.-J.; Turner, B. L., *Global change and the earth system: a planet under pressure*. Springer Science & Business Media: 2006.
5. Rockström, J.; Steffen, W.; Noone, K.; Persson, Å.; Chapin, F. S.; Lambin, E. F.; Lenton, T. M.; Scheffer, M.; Folke, C.; Schellnhuber, H. J.; Nykvist, B.; De Wit, C. A.; Hughes, T.; Van Der Leeuw, S.; Rodhe, H.; Sörlin, S.; Snyder, P. K.; Costanza, R.; Svedin, U.; Falkenmark, M.; Karlberg, L.; Corell, R. W.; Fabry, V. J.; Hansen, J.; Walker, B.; Liverman, D.; Richardson, K.; Crutzen, P.; Foley, J. A., A safe operating space for humanity. *Nature* **2009**, *461*, (7263), 472-475.
6. Sutton, M.; Raghuram, N.; Adhya, T. K.; Baron, J.; Cox, C.; de Vries, W.; Hicks, K.; Howard, C.; Ju, X.; Kanter, D., The nitrogen fix: from nitrogen cycle pollution to nitrogen circular economy-frontiers 2018/19: emerging issues of environmental concern chapter 4. *Frontiers 2018/19: Emerging Issues of Environmental Concern* **2019**.
7. Galloway, J. N.; Aber, J. D.; Erisman, J. W.; Seitzinger, S. P.; Howarth, R. W.; Cowling, E. B.; Cosby, B. J., The Nitrogen Cascade. *BioScience* **2003**, *53*, (4), 341.
8. Sutton, M. A.; Oenema, O.; Erisman, J. W.; Leip, A.; Van Grinsven, H.; Winiwarter, W., Too much of a good thing. *Nature* **2011**, *472*, (7342), 159-161.
9. Strock, J. S., Ammonification. In *Encyclopedia of Ecology, Five-Volume Set*, Elsevier Inc.: 2008; pp 162-165.
10. Erisman, J. W.; Sutton, M. A.; Galloway, J.; Klimont, Z.; Winiwarter, W., How a century of ammonia synthesis changed the world. *Nature Geoscience* **2008**, *1*, (10), 636-639.
11. Lenders, S.; Oeyen, A.; D'hooghe, J.; Overloop, S., Bodembalans van de Vlaamse landbouw, cijfers voor 2007–2009. *Departement Landbouw en Visserij and Vlaamse Milieumaatschappij, Brussel* **2012**.
12. Coppens, J.; Meers, E.; Boon, N.; Buysse, J.; Vlaeminck, S. E., Follow the N and P road: high-resolution nutrient flow analysis of the Flanders region as precursor for sustainable resource management. *Resources, Conservation and Recycling* **2016**, *115*, 9-21.
13. Smil, V., *Enriching the earth: Fritz Haber, Carl Bosch, and the transformation of world food production*. MIT press: 2001.

14. Trejo-Téllez, L. I.; Gómez-Merino, F. C., Nutrient solutions for hydroponic systems. *Hydroponics-a standard methodology for plant biological researches* **2012**, 1-22.
15. Jones Jr, J. B., *Complete guide for growing plants hydroponically*. CRC Press: 2014.
16. Hoagland, D. R.; Arnon, D. I., The water-culture method for growing plants without soil. *Circular. California agricultural experiment station* **1950**, 347, (2nd edit).
17. Hershey, D. R., Pardon me, but your roots are showing. *The Science Teacher* **1990**, 57, (2), 42.
18. Steiner, A. A., A universal method for preparing nutrient solutions of a certain desired composition. *Plant and soil* **1961**, 15, (2), 134-154.
19. Faulkner, S., The modified Steiner solution: A complete nutrient solution. *The Growing Edge* **1998**, 9, (4), 43-49.
20. AlShrouf, A., Hydroponics, aeroponic and aquaponic as compared with conventional farming. *American Scientific Research Journal for Engineering, Technology, and Sciences (ASRJETS)* **2017**, 27, (1), 247-255.
21. Brechner, M., Both AJ Cornell Controlled Environment Agriculture. *Cornell University* **2014**.
22. Alexandratos, N.; Bruinsma, J., World agriculture towards 2030/2050: the 2012 revision. **2012**.
23. Galloway, J. N., The global nitrogen cycle: changes and consequences. *Environmental pollution* **1998**, 102, (1), 15-24.
24. Bodirsky, B. L.; Popp, A.; Lotze-Campen, H.; Dietrich, J. P.; Rolinski, S.; Weindl, I.; Schmitz, C.; Müller, C.; Bonsch, M.; Humpenöder, F., Reactive nitrogen requirements to feed the world in 2050 and potential to mitigate nitrogen pollution. *Nature communications* **2014**, 5, (1), 1-7.
25. UNEP, U. N. E. P., UNEP Year Book 2014 **2014**.
26. Kanter, D. R.; Winiwarter, W.; Bodirsky, B. L.; Bouwman, L.; Boyer, E.; Buckle, S.; Compton, J. E.; Dalgaard, T.; De Vries, W.; Leclère, D.; Leip, A.; Müller, C.; Popp, A.; Raghuram, N.; Rao, S.; Sutton, M. A.; Tian, H.; Westhoek, H.; Zhang, X.; Zurek, M., A framework for nitrogen futures in the shared socioeconomic pathways. *Global Environmental Change* **2020**, 61, 102029.
27. Sutton, M. A.; Bleeker, A.; Howard, C.; Erismann, J.; Abrol, Y.; Bekunda, M.; Datta, A.; Davidson, E.; De Vries, W.; Oenema, O. *Our nutrient world. The challenge to produce more food & energy with less pollution*; Centre for Ecology & Hydrology: 2013.
28. Craig, R. K., Local or national-the increasing federalization of nonpoint source pollution regulation. *J. Env'tl. L. & Litig.* **2000**, 15, 179.
29. Suslick, K. S., Encyclopedia of physical science and technology. *Sonoluminescence and Sonochemistry Massachusetts: Elsevier Science Ltd* **2001**, 1-20.
30. Commission, E., Circular Economy Package: Questions & Answers. **2015**.
31. Wan, Y.; Huang, Z.; Zhou, L.; Li, T.; Liao, C.; Yan, X.; Li, N.; Wang, X., Bioelectrochemical Ammoniation Coupled with Microbial Electrolysis for Nitrogen Recovery from Nitrate in Wastewater. *Environmental Science & Technology* **2020**, 54, (5), 3002-3011.
32. Smil, V., Nitrogen and food production: proteins for human diets. *AMBIO: A Journal of the Human Environment* **2002**, 31, (2), 126-131.

33. Ukwuani, A. T.; Tao, W., Developing a vacuum thermal stripping – acid absorption process for ammonia recovery from anaerobic digester effluent. *Water Research* **2016**, *106*, 108-115.
34. Qin, M.; Molitor, H.; Brazil, B.; Novak, J. T.; He, Z., Recovery of nitrogen and water from landfill leachate by a microbial electrolysis cell–forward osmosis system. *Bioresource Technology* **2016**, *200*, 485-492.
35. Wu, X.; Modin, O., Ammonium recovery from reject water combined with hydrogen production in a bioelectrochemical reactor. *Bioresource Technology* **2013**, *146*, 530-536.
36. Sun, D.; Gao, Y.; Hou, D.; Zuo, K.; Chen, X.; Liang, P.; Zhang, X.; Ren, Z. J.; Huang, X., Energy-neutral sustainable nutrient recovery incorporated with the wastewater purification process in an enlarged microbial nutrient recovery cell. *Journal of Power Sources* **2018**, *384*, 160-164.
37. Zhang, C.; Ma, J.; Song, J.; He, C.; Waite, T. D., Continuous Ammonia Recovery from Wastewaters Using an Integrated Capacitive Flow Electrode Membrane Stripping System. *Environmental Science & Technology* **2018**, *52*, (24), 14275-14285.
38. Zamora, P.; Georgieva, T.; Ter Heijne, A.; Sleutels, T. H. J. A.; Jeremiasse, A. W.; Saakes, M.; Buisman, C. J. N.; Kuntke, P., Ammonia recovery from urine in a scaled-up Microbial Electrolysis Cell. *Journal of Power Sources* **2017**, *356*, 491-499.
39. Rodríguez Arredondo, M.; Kuntke, P.; Ter Heijne, A.; Hamelers, H. V. M.; Buisman, C. J. N., Load ratio determines the ammonia recovery and energy input of an electrochemical system. *Water Research* **2017**, *111*, 330-337.
40. Luther, A. K.; Desloover, J.; Fennell, D. E.; Rabaey, K., Electrochemically driven extraction and recovery of ammonia from human urine. *Water Research* **2015**, *87*, 367-377.
41. Kuntke, P.; Rodríguez Arredondo, M.; Widyakristi, L.; Ter Heijne, A.; Sleutels, T. H. J. A.; Hamelers, H. V. M.; Buisman, C. J. N., Hydrogen Gas Recycling for Energy Efficient Ammonia Recovery in Electrochemical Systems. *Environmental Science & Technology* **2017**, *51*, (5), 3110-3116.
42. Kuntke, P.; Zamora, P.; Saakes, M.; Buisman, C. J. N.; Hamelers, H. V. M., Gas-permeable hydrophobic tubular membranes for ammonia recovery in bio-electrochemical systems. *Environmental Science: Water Research & Technology* **2016**, *2*, (2), 261-265.
43. Antonini, S.; Paris, S.; Eichert, T.; Clemens, J., Nitrogen and Phosphorus Recovery from Human Urine by Struvite Precipitation and Air Stripping in Vietnam. *CLEAN - Soil, Air, Water* **2011**, *39*, (12), 1099-1104.
44. Beckinghausen, A.; Odlare, M.; Thorin, E.; Schwede, S., From removal to recovery: An evaluation of nitrogen recovery techniques from wastewater. *Applied Energy* **2020**, *263*, 114616.
45. Guo, C. H.; Stabnikov, V.; Ivanov, V., The removal of nitrogen and phosphorus from reject water of municipal wastewater treatment plant using ferric and nitrate bioreductions. *Bioresource technology* **2010**, *101*, (11), 3992-3999.
46. Mobley, H.; Hausinger, R., Microbial ureases: significance, regulation, and molecular characterization. *Microbiological reviews* **1989**, *53*, (1), 85-108.

47. Tao, W.; Bayrakdar, A.; Wang, Y.; Agyeman, F., Three-stage treatment for nitrogen and phosphorus recovery from human urine: Hydrolysis, precipitation and vacuum stripping. *Journal of environmental management* **2019**, *249*, 109435.
48. Buchner, G. A.; Stepputat, K. J.; Zimmermann, A. W.; Schomäcker, R., Specifying Technology Readiness Levels for the Chemical Industry. *Industrial & Engineering Chemistry Research* **2019**, *58*, (17), 6957-6969.
49. Yang, X.; Pang, H.; Zhang, J.; Liubinas, A.; Duke, M., Sustainable waste water deammonification by vacuum membrane distillation without pH adjustment: Role of water chemistry. *Chemical Engineering Journal* **2017**, *328*, 884-893.
50. Kwon, G.; Kang, J.; Nam, J.-H.; Kim, Y.-O.; Jahng, D., Recovery of ammonia through struvite production using anaerobic digestate of piggery wastewater and leachate of sewage sludge ash. *Environmental Technology* **2018**, *39*, (7), 831-842.
51. Tao, W.; Ukwuani, A. T., Coupling thermal stripping and acid absorption for ammonia recovery from dairy manure: Ammonia volatilization kinetics and effects of temperature, pH and dissolved solids content. *Chemical Engineering Journal* **2015**, *280*, 188-196.
52. Dube, P.; Vanotti, M.; Szogi, A.; García-González, M., Enhancing recovery of ammonia from swine manure anaerobic digester effluent using gas-permeable membrane technology. *Waste management* **2016**, *49*, 372-377.
53. Sancho, I.; Licon, E.; Valderrama, C.; De Arespacochaga, N.; López-Palau, S.; Cortina, J. L., Recovery of ammonia from domestic wastewater effluents as liquid fertilizers by integration of natural zeolites and hollow fibre membrane contactors. *Science of The Total Environment* **2017**, *584-585*, 244-251.
54. Christiaens, M. E. R.; Gildemyn, S.; Matassa, S.; Ysebaert, T.; De Vrieze, J.; Rabaey, K., Electrochemical Ammonia Recovery from Source-Separated Urine for Microbial Protein Production. *Environmental Science & Technology* **2017**, *51*, (22), 13143-13150.
55. Moral, R.; Paredes, C.; Bustamante, M.; Marhuenda-Egea, F.; Bernal, M., Utilisation of manure composts by high-value crops: Safety and environmental challenges. *Bioresource Technology* **2009**, *100*, (22), 5454-5460.
56. Chantigny, M. H.; Angers, D. A.; Rochette, P., Fate of carbon and nitrogen from animal manure and crop residues in wet and cold soils. *Soil Biology and Biochemistry* **2002**, *34*, (4), 509-517.
57. Rigo, E.; Ninow, J. L.; Di Luccio, M.; Oliveira, J. V.; Polloni, A. E.; Remonato, D.; Arbter, F.; Vardanega, R.; De Oliveira, D.; Treichel, H., Lipase production by solid fermentation of soybean meal with different supplements. *LWT - Food Science and Technology* **2010**, *43*, (7), 1132-1137.
58. Gao, M.; Liang, F.; Yu, A.; Li, B.; Yang, L., Evaluation of stability and maturity during forced-aeration composting of chicken manure and sawdust at different C/N ratios. *Chemosphere* **2010**, *78*, (5), 614-619.
59. Treball, B., Agro-Food Industry–Sector Report 2013. In 2013.
60. Diaz, M.; Madejon, E.; Lopez, F.; Lopez, R.; Cabrera, F., Optimization of the rate vinasse/grape marc for co-composting process. *Process Biochemistry* **2002**, *37*, (10), 1143-1150.
61. Cayuela, M. L.; Mondini, C.; Insam, H.; Sinicco, T.; Franke-Whittle, I., Plant and

- animal wastes composting: Effects of the N source on process performance. *Bioresource Technology* **2009**, *100*, (12), 3097-3106.
62. Parnaudeau, V.; Nicolardot, B.; Robert, P.; Alavoine, G.; Pagès, J.; Duchiron, F., Organic matter characteristics of food processing industry wastewaters affecting their C and N mineralization in soil incubation. *Bioresource Technology* **2006**, *97*, (11), 1284-1295.
63. Wang, S.; Zeng, Y., Ammonia emission mitigation in food waste composting: A review. *Bioresource Technology* **2018**, *248*, 13-19.
64. Rose, C.; Parker, A.; Jefferson, B.; Cartmell, E., The Characterization of Feces and Urine: A Review of the Literature to Inform Advanced Treatment Technology. *Critical Reviews in Environmental Science and Technology* **2015**, *45*, (17), 1827-1879.
65. Jeyabal, A.; Kuppuswamy, G., Recycling of organic wastes for the production of vermicompost and its response in rice–legume cropping system and soil fertility. *European Journal of Agronomy* **2001**, *15*, (3), 153-170.
66. Meunchang, S.; Panichsakpatana, S.; Weaver, R. W., Co-composting of filter cake and bagasse; by-products from a sugar mill. *Bioresource technology* **2005**, *96*, (4), 437-442.
67. Ramdani, A.; Dold, P.; Gadbois, A.; Déléris, S.; Houweling, D.; Comeau, Y., Characterization of the heterotrophic biomass and the endogenous residue of activated sludge. *Water Research* **2012**, *46*, (3), 653-668.
68. Udert, K. M.; Larsen, T. A.; Gujer, W., Fate of major compounds in source-separated urine. *Water Science and Technology* **2006**, *54*, (11-12), 413-420.
69. Erisman, J. W.; Galloway, J. N.; Seitzinger, S.; Bleeker, A.; Dise, N. B.; Petrescu, A. R.; Leach, A. M.; de Vries, W., Consequences of human modification of the global nitrogen cycle. *Philosophical Transactions of the Royal Society B: Biological Sciences* **2013**, *368*, (1621), 20130116.
70. Huang, H.; Xiao, D.; Liu, J.; Hou, L.; Ding, L., Recovery and removal of nutrients from swine wastewater by using a novel integrated reactor for struvite decomposition and recycling. *Scientific Reports* **2015**, *5*, (1), 10183.
71. Booker, N.; Priestley, A.; Fraser, I., Struvite formation in wastewater treatment plants: opportunities for nutrient recovery. *Environmental technology* **1999**, *20*, (7), 777-782.
72. Hao, X.-D.; Wang, C.-C.; Lan, L.; Van Loosdrecht, M., Struvite formation, analytical methods and effects of pH and Ca²⁺. *Water Science and technology* **2008**, *58*, (8), 1687-1692.
73. Dube, P. J.; Vanotti, M. B.; Szogi, A. A.; García-González, M. C., Enhancing recovery of ammonia from swine manure anaerobic digester effluent using gas-permeable membrane technology. *Waste Management* **2016**, *49*, 372-377.
74. Vanotti, M. B.; Dube, P. J.; Szogi, A. A.; García-González, M. C., Recovery of ammonia and phosphate minerals from swine wastewater using gas-permeable membranes. *Water Research* **2017**, *112*, 137-146.
75. Riaño, B.; Molinuevo-Salces, B.; Vanotti, M. B.; García-González, M. C., Application of Gas-Permeable Membranes For-Semi-Continuous Ammonia Recovery from Swine Manure. *Environments* **2019**, *6*, (3), 32.
76. Jiang, A.; Zhang, T.; Zhao, Q.-B.; Li, X.; Chen, S.; Frear, C. S., Evaluation of an

integrated ammonia stripping, recovery, and biogas scrubbing system for use with anaerobically digested dairy manure. *Biosystems Engineering* **2014**, *119*, 117-126.

77. Arredondo, M. R.; Kuntke, P.; Jeremiasse, A.; Sleutels, T.; Buisman, C.; Ter Heijne, A., Bioelectrochemical systems for nitrogen removal and recovery from wastewater. *Environmental Science: Water Research & Technology* **2015**, *1*, (1), 22-33.

78. Wang, H.; Ren, Z. J., A comprehensive review of microbial electrochemical systems as a platform technology. *Biotechnology advances* **2013**, *31*, (8), 1796-1807.

79. Qin, M.; Liu, Y.; Luo, S.; Qiao, R.; He, Z., Integrated experimental and modeling evaluation of energy consumption for ammonia recovery in bioelectrochemical systems. *Chemical Engineering Journal* **2017**, *327*, 924-931.

80. Gaskell, M.; Smith, R., Nitrogen Sources for Organic Vegetable Crops. *HortTechnology* **2007**, *17*, (4), 431-441.

81. Mikkelsen, R.; Hartz, T., Nitrogen sources for organic crop production. *Better crops* **2008**, *92*, (4), 16-19.

82. Azim, K.; Soudi, B.; Boukhari, S.; Perissol, C.; Roussos, S.; Thami Alami, I., Composting parameters and compost quality: a literature review. *Organic Agriculture* **2018**, *8*, (2), 141-158.

83. Antizar-Ladislao, B.; Lopez-Real, J.; Beck, A. J., Investigation of organic matter dynamics during in-vessel composting of an aged coal-tar contaminated soil using fluorescence excitation-emission spectroscopy. *Chemosphere* **2006**, *64*, (5), 839-847.

84. Soobhany, N.; Mohee, R.; Garg, V. K., Comparative assessment of heavy metals content during the composting and vermicomposting of municipal solid waste employing *Eudrilus eugeniae*. *Waste Management* **2015**, *39*, 130-145.

85. Soobhany, N., Insight into the recovery of nutrients from organic solid waste through biochemical conversion processes for fertilizer production: A review. *Journal of Cleaner Production* **2019**, *241*, 118413.

86. Muys, M. Microbial Protein as Sustainable Feed and Food Ingredient: Production and Nutritional Quality of Phototrophs and Aerobic Heterotrophs: Thesis. 2019.

87. Falletti, L.; Conte, L.; Zaggia, A.; Battistini, T.; Garosi, D., Food industry wastewater treatment plant based on flotation and MBBR. *Modern Environment Science and Engineering* **2014**, *1*, 562-566.

88. Spanoghe, J.; Grunert, O.; Wambacq, E.; Sakarika, M.; Papini, G.; Alloul, A.; Spiller, M.; Derycke, V.; Stragier, L.; Verstraete, H.; Fauconnier, K.; Verstraete, W.; Haesaert, G.; Vlaeminck, S. E., Storage, fertilization and cost properties highlight the potential of dried microbial biomass as organic fertilizer. *Microbial Biotechnology* **2020**, *13*, (5), 1377-1389.

89. Vriens, L.; Van den Eynde, E.; Verachtert, H., Parameters affecting protein production from brewery waste water in a multi-channel laboratory-scale activated sludge system. *European journal of applied microbiology and biotechnology* **1983**, *18*, (1), 52-59.

90. Spiller, M.; Muys, M.; Papini, G.; Sakarika, M.; Buyle, M.; Vlaeminck, S. E., Environmental impact of microbial protein from potato wastewater as feed ingredient: Comparative consequential life cycle assessment of three production systems and soybean meal. *Water Research* **2020**, *171*, 115406.

91. Wang, S. C.; Khin, M. C.; Chua, P. Q. D.; Luo, Y. D., Use of *Spirulina* biomass

produced from treatment of aquaculture wastewater as agricultural fertilizers. *Algal research* **2016**, *15*, 59-64.

92. Stanford, G.; Epstein, E., Nitrogen mineralization - water relations in soils. *Soil Science Society of America Journal* **1974**, *38*, (1), 103-107.

93. Kreij, C. d.; Voogt, W.; Baas, R., Nutrient solutions and water quality for soilless cultures. *Brochure/Research Station for Floriculture and Glasshouse Vegetables (Netherlands)* **1999**.

94. Maucieri, C.; Nicoletto, C.; Van Os, E.; Anseeuw, D.; Van Havermaet, R.; Junge, R., Hydroponic technologies. *Aquaponics Food Production Systems* **2019**, *77*.

95. Alsanus, B. W.; Wohanka, W., Root Zone Microbiology of Soilless Cropping Systems. In Elsevier: 2019; pp 149-194.

96. Zaman, M.; Di, H.; Cameron, K., A field study of gross rates of N mineralization and nitrification and their relationships to microbial biomass and enzyme activities in soils treated with dairy effluent and ammonium fertilizer. *Soil Use and Management* **1999**, *15*, (3), 188-194.

97. Khatoon, H.; Solanki, P.; Narayan, M.; Tewari, L.; Rai, J.; Hina Khatoon, C., Role of microbes in organic carbon decomposition and maintenance of soil ecosystem. *International Journal of Chemical Studies* **2017**, *5*, (6), 1648-1656.

98. Bridgham, S. D.; Ye, R., Organic matter mineralization and decomposition. *Methods in biogeochemistry of wetlands* **2013**, *10*, 385-406.

99. Blom, T.; Straver, W.; Ingratta, F.; Khosla, S., Carbon Dioxide in Greenhouses. Available at:(Accessed 10 November 2015) <http://www.omafra.gov.on.ca/english/crops/facts/00-077.htm> **2009**.

100. Reis, S.; Bekunda, M.; Howard, C. M.; Karanja, N.; Winiwarter, W.; Yan, X.; Bleeker, A.; Sutton, M. A., Synthesis and review: tackling the nitrogen management challenge: from global to local scales. *Environmental Research Letters* **2016**, *11*, (12), 120205.

101. Van Winckel, T. Towards intensification of water resource recovery facilities: smart metabolic and physical selection for design and control of mainstream processes. Ghent University, 2019.

102. Brochier-Armanet, C.; Boussau, B.; Gribaldo, S.; Forterre, P., Mesophilic Crenarchaeota: proposal for a third archaeal phylum, the Thaumarchaeota. *Nature Reviews Microbiology* **2008**, *6*, (3), 245-252.

103. Hatzenpichler, R., Diversity, physiology, and niche differentiation of ammonia-oxidizing archaea. *Applied and environmental microbiology* **2012**, *78*, (21), 7501-7510.

104. Stahl, D. A.; de la Torre, J. R., Physiology and diversity of ammonia-oxidizing archaea. *Annual review of microbiology* **2012**, *66*, 83-101.

105. Walker, C. B.; De La Torre, J.; Klotz, M.; Urakawa, H.; Pinel, N.; Arp, D.; Brochier-Armanet, C.; Chain, P.; Chan, P.; Gollabgir, A., Nitrosopumilus maritimus genome reveals unique mechanisms for nitrification and autotrophy in globally distributed marine crenarchaea. *Proceedings of the National Academy of Sciences* **2010**, *107*, (19), 8818-8823.

106. Daims, H.; Lücker, S.; Wagner, M., A New Perspective on Microbes Formerly Known as Nitrite-Oxidizing Bacteria. *Trends in Microbiology* **2016**, *24*, (9), 699-712.

107. Liu, G.; Wang, J., Probing the stoichiometry of the nitrification process using the

- respirometric approach. *Water Research* **2012**, *46*, (18), 5954-5962.
108. Benninger, R. W.; Sherrard, J. H., Nitrification and alkalinity relationships in activated sludge. *Journal (Water Pollution Control Federation)* **1978**, 2132-2142.
109. Metcalf; Eddy, I., Wastewater engineering: Treatment, disposal and reuse. In McGraw-Hill New York,, USA: 1991.
110. Shamas, N. K., Interactions of temperature, pH, and biomass on the nitrification process. *Journal (Water Pollution Control Federation)* **1986**, 52-59.
111. Grady Jr, C. L.; Smets, B. F.; Barbeau, D. S., Variability in kinetic parameter estimates: a review of possible causes and a proposed terminology. *Water Research* **1996**, *30*, (3), 742-748.
112. Henze, M.; van Loosdrecht, M. C.; Ekama, G. A.; Brdjanovic, D., *Biological wastewater treatment*. IWA publishing: 2008.
113. Anthonisen, A. C.; Loehr, R. C.; Prakasam, T.; Srinath, E., Inhibition of nitrification by ammonia and nitrous acid. *Journal (Water Pollution Control Federation)* **1976**, 835-852.
114. Vlaeminck, S.; De Clippeleir, H.; Verstraete, W., Microbial resource management of one - stage partial nitrification/anammox. *Microbial Biotechnology* **2012**, *5*, (3), 433-448.
115. Vandekerckhove, T. Technology for thermophilic nitrogen removal from wastewater: developing combined nitrification/denitrification and proving anammox. Ghent University, 2018.
116. Liu, L.; Koenig, A., Use of limestone for pH control in autotrophic denitrification: batch experiments. *Process Biochemistry* **2002**, *37*, (8), 885-893.
117. Koenig, A.; Liu, L., Kinetic model of autotrophic denitrification in sulphur packed-bed reactors. *Water research* **2001**, *35*, (8), 1969-1978.
118. Val del Río, Á.; Campos Gómez, J. L.; Mosquera Corral, A., *Technologies for the treatment and recovery of nutrients from industrial wastewater*. IGI Global: 2016.
119. Sahinkaya, E.; Dursun, N.; Kilic, A.; Demirel, S.; Uyanik, S.; Cinar, O., Simultaneous heterotrophic and sulfur-oxidizing autotrophic denitrification process for drinking water treatment: Control of sulfate production. *Water Research* **2011**, *45*, (20), 6661-6667.
120. Park, J. Y.; Yoo, Y. J., Biological nitrate removal in industrial wastewater treatment: which electron donor we can choose. *Applied Microbiology and Biotechnology* **2009**, *82*, (3), 415-429.
121. Wan, D.; Li, Q.; Liu, Y.; Xiao, S.; Wang, H., Simultaneous reduction of perchlorate and nitrate in a combined heterotrophic-sulfur-autotrophic system: Secondary pollution control, pH balance and microbial community analysis. *Water Research* **2019**, *165*, 115004.
122. Henze, M., Capabilities of biological nitrogen removal processes from wastewater. *Water Science and Technology* **1991**, *23*, (4-6), 669-679.
123. Sözen, S.; Orhon, D., The effect of nitrite correction on the evaluation of the rate of nitrate utilization under anoxic conditions. *Journal of Chemical Technology & Biotechnology: International Research in Process, Environmental & Clean Technology* **1999**, *74*, (8), 790-800.
124. Koren, D.; Gould, W. D.; Bedard, P., Biological removal of ammonia and nitrate

- from simulated mine and mill effluents. *Hydrometallurgy* **2000**, *56*, (2), 127-144.
125. Campos, J. L.; Carvalho, S.; Portela, R.; Mosquera-Corral, A.; Méndez, R., Kinetics of denitrification using sulphur compounds: Effects of S/N ratio, endogenous and exogenous compounds. *Bioresource Technology* **2008**, *99*, (5), 1293-1299.
126. Vandekerckhove, T. G.; Kobayashi, K.; Janda, J.; Van Nevel, S.; Vlaeminck, S. E., Sulfur-based denitrification treating regeneration water from ion exchange at high performance and low cost. *Bioresource technology* **2018**, *257*, 266-273.
127. Shao, M.-F.; Zhang, T.; Fang, H. H.-P., Sulfur-driven autotrophic denitrification: diversity, biochemistry, and engineering applications. *Applied Microbiology and Biotechnology* **2010**, *88*, (5), 1027-1042.
128. Chang, C. C.; Tseng, S. K.; Huang, H. K., Hydrogenotrophic denitrification with immobilized *Alcaligenes eutrophus* for drinking water treatment. *Bioresource technology* **1999**, *69*, (1), 53-58.
129. Zhang, T. C.; Lampe, D. G., Sulfur: limestone autotrophic denitrification processes for treatment of nitrate-contaminated water: batch experiments. *Water Research* **1999**, *33*, (3), 599-608.
130. Oh, S.-E.; Kim, K.-S.; Choi, H.-C.; Cho, J.; Kim, I., Kinetics and physiological characteristics of autotrophic denitrification by denitrifying sulfur bacteria. *Water science and technology* **2000**, *42*, (3-4), 59-68.
131. Wiesmann, U., Advances in biochemical engineering. *Biotechnology* **1994**, *51*, 113-154.
132. Alexander, M., Introduction to soil microbiology. *Soil Science* **1978**, *125*, (5), 331.
133. Cao, S.; Peng, Y.; Du, R.; Wang, S., Feasibility of enhancing the DENitrifying AMmonium OXidation (DEAMOX) process for nitrogen removal by seeding partial denitrification sludge. *Chemosphere* **2016**, *148*, 403-407.
134. Cui, B.; Yang, Q.; Liu, X.; Wu, W.; Liu, Z.; Gu, P., Achieving partial denitrification-anammox in biofilter for advanced wastewater treatment. *Environment International* **2020**, *138*, 105612.
135. Cao, S.; Wang, S.; Peng, Y.; Wu, C.; Du, R.; Gong, L.; Ma, B., Achieving partial denitrification with sludge fermentation liquid as carbon source: the effect of seeding sludge. *Bioresource technology* **2013**, *149*, 570-574.
136. Cui, B.; Liu, X.; Yang, Q.; Li, J.; Zhou, X.; Peng, Y., Achieving partial denitrification through control of biofilm structure during biofilm growth in denitrifying biofilter. *Bioresource technology* **2017**, *238*, 223-231.
137. Du, R.; Cao, S.; Li, B.; Niu, M.; Wang, S.; Peng, Y., Performance and microbial community analysis of a novel DEAMOX based on partial-denitrification and anammox treating ammonia and nitrate wastewaters. *Water research* **2017**, *108*, 46-56.
138. Li, W.; Li, H.; Liu, Y.-d.; Zheng, P.; Shapleigh, J. P., Salinity-aided selection of progressive onset denitrifiers as a means of providing nitrite for anammox. *Environmental science & technology* **2018**, *52*, (18), 10665-10672.
139. Cao, Y.; van Loosdrecht, M. C.; Daigger, G. T., Mainstream partial nitrification-anammox in municipal wastewater treatment: status, bottlenecks, and further studies. *Applied microbiology and biotechnology* **2017**, *101*, (4), 1365-1383.
140. Du, R.; Cao, S.; Li, B.; Zhang, H.; Wang, S.; Peng, Y., Synergy of partial-

denitrification and anammox in continuously fed upflow sludge blanket reactor for simultaneous nitrate and ammonia removal at room temperature. *Bioresource Technology* **2019**, *274*, 386-394.

141. Le, T.; Peng, B.; Su, C.; Massoudieh, A.; Torrents, A.; Al - Omari, A.; Murthy, S.; Wett, B.; Chandran, K.; DeBarbadillo, C., Impact of carbon source and COD/N on the concurrent operation of partial denitrification and anammox. *Water Environment Research* **2019**, *91*, (3), 185-197.

142. Du, R.; Cao, S.; Li, B.; Zhang, H.; Li, X.; Zhang, Q.; Peng, Y., Step-feeding organic carbon enhances high-strength nitrate and ammonia removal via DEAMOX process. *Chemical Engineering Journal* **2019**, *360*, 501-510.

143. Du, R.; Peng, Y.; Ji, J.; Shi, L.; Gao, R.; Li, X., Partial denitrification providing nitrite: Opportunities of extending application for anammox. *Environment International* **2019**, *131*, 105001.

144. Qian, W.; Ma, B.; Li, X.; Zhang, Q.; Peng, Y., Long-term effect of pH on denitrification: High pH benefits achieving partial-denitrification. *Bioresource Technology* **2019**, *278*, 444-449.

145. Chen, F.; Li, X.; Gu, C.; Huang, Y.; Yuan, Y., Selectivity control of nitrite and nitrate with the reaction of SO and achieved nitrite accumulation in the sulfur autotrophic denitrification process. *Bioresource Technology* **2018**, *266*, 211-219.

146. Deng, Y.-F.; Wu, D.; Huang, H.; Cui, Y.-X.; Van Loosdrecht, M. C. M.; Chen, G.-H., Exploration and verification of the feasibility of sulfide-driven partial denitrification coupled with anammox for wastewater treatment. *Water Research* **2021**, *193*, 116905.

147. Qian, J.; Zhang, M.; Wu, Y.; Niu, J.; Chang, X.; Yao, H.; Hu, S.; Pei, X., A feasibility study on biological nitrogen removal (BNR) via integrated thiosulfate-driven denitrification with anammox. *Chemosphere* **2018**, *208*, 793-799.

148. Deng, Y.-F.; Ekama, G. A.; Cui, Y.-X.; Tang, C.-J.; Van Loosdrecht, M. C. M.; Chen, G.-H.; Wu, D., Coupling of sulfur(thiosulfate)-driven denitrification and anammox process to treat nitrate and ammonium contained wastewater. *Water Research* **2019**, *163*, 114854.

149. Yamamoto-Ikemoto, R.; Komori, T.; Nomuri, M.; Ide, Y.; Matsukami, T., Nitrogen removal from hydroponic culture wastewater by autotrophic denitrification using thiosulfate. *Water Science and Technology* **2000**, *42*, (3-4), 369-376.

150. Wang, Y.; Sabba, F.; Bott, C.; Nerenberg, R., Using kinetics and modeling to predict denitrification fluxes in elemental - sulfur - based biofilms. *Biotechnology and Bioengineering* **2019**, *116*, (10), 2698-2709.

151. Wang, Y.; Bott, C.; Nerenberg, R., Sulfur-based denitrification: Effect of biofilm development on denitrification fluxes. *Water Research* **2016**, *100*, 184-193.

152. Weißbach, M.; Criddle, C. S.; Drewes, J. E.; Koch, K., A proposed nomenclature for biological processes that remove nitrogen. *Environmental Science: Water Research & Technology* **2017**, *3*, (1), 10-17.

153. Dietl, A.; Ferousi, C.; Maalcke, W. J.; Menzel, A.; de Vries, S.; Keltjens, J. T.; Jetten, M. S.; Kartal, B.; Barends, T. R., The inner workings of the hydrazine synthase multiprotein complex. *Nature* **2015**, *527*, (7578), 394-397.

154. Maalcke, W. J.; Reimann, J.; de Vries, S.; Butt, J. N.; Dietl, A.; Kip, N.; Mersdorf,

- U.; Barends, T. R.; Jetten, M. S.; Keltjens, J. T., Characterization of anammox hydrazine dehydrogenase, a key N₂-producing enzyme in the global nitrogen cycle. *Journal of Biological Chemistry* **2016**, *291*, (33), 17077-17092.
155. Gori, F.; Tringe, S. G.; Kartal, B.; Marchiori, E.; Jetten, M., The metagenomic basis of anammox metabolism in Candidatus' Brocadia fulgida'. *Biochemical Society Transactions* **2011**, *39*, (6), 1799-1804.
156. Strous, M.; Heijnen, J. J.; Kuenen, J. G.; Jetten, M. S. M., The sequencing batch reactor as a powerful tool for the study of slowly growing anaerobic ammonium-oxidizing microorganisms. *Applied Microbiology and Biotechnology* **1998**, *50*, (5), 589-596.
157. Oshiki, M.; Satoh, H.; Okabe, S., Ecology and physiology of anaerobic ammonium oxidizing bacteria. *Environmental microbiology* **2016**, *18*, (9), 2784-2796.
158. Kuenen, J. G., Anammox bacteria: from discovery to application. *Nature Reviews Microbiology* **2008**, *6*, (4), 320-326.
159. Fernández, I.; Dosta, J.; Fajardo, C.; Campos, J. L.; Mosquera-Corral, A.; Méndez, R., Short- and long-term effects of ammonium and nitrite on the Anammox process. *Journal of Environmental Management* **2012**, *95*, S170-S174.
160. Egli, K.; Fanger, U.; Alvarez, P. J.; Siegrist, H.; van der Meer, J. R.; Zehnder, A. J., Enrichment and characterization of an anammox bacterium from a rotating biological contactor treating ammonium-rich leachate. *Archives of microbiology* **2001**, *175*, (3), 198-207.
161. Strous, M.; Kuenen, J. G.; Jetten, M. S., Key physiology of anaerobic ammonium oxidation. *Applied and environmental microbiology* **1999**, *65*, (7), 3248-3250.
162. Dapena-Mora, A.; Fernandez, I.; Campos, J.; Mosquera-Corral, A.; Mendez, R.; Jetten, M., Evaluation of activity and inhibition effects on Anammox process by batch tests based on the nitrogen gas production. *Enzyme and Microbial Technology* **2007**, *40*, (4), 859-865.
163. Hoover, S. R.; Porges, N., Assimilation of dairy wastes by activated sludge: II. The equation of synthesis and rate of oxygen utilization. *Sewage and Industrial Wastes* **1952**, 306-312.
164. Takács, I.; Vanrolleghem, P. In *Elemental balances in activated sludge modelling*, Proceedings of IWA World Water Congress, 2006; 2006; pp 10-14.
165. Blackburne, R.; Yuan, Z.; Keller, J., Partial nitrification to nitrite using low dissolved oxygen concentration as the main selection factor. *Biodegradation* **2008**, *19*, (2), 303-312.
166. Hellinga, C.; Schellen, A.; Mulder, J. W.; van Loosdrecht, M. v.; Heijnen, J., The SHARON process: an innovative method for nitrogen removal from ammonium-rich waste water. *Water science and technology* **1998**, *37*, (9), 135-142.
167. Kornaros, M.; Dokianakis, S.; Lyberatos, G., Partial nitrification/denitrification can be attributed to the slow response of nitrite oxidizing bacteria to periodic anoxic disturbances. *Environmental science & technology* **2010**, *44*, (19), 7245-7253.
168. Lackner, S.; Terada, A.; Smets, B. F., Heterotrophic activity compromises autotrophic nitrogen removal in membrane-aerated biofilms: results of a modeling study. *Water research* **2008**, *42*, (4-5), 1102-1112.
169. Lackner, S.; Gilbert, E. M.; Vlaeminck, S. E.; Joss, A.; Horn, H.; van Loosdrecht, M.

- C., Full-scale partial nitrification/anammox experiences—an application survey. *Water research* **2014**, *55*, 292-303.
170. Agrawal, S.; Seuntjens, D.; De Cocker, P.; Lackner, S.; Vlaeminck, S. E., Success of mainstream partial nitrification/anammox demands integration of engineering, microbiome and modeling insights. *Current opinion in biotechnology* **2018**, *50*, 214-221.
171. Laurenzi, M.; Falås, P.; Robin, O.; Wick, A.; Weissbrodt, D. G.; Nielsen, J. L.; Ternes, T. A.; Morgenroth, E.; Joss, A., Mainstream partial nitrification and anammox: long-term process stability and effluent quality at low temperatures. *Water Research* **2016**, *101*, 628-639.
172. Peng, L.; Xie, Y.; Van Beeck, W.; Zhu, W.; Van Tendeloo, M.; Tytgat, T.; Lebeer, S.; Vlaeminck, S. E., Return-Sludge Treatment with Endogenous Free Nitrous Acid Limits Nitrate Production and N₂O Emission for Mainstream Partial Nitrification/Anammox. *Environmental Science & Technology* **2020**, *54*, (9), 5822-5831.
173. Zhang, M.; Wang, S.; Ji, B.; Liu, Y., Towards mainstream deammonification of municipal wastewater: Partial nitrification-anammox versus partial denitrification-anammox. *Science of The Total Environment* **2019**, *692*, 393-401.
174. Ma, B.; Xu, X.; Wei, Y.; Ge, C.; Peng, Y., Recent advances in controlling denitrification for achieving denitrification/anammox in mainstream wastewater treatment plants. *Bioresource Technology* **2020**, *299*, 122697.
175. An, S.; Loden, B.; Nemati, M., Evaluation of heterotrophic nitrite removal by a sulphide and acetate oxidizing mixed culture originated from an oil reservoir. *Journal of Chemical Technology & Biotechnology* **2012**, *87*, (3), 410-417.
176. Machineni, L., Review on biological wastewater treatment and resources recovery: attached and suspended growth systems. *Water Science and Technology* **2019**, *80*, (11), 2013-2026.
177. Rittmann, B. E.; McCarty, P. L., *Environmental biotechnology: principles and applications*. McGraw-Hill Education: 2001.
178. Jenkins, D.; Richard, M. G.; Daigger, G. T., *Manual on the causes and control of activated sludge bulking, foaming, and other solids separation problems*. Lewis publishers Boca Raton, FL: 2004.
179. Li, L.; Pagilla, K. R., Biomass density-function relationships in suspended growth biological processes – A critical review. *Water Research* **2017**, *111*, 274-287.
180. Abdelfattah, A.; Hossain, M. I.; Cheng, L., High-strength wastewater treatment using microbial biofilm reactor: a critical review. *World Journal of Microbiology and Biotechnology* **2020**, *36*, 1-10.
181. Daigger, G. T.; Boltz, J. P., Trickling filter and trickling filter - suspended growth process design and operation: A state - of - the - art review. *Water Environment Research* **2011**, *83*, (5), 388-404.
182. Farabegoli, G.; Chiavola, A.; Rolle, E., The Biological Aerated Filter (BAF) as alternative treatment for domestic sewage. Optimization of plant performance. *Journal of Hazardous Materials* **2009**, *171*, (1-3), 1126-1132.
183. De Clippeleir, H.; Yan, X.; Verstraete, W.; Vlaeminck, S. E., OLAND is feasible to treat sewage-like nitrogen concentrations at low hydraulic residence times. *Applied Microbiology and Biotechnology* **2011**, *90*, (4), 1537-1545.

184. SirianuntaPiboon, S., Some properties of packed cage RBC system on the treatment of synthetic domestic wastewater. *Science & Technology Asia* **2000**, 40-49.
185. Meulman, B.; Elzinga, N.; Gorter, K.; Zeeman, G.; Buisman, C.; Vlaeminck, S.; Verstraete, W. In *Pilot-scale demonstration of sustainable C and N removal from concentrated black water*, IWA World Water Congress & Exhibition, 2010; 2010.
186. Courtens, E. N. P.; Boon, N.; De Clippeleir, H.; Berckmoes, K.; Mosquera, M.; Seuntjens, D.; Vlaeminck, S. E., Control of nitrification in an oxygen-limited autotrophic nitrification/denitrification rotating biological contactor through disc immersion level variation. *Bioresource Technology* **2014**, *155*, 182-188.
187. Ødegaard, H., Innovations in wastewater treatment:—the moving bed biofilm process. *Water science and technology* **2006**, *53*, (9), 17-33.
188. Leyva-Díaz, J.; Martín-Pascual, J.; Poyatos, J., Moving bed biofilm reactor to treat wastewater. *International journal of environmental science and technology* **2017**, *14*, (4), 881-910.
189. Burghate, S.; Ingole, N., Fluidized bed biofilm reactor—a novel wastewater treatment reactor. *International Journal of Research in Environmental Science and Technology* **2013**, *3*, (4), 145-155.
190. Rittmann, B., The membrane biofilm reactor: the natural partnership of membranes and biofilm. *Water Science and Technology* **2006**, *53*, (3), 219-225.
191. Martin, K. J.; Nerenberg, R., The membrane biofilm reactor (MBfR) for water and wastewater treatment: principles, applications, and recent developments. *Bioresource technology* **2012**, *122*, 83-94.
192. Nerenberg, R., The membrane-biofilm reactor (MBfR) as a counter-diffusional biofilm process. *Current opinion in biotechnology* **2016**, *38*, 131-136.
193. Vlaeminck, S. E.; Terada, A.; Smets, B. F.; De Clippeleir, H. E.; Schaubroeck, T.; Bolca, S.; Demeestere, L.; Mast, J.; Boon, N.; Carballa, M.; Verstraete, W., Aggregate Size and Architecture Determine Microbial Activity Balance for One-Stage Partial Nitrification and Anammox. *Applied and Environmental Microbiology* **2010**, *76*, (3), 900-909.
194. Kim, H.-S.; Gellner, J. W.; Boltz, J. P.; Freudenberg, R. G.; Gunsch, C. K.; Schuler, A. J., Effects of integrated fixed film activated sludge media on activated sludge settling in biological nutrient removal systems. *Water Research* **2010**, *44*, (5), 1553-1561.
195. Malovanyy, A.; Trela, J.; Plaza, E., Mainstream wastewater treatment in integrated fixed film activated sludge (IFAS) reactor by partial nitrification/anammox process. *Bioresource Technology* **2015**, *198*, 478-487.
196. Loupasaki, E.; Diamadopoulou, E., Attached growth systems for wastewater treatment in small and rural communities: a review. *Journal of Chemical Technology & Biotechnology* **2013**, *88*, (2), 190-204.
197. Huang, Z.; Hejazi, M.; Tang, Q.; Vernon, C. R.; Liu, Y.; Chen, M.; Calvin, K., Global agricultural green and blue water consumption under future climate and land use changes. *Journal of Hydrology* **2019**, *574*, 242-256.
198. Hollevoet, L.; Jardali, F.; Gorbanev, Y.; Creel, J.; Bogaerts, A.; Martens, J. A., Towards Green Ammonia Synthesis through Plasma - Driven Nitrogen Oxidation and Catalytic Reduction. *Angewandte Chemie* **2020**.
199. Griffis, T. J.; Baker, J. M., Nitrogen management and air quality in China. *Nature*

Food **2020**, *1*, (10), 597-598.

200. Lacour, C.; Seconda, L.; Allès, B.; Hercberg, S.; Langevin, B.; Pointereau, P.; Lairon, D.; Baudry, J.; Kesse-Guyot, E., Environmental Impacts of Plant-Based Diets: How Does Organic Food Consumption Contribute to Environmental Sustainability? *Frontiers in Nutrition* **2018**, *5*.
201. Ramírez, W. A.; Domene, X.; Andrés, P.; Alcañiz, J. M., Phytotoxic effects of sewage sludge extracts on the germination of three plant species. *Ecotoxicology* **2008**, *17*, (8), 834-844.
202. Cabello, P.; Roldán, M. D.; Castillo, F.; Moreno-Vivián, C., Nitrogen Cycle. In *Encyclopedia of Microbiology (Third Edition)*, Schaechter, M., Ed. Academic Press: Oxford, 2009; pp 299-321.
203. Crohn, D. In *Nitrogen mineralization and its importance in organic waste recycling*, Proceedings, National Alfalfa Symposium, 2004; 2004; pp 13-5.
204. Botheju, D., Oxygen Effects in Anaerobic Digestion – A Review. *The Open Waste Management Journal* **2011**, *4*, (1), 1-19.
205. Veeken, A.; Hamelers, B., Effect of temperature on hydrolysis rates of selected biowaste components. *Bioresource Technology* **1999**, *69*, (3), 249-254.
206. Johansen, J.-E.; Bakke, R., Enhancing hydrolysis with microaeration. *Water science and Technology* **2006**, *53*, (8), 43-50.
207. Niu, T.; Zhou, Z.; Shen, X.; Qiao, W.; Jiang, L.-M.; Pan, W.; Zhou, J., Effects of dissolved oxygen on performance and microbial community structure in a micro-aerobic hydrolysis sludge in situ reduction process. *Water research* **2016**, *90*, 369-377.
208. Katipoglu-Yazan, T.; Cokgor, E. U.; Insel, G.; Orhon, D., Is ammonification the rate limiting step for nitrification kinetics? *Bioresource Technology* **2012**, *114*, 117-125.
209. Garland, J. L.; Mackowiak, C. L.; Strayer, R. F.; Finger, B. W., Integration of waste processing and biomass production systems as part of the KSC Breadboard project. **1997**, *20*, (10), 1821-1826.
210. Grunert, O.; Reheul, D.; Van Labeke, M.-C.; Perneel, M.; Hernandez-Sanabria, E.; Vlaeminck, S. E.; Boon, N., Growing media constituents determine the microbial nitrogen conversions in organic growing media for horticulture. **2016**, *9*, (3), 389-399.
211. Shinohara, M.; Aoyama, C.; Fujiwara, K.; Watanabe, A.; Ohmori, H.; Uehara, Y.; Takano, M., Microbial mineralization of organic nitrogen into nitrate to allow the use of organic fertilizer in hydroponics. *Soil science and plant nutrition* **2011**, *57*, (2), 190-203.
212. Garland, J. L.; Mackowiak, C. L.; Sager, J. C., Hydroponic crop production using recycled nutrients from inedible crop residues. *SAE Transactions* **1993**, 1103-1110.
213. Lee, S.; Ge, C.; Bohrerova, Z.; Grewal, P. S.; Lee, J., Enhancing plant productivity while suppressing biofilm growth in a windowfarm system using beneficial bacteria and ultraviolet irradiation. *Canadian journal of microbiology* **2015**, *61*, (7), 457-466.
214. Yaron, S.; Römling, U., Biofilm formation by enteric pathogens and its role in plant colonization and persistence. *Microbial Biotechnology* **2014**, *7*, (6), 496-516.
215. Clesceri, L.; Greenberg, A.; Eaton, A., Standard Methods for the Examination of Water and Wastewater, APHA, Washington, DC. *Standard methods for the examination of water and wastewater. 20th ed.* APHA, Washington, DC. **1998**, -.
216. Wang, Q.; Garrity, G. M.; Tiedje, J. M.; Cole, J. R., Naive Bayesian classifier for

- rapid assignment of rRNA sequences into the new bacterial taxonomy. *Applied and environmental microbiology* **2007**, *73*, (16), 5261-5267.
217. van Os, E.; Blok, C.; Voogt, W.; Waked, L. *Water quality and salinity aspects in hydroponic cultivation*; WUR Glastuinbouw: 2016.
218. Roman, M.-D.; Mureşan, M.-V., Analysis of oxygen requirements and transfer efficiency in a wastewater treatment plant. *Int. J. Latest Res. Sci. Technol* **2014**, *3*, 30-33.
219. Eurostat, S. E., Electricity price statistics. *Electricity prices for non-household consumers. ISSN* **2018**, 2443-8219.
220. Gentry, M., Local heat, local food: Integrating vertical hydroponic farming with district heating in Sweden. *Energy* **2019**, *174*, 191-197.
221. Gbadamosi, S. L.; Nwulu, N. I., Optimal Power Dispatch and Reliability Analysis of Hybrid CHP-PV-Wind Systems in Farming Applications. *Sustainability* **2020**, *12*, (19), 8199.
222. Arif, A. U. A.; Sorour, M. T.; Aly, S. A., Cost analysis of activated sludge and membrane bioreactor WWTPs using CapdetWorks simulation program: Case study of Tikrit WWTP (middle Iraq). *Alexandria Engineering Journal* **2020**, *59*, (6), 4659-4667.
223. Diamantis, V., Performance of a Micro-Scale Membrane Reactor for Greywater Treatment at Household Level. *Membranes* **2021**, *11*, (1), 63.
224. Kraus, T. E. C.; Dahlgren, R. A.; Zasoski, R. J., Tannins in nutrient dynamics of forest ecosystems - a review. *Plant and Soil* **2003**, *256*, (1), 41-66.
225. Campos, C. R.; Mesquita, V. A.; Silva, C. F.; Schwan, R. F., Efficiency of physicochemical and biological treatments of vinasse and their influence on indigenous microbiota for disposal into the environment. *Waste Management* **2014**, *34*, (11), 2036-2046.
226. Duff, S. J.; Murray, W. D., Bioconversion of forest products industry waste cellulose to fuel ethanol: a review. *Bioresour. Technol.* **1996**, *55*, (1), 1-33.
227. Sathiyamoorthi, E.; Kumar, P.; Kim, B. S., Lipid production by *Cryptococcus albidus* using biowastes hydrolysed by indigenous microbes. *Bioprocess and Biosystems Engineering* **2019**, *42*, (5), 687-696.
228. Carlsson, H., Calcium phosphate precipitation in biological phosphorus removal systems. *Water Research* **1997**, *31*, (5), 1047-1055.
229. Sindhu, M. t.; Cornfield, A., Comparative effects of varying levels of chlorides and sulphates of sodium, potassium, calcium, and magnesium on ammonification and nitrification during incubation of soil. *Plant and Soil* **1967**, *27*, (3), 468-472.
230. Smith, S. R.; Durham, E., Nitrogen Release and Fertiliser Value of Thermally-Dried Biosolids. *Water and Environment Journal* **2002**, *16*, (2), 121-126.
231. Masunga, R. H.; Uzokwe, V. N.; Mlay, P. D.; Odeh, I.; Singh, A.; Buchan, D.; De Neve, S., Nitrogen mineralization dynamics of different valuable organic amendments commonly used in agriculture. *Applied Soil Ecology* **2016**, *101*, 185-193.
232. Lazicki, P.; Geisseler, D.; Lloyd, M., Nitrogen mineralization from organic amendments is variable but predictable. *Journal of Environmental Quality* **2020**, *49*, (2), 483-495.
233. Rigby, H.; Clarke, B. O.; Pritchard, D. L.; Meehan, B.; Beshah, F.; Smith, S. R.; Porter, N. A., A critical review of nitrogen mineralization in biosolids-amended soil, the associated fertilizer value for crop production and potential for emissions to the

- environment. *Science of The Total Environment* **2016**, 541, 1310-1338.
234. Geisseler, D.; Miller, K. S.; Aegerter, B. J.; Clark, N. E.; Miyao, E. M., Estimation of Annual Soil Nitrogen Mineralization Rates using an Organic - Nitrogen Budget Approach. *Soil Science Society of America Journal* **2019**, 83, (4), 1227-1235.
235. Ribeiro, H. M.; Fangueiro, D.; Alves, F.; Vasconcelos, E.; Coutinho, J.; Bol, R.; Cabral, F., Carbon-mineralization kinetics in an organically managed Cambic Arenosol amended with organic fertilizers. *Journal of Plant Nutrition and Soil Science* **2010**, 173, (1), 39-45.
236. Guo, Z.; Han, J.; Li, J.; Xu, Y.; Wang, X., Effects of long-term fertilization on soil organic carbon mineralization and microbial community structure. *PLOS ONE* **2019**, 14, (1), e0211163.
237. DİNÇER, A. R.; ARAL, İ. F., CARBON DIOXIDE EMISSION IN THRACE REGION AND NEIGHBORING COUNTRIES AS A RESULT OF AEROBIC STABILIZATION OF URBAN TREATMENT SLUDGES. *Sigma: Journal of Engineering & Natural Sciences/Mühendislik ve Fen Bilimleri Dergisi* **2020**, 38, (4).
238. Seo, K. W.; Choi, Y.-S.; Gu, M. B.; Kwon, E. E.; Tsang, Y. F.; Rinklebe, J.; Park, C., Pilot-scale investigation of sludge reduction in aerobic digestion system with endospore-forming bacteria. *Chemosphere* **2017**, 186, 202-208.
239. Yang, C.; Zhang, W.; Liu, R.; Li, Q.; Li, B.; Wang, S.; Song, C.; Qiao, C.; Mulchandani, A., Phylogenetic Diversity and Metabolic Potential of Activated Sludge Microbial Communities in Full-Scale Wastewater Treatment Plants. *Environmental Science & Technology* **2011**, 45, (17), 7408-7415.
240. Eichorst, S. A.; Varanasi, P.; Stavila, V.; Zemla, M.; Auer, M.; Singh, S.; Simmons, B. A.; Singer, S. W., Community dynamics of cellulose-adapted thermophilic bacterial consortia. *Environmental Microbiology* **2013**, 15, (9), 2573-2587.
241. Cabrol, L.; Malhautier, L.; Poly, F.; Lepeuple, A.-S.; Fanlo, J.-L., Bacterial dynamics in steady-state biofilters: beyond functional stability. *FEMS Microbiology Ecology* **2012**, 79, (1), 260-271.
242. Lu, S.; Liu, X.; Liu, C.; Wang, X.; Cheng, G., Review of ammonia-oxidizing bacteria and archaea in freshwater ponds. *Reviews in Environmental Science and Bio/Technology* **2019**, 18, (1), 1-10.
243. Pan, Z.; Zhou, J.; Lin, Z.; Wang, Y.; Zhao, P.; Zhou, J.; Liu, S.; He, X., Effects of COD/TN ratio on nitrogen removal efficiency, microbial community for high saline wastewater treatment based on heterotrophic nitrification-aerobic denitrification process. *Bioresource Technology* **2020**, 301, 122726.
244. Duan, S.; Zhang, Y.; Zheng, S., Heterotrophic nitrifying bacteria in wastewater biological nitrogen removal systems: A review. *Critical Reviews in Environmental Science and Technology* **2021**, 1-37.
245. Wang, X.; Wang, W.; Li, Y.; Zhang, J.; Zhang, Y.; Li, J., Biofilm activity, ammonia removal and cell growth of the heterotrophic nitrifier, *Acinetobacter* sp., facilitated by exogenous N-acyl-homoserine lactones. *RSC advances* **2018**, 8, (54), 30783-30793.
246. Lang, X.; Li, Q.; Xu, Y.; Ji, M.; Yan, G.; Guo, S., Aerobic denitrifiers with petroleum metabolizing ability isolated from caprolactam sewage treatment pool. *Bioresource technology* **2019**, 290, 121719.

247. Sonneveld, C.; Voogt, W., Nutrient management in substrate systems. In *Plant nutrition of greenhouse crops*, Springer: 2009; pp 277-312.
248. Mikunda, T.; Neele, F.; Wilschut, F.; Hanegraaf, M., *A secure and affordable CO2 supply for the Dutch greenhouse sector*. TNO, Earth, Life & Social Sciences: 2015.
249. Lyman, W. J.; Reehl, W. F.; Rosenblatt, D. H., Handbook of chemical property estimation methods. **1990**.
250. Brodt, S.; Six, J.; Feenstra, G.; Ingels, C.; Campbell, D., Sustainable agriculture. *Nat. Educ. Knowl* **2011**, *3*, (1).
251. Bischel, H. N.; Schertenleib, A.; Fumasoli, A.; Udert, K. M.; Kohn, T., Inactivation kinetics and mechanisms of viral and bacterial pathogen surrogates during urine nitrification. *Environmental Science: Water Research & Technology* **2015**, *1*, (1), 65-76.
252. Zeeman, G.; Kujawa, K.; De Mes, T.; Hernandez, L.; De Graaff, M.; Abu-Ghunmi, L.; Mels, A.; Meulman, B.; Temmink, H.; Buisman, C., Anaerobic treatment as a core technology for energy, nutrients and water recovery from source-separated domestic waste (water). *Water Science and Technology* **2008**, *57*, (8), 1207-1212.
253. Randall, D.; Naidoo, V., Urine: The liquid gold of wastewater. *Journal of Environmental Chemical Engineering* **2018**, *6*, (2), 2627-2635.
254. De Paepe, J. Urine treatment technologies for a circular future within and beyond terrestrial boundaries. Ghent University, 2020.
255. Larsen, T. A.; Peters, I.; Alder, A.; Eggen, R.; Maurer, M.; Muncke, J., Peer reviewed: re-engineering the toilet for sustainable wastewater management. In ACS Publications: 2001.
256. Mobley, H.; Hausinger, R., Microbial ureases: significance, regulation, and molecular characterization. *Microbiology and Molecular Biology Reviews* **1989**, *53*, (1), 85-108.
257. Udert, K.; Fux, C.; Münster, M.; Larsen, T.; Siegrist, H.; Gujer, W., Nitrification and autotrophic denitrification of source-separated urine. *Water science and technology* **2003**, *48*, (1), 119-130.
258. Udert, K. M. The fate of nitrogen and phosphorus in source-separated urine. ETH Zurich, 2002.
259. Randall, D. G.; Krähenbühl, M.; Köpping, I.; Larsen, T. A.; Udert, K. M., A novel approach for stabilizing fresh urine by calcium hydroxide addition. *Water Research* **2016**, *95*, 361-369.
260. Udert, K. M.; Wächter, M., Complete nutrient recovery from source-separated urine by nitrification and distillation. *Water Research* **2012**, *46*, (2), 453-464.
261. Bornemann, G.; Waßer, K.; Tonat, T.; Moeller, R.; Bohmeier, M.; Hauslage, J., Natural microbial populations in a water-based biowaste management system for space life support. *Life Sciences in Space Research* **2015**, *7*, 39-52.
262. Bornemann, G.; Waßer, K.; Hauslage, J., The influence of nitrogen concentration and precipitation on fertilizer production from urine using a trickling filter. *Life Sciences in Space Research* **2018**, *18*, 12-20.
263. Islam, A.; Edwards, D.; Asher, C., pH optima for crop growth. *Plant and soil* **1980**, *54*, (3), 339-357.
264. Jiang, F.; Chen, Y.; Mackey, H. R.; Chen, G.; Van Loosdrecht, M., Urine nitrification

- and sewer discharge to realize in-sewer denitrification to simplify sewage treatment in Hong Kong. *Water Science and Technology* **2011**, *64*, (3), 618-626.
265. Coppens, J.; Lindeboom, R.; Muys, M.; Coessens, W.; Alloul, A.; Meerbergen, K.; Lievens, B.; Clauwaert, P.; Boon, N.; Vlaeminck, S. E., Nitrification and microalgae cultivation for two-stage biological nutrient valorization from source separated urine. *Bioresource Technology* **2016**, *211*, 41-50.
266. De Paepe, J.; Lindeboom, R. E. F.; Vanoppen, M.; De Paepe, K.; Demey, D.; Coessens, W.; Lamaze, B.; Verliefdde, A. R. D.; Clauwaert, P.; Vlaeminck, S. E., Refinery and concentration of nutrients from urine with electro dialysis enabled by upstream precipitation and nitrification. *Water Research* **2018**, *144*, 76-86.
267. De Paepe, J.; De Paepe, K.; Gòdia, F.; Rabaey, K.; Vlaeminck, S. E.; Clauwaert, P., Bio-electrochemical COD removal for energy-efficient, maximum and robust nitrogen recovery from urine through membrane aerated nitrification. *Water Research* **2020**, *185*, 116223.
268. Feng, D.; Wu, Z.; Xu, S., Nitrification of human urine for its stabilization and nutrient recycling. *Bioresource Technology* **2008**, *99*, (14), 6299-6304.
269. Wohlsager, S.; Clemens, J.; Nguyet, P. T.; Rechenburg, A.; Arnold, U., Urine - A Valuable Fertilizer with Low Risk after Storage in the Tropics. *Water Environment Research* **2010**, *82*, (9), 840-847.
270. Greenberg, A.; Clesceri, L.; Eaton, A. In *Standard methods for the examination of water and wastewater. Published by American public health association 18th edition Washington, DC*, Library congress ISBN 0-87553-207-1, 1992; 1992.
271. Fair, G. M., The trickling filter fly (*Psychoda alternata*), its habits and control. *Sewage Works Journal* **1934**, 966-981.
272. Le, T. T. H.; Fetting, J.; Meon, G., Kinetics and simulation of nitrification at various pH values of a polluted river in the tropics. *Ecohydrology & Hydrobiology* **2019**, *19*, (1), 54-65.
273. Udert, K. M.; Larsen, T. A.; Gujer, W., Biologically induced precipitation in urine-collecting systems. *Water Supply* **2003**, *3*, (3), 71-78.
274. Janiak, K.; Jurga, A.; Wizimirska, A.; Miodoński, S.; Muszyński-Huhajło, M.; Ratkiewicz, K.; Zięba, B., Urine nitrification robustness for application in space: Effect of high salinity and the response to extreme free ammonia concentrations. *Journal of Environmental Management* **2021**, *279*, 111610.
275. Sarigul, N.; Korkmaz, F.; Kurultak, İ., A New Artificial Urine Protocol to Better Imitate Human Urine. *Scientific Reports* **2019**, *9*, (1).
276. EPA, E. P. A., Wastewater technology fact sheet: Trickling filter nitrification. In 2000.
277. Andersson, B.; Aspegren, H.; Parker, D.; Lutz, M., High rate nitrifying trickling filters. *Water science and technology* **1994**, *29*, (10-11), 47.
278. Afzalimehr, H.; Anctil, F., Accelerating shear velocity in gravel-bed channels. *Hydrological Sciences Journal* **2000**, *45*, (1), 113-124.
279. Bansal, M. K., Nitrification in natural streams. *Journal (Water Pollution Control Federation)* **1976**, 2380-2393.
280. Timmons, M. B.; Losordo, T., *Aquaculture water reuse systems*. Elsevier: 1994.

281. Cheng, F.; Dai, Z.; Shen, S.; Wang, S.; Lu, X., Characteristics of rural domestic wastewater with source separation. *Water Science and Technology* **2021**, *83*, (1), 233-246.
282. Spellman, F. R., *Handbook of water and wastewater treatment plant operations*. CRC press: 2013.
283. Udert, K. M.; Larsen, T. A.; Biebow, M.; Gujer, W., Urea hydrolysis and precipitation dynamics in a urine-collecting system. *Water research* **2003**, *37*, (11), 2571-2582.
284. Mulder, A., The quest for sustainable nitrogen removal technologies. *Water Science and Technology* **2003**, *48*, (1), 67-75.
285. Gilbert, E. M.; Agrawal, S.; Schwartz, T.; Horn, H.; Lackner, S., Comparing different reactor configurations for Partial Nitrification/Anammox at low temperatures. *Water research* **2015**, *81*, 92-100.
286. De Clippeleir, H.; Vlaeminck, S. E.; De Wilde, F.; Daeninck, K.; Mosquera, M.; Boeckx, P.; Verstraete, W.; Boon, N., One-stage partial nitrification/anammox at 15 °C on pretreated sewage: feasibility demonstration at lab-scale. *Applied Microbiology and Biotechnology* **2013**, *97*, (23), 10199-10210.
287. Augusto, M. R.; Camiloti, P. R.; Souza, T. S. O. D., Fast start-up of the single-stage nitrogen removal using anammox and partial nitrification (SNAP) from conventional activated sludge in a membrane-aerated biofilm reactor. *Bioresource Technology* **2018**, *266*, 151-157.
288. Bunse, P.; Orschler, L.; Agrawal, S.; Lackner, S., Membrane aerated biofilm reactors for mainstream partial nitrification/anammox: Experiences using real municipal wastewater. *Water Research X* **2020**, *9*, 100066.
289. Malovanyy, A.; Yang, J.; Trela, J.; Plaza, E., Combination of upflow anaerobic sludge blanket (UASB) reactor and partial nitrification/anammox moving bed biofilm reactor (MBBR) for municipal wastewater treatment. *Bioresource Technology* **2015**, *180*, 144-153.
290. Szatkowska, B.; Cema, G.; Plaza, E.; Trela, J.; Hultman, B., A one-stage system with partial nitrification and Anammox processes in the moving-bed biofilm reactor. *Water Science and Technology* **2007**, *55*, (8-9), 19-26.
291. Liu, T.; Li, D.; Zhang, J., Biochemical characteristic along UBAF in a one-stage autotrophic nitrogen removal reactor. *Water Science and Technology* **2016**, *74*, (11), 2656-2665.
292. Liu, T.; Quan, X.; Li, D., Evaluations of biofilm thickness and dissolved oxygen on single stage anammox process in an up-flow biological aerated filter. **2017**, *119*, 20-26.
293. Antwi, P.; Zhang, D.; Luo, W.; Xiao, L. W.; Meng, J.; Kabutey, F. T.; Ayivi, F.; Li, J., Performance, microbial community evolution and neural network modeling of single-stage nitrogen removal by partial-nitrification/anammox process. *Bioresource Technology* **2019**, *284*, 359-372.
294. Wang, X.; Gao, D., In-situ restoration of one-stage partial nitrification-anammox process deteriorated by nitrate build-up via elevated substrate levels. *Scientific Reports* **2016**, *6*, (1), 37500.
295. Vlaeminck, S. E.; Terada, A.; Smets, B. F.; Linden, D. V. D.; Boon, N.; Verstraete,

- W.; Carballa, M., Nitrogen Removal from Digested Black Water by One-Stage Partial Nitrification and Anammox. *Environmental Science & Technology* **2009**, *43*, (13), 5035-5041.
296. Luo, W.; Yang, C.; He, H.; Zeng, G.; Yan, S.; Cheng, Y., Novel two-stage vertical flow biofilter system for efficient treatment of decentralized domestic wastewater. *Ecological Engineering* **2014**, *64*, 415-423.
297. Bressani-Ribeiro, T.; Almeida, P.; Volcke, E.; Chernicharo, C., Trickling filters following anaerobic sewage treatment: state of the art and perspectives. *Environmental Science: Water Research & Technology* **2018**, *4*, (11), 1721-1738.
298. The Water Environment, F., *Biofilm Reactors - WEF MoP 35*. McGraw-Hill Education: New York, 2011.
299. Sánchez Guillén, J. A.; Jayawardana, L. K. M. C. B.; Lopez Vazquez, C. M.; De Oliveira Cruz, L. M.; Brdjanovic, D.; Van Lier, J. B., Autotrophic nitrogen removal over nitrite in a sponge-bed trickling filter. *Bioresource Technology* **2015**, *187*, 314-325.
300. Watari, T.; Vazquez, C. L.; Hatamoto, M.; Yamaguchi, T.; Van Lier, J. B., Development of a single-stage mainstream anammox process using a sponge-bed trickling filter. *Environmental Technology* **2020**, 1-12.
301. Lekang, O.-I.; Kleppe, H., Efficiency of nitrification in trickling filters using different filter media. *Aquacultural engineering* **2000**, *21*, (3), 181-199.
302. Kuai, L.; Verstraete, W., Ammonium Removal by the Oxygen-Limited Autotrophic Nitrification-Denitrification System. *Applied and Environmental Microbiology* **1998**, *64*, (11), 4500-4506.
303. Hao, X.; Heijnen, J. J.; Van Loosdrecht, M. C. M., Sensitivity analysis of a biofilm model describing a one-stage completely autotrophic nitrogen removal (CANON) process. *Biotechnology and Bioengineering* **2002**, *77*, (3), 266-277.
304. Pynaert, K.; Smets, B. F.; Wyffels, S.; Beheydt, D.; Siciliano, S. D.; Verstraete, W., Characterization of an autotrophic nitrogen-removing biofilm from a highly loaded lab-scale rotating biological contactor. *Applied and environmental microbiology* **2003**, *69*, (6), 3626-3635.
305. Bernet, N.; Dangcong, P.; Delgenès, J.-P.; Moletta, R., Nitrification at low oxygen concentration in biofilm reactor. *Journal of environmental engineering* **2001**, *127*, (3), 266-271.
306. Hu, X.; Lin, R.; Wei, J.; Chang, J.; Wang, K.; Zhong, M.; Chen, L., Effects of Internal Diameter Size of Carriers on Biofilm Characteristics in Wastewater Treatment. *Environmental Engineering Science* **2020**, *37*, (10), 679-688.
307. Melo, L. F.; Vieira, M. J., Physical stability and biological activity of biofilms under turbulent flow and low substrate concentration. *Bioprocess Engineering* **1999**, *20*, (4), 363.
308. Kindaichi, T.; Ito, T.; Okabe, S., Ecophysiological Interaction between Nitrifying Bacteria and Heterotrophic Bacteria in Autotrophic Nitrifying Biofilms as Determined by Microautoradiography-Fluorescence In Situ Hybridization. *Applied and Environmental Microbiology* **2004**, *70*, (3), 1641-1650.
309. Gieseke, A.; Bjerrum, L.; Wagner, M.; Amann, R., Structure and activity of multiple nitrifying bacterial populations co-existing in a biofilm. **2003**, *5*, (5), 355-369.
310. Van Der Star, W. R. L.; Abma, W. R.; Blommers, D.; Mulder, J.-W.; Tokutomi, T.;

- Strous, M.; Picioreanu, C.; Van Loosdrecht, M. C. M., Startup of reactors for anoxic ammonium oxidation: Experiences from the first full-scale anammox reactor in Rotterdam. *Water Research* **2007**, *41*, (18), 4149-4163.
311. Mathure, P.; Patwardhan, A., Comparison of mass transfer efficiency in horizontal rotating packed beds and rotating biological contactors. **2005**, *80*, (4), 413-419.
312. Wett, B.; Nyhuis, G.; Takács, I.; Murthy, S., Development of enhanced deammonification selector. *WATER ENVIRONMENT FEDERATION, WEFTEC* **2010**, 2-6.
313. Poot, V.; Hoekstra, M.; Geleijnse, M. A. A.; Van Loosdrecht, M. C. M.; Pérez, J., Effects of the residual ammonium concentration on NOB repression during partial nitrification with granular sludge. *Water Research* **2016**, *106*, 518-530.
314. Directive, E. C., Directive 98/15/EEC amending directive 91/271/EEC. *Urban waste water treatment* **1998**.
315. Cao, S.; Du, R.; Peng, Y.; Li, B.; Wang, S., Novel two stage partial denitrification (PD)-Anammox process for tertiary nitrogen removal from low carbon/nitrogen (C/N) municipal sewage. *Chemical Engineering Journal* **2019**, *362*, 107-115.
316. Du, R.; Cao, S.; Li, X.; Wang, J.; Peng, Y., Efficient partial-denitrification/anammox (PD/A) process through gas-mixing strategy: System evaluation and microbial analysis. *Bioresource Technology* **2020**, *300*, 122675.
317. Du, R.; Cao, S.; Zhang, H.; Li, X.; Peng, Y., Flexible Nitrite Supply Alternative for Mainstream Anammox: Advances in Enhancing Process Stability. *Environmental Science & Technology* **2020**, *54*, (10), 6353-6364.
318. Li, X.; Yuan, Y.; Huang, Y.; Bi, Z., Simultaneous removal of ammonia and nitrate by coupled S₀-driven autotrophic denitrification and Anammox process in fluorine-containing semiconductor wastewater. *Science of The Total Environment* **2019**, *661*, 235-242.
319. Kumar, M.; Lin, J.-G., Co-existence of anammox and denitrification for simultaneous nitrogen and carbon removal—strategies and issues. *Journal of Hazardous Materials* **2010**, *178*, (1-3), 1-9.
320. Ge, S.; Peng, Y.; Wang, S.; Lu, C.; Cao, X.; Zhu, Y., Nitrite accumulation under constant temperature in anoxic denitrification process: The effects of carbon sources and COD/NO₃-N. *Bioresource technology* **2012**, *114*, 137-143.
321. Wang, Y.; Pavissich, J. P.; Sabba, F.; Bott, C.; Nerenberg, R., Elemental sulfur (S) as a supplemental electron donor for wastewater denitrification. *Proceedings of the Water Environment Federation* **2011**, *2011*, (15), 1590-1597.
322. Rohwerder, T.; Sand, W., The sulfane sulfur of persulfides is the actual substrate of the sulfur-oxidizing enzymes from *Acidithiobacillus* and *Acidiphilium* spp. *Microbiology* **2003**, *149*, (7), 1699-1710.
323. Suzuki, I., Oxidation of inorganic sulfur compounds: chemical and enzymatic reactions. *Canadian Journal of Microbiology* **1999**, *45*, (2), 97-105.
324. Boyd, E. S.; Druschel, G. K., Involvement of Intermediate Sulfur Species in Biological Reduction of Elemental Sulfur under Acidic, Hydrothermal Conditions. *Applied and Environmental Microbiology* **2013**, *79*, (6), 2061-2068.
325. An, S.; Tang, K.; Nemati, M., Simultaneous biodesulphurization and denitrification using an oil reservoir microbial culture: effects of sulphide loading rate and

- sulphide to nitrate loading ratio. *Water research* **2010**, *44*, (5), 1531-1541.
326. Simard, M.-C.; Masson, S.; Mercier, G.; Benmoussa, H.; Blais, J.-F.; Coudert, L., Autotrophic denitrification using elemental sulfur to remove nitrate from saline aquarium waters. *Journal of Environmental Engineering* **2015**, *141*, (12), 04015037.
327. Pan, Y.; Ni, B.-J.; Yuan, Z., Modeling electron competition among nitrogen oxides reduction and N₂O accumulation in denitrification. *Environmental science & technology* **2013**, *47*, (19), 11083-11091.
328. Van De Graaf, A. A.; De Bruijn, P.; Robertson, L. A.; Jetten, M. S. M.; Kuenen, J. G., Autotrophic growth of anaerobic ammonium-oxidizing micro-organisms in a fluidized bed reactor. *Microbiology* **1996**, *142*, (8), 2187-2196.
329. APHA, A., Standard methods for the examination of water and wastewater analysis. *American Public Health Association, Washington DC* **1998**.
330. Hjortso, M., *Cell adhesion in bioprocessing and biotechnology*. CRC Press: 1994; Vol. 20.
331. Almeida, J.; Reis, M.; Carrondo, M., Competition between nitrate and nitrite reduction in denitrification by *Pseudomonas fluorescens*. *Biotechnology and Bioengineering* **1995**, *46*, (5), 476-484.
332. Meijer, E. M.; Zwaan, J. W.; Stouthamer, A. H.; Wever, R., Anaerobic Respiration and Energy Conservation in *Paracoccus denitrificans*. Functioning of Iron-Sulfur Centers and the Uncoupling Effect of Nitrite. *European Journal of Biochemistry* **1979**, *96*, (1), 69-76.
333. Glass, C.; Silverstein, J., Denitrification kinetics of high nitrate concentration water: pH effect on inhibition and nitrite accumulation. *Water Research* **1998**, *32*, (3), 831-839.
334. Zhou, W.; Li, Y.; Liu, X.; He, S.; Huang, J. C., Comparison of microbial communities in different sulfur-based autotrophic denitrification reactors. *Applied Microbiology and Biotechnology* **2017**, *101*, (1), 447-453.
335. Lv, P.-L.; Shi, L.-D.; Dong, Q.-Y.; Rittmann, B.; Zhao, H.-P., How nitrate affects perchlorate reduction in a methane-based biofilm batch reactor. *Water Research* **2020**, *171*, 115397.
336. Ishaque, M.; Aleem, M., Intermediates of denitrification in the chemoautotroph *Thiobacillus denitrificans*. *Archiv für Mikrobiologie* **1973**, *94*, (3), 269-282.
337. Zhang, L.; Zhang, C.; Hu, C.; Liu, H.; Bai, Y.; Qu, J., Sulfur-based mixotrophic denitrification corresponding to different electron donors and microbial profiling in anoxic fluidized-bed membrane bioreactors. *Water Research* **2015**, *85*, 422-431.
338. Maurer, M.; Schwegler, P.; Larsen, T. A., Nutrients in urine: energetic aspects of removal and recovery. *Water Science and Technology* **2003**, *48*, (1), 37-46.
339. McMichael, A. J.; Butler, C. D.; Folke, C., New visions for addressing sustainability. *Science* **2003**, *302*, (5652), 1919-1920.
340. Ghosh, P.; Westhoff, P.; Debnath, D., Biofuels, food security, and sustainability. In *Biofuels, Bioenergy and Food Security*, Elsevier: 2019; pp 211-229.
341. Parravicini, V.; Svardal, K.; Krampe, J., Greenhouse Gas Emissions from Wastewater Treatment Plants. *Energy Procedia* **2016**, *97*, 246-253.
342. Lv, Y.; Zhang, S.; Yang, Y.; Liu, Y.; Xie, K.; Zhong, J., N₂O emission and control

- strategy in different wastewater treatment processes. *E3S Web of Conferences* **2019**, *118*, 04029.
343. Lin, Y.; Guo, M.; Shah, N.; Stuckey, D. C., Economic and environmental evaluation of nitrogen removal and recovery methods from wastewater. *Bioresource Technology* **2016**, *215*, 227-238.
344. Bao, Z.; Sun, S.; Sun, D., Characteristics of direct CO₂ emissions in four full-scale wastewater treatment plants. *Desalination and Water Treatment* **2015**, *54*, (4-5), 1070-1079.
345. Alves, M. S.; Silva, F. J. A. D.; Araújo, A. L. C.; Pereira, E. L., Performance evaluation and coefficients of reliability for waste stabilization ponds in northeast Brazil. *Ambiente e Agua - An Interdisciplinary Journal of Applied Science* **2021**, *16*, (1), 1.
346. Kool, A.; Marinussen, M.; Blonk, H., LCI data for the calculation tool Feedprint for greenhouse gas emissions of feed production and utilization. *GHG Emissions of N, P and K fertiliser production* **2012**.
347. Kjrgard, B.; Land, B.; Bransholm Pedersen, K., Health and sustainability. *Health Promotion International* **2014**, *29*, (3), 558-568.
348. Godfray, H.; Crute, I.; Haddad, L.; Lawrence, D.; Muir, J.; Pretty, J.; Robinson, S.; Toulmin, C., The Future of food and farming; Challenges and choices for global sustainability, London, UK, The Government office for Science. *Foresight Report* **2011**.
349. Lancet, T., A Commission on climate change. In Elsevier: 2009.
350. Muys, M.; Papini, G.; Spiller, M.; Sakarika, M.; Schwaiger, B.; Lesueur, C.; Vermeir, P.; Vlaeminck, S. E., Dried aerobic heterotrophic bacteria from treatment of food and beverage effluents: Screening of correlations between operation parameters and microbial protein quality. *Bioresource Technology* **2020**, *307*, 123242.
351. Parliament, E.; Union, C. o. t. E., Regulation (EU) 2019/1009 of the European Parliament and of the Council of 5 June 2019 laying down rules on the making available on the market of EU fertilising products and amending Regulations (EC) No 1069/2009 and (EC) No 1107/2009 and repealing Regulation (EC) No 2003/2003. Official Journal of the European Union, L 170/1. *Off. J. Eur. Union* **2019**, *62*, 1-132.
352. Viskari, E.-L.; Grobler, G.; Karimäki, K.; Gorbatova, A.; Vilpas, R.; Lehtoranta, S., Nitrogen Recovery With Source Separation of Human Urine—Preliminary Results of Its Fertiliser Potential and Use in Agriculture. *Frontiers in Sustainable Food Systems* **2018**, *2*.
353. Winker, M.; Vinnerås, B.; Muskolus, A.; Arnold, U.; Clemens, J., Fertiliser products from new sanitation systems: their potential values and risks. *Bioresource technology* **2009**, *100*, (18), 4090-4096.
354. Schönning, C.; Leaning, R.; Stenstrom, T. In *Evaluation of microbial health risks associated with the reuse of source separated human urine*, Proceedings of the international conference on ecological sanitation, Nanning, China, 2001; 2001.
355. Farrell, J. B.; Smith Jr, J. E.; Hathaway, S. W.; Dean, R. B., Lime stabilization of primary sludges. *Journal (Water Pollution Control Federation)* **1974**, 113-122.
356. Doll, T. E.; Frimmel, F. H., Fate of pharmaceuticals—photodegradation by simulated solar UV-light. *Chemosphere* **2003**, *52*, (10), 1757-1769.
357. Winker, M.; Clemens, J.; Reich, M.; Gulyas, H.; Otterpohl, R., Ryegrass uptake of carbamazepine and ibuprofen applied by urine fertilization. *Science of the Total*

Environment **2010**, *408*, (8), 1902-1908.

358. Ayres, R.; Turton, H.; Casten, T., Energy efficiency, sustainability and economic growth. *Energy* **2007**, *32*, (5), 634-648.

359. Patel, K. K.; Kar, A., Heat pump assisted drying of agricultural produce—an overview. *Journal of food science and technology* **2012**, *49*, (2), 142-160.

360. Van Den Hende, S. Microalgal bacterial flocs for wastewater treatment: from concept to pilot scale. Ghent University, 2014.

361. Muys, M.; Phukan, R.; Brader, G.; Samad, A.; Moretti, M.; Haiden, B.; Pluchon, S.; Roest, K.; Vlaeminck, S. E.; Spiller, M., A systematic comparison of commercially produced struvite: Quantities, qualities and soil-maize phosphorus availability. *Science of The Total Environment* **2021**, *756*, 143726.

362. Winkler, M. K.; Straka, L., New directions in biological nitrogen removal and recovery from wastewater. *Current Opinion in Biotechnology* **2019**, *57*, 50-55.

363. Guo, X.; Chen, G.; Liu, F.; Wang, C.; Gao, K.; Cheng, Z.; Yan, B.; Ma, W., Promoting air gasification of corn straw through biological pretreatment by biogas slurry: An initiative experimental study. *Fuel Processing Technology* **2019**, *191*, 60-70.

364. Xiang, S.; Liu, Y.; Zhang, G.; Ruan, R.; Wang, Y.; Wu, X.; Zheng, H.; Zhang, Q.; Cao, L., New progress of ammonia recovery during ammonia nitrogen removal from various wastewaters. *World Journal of Microbiology and Biotechnology* **2020**, *36*, (10).

365. Fang, K.; Gong, H.; He, W.; Peng, F.; He, C.; Wang, K., Recovering ammonia from municipal wastewater by flow-electrode capacitive deionization. *Chemical Engineering Journal* **2018**, *348*, 301-309.

366. Yeh, C.-L.; Hsi, H.-C.; Li, K.-C.; Hou, C.-H., Improved performance in capacitive deionization of activated carbon electrodes with a tunable mesopore and micropore ratio. *Desalination* **2015**, *367*, 60-68.

367. Kim, D.-J.; Ahn, D. H.; Lee, D.-I., Effects of free ammonia and dissolved oxygen on nitrification and nitrite accumulation in a biofilm airlift reactor. *Korean Journal of Chemical Engineering* **2005**, *22*, (1), 85-90.

Acknowledgments

Siegfried, thanks for accepting me to the research group, which was a new start to my career. It was precious to work together in the past four years. Honestly, I have grown and matured during my Ph.D., owing to your support and supervision.

Lai, thanks for introducing me to Siegfried. I still remember the first time we met in the winter of 2016 at Hunan University. After I arrived here, you took care of my new life and career as an old brother. All of your contributions make me feel warm and confident in my Ph.D. life.

Marc, much appreciation for your contribution to my research. I am glad to have my first paper together with you. Thanks for your response to my academic questions, even during your weekends and holidays, making me feel more secure.

Mingsheng, extremely lucky and happy to know you and work together during my Ph.D. Significantly during the second half of my Ph.D. career, your warm and sincere talk, support, and guidance rescued me from the dark dilemma. Good luck to your postdoc and future. Hopefully, in the future, we can still collaborate.

Michiel, nice to be each other's RBC buddy in our Ph.D. I will miss the moments we shared during work, travel, party, and many others.

Weiqiang, great to have you from the beginning of our Ph.D. as well. I learned a lot from you, which makes me stronger and more mature. I have to say it was very nice working with you.

Marijn, Tim, Jolien, Wannes, Olivier and Veerle, really nice to work with you, and thanks for all your help with my research.

Hilde and Annelize, thanks for all your dedicated support to my Ph.D. You made me feel warm and secure when I worked in the lab. I wish you all the best.

Gustavo, buddy, nice to know you and work with you. You are a good man. Every time I came to you, you always tried your best to help me. Good luck with your career and life.

Abbas and Janne, I cannot believe each of you guys already has a lovely baby and a happy family. Well done!

Julia, Joris, Naïm, and Waut, welcome to the group, and good luck.

Sui, Radu, Maarten, Michele, Myrsini, Rishav, Marnix, although you have been away, the time we spent together will always be remembered.

For our air buddies, I would like to thank all of you for the fun times we had, **Ritu, Rajesh, Tess, Griet, Myrthe, Natan, Lore, Laurens, Ramesh, Ritu, Sammy, Siegfried D, Jelle, Jeroen**, and many more!

Leen, Bea, Katrien, Tom, and the whole BIR, nice to work with you. Thank all of you for your support.

Gilles, Björn, and Eddie, thanks guys for building and maintaining all my reactors.

Luka, thank you for all the sludge you provided.

A special thanks to the students involved in my Ph.D.: **Inaki, Quinten, Thomas, Vincent, Daphné, and many more lovely people that I have met**. It was very nice working with you.

Kaimin and Jinxin, thanks for making me feel at home sometimes. Best wishes to your Ph.D. and your marriage life. I am looking forward to reuniting with you in China.

Xiaoquan, Zhouyan, Xuezhang, Yi Feng, Fangwei and Wang Yang, best buddies ever.

Yang Hong, you are one of the most important people in my life. Thank you for your care and company all alone.

Meng jun, you know you are always my first and last support, and I will be yours as well.

Prof. Haoran Dong, you are the great man of my life and always my role model. I was so lucky to be your student. I have been under your guidance, care, and encouragement for years.

Finally, I would like to thank my family. **Mum and Dad**, thank you for your unconditional

love and support. **My parents-in-law**, without your care and support, I will never complete this journey. I hope you live long and prosper. My brother, sister, grandpa, uncles, aunties, and nephews, thanks for giving me such a nice family. My maternal grandfather, grandmother, and grandma, you would be proud of me if you were here. Miss you.

Yuan, my dear wife, thank you for your pure love and companionship for all these years. I want to say, to hold your hand, to grow old with you.

YANKAI XIE

09-10-1992, Henan, China

yankaixie@163.com



EDUCATION

- **PhD Bioscience Engineering**
2017-2021, University of Antwerp
- **MSc Environmental Science and Engineering**
2014-2017, Hunan University
- **BSc Environmental Engineering**
2010-2014, Zhongyuan University of Technology

SELECTED HONORS AND AWARDS

- **Scholarship under the State Scholarship Fund**
2017-2021, China scholarship council
- **National Scholarship for Postgraduate students**
2016, Ministry of Education (China)

SELECTED PUBLICATIONS

▪ Published

1. **Xie, Y.**; Spiller, M.; Vlaeminck, S. E.. (2021). A bioreactor and nutrient balancing approach for the conversion of solid organic fertilizers to liquid nitrate-rich fertilizers: Mineralization and nitrification performance complemented with economic aspects. *Science of the Total Environment*, 806, 150415.
2. Van Tendeloo, M.*; **Xie, Y.***; Van Beeck, W.; Zhu, W.; Lebeer, S.; Vlaeminck, S. E. (2021). Oxygen control and stressor treatments for complete and long-term suppression of nitrite-oxidizing bacteria in biofilm-based partial nitrification/anammox. (*shared first co-authorship) *Bioresource Technology*, 342, 125996.

3. Peng, L.; **Xie, Y.**; Van Beeck, W.; Zhu, W.; Van Tendeloo, M.; Tytgat, T.; Lebeer, S.; Vlaeminck, S. E. (2020). Return-Sludge Treatment with Endogenous Free Nitrous Acid Limits Nitrate Production and N₂O Emission for Mainstream Partial Nitritation/Anammox. *Environmental Science & Technology*, 54, (9), 5822-5831.
4. **Xie, Y.**; Dong, H.; Zeng, G.; Zhang, L.; Cheng, Y.; Hou, K.; Jiang, Z.; Zhang, C.; Deng, J. (2017), The comparison of Se(IV) and Se(VI) sequestration by nanoscale zero-valent iron in aqueous solutions: The roles of solution chemistry. *Journal of Hazardous Materials*, 338, 306-312.
5. **Xie, Y.**; Dong, H.; Zeng, G.; Tang, L.; Jiang, Z.; Zhang, C.; Deng, J.; Zhang, L.; Zhang, Y. (2017), The interactions between nanoscale zero-valent iron and microbes in the subsurface environment: A review. *Journal of Hazardous Materials*, 321, 390-407.
6. Dong, H.; Deng, J.; **Xie, Y.**; Zhang, C.; Jiang, Z.; Cheng, Y.; Hou, K.; Zeng, G. (2017), Stabilization of nanoscale zero-valent iron (nZVI) with modified biochar for Cr(VI) removal from aqueous solution. *Journal of Hazardous Materials* 2017, 332, 79-86.
7. Dong, H.; **Xie, Y.**; Zeng, G.; Tang, L.; Liang, J.; He, Q.; Zhao, F.; Zeng, Y.; Wu, Y. (2016), The dual effects of carboxymethyl cellulose on the colloidal stability and toxicity of nanoscale zero-valent iron. *Chemosphere*, 144, 1682-1689.

▪ In preparation

8. **Xie, Y.**; Jia, M.; Timmer, M. J.; De Paepe, J.; Spiller, M.; Vlaeminck, S. E., A nitrification trickling filter as key to produce hydroponic nutrient solutions from real urine.
9. **Xie, Y.**; Jia, M.; De Wilde F., Daeninck, K.; De Clippeleir, H.; Verstraete, W.; Vlaeminck, S. E., Feasibility of a trickling filter for partial nitritation/anammox: Effects of carrier material, passive ventilation and hydraulic loading rate at lab scale.
10. **Xie, Y.**; Van Tendeloo, M.; Zhu, W.; Peng, L.; Vlaeminck, S. E., Autotrophic nitrogen polishing of secondary effluents: Challenges in obtaining sulfur-driven denitratation for downstream anammox treatment.

International conferences

▪ Oral presentations:

1. Improving ammonification for nitrate production in bioconversion of organic fertilizers to liquid products. The 6th MELiSSA Conference, 3-5 November 2020 (virtual).
2. Bioconversion of organic fertilizers to liquid products: Optimizing ammonification as a bottleneck to nitrate production. The 6th YWP BeNeLux conference, 12-14 February 2020 (Luxembourg).
3. Recurrent free nitrous acid exposure insufficiently suppressed nitrate formation in a mainstream partial nitritation/anammox system. The 24th National Symposium for Applied Biological Sciences, NSABS, 4 Feb 2019 (Ghent).

Supervision of students

1. 2019, Inaki Thys, Karel de Grote Hogeschool. AnAMMOX process in a packed bed reactor: set-up and performance in nitrogen removal. (Bachelor's thesis)

2. 2020, Quinten Segers, Karel de Grote Hogeschool. Bioconversion of organic fertilizers to liquid products: optimizing ammonification as a bottleneck to nitrate production. (Bachelor's thesis)